

SYNTHESIS, CHARACTERIZATION, AND CATALYTIC REACTIVITY OF
FIRST-ROW TRANSITION METAL CCC PINCER COMPLEXES

BY
BAILEY JEANNE JACKSON

DISSERTATION

Submitted in partial fulfillment of the requirements
for the degree of Doctor of Philosophy in Chemistry
in the Graduate College of the
University of Illinois at Urbana-Champaign, 2018

Urbana, Illinois

Doctoral Committee:

Associate Professor Alison Fout, Chair
Professor Gregory Girolami
Professor Catherine Murphy
Professor Renske van der Veen

Abstract

Catalysis is such a ubiquitous process that over 75% of existing chemical processes and 90% of newly developed processes utilize catalysts. Understanding how to improve and create new catalysts is therefore essential to developing new products as well as greener and more efficient processes. One way to improve the environmental impact of these reactions is to move away from using less biocompatible second- and third-row transition metal catalysts and replace them with first-row transition metal catalysts. However, first-row metals tend to engage in one-electron radical chemistry much more readily than the typically desired two-electron reactions.

One way to induce first-row transition metals to engage in the desired reactions is to use strong-field ligand frameworks. Strong-field ligands cause the d-orbital splitting of the metal center to increase in energy, often leading to low-spin electronic configurations which favor two-electron reactivity. *N*-heterocyclic carbenes (NHCs) are popular strong-field ligands due to their inherent stability and oxidative robustness, especially compared to phosphines. Combining NHCs with pincer ligand frameworks provides even more stable complexes. Therefore, we investigated a variety of monoanionic, bis(carbene), strong-field pincers with first-row transition metals.

A variety of ^{Ar}CCC (Ar = Mes, DIPP) and ^RCcCcC (R = benzyl, t-butyl) pincer ligand frameworks were developed and their metalation investigated. The ^RCcCcC pincers were successfully metalated with nickel generating (^RCcCcC)Ni(II)Br complexes (R = benzy, t-butyl). ^{DIPP}CCC pincers, previously metalated with nickel and cobalt in our group, have been extended to iron as well. The metalation method first goes through a zwitterionic intermediate which was isolated and characterized before being reduced *in situ* to yield the (^{DIPP}CCC)Fe(II)H(L)(L') complexes. A distinct electronic effect was observed on the Fe–H when varying the L-type ligands coordinated to the iron center. Reactivity of these iron hydrides with CO₂ showed insertion into

the Fe–H bond to form a κ^2 -OOCH complex ($L = \text{PMe}_3$, $L' = \text{N}_2$). This complex was also independently synthesized starting from $(^{\text{DIPP}}\text{CCC})\text{Fe}(\text{II})\text{Cl}(\text{PMe}_3)_2$.

The zwitterionic metalation method was also extended to other first-row transition metals. The synthesis and characterization of zwitterionic complexes, $\text{H}_2(^{\text{DIPP}}\text{CCC})\text{M}(\text{II})\text{Cl}_3$ ($\text{M} = \text{Mn}, \text{Co}, \text{Ni}$), was accomplished and the *in situ* reduction lead to metalation using cobalt and nickel. An alternate metalation method, transmetalation from zirconium, into similar CCC pincer ligand frameworks has been previously established by the Hollis group. Utilizing a similar procedure zirconium complexes were synthesized and characterized $(^{\text{Ar}}\text{CCC})\text{Zr}(\text{IV})\text{X}_3$ ($\text{Ar} = \text{Mes}, \text{DIPP}$). The transmetalation to iron, cobalt, and nickel were all successful with both ligand derivatives.

Our group has studied cobalt catalysts, $(^{\text{Mes}}\text{CCC})\text{Co}(\text{I})\text{L}$, for the hydrogenation of alkenes and semi-hydrogenation of alkynes and were interested in extending the hydrogenation further to more polar functional groups. Nitrile hydrogenation is a difficult reaction both in terms of activating the C–N triple bond and selectivity among products. We discovered a mild set of reaction conditions that selectively formed the primary amine for a variety of different substrates.

During our mechanistic work we determined that the process is actually Lewis acid-assisted and is in fact undergoing a two-electron catalytic process. During the investigation and subsequent publication of this work another product, the secondary aldimine, was seen under some reaction conditions. Modifying our reaction parameters, we discovered we could also selectively form the secondary aldimine product starting from the nitrile. This represents only the second example of a cobalt catalyst that can perform the hydrogenation of nitriles with selectivity to the secondary aldimine. Our condition switchable system also provided exceptionally mild reaction conditions compared to other first-row transition metal catalysts for nitrile hydrogenation.

To My Family

Acknowledgements

I would like to thank my family, including all the friends I consider family, for all their support throughout life and especially during graduate school. You have all always encouraged me to follow my dreams and work hard. Even if you didn't understand a word of technical chemistry you always asked how things were going and listened to me talk about my research projects. I would especially like to thank my parents who always encouraged my siblings and I to find our passion and turn it into a career.

I would like to thank my advisor Professor Alison Fout for her help and guidance on projects and for always challenging me to think outside the box. I would also like to thank my committee members Professor Greg Girolami, Professor Catherine Murphy, and Professor Renske van der Veen for their knowledge of chemistry and ability to ask excellent questions.

My colleagues in the lab made coming to work every day much less work and much more fun, even in spite of our rather varied taste in music. Past co-workers; Yun Ji Park, Abdulrahman Ibrahim, Gabriel Espinosa Martinez, Zack Gordon, Jack Killion, Courtney Ford, Ellen Matson, and Marshall Brennan and current co-workers; Kenan Tokmic, Michael Drummond, Tabitha Miller, Joe Nugent, Safiyah Muhammad, Claire Leahy, and Daniel Najera as well as all of our excellent undergraduates provided scientific discussions and friendship throughout the years.

I would like to thank the local ACS section as well as my fellow Younger Chemists' Committee board members for excellent years of hard work and cooperation. Additionally, I would like to thank the NMR and X-ray facility staff for all their help and support with instrumentation. Finally, I would like to thank the IMP office for their help with the YCC and myself personally. I never left the office without a smile and, more often than not, some sort of treat. You truly helped make the department feel like home.

Table of Contents

Chapter 1: Introduction.....	1
Chapter 2: Synthesis and Characterization of Ligand Scaffolds: Metalation using Iron and Nickel.....	15
Chapter 3: Extending the Metalation Methods.....	65
Chapter 4: Cobalt Catalyzed Nitrile Hydrogenation to Primary Amines.....	88
Chapter 5: Cobalt Catalyzed Semi-Hydrogenation of Nitriles and Lewis Acid Controlled Condensation to Secondary Aldimines.....	131

Chapter 1

Introduction

1.1 Introduction to Homogeneous First-Row Transition Metal Two-Electron Catalysis

The use of catalysts to undergo organic transformations has revolutionized the types of products and materials that many people take advantage of in their everyday lives. Almost 75% of existing processes and 90% of new processes developed involve the use of catalysts. Understanding these catalysts at their fundamental levels is essential for continued improvements and the development of novel systems. Though heterogeneous catalysts are used by many of the major industrial feedstock reactions subsequent steps that add complexity are often catalyzed by homogeneous methods (Figure 1.1).¹

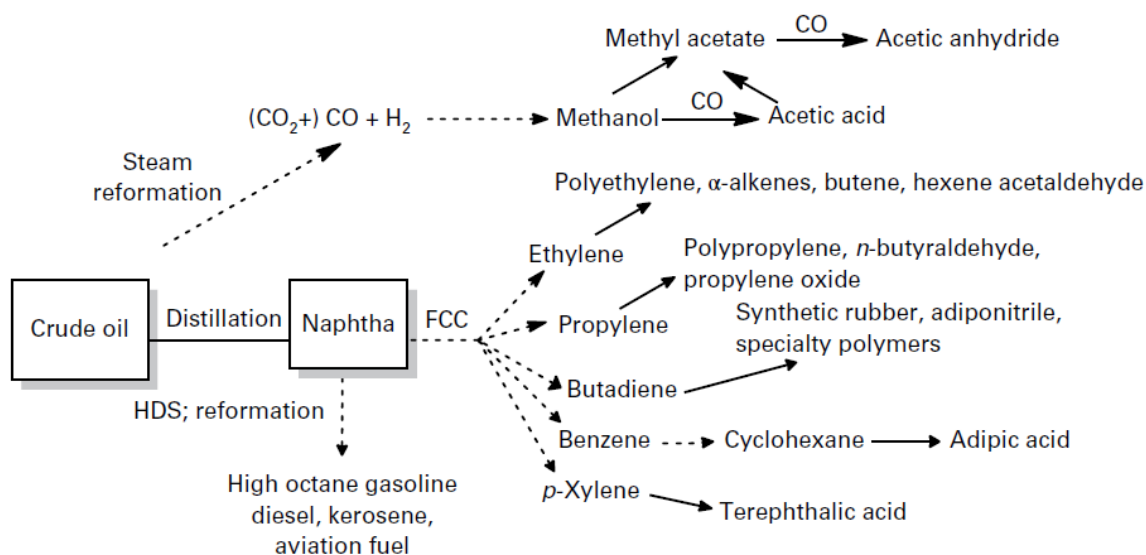


Figure 1.1. Heterogeneous reactions (dotted arrows) feeding into homogeneous reactions (solid arrows).¹

Transition metal catalysts in particular have dominated the realm of homogeneous catalysis when it comes to adding complexity,¹⁻³ though non-transition metal organic catalysts are growing in prominence.⁴⁻⁶ Within transition metals by far the most widely used and studied includes the late second- and third-row transition metals, like rhodium, palladium, iridium, and platinum, which often exhibit well-defined, two-electron catalytic steps.⁷⁻¹³ These metals have allowed chemists to

develop a variety of reactions including cross-couplings, hydrofunctionalizations, and carbon-bond metatheses to name only a few examples.⁷⁻¹³ Their well-behaved nature allows for the minutiae adjustment of ligands and conditions to obtain specific regioselectivity and often stereoselectivity. However, while second- and third-row transition metal catalysts are well understood they are also more expensive and can be less biocompatible than their first-row congeners. The latter of which is incredibly important especially in the pharmaceutical industry. Replacement of these robust catalysts presents a difficult challenge that chemists are exploring, often through the use of first-row transition metals. The difficulty of using these metals as replacement catalysts arises due to their propensity to undergo one-electron side reactions that are often undesired. The use of these first-row metals offers cheaper and more environmentally benign alternatives if this limitation can be overcome or harnessed for catalytic reactivity.¹⁴

The radical reactivity, or single electron transfer (SET), of first-row transition metals can be utilized to undergo transformations including C–H activation, hydrofunctionalization of unsaturated bonds, and a suite of polymerizations.¹⁵⁻¹⁸ Often these transformations offer unique reactivity that even second- and third-row metals do not confer and have been used for a number of different applications.^{19,20} However, replacing second- and third-row metals in catalysis usually requires replicating or mimicking the two-electron reactions they facilitate. To do this with first-row transition metals their electronic structure must either be perturbed to favor two-electron reactivity or metal-ligand cooperativity must be accessed. Therefore, two methods for this are the use of redox active ligands or strongly σ -donating ligands.

Redox active or redox non-innocent ligands can store electrons which can then be utilized by a metal center to catalyze organic reactions, sometimes without any formal oxidation state change of the metal. The overall reaction therefore, can be either two subsequent one-electron

steps or a two-electron step with at least one electron coming from the ligand itself.^{21,22} A prominent example of this type of ligand includes the use of bis(imino)pyridine ligands first reported by Bennett, Brookhart, and Gibson.²³⁻²⁵ The pyridine backbone directly connects to the imino moiety with N-substituted aryl groups to give a tridentate ligand connected through the three nitrogen atoms (Figure 1.2). Both of the imine groups can be reduced allowing the ligand to store up to two electrons at a time. Chirik's group, in particular, has made use of this ligand's redox-active ability and has investigated a number of reactions including hydrogenations,²⁶ hydrosilylations,²⁷ and ethylene polymerizations^{28,29} with iron and cobalt catalysts. Sometimes this approach can even be used to access the same reactivity and products as second- and third-row transition metals. However, understanding and improving these catalysts requires intensive characterization of their electronic structures. They are also prone to deactivation due to the nature of their radical reactivity.^{30,31}

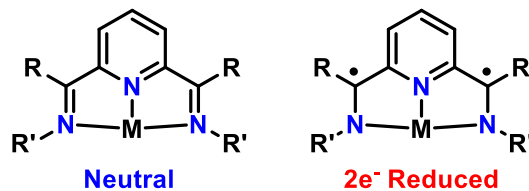


Figure 1.2. Bis(imino)pyridine ligand platform and its redox non-innocent reactivity.

Alternatively, strongly σ -donating ligands can be used to induce two-electron reactivity at the metal center itself, mirroring classic second- and third-row transition metal catalysts. Strongly σ -donating ligands include phosphines, carbon-based ligands, or other electron-rich ligands.^{32,33} These ligands increase the electron splitting of the metal d-orbitals, often resulting in low-spin electronic configurations (Figure 1.3).^{34,35}

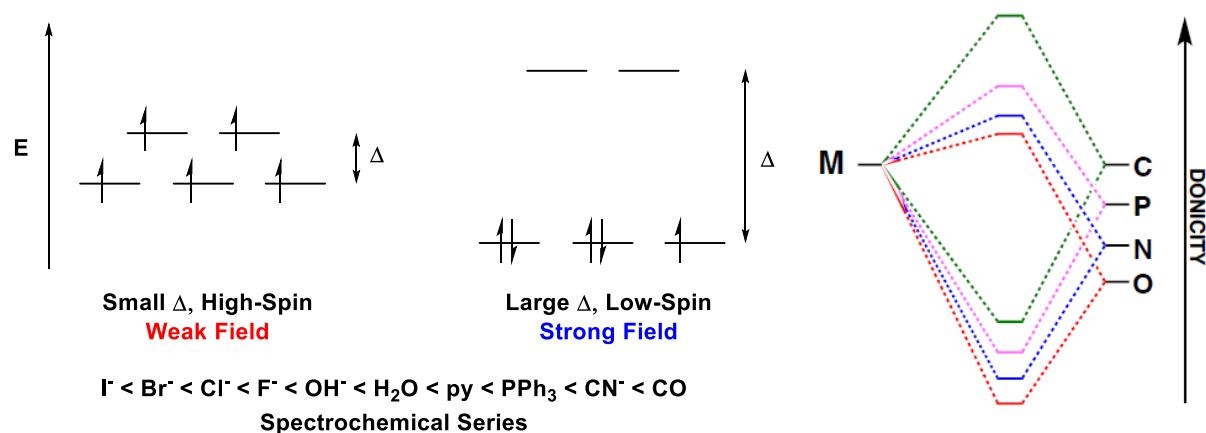


Figure 1.3. Weak vs. strong field ligand effects (left) and metal-ligand orbital overlap (right).^{34,35}

Low-spin electronic configurations help to induce two-electron reactivity instead of the more common radical reactivity seen for first-row transition metal complexes. Traditionally phosphines have dominated the realm of strongly σ -donating ligands utilized in catalysis, however, carbon-based ligands are considered even more strongly donating than phosphines based on orbital overlap with the metal center (Figure 1.3). Carbenes, in particular, have garnered much attention as ligands for transition metal catalysts and were first reported in 1964 by Fischer.³⁶ There are a number of different types of carbenes, defined as a neutral carbon atom with two unshared valence electrons ($R-(C:)-R$ or $R=C:$) including Fischer, Schrock, radical carbenes, and *N*-heterocyclic carbenes (NHCs).³⁶⁻³⁹

The use of *N*-heterocyclic carbenes (NHCs) as strongly σ -donating ligands has been rapidly gaining attention due to a number of factors including ease of synthesis, modularity, and their incredible stability especially when compared to other types of carbenes. NHCs are heterocyclic groups containing at least one nitrogen atom and a carbene. They are often called Arduengo carbenes after Anthony Arduengo who published the first isolable and ‘bottleable’ carbene in 1991.³⁷ A few examples of the most widely used and popular NHCs have been depicted (Figure 1.4).³⁷⁻³⁹ The most common structure of an NHC is a five-membered ring with two substituted

nitrogen atoms adjacent to the carbene carbon. The nitrogen atoms are critical to the electronic structure because they act as σ -withdrawing and π -donating groups which stabilize the structure inductively and mesomerically.^{40,41} The strain of the five-membered ring is also important as it results

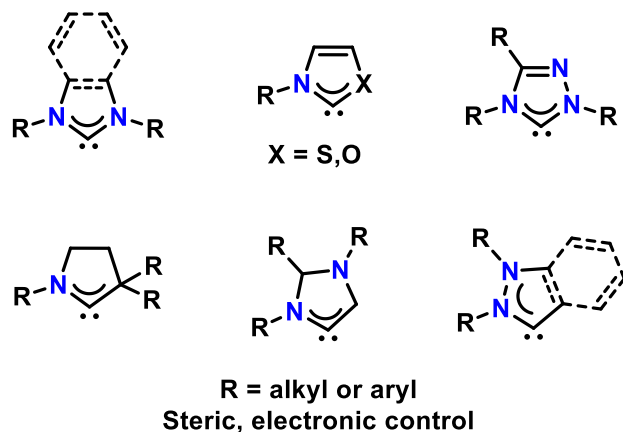


Figure 1.4. Common types of NHC ligands.

in more sp^2 bonding character of the carbene carbon. This structure helps to favor a singlet electronic ground state carbene which can render these NHCs nucleophilic. These unique electronic properties make them ideal ligands for first-row transition metal catalysts since they are very strongly σ -donating but typically poor π -acceptors leading to very strong and robust metal-carbon bonds.⁴² A prominent example of the advantage of NHCs over phosphines can be seen when examining Grubbs' first- and second-generation catalysts for olefin metathesis (Figure 1.5).⁴³⁻⁴⁵ Grubbs' second-generation catalyst makes use of a saturated NHC that renders the catalyst air and moisture stable along with exhibiting higher catalytic reactivity and stability than its predecessor.

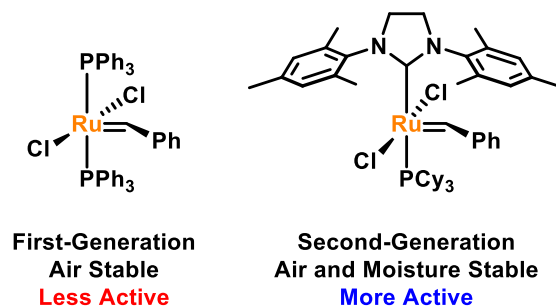


Figure 1.5. Grubbs' first- and second-generation.

While NHCs by themselves offer excellent stability and can be easily modified their incorporation into pincer frameworks even further accelerates this effect. Pincers are defined as tridentate contiguous ligand frameworks that bind in a meridional fashion, though the term has been extended to include non-meridional binding as well. Metal complexes using pincers are much

more stable, helping to prevent catalyst decomposition, and are often easier to isolate and study which is especially relevant when investigating mechanistic details.^{46,47} The strongly σ -donating nature of NHCs combined with the stability of pincers has enabled many groups, including our own, to synthesize a metal complexes and investigate their catalytic reactivity (Figure 1.6).⁴⁶⁻⁵⁷

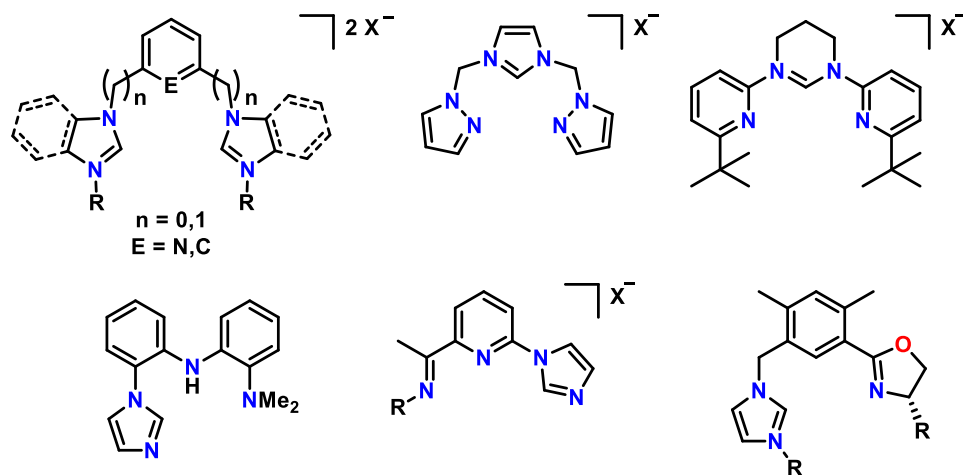


Figure 1.6. Examples of NHC incorporation into pincer ligand frameworks.⁴⁸⁻⁵⁷

Our ligand framework is a monoanionic bis(carbene) pincer platform that has been investigated with iron, cobalt, and nickel (Figure 1.7). The metalation of these ligands with first-row transition metals has been undertaken using a variety of methods including C–H activation by low-valent metals, the synthesis of a zwitterionic precursor, transmetalation from zirconium, and the use of internal bases. Various coordination complexes were synthesized and analyzed looking at electronic trends particularly with iron-hydride molecules. The catalytic hydrogenation of

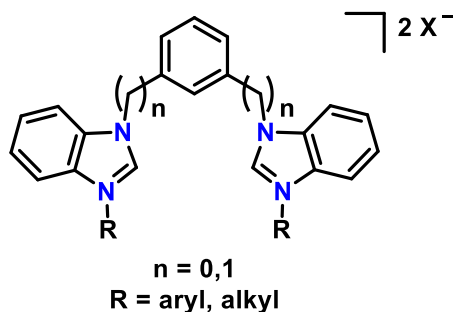


Figure 1.7. Monoanionic bis(carbene) CCC pincer ligand platform.

nitriles was also extensively investigated using previously synthesized cobalt complexes with condition switchable selectivity for the primary amines and secondary aldimines, respectively. Mechanistic studies supported a two-electron catalytic cycle for these reactions. Often our catalytic conditions more closely resemble those of second- and third-row transition metals rather than other first-row metal catalysts, indicating the influence of our ligand framework.

1.2 References

1. Bhaduri, S.; Mukesh, D. *Homogeneous Catalysis: Mechanisms and Industrial Applications*, Second Ed.; John Wiley & Sons, Inc.: New Jersey, 2014.
2. Hagen, Jens. *Industrial Catalysis: A Practical Approach*, Third Ed.; Wiley-VCH Verlag GmbH & Co. KGaA: Weinheim, Germany, 2015.
3. *Applied Homogeneous Catalysis with Organometallic Compounds*, Third Ed.; Vol. 1; Bornils, B.; Herrmann, W. A.; Beller, M.; Paciello, R., Ed.; Wiley-VCH Verlag GmbH & Co. KGaA: Weinheim, Germany, 2018.
4. Sun, C.; Shi, Z.; Transition-Metal-Free Coupling Reactions. *Chem. Rev.* **2014**, *114*, 9219-9280.
5. Qin, Y.; Zhu, L.; Luo, S.; Organocatalysis in Inert C-H Bond Functionalization. *Chem. Rev.* **2017**, *117*, 9433-9520.
6. Romero, N. A.; Nicewicz, D. A.; Organic Photoredox Catalysis. *Chem. Rev.* **2016**, *116*, 10075-10166.
7. Leeuwen, P. W.N.M. van. *Homogeneous Catalysis: Understanding the Art*. Kluwer Academic Publishers: Dordrecht, Netherlands, 2004.
8. Hartwig, J. F. *Organotransition Metal Chemistry: From Bonding to Catalysis*. University Science Books: California, 2011.
9. Meijere, A.; Bräse, S.; Oestreich, M. *Metal-Catalyzed Cross-Coupling Reactions and More*. Wiley-VCH Verlag GmbH & Co. KGaA: Weinheim, Germany, 2014.
10. Magano, J.; Dunetz, J. R. *Transition Metal-Catalyzed Couplings in Process Chemistry: Case Studies from the Pharmaceutical Industry*. Wiley-VCH Verlag GmbH & Co. KGaA: Weinheim, Germany, 2013.

11. Ananikov, V. P.; Tanaka, M. *Hydrofunctionalization: Topics in Organometallic Chemistry*. Springer-Verlag: Berlin, Germany, 2013.
12. Astruc, D. The metathesis reactions: from a historical perspective to recent developments. *New J. Chem.* **2005**, *29*, 42-56.
13. Hoff, R. *Handbook of Transition Metal Polymerization Catalysts*. John Wiley & Sons, Inc.: New Jersey, 2018.
14. Ludwig, J. R.; Schindler, C. S.; Catalyst: Sustainable Catalysis. *Chem.* **2017**, *2*, 313-316.
15. Smith, K. Single Electron Transfer Reactions in the Synthetic Organometallic Chemistry of First-Row Transition Metals. *Organometallics* **2005**, *24*, 778-784.
16. Yi, H.; Zhang, G.; Wang, H.; Huang, Z.; Wang, J.; Singh, A. K.; Lei, A. Recent Advances in Radical C-H Activation/Radical Cross-Coupling. *Chem. Rev.* **2017**, *117*, 9016-9085.
17. Crossley, S. W. M.; Obraors, C.; Martinez, R. M.; Shenvi, R. A. Mn-, Fe-, and Co-Catalyzed Radical Hydrofunctionalizations of Olefins. *Chem. Rev.* **2016**, *116*, 8912-9000.
18. Zhang, N.; Samanta, S. R.; Rosen, B. M.; Percec, V. Single Electron Transfer in Radical Ion and Radical-Mediated Organic, Materials, and Polymer Synthesis. *Chem. Rev.* **2014**, *114*, 5848-5958.
19. Liu, C.; Liu, D.; Lei, A. Recent Advances of Transition-Metal Catalyzed Radical Oxidative Cross-Couplings. *Acc. Chem. Res.* **2014**, *47*, 3459-3470.
20. Zweig, J. E.; Kim, D. E.; Newhouse, T. R. Methods Utilizing First-Row Transition Metals in natural Product Total Synthesis. *Chem. Rev.* **2017**, *117*, 11680-11752.
21. Lyaskovskyy, V.; Bruin, B. Redox Non-Innocent Ligands: Versatile New Tools to Control Catalytic Reactions. *ACS Catal.* **2012**, *2*, 270-279.

22. Peters, R. *Cooperative Catalysis: Designing Efficient Catalysts for Synthesis*. Wiley-VCH Verlag GmbH & Co. KGaA: Weinheim, Germany, 2015.
23. A. M. A. Bennett, *World Pat.*, WO 98/2714 (DuPont), 1998; A. M. A. Bennett, *Chem. Abstr.* **1998**, 129, 122973.
24. Small, B. L.; Brookhart, M. S.; Bennett, A. M. Highly Active Iron and Cobalt Catalysts for the Polymerization of Ethylene. *J. Am. Chem. Soc.* **1998**, 120, 4049–4050.
25. J. P. Britovsek, G.; C. Gibson, V.; J. McTavish, S.; A. Solan, G.; J. P. White, A.; J. Williams, D.; J. P. Britovsek, G.; S. Kimberley, B.; J. Maddox, P. Novel Olefin Polymerization Catalysts Based on Iron and Cobalt. *Chem. Commun.* **1998**, 7, 849–850.
26. Monfette, S.; Turner, Z. R.; Semproni, S. P.; Chirik, P. J. Enantiopure C₁-Symmetric bis(imino)pyridine Cobalt Complexes for Asymmetric Alkene Hydrogenation. *J. Am. Chem. Soc.* **2012**, 134, 4561-4564.
27. Tondreau, A. M.; Atienza, C. C. H.; Weller, K. J.; Nye, S. A.; Lewis, K. M.; Delis, J. G. P.; Chirik, P. J. Iron Catalysts for Selective Anti-Markovnikov Alkene Hydrosilylation Using Tertiary Silanes. *Science* **2012**, 335, 567-570.
28. Schaefer, B. A.; Margulieux, G. W.; Tiedemann, M. A.; Small, B. L.; Chirik, P. J. Synthesis and Electronic Structure of Iron Borate Betaine Complexes as a Route to Single-Component Iron Ethylene Oligomerization and Polymerization Catalysts. *Organometallics* **2015**, 34, 5615-5623.
29. Atienza, C. C. H.; Milsmann, C.; Lobkovsky, E.; Chirik, P. J. Synthesis, Electronic Structure, and Ethylene Polymerization Activity of Bis(imino)pyridine Cobalt Alkyl Cations. *Angew. Chem. Int. Ed.* **2011**, 50, 8143-8147.

30. Archer, A. M.; Bouwkamp, M. W.; Cortez, M.; Lobkovsky, E.; Chirik, P. J. Arene Coordination in Bis(imino)pyridine Iron Complexes: Identification of Catalyst Deactivation Pathways in Iron-Catalyzed Hydrogenation and Hydrosilylation. *Organometallics* **2006**, *25*, 4269-4278.
31. Crabtree, R. H. Deactivation in Homogeneous Transition Metal Catalysis: Causes, Avoidance, and Cure. *Chem. Rev.* **2014**, *115*, 127-150.
32. Mitoraj, M. P.; Michalak, A. σ -Donor and π -Acceptor Properties of Phosphorus Ligands: An Insight from the Natural Orbitals for Chemical Valence. *Inorg. Chem.* **2010**, *49*, 578-582.
33. Crabtree, R. H. *The Organometallic Chemistry of the Transition Metals*, 6th ed.; John Wiley & Sons: New York, 2005.
34. Volpe, E. C., Wolczanski, P. T.; Lobkovsky, E. B. Aryl-Containing Pyridine-Imine and Azaallyl Chelates of Iron toward Strong Field Coordination Compounds. *Organometallics* **2010**, *29*, 364-377.
35. Miessler, G.; Tarr, D. *Inorganic Chemistry*, 4th ed.; Prentice Hall: Upper Saddle River, 2011.
36. Fischer, E. O.; Maasböl, A. On the Existence of a Tungsten Carbonyl Carbene Complex. *Angew. Chem. Int. Ed. Engl.* **1964**, *3*, 580-581.
37. Arduengo, A. J.; Harlow, R. L.; Kline, M. A Stable Crystalline Carbene. *J. Am. Chem. Soc.* **1991**, *113*, 361-363.
38. Benhamou, L.; Chardon, E.; Lavigne, G.; Bellemin-Laponnaz, S.; Cesar, V. Synthetic Routes to N-Heterocyclic Carbene Precursors. *Chem. Rev.* **2011**, *111*, 2705-2733.

39. Hopinson, M. N.; Richter, C.; Schedler, M.; Glorius, F. An overview of N-heterocyclic carbenes. *Nature* **2014**, *510*, 485-496.
40. Jacobsen, H.; Correa, A.; Poater, A.; Costabile, C.; Cavallo, L. Understanding the M-(NHC) (NHC= N-heterocyclic carbene) bond. *Coord. Chem. Rev.* **2009**, *253*, 687-703.
41. Huynh, H. V. Electronic Properties of N-Heterocyclic Carbenes and Their Experimental Determination. *Chem. Rev.* **2018**.
42. Díez-González, S.; Marion, N.; Nolan, S. P. N-Heterocyclic Carbenes in Late Transition Metal Catalysis. *Chem. Rev.* **2009**, *109*, 3612-3676.
43. Schwab, P.; France, M. B.; Ziller, J. W.; Grubbs, R. H. A Series of Well-Defined Metathesis Catalysts – Synthesis of $[\text{RuCl}_2(=\text{CHR}')(\text{PR}_3)_2]$ and Its Reactions. *Angew. Chem. Int. Ed. Engl.* **1995**, *34*, 2039-2041.
44. Schwab, P.; Grubbs, R. H.; Ziller, J. W. Synthesis and Applications of $\text{RuCl}_2(=\text{CHR}')(\text{PR}_3)_2$: The Influence of the Alkylidene Moiety on Metathesis Activity. *J. Am. Chem. Soc.* **1996**, *118*, 100-110.
45. Scholl, M.; Ding, S.; Lee, C. W.; Grubbs, R. H. Synthesis and Activity of a New Generation of Ruthenium-Based Olefin Metathesis Catalysts Coordinated with 1,3-Dimesityl-4,5-dihydroimidazol-2-ylidene Ligands. *Org. Lett.* **1999**, *1*, 953-956.
46. Morales-Morales, D. *Pincer Compounds: Chemistry and Applications*. Elsevier Inc.: Amsterdam, Netherlands, 2018.
47. Peris, E.; Crabtree, R. H. Recent homogeneous catalytic applications of chelate and pincer N-heterocyclic carbenes. *Coord. Chem. Rev.* **2004**, *248*, 2239-2246.
48. Peris, E.; Loch, J. A.; Mata, J.; Crabtree, R. H. A Pd complex of a tridentate pincer CNC bis-carbene ligand as a robust homogenous Heck catalyst. *Chem. Commun.* **2001**, 201-202.

49. Gründemann, S.; Albrecht, M.; Loch, J. A.; Faller, J. W.; Crabtree, R. H. Tridentate CCC and CNC Pincer Palladium(II) Complexes: Structure, Fluxionality, and Catalytic Activity. *Organometallics* **2001**, *20*, 5485-5488.
50. Vargas, V. C.; Rubio, R. J.; Hollis, T. K.; Salcido, M. E. Efficient Route to 1,3-Di-*N*-imidazolylbenzene. A Comparison of Monodentate vs Bidentate Carbenes in Pd-Catalyzed Cross Coupling. *Org. Lett.* **2003**, *5*, 4847-4849.
51. Hah, F. E.; Jahnke, M. C.; Pape, T. Synthesis of Pincer-Type Bis(benzimidazolin-2-ylidene) Palladium Complexes and Their Application in C-C Coupling Reactions. *Organometallics* **2007**, *26*, 150-154.
52. Ghavale, N.; Manjare, S. T.; Singh, H. B.; Butcher, R. J. Bis(chalcogenones) as pincer ligands: isolation and Heck activity of the selone-ligated unsymmetrical C,C,Se-Pd pincer complex. *Dalton Trans.* **2015**, *44*, 11893-11900.
53. Mancano, G.; Page, M. J.; Bhadbhade, M.; Messerle, B. A. Hemilabile and Bimetallic Coordination in Rh and Ir Complexes of NCN Pincer Ligands. *Inorg. Chem.* **2014**, *53*, 10159-10170.
54. Jiang, Y.; Gendy, C.; Roesler, R. Nickel, Ruthenium, and Rhodium NCN-Pincer Complexes Featuring a Six-Membered N-Heterocyclic Carbene Central Moiety and Pyridyl Pendant Arms. *Organometallics* **2018**, *37*, 1123-1132.
55. Wang, Z.; Li, X.; Sun, H.; Fuhr, O.; Fenske, D. Synthesis of NHC Pincer Hydrido Nickel Complexes and Their Catalytic Applications in Hydrodehalogenation. *Organometallics* **2018**, *37*, 539-544.

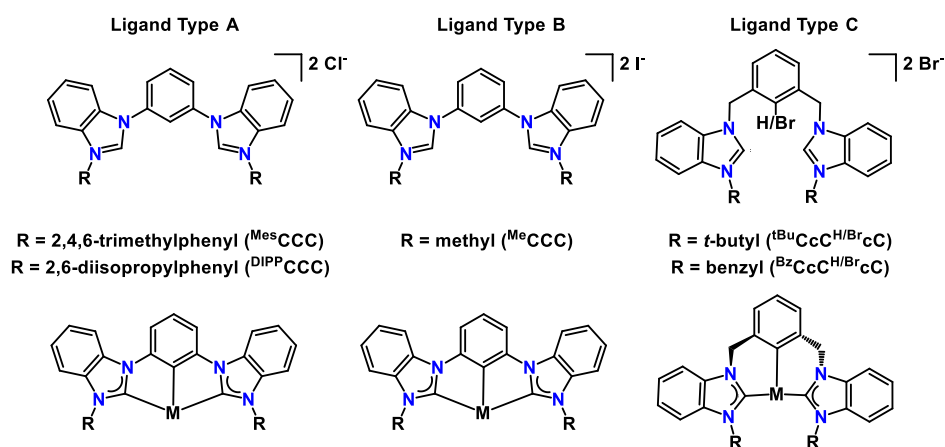
56. He, F.; Danopoulos, A. A.; Braunstein, P. Trifunctional pNHC, Imine, Pyridine Pincer-Type Iridium(III) Complexes: Synthetic, Structural, and Reactivity Studies. *Organometallics* **2015**, *35*, 198-206.
57. Ito, J.; Sugino, K.; Matsushima, S.; Sakaguchi, H.; Iwata, H.; Ishihara, T.; Nishiyama, H. Synthesis of NHC-Oxazoline Pincer Complexes of Rh and Ru and Their Catalytic Activity for Hydrogenation and Conjugate Reduction. *Organometallics* **2016**, *35*, 1885-1894.

Chapter 2

Synthesis and Characterization of Ligand Scaffolds: Metalation using Iron and Nickel

2.1 Ligand Platforms, Synthesis, and Metalation Methods

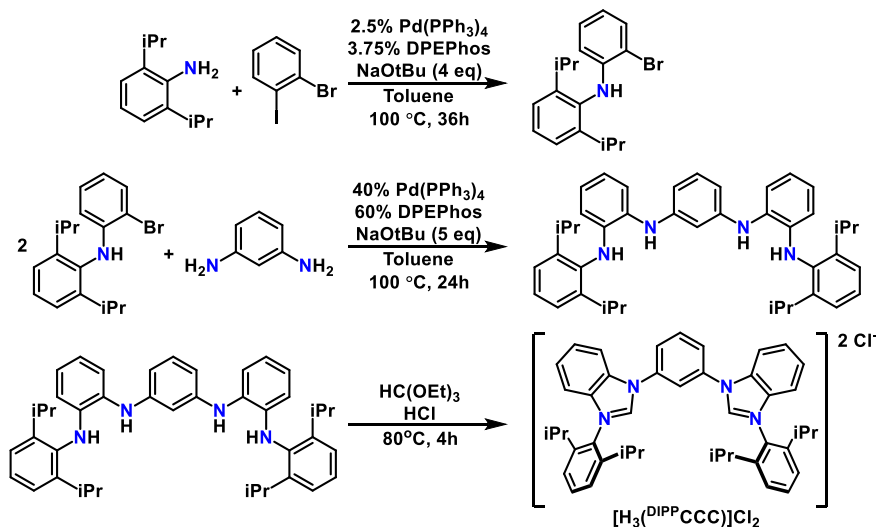
Our general ligand platform consists of a phenyl backbone group with two flanking *N*-heterocyclic carbene (NHC) moieties giving a monoanionic pincer ligand. These carbenes have been substituted with a variety of aryl and alkyl groups along with the addition of methylene group linkers between the NHCs and phenyl backbone. These ligand frameworks are strongly σ -donating due to both the aryl backbone ($M-C_{Ar}$) and NHCs ($M-C_{NHC}$) that are combined in a pincer conformation which helps to impart stability to the generated complexes. The structure of these ligand frameworks is outlined below (Scheme 2.1).



Scheme 2.1. CCC and CcCcC pincer ligand platforms shown as the benzimidazolium salts (top) and with a metal coordinated (bottom).

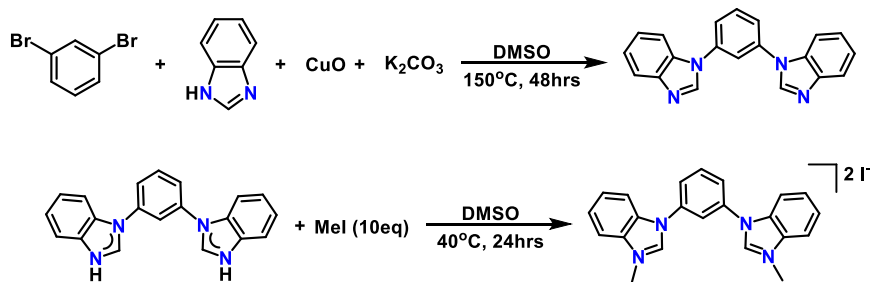
Ligand type A, with aryl substituted *N*-heterocyclic carbenes, is synthesized by two subsequent Buchwald-Hartwig palladium cross-couplings forming the C–N bonds to the aryl group and the phenyl backbone to give the tetraamine product. This compound can then be cyclized using triethylorthoformate and hydrochloric acid to give the final benzimidazolium salt of the ligand shown (Scheme 2.2). $[H_3(^{Mes}CCC)]Cl_2$ (^{Mes}CCC = bis(2,4,6-trimethylphenyl-benzimidazol-2-ylidene)phenyl) and $[H_3(^{DIPP}CCC)]Cl_2$ (^{DIPP}CCC = bis(2,6-diisopropylphenyl-benzimidazol-2-

ylidene)phenyl) have both been synthesized and reported in the literature previously, but modifications were made to the procedure by our group as detailed in our previous publications.^{1,2}



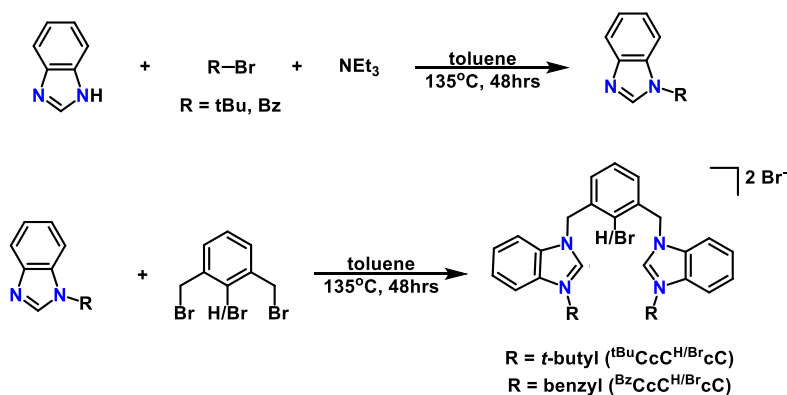
Scheme 2.2. Synthesis of Ligand type A, $[H_3^{(DIPPCCC)}]Cl_2$ shown.^{1,2}

Ligand type B, with alkyl substituted *N*-heterocyclic carbenes and no methylene spacer, is instead synthesized using a modified ligand procedure starting with benzimidazole and phenyl dibromide which is coupled using copper oxide to give the unsubstituted CCC backbone. The use of excess methyl iodide then yields the benzimidazolium salt of the ligand $[H_3^{(MeCCC)}]I_2$ ($MeCCC$ = bis(methyl-benzimidazol-2-ylidene)phenyl) (Scheme 2.3). This ligand is particularly insoluble and was not able to be metalated due to this limitation but improvements to the synthetic procedure were made (See 2.4 Experimental).³



Scheme 2.3. Synthesis of Ligand type B, $[H_3^{(MeCCC)}]I_2$.³

Ligand type C, with methylene spacers, is synthesized by first installing the R-groups on benzimidazole via an S_N2 reaction. The substituted benzimidazole is then reacted with 2-bromo-bis(1,3-bromomethyl)benzene via an S_N2 copper reaction to yield the benzimidazolium salt of the ligand. The protonated version was also synthesized using 1,3-(bromomethyl)benzene instead (Scheme 2.4). This platform is especially attractive due to its modularity and simplicity as well as lack of palladium couplings. [H₃(^{Bz}CcCcC)]Br₂ (^{Bz}CcCcC = 2,6-bis(benzyl-methylenebenzimidazol-2-ylidene)phenyl) and [H₂(^{Bz}CcC^{Br}cC)]Br₂ (^{Bz}CcC^{Br}cC = 2,6-bis(benzyl-methylenebenzimidazol-2-ylidene)-1-bromobenzene) have been previously synthesized, though only as the PF₆ salt for the former.^{4,5} Other alkyl groups with this ligand type have also been investigated including [H₂(^{tBu}CcC^{Br}cC)]Br₂ (^{tBu}CcC^{Br}cC = 2,6-bis(*t*-butyl-methylenebenzimidazol-2-ylidene)-1-bromobenzene) but the protonated version, [H₃(^{tBu}CcCcC)]Br₂ (^{tBu}CcCcC = 2,6-bis(*t*-butyl-methylenebenzimidazol-2-ylidene)), has not yet been reported.⁶ The only d-block transition metals reported with these ligand platforms are silver and palladium.^{4,7}

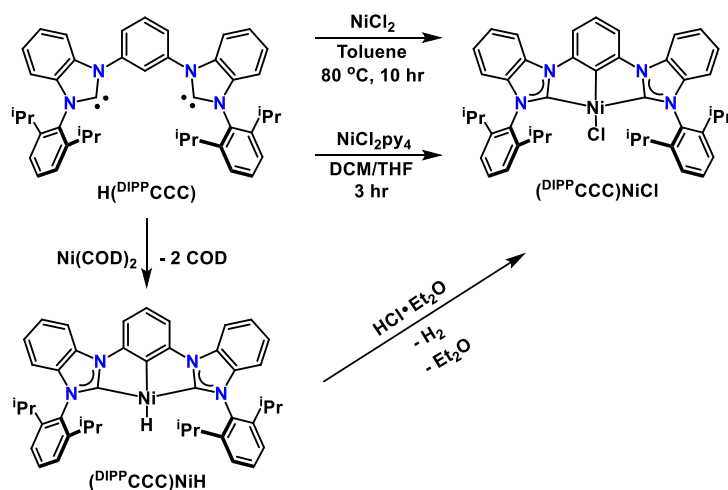


Scheme 2.4. Synthesis of Ligand type C, [H₃(^RCcC^{H/Br}cC)]Br₂.⁴⁻⁷

Ligand types A and B form rigid pincers in which the metal binds in the traditional tridentate, meridional fashion. However, ligand type C has much more flexibility due to the methylene carbons and, while still binding tridentate, that flexibility causes the ligand to twist out

of plane when a metal is bound as evidenced in the solid-state structures following. Metalation of these CCC type pincer ligands is particularly difficult due to many of their intrinsic properties. The salts can be easily deprotonated to give the bis(carbenes) by any sufficiently Lewis basic functionality, but the activation of the phenyl backbone then requires a Lewis acidic group which is often incompatible with the previous step. A variety of methods have been employed to circumvent this incompatibility.

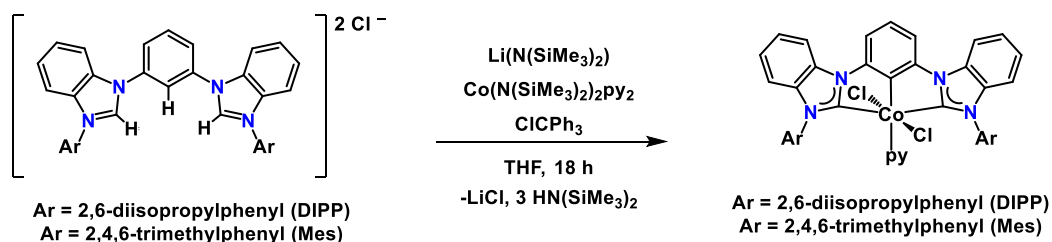
Metalation of these CCC ligand frameworks has been accomplished by transmetalation from silver^{3,8-10} and zirconium,¹¹⁻¹⁷ salt metathesis with excess base,^{1,18-19} metal sources with internal bases,² and using zero valent metal sources to perform oxidative addition across C–H or C–Br bonds.^{5,7,20} Noble metals including rhodium,^{3,13,14} palladium,^{5,7,9} osmium,¹⁸ iridium,^{1,9,14} and platinum^{15,16} have been installed in similar CCC systems by these methods. However, our group was the first to metalate this type of CCC framework using a late first-row transition metal. This was accomplished by two different methods using nickel 1) salt metathesis and 2) the use of a zero-valent nickel source (Scheme 2.5).²⁰



Scheme 2.5. $(\text{DIPPCCC})\text{Ni}$ complexes.

The synthesis of $(^{\text{DIPP}}\text{CCC})\text{Ni}(\text{II})\text{Cl}$ was first achieved by the *in situ* generation of the free carbene, $\text{H}(^{\text{DIPP}}\text{CCC})$, using two equivalents of base which was then refluxed with NiCl_2 in toluene to give $(^{\text{DIPP}}\text{CCC})\text{Ni}(\text{II})\text{Cl}$ in low yields ($\sim 35\%$). However, it was also discovered that treating the carbene with NiCl_2py_4 in a DCM/THF mixture gave the same complex in quantitative yields. The nickel hydride complex can also be synthesized starting with the isolated bis(carbene) and adding $\text{Ni}(\text{0})(\text{COD})_2$. Oxidative addition across the aryl C–H bond then generated the nickel hydride in decent yields (41%) (Scheme 2.5).²⁰

Subsequently, our group was also able to synthesize the cobalt derivatives of both the $(^{\text{DIPP}}\text{CCC})$ and $(^{\text{Mes}}\text{CCC})$ ligands using a metal source containing an internal base, $\text{Co}(\text{N}(\text{SiMe}_3)_2)_2\text{py}_2$ (Scheme 2.6). These complexes were found to reduce easily to the Co(II) and Co(I) oxidation states and were also investigated for catalytic reactivity.^{2,21-24}



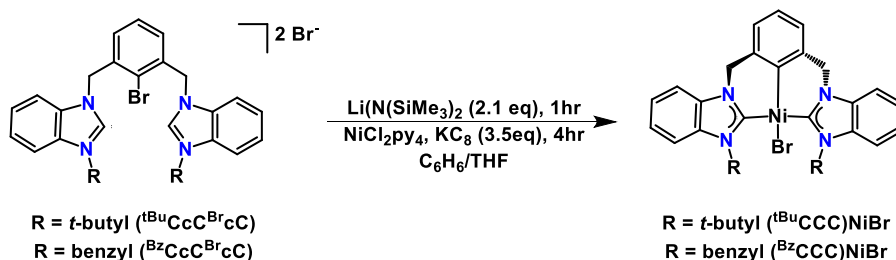
Scheme 2.6. $(^{\text{R}}\text{CCC})\text{Co}$ complexes.

The use of these CCC pincer ligand frameworks with first-row transition metals has demonstrated their ability to stabilize complexes, catalyze numerous organic transformations, and enable two-electron catalytic reactivity. Therefore, synthesizing derivatives of the ligands as well as applying them to new first-row metals, like iron and manganese, would allow for the development of new catalysts and a better understanding of these systems.

2.2 Synthesis and Characterization of New Complexes - Nickel

Ligand Type C, with the methylene spacer, was first investigated with iron, cobalt, and nickel due to its ease of synthesis and lack of palladium couplings. $[\text{H}_2(\text{R}^{\text{C}}\text{C}^{\text{Br}}\text{C})]\text{Br}_2$ (R = benzyl, t-butyl) was treated with two equivalents of various bases to determine if the free carbene could be generated or if the benzylic C–H bonds were susceptible to activation first. It was found that the free carbenes, $(\text{Bz}^{\text{C}}\text{C}^{\text{Br}}\text{C})$ and $(\text{tBu}^{\text{C}}\text{C}^{\text{Br}}\text{C})$, could be generated upon the addition of two equivalents of $\text{Li}(\text{N}(\text{SiMe}_3)_2)$ with no activation of the benzylic C–H bonds. This is clearly evidenced by the loss of the downfield NHC resonances in the ^1H NMR spectra and the increased solubility of the generated free carbenes (See 2.4 Experimental).

The next step was to activate the C–Br bond with a metal or base which should be more easily accessed than a C–H bond in the same position. The free carbene was generated *in situ* and then $\text{Ni}(\text{COD})_2$, a zero-valent nickel source, was added to the reaction mixture. The isolation of



Scheme 2.7. Synthesis of $(\text{R}^{\text{C}}\text{C}^{\text{C}}\text{C})\text{Ni}$ complexes.

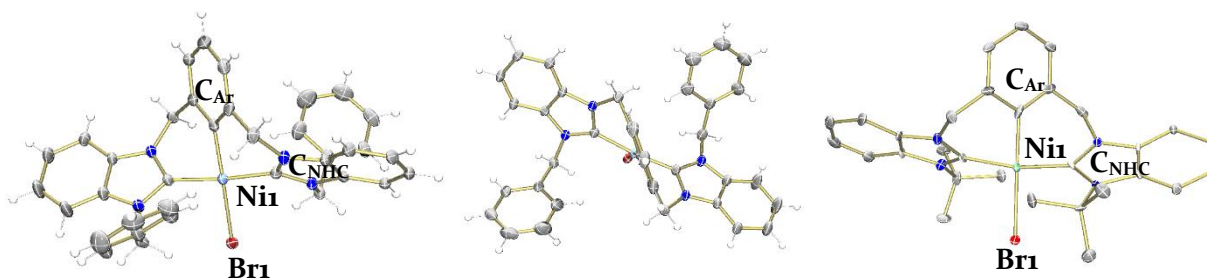


Figure 2.1. Molecular structures of $(\text{Bz}^{\text{C}}\text{C}^{\text{C}}\text{C})\text{Ni}(\text{II})\text{Br}$ (left, center) and $(\text{tBu}^{\text{C}}\text{C}^{\text{C}}\text{C})\text{Ni}(\text{II})\text{Br}$ (right) shown with 50% probability ellipsoids. Solvent molecules and selected hydrogen atoms have been omitted for clarity.

$(^{\text{Bz}}\text{CcCcC})\text{Ni}(\text{II})\text{Br}$ attested to the C–Br bond being activated but a lower yield (~60%) led to further investigation into this metalation. Substituting instead $\text{Ni}(\text{II})\text{Cl}_2\text{py}_4$ with two equivalents of a reductant (KC_8) to generate the $\text{Ni}(0)$ *in situ* led to much higher yields (80-90%) for both $(^{\text{tBu}}\text{CcBrcC})\text{Ni}(\text{II})\text{Br}$ and $(^{\text{Bz}}\text{CcBrcC})\text{Ni}(\text{II})\text{Br}$ (Scheme 2.7). This is likely due to the nickel first coordinating to the free carbene before being reduced to $\text{Ni}(0)$ *in situ* and undergoing oxidative addition. Both complexes were characterized crystallographically and orienting to the plane of the phenyl backbone you can very clearly see the flexibility of the ligand as the two benzimidazole groups end up nearly perpendicular to one another (Figure 2.1, center). Both nickel centers have a slightly distorted square planar geometry with similar $\text{Ni}-\text{C}_{\text{Ar}}$ bond lengths, 2.4188(3) Å and 2.4379(8) Å for $(^{\text{Bz}}\text{CcCcC})\text{Ni}(\text{II})\text{Br}$ and $(^{\text{tBu}}\text{CcCcC})\text{Ni}(\text{II})\text{Br}$, respectively, and $\text{Ni}-\text{C}_{\text{NHC}}$ bond lengths, 1.906(2) Å and 1.902(2) Å for $(^{\text{Bz}}\text{CcCcC})\text{Ni}(\text{II})\text{Br}$ and 1.916(6) Å and 1.903(5) Å for $(^{\text{tBu}}\text{CcCcC})\text{Ni}(\text{II})\text{Br}$.

Investigating these complexes by ^1H NMR spectroscopy revealed C_2 symmetric spectra (Figure 2.2). The NHC resonances of the benzimidazolium ligand salts have disappeared and the previous methylene CH_2 singlet resonances ($\text{R} = \text{Bz}$: 6.04 and 5.91 ppm, $\text{R} = \text{tBu}$: 5.91 ppm) have become diastereotopic. However, $(^{\text{Bz}}\text{CcCcC})\text{Ni}(\text{II})\text{Br}$ appeared to only have three sets of doublet resonances ($3 \times 2\text{H}$) for the methylene CH_2 groups in the region from 4-6 ppm. Integration of the aryl region revealed that the extra resonance has likely been shifted downfield into the aromatic region. This could indicate a significant interaction between the nickel center and one of the methylene groups in solution since no close interaction is evident in the solid-state structure. Investigating the coupling constants between the visible doublets corroborates this hypothesis since the constants, which should be identical, do not match ($J = 16.9, 13.2, \text{ and } 12.3$ Hz) which indicates possible non-symmetry in the solution state. Analysis of the isolated crystals by ^1H NMR

spectroscopy gave the same spectrum. (¹BuCcCcC)Ni(II)Br, on the other hand, displays a much more symmetric ¹H NMR spectrum with no indication of a nickel-methylene interaction and matching coupling constants for the methylene doublet resonances (*J* = 13.6 Hz) (Figure 2.2).

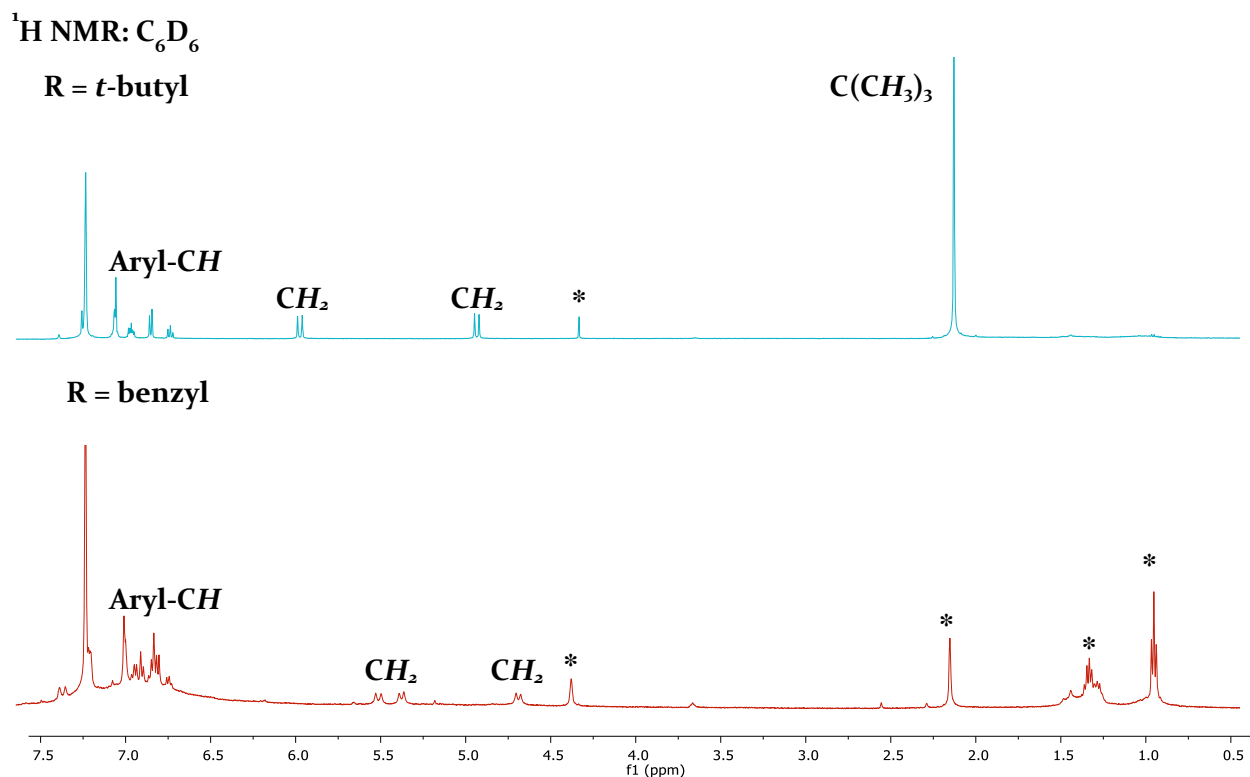


Figure 2.2. ¹H NMR spectra (C₆D₆) of (^RCcCcC)Ni(II)Br (R = *t*-butyl (top, blue), benzyl (bottom, red)), *indicates solvent.

The addition of NaHBET₃ to (¹BuCcCcC)Ni(II)Br yielded (¹BuCcCcC)Ni(II)H via ¹H NMR spectroscopy (Figure 2.3). The deep purple complex has a hydridic resonance that appears as a singlet at -7.77 ppm and the diastereotopic methylene protons appear at 5.4 ppm and 5.1 ppm as doublets (*J* = 13.5 Hz). (¹BuCcCcC)Ni(II)H exhibited thermal instability when in solution at room temperature but appeared much more stable as a solid at -35 °C. The independent synthesis of this complex was attempted from the protonated version of the benzimidazolium ligand salt, [H₃(¹BuCcCcC)]Br₂, following the same metalation procedure but was unsuccessful. It was verified that the generation of the free carbene, as previously described, also worked with the protonated

ligand (See 2.4 Experimental). The sensitive nature of the hydride appeared to lead to decomposition before it could be fully isolated from the reaction mixture. A distinct color change could be seen during work-up from the purple color of the hydride to a dark red color previously observed from the decomposition of the nickel hydride complex.

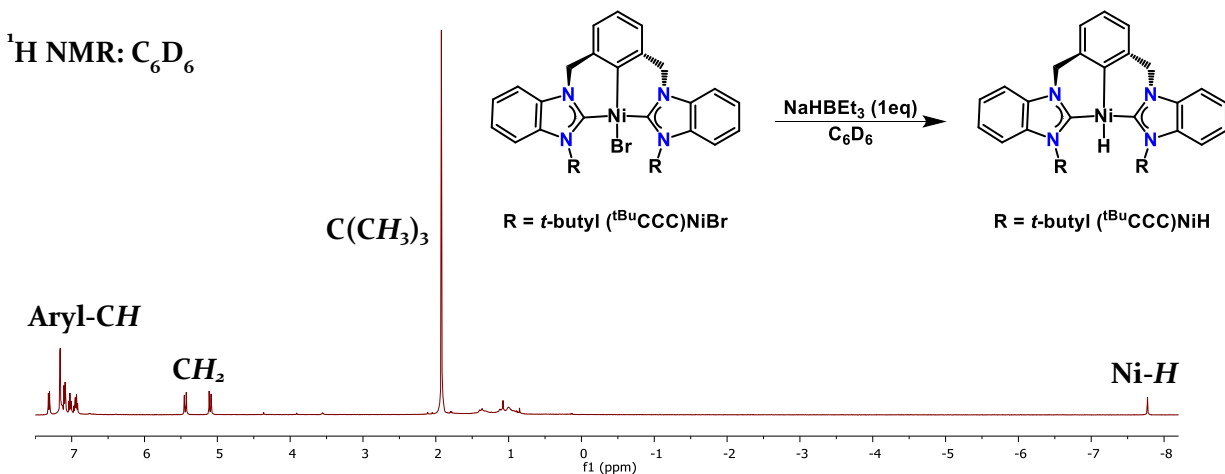
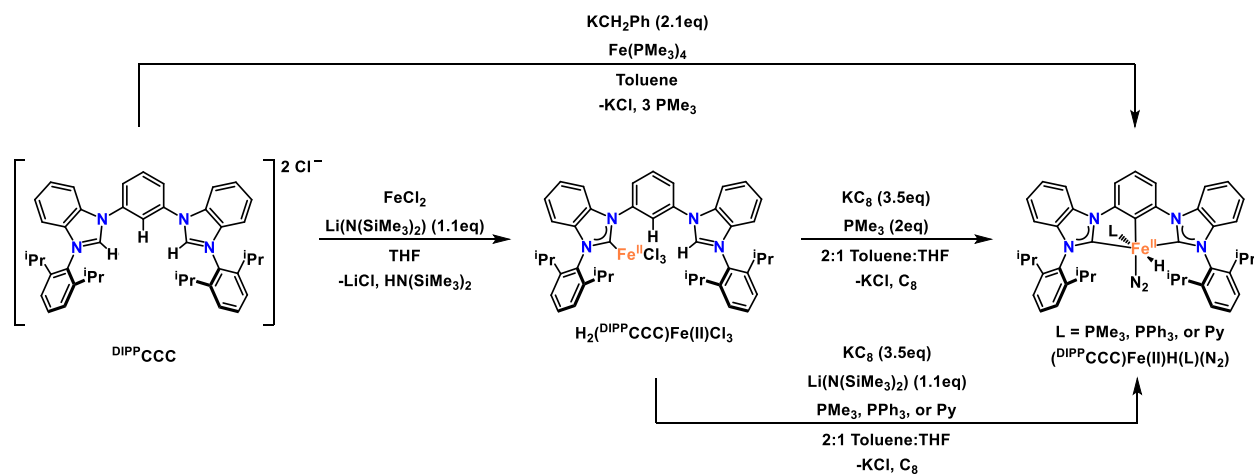


Figure 2.3. Synthesis of (^tBuCcCcC)Ni(II)H and ¹H NMR spectrum (C₆D₆).

Unfortunately, the synthesis of the iron and cobalt derivatives was unsuccessful. Interested in pursuing a variety of first-row transition metal catalysts we turned our attention to Ligand Type A, [H₃(^{Ar}CCC)]Cl₂, for the development of iron catalysts.

2.3 Synthesis and Characterization of New Complexes - Iron

Ligand Type A has been metalated by our group using nickel and cobalt, as previously described, but applying these same routes to iron did not afford the desired products in appreciable yield. An Fe(II)–H molecule, later identified as (^{DIPP}CCC)Fe(II)H(PMe₃)(N₂), could be generated using two equivalents of benzyl potassium and Fe(PMe₃)₄ but only in low yield (30%). Therefore, we sought a different synthetic route to access the iron complexes. Treatment of [H₃(^{DIPP}CCC)]Cl₂ with FeCl₂ and Li(N(SiMe₃)₂) (1.1equiv) in THF generates the zwitterionic complex, H₂(^{DIPP}CCC)Fe(II)Cl₃, in quantitative yields (Scheme 2.8).²⁵



Scheme 2.8. Synthesis of $(\text{DIPPCCC})\text{Fe}(\text{II})$ complexes.

This compound displays a broadened, paramagnetic ^1H NMR spectrum. The solution magnetic moment of $\text{H}_2(\text{DIPPCCC})\text{Fe}(\text{II})\text{Cl}_3$, as determined by Evans' method, was found to be $5.73(5) \mu_{\text{B}}$, which is at the high end of the calculated spin-orbit coupled magnetic moment of high spin $S=2$ tetrahedral $\text{Fe}(\text{II})$ complexes which typically range from 5.1 - $5.7 \mu_{\text{B}}$.^{26,27} In order to gain a better understanding of the bonding in this complex X-ray quality crystals of $\text{H}_2(\text{DIPPCCC})\text{Fe}(\text{II})\text{Cl}_3$ were grown from DCM and hexanes at -35°C . The iron center is coordinated to a single carbene ligand and three chlorides bound in a tetrahedral fashion. The other NHC remains protonated and is charge balanced by the extra chloride ligand on the iron center giving a zwitterionic complex (Figure 2.4).²⁵

$\text{H}_2(\text{DIPPCCC})\text{Fe}(\text{II})\text{Cl}_3$ can be treated with an excess of reductant (KC_8 , 3.5equiv) to generate an Fe^0 *in situ* in the presence of two equivalents of trimethylphosphine (PMe_3) giving $(\text{DIPPCCC})\text{Fe}(\text{II})\text{H}(\text{PMe}_3)(\text{N}_2)$ in quantitative yield (Scheme 2.8). Characterization of $(\text{DIPPCCC})\text{Fe}(\text{II})\text{H}(\text{PMe}_3)(\text{N}_2)$ by ^1H NMR spectroscopy reveals a C_s symmetric spectrum with a doublet at -9.67 ppm assigned to the $\text{Fe}-\text{H}$ ($J_{\text{P-H}} = 13$ Hz) (Figure 2.5). Given the low coupling constant of under 20 Hz, we tentatively assigned the phosphine ligand as *cis* to the hydride. Typical coupling constants are much higher in magnitude for *trans* $\text{P}-\text{H}$ ($J_{\text{P-H}(\text{trans})} = 90$ - 150 Hz) while *cis*

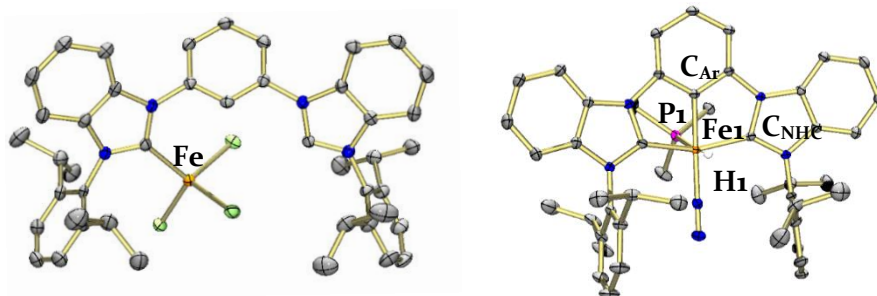


Figure 2.4. Molecular structures of $\text{H}_2(\text{DIPPCCC})\text{Fe}(\text{II})\text{Cl}_3$ (left) and $(\text{DIPPCCC})\text{Fe}(\text{II})\text{H}(\text{PMe}_3)(\text{N}_2)$ (right) shown with 50% probability ellipsoids. Solvent molecules and selected hydrogen atoms have been omitted for clarity.

P–H coupling is lower ($J_{\text{P-H}(\text{trans})} = 15\text{-}30$ Hz).^{29,30} However, X-ray crystallography reveals a slightly distorted octahedral geometry with the PMe_3 trans to the hydride ligand while a bound N_2 occupies the position trans to the C_{Ar} carbon (Figure 2.4). Some Fe systems in the literature see a reversal wherein $J_{\text{P-H}(\text{cis})} > J_{\text{P-H}(\text{trans})}$ which appears to also be true for our system.²⁹ The Fe–H bond distance, 1.52(2) Å, is within the expected range for other Fe–H’s and the N–N bond distance is relatively un-activated at 1.1078(17) Å. Vibrational frequencies for the Fe–H and N_2 are observed by IR spectroscopy at 1724 and 2099 cm^{-1} , respectively. $(\text{DIPPCCC})\text{Fe}(\text{II})\text{H}(\text{PMe}_3)(\text{N}_2)$ represents a rare example of an Fe monoanionic bis(*N*-heterocyclic carbene) pincer complex with the ligand bound in a tridentate fashion. The only other example, by Meyer and co-workers, features two tetradentate ligands, amide functionalized bis(imidazolium) salts, coordinated in a tridentate (NCC) fashion to one iron center.³¹

Accessing a zwitterionic intermediate for metalation has not been previously reported for monoanionic bis(carbene) pincer complexes, despite the generation of the singly coordinated NHC complexes with rhodium and iridium. However, these noble metal systems feature a ratio of two metal centers to one ligand.³²⁻³³ With this new metalation method in hand, which quantitatively generates both $\text{H}_2(\text{DIPPCCC})\text{Fe}(\text{II})\text{Cl}_3$ and $(\text{DIPPCCC})\text{Fe}(\text{II})\text{H}(\text{PMe}_3)(\text{N}_2)$, the synthesis and characterization of a family of iron complexes has been accomplished.

Following the synthetic protocol established with $(^{\text{DIPP}}\text{CCC})\text{Fe}(\text{II})\text{H}(\text{PMe}_3)(\text{N}_2)$ the addition of the less Lewis basic PPh_3 and pyridine (py) bound complexes was sought. Addition of two equivalents of PPh_3 or pyridine to the zwitterionic complex with reductant (KC_8 , 3.5 equiv) did not result in the desired complexes. Similarly, reduction in the absence of an L-type ligand did not result in the isolation of an Fe–H complex. Surprisingly, despite only one phosphine being bound to the iron center, the addition of a single equivalent of PMe_3 resulted in very little formation of the desired complex (<20%). Therefore, we hypothesize that metalation of the ligand requires an additional equivalent of PMe_3 to act as a Lewis base, possibly after coordination to the metal center. The lower basicity of PPh_3 (7.64 pKa) and pyridine (12.53 pKa) compared to PMe_3 (15.5 pKa) could result in no deprotonation and no subsequent formation of the Fe–H complexes.³⁴

The addition of a single equivalent of PPh_3 or pyridine in the presence of the strong Lewis base $\text{Li}(\text{N}(\text{SiMe}_3)_2)$ (26 pKa) to $\text{H}_2(^{\text{DIPP}}\text{CCC})\text{Fe}(\text{II})\text{Cl}_3$ resulted in formation of $(^{\text{DIPP}}\text{CCC})\text{Fe}(\text{II})\text{H}(\text{PPh}_3)(\text{N}_2)$ and $(^{\text{DIPP}}\text{CCC})\text{Fe}(\text{II})\text{H}(\text{py})(\text{N}_2)$ (Scheme 2.8). Both display similar ^1H NMR spectra to complex $(^{\text{DIPP}}\text{CCC})\text{Fe}(\text{II})\text{H}(\text{PMe}_3)(\text{N}_2)$ with the most noticeable difference being the Fe–H resonance, which shifts upfield from -9.67 ppm (PMe_3) to -11.11 ppm (PPh_3) and -18.70 ppm (py) (Figure 2.5, Table 2.1) Akin to $(^{\text{DIPP}}\text{CCC})\text{Fe}(\text{II})\text{H}(\text{PMe}_3)(\text{N}_2)$ the hydride resonance for $(^{\text{DIPP}}\text{CCC})\text{Fe}(\text{II})\text{H}(\text{PPh}_3)(\text{N}_2)$ is the expected doublet ($J_{\text{P-H}} = 22.5$ Hz) due to the coupling of the hydride and phosphine ligand. Both the phosphine iron hydrides have ATR-IR N_2 stretches at 2099 cm^{-1} , while the pyridine hydride features a red-shifted N_2 stretch at 2081 cm^{-1} . The ATR-IR spectra for $(^{\text{DIPP}}\text{CCC})\text{Fe}(\text{II})\text{H}(\text{PPh}_3)(\text{N}_2)$ and $(^{\text{DIPP}}\text{CCC})\text{Fe}(\text{II})\text{H}(\text{py})(\text{N}_2)$ include an Fe–H absorption at $\nu_{\text{Fe-H}} = 1791$ and 1794 cm^{-1} , respectively, which is blue-shifted from that of $(^{\text{DIPP}}\text{CCC})\text{Fe}(\text{II})\text{H}(\text{PMe}_3)(\text{N}_2)$ (1722 cm^{-1}) (Table 2.1). $(^{\text{DIPP}}\text{CCC})\text{Fe}(\text{II})\text{H}(\text{PMe}_3)(\text{N}_2)$ could also be synthesized in quantitative yield using PMe_3 (1equiv) and $\text{Li}(\text{N}(\text{SiMe}_3)_2)$ (1equiv) (Scheme 2.8).

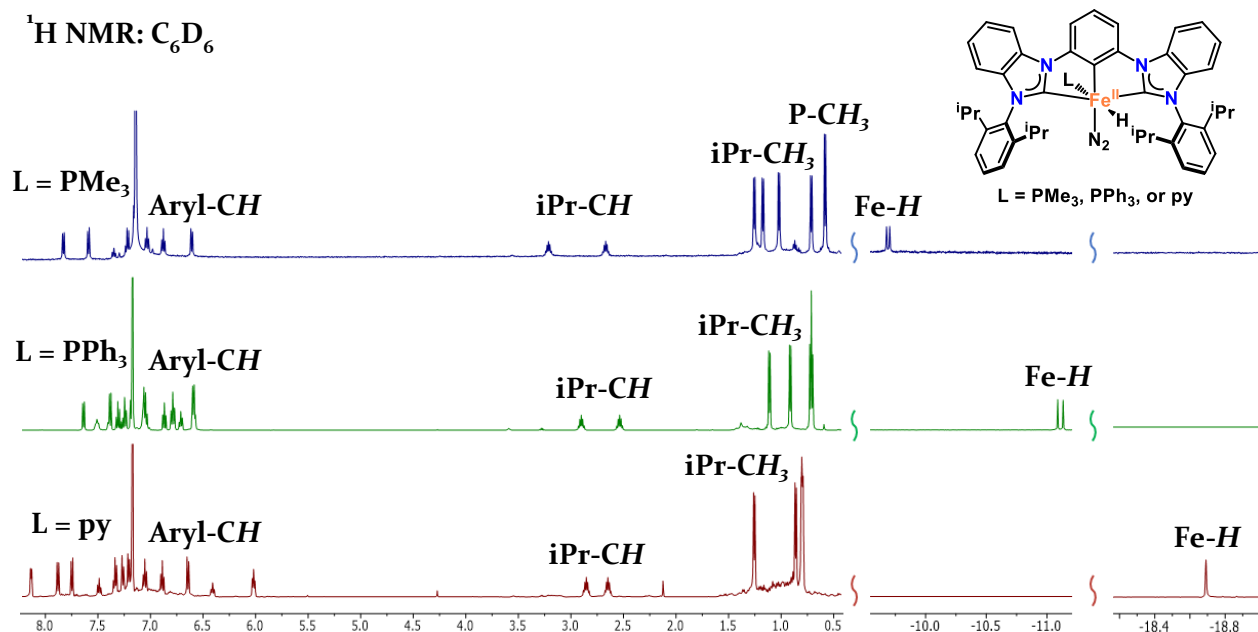
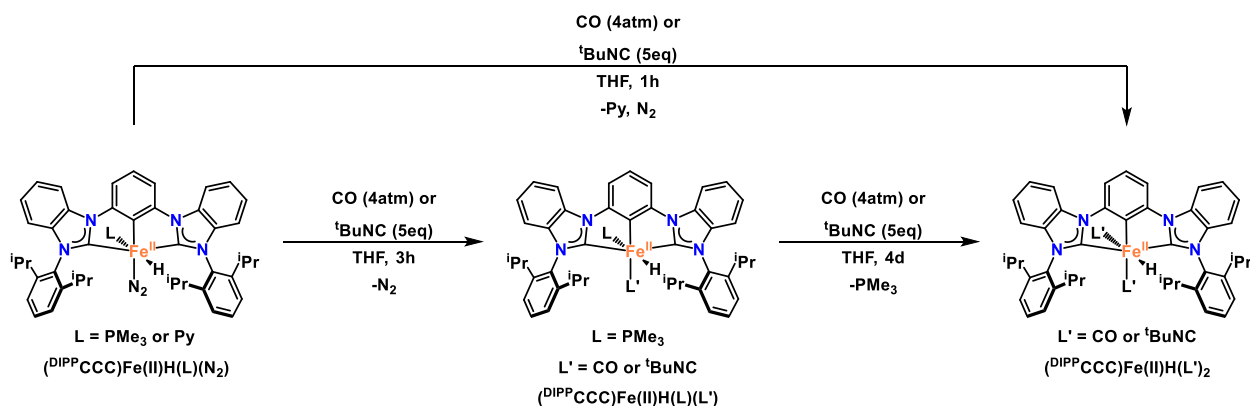


Figure 2.5. ^1H NMR spectra of $(^{\text{DIPP}}\text{CCC})\text{Fe}(\text{II})\text{H}(\text{L})(\text{N}_2)$ ($\text{L} = \text{PMe}_3, \text{PPh}_3, \text{py}$).

The shifts of the hydride resonances by ^1H NMR spectroscopy can be rationalized by looking at the trans-effect of the L-type ligand. Though only $(^{\text{DIPP}}\text{CCC})\text{Fe}(\text{II})\text{H}(\text{PMe}_3)(\text{N}_2)$ was characterized crystallographically it is likely that the other two complexes have similar orientations of the ligands, which is supported by the coupling constant for $(^{\text{DIPP}}\text{CCC})\text{Fe}(\text{II})\text{H}(\text{PPh}_3)(\text{N}_2)$ ($J_{\text{P-H}} = 22.5$ Hz). Interested in understanding the influence the σ -donating and π -accepting abilities of the trans L-type ligand has on the hydride resonance shift, we sought to directly compare these complexes. Although PPh_3 is a better π -acceptor than PMe_3 the steric constraints afforded by the PPh_3 cause an upfield shift of the hydride resonance when compared to the PMe_3 complex (-11.11 ppm vs -9.67 ppm, respectively). These effects were further validated when comparing these to the pyridine complex, as pyridine is an even poorer π -acceptor, the hydride resonance shifts even further upfield to -18.70 ppm.³⁵ This increase in hydridic character is also clearly evident in the greater thermal instability of the pyridine iron hydride which decomposes over a few days if stored at room temperature.



Scheme 2.9. Synthesis of $(^{\text{DIPP}}\text{CCC})\text{Fe(II)H(L)(L')}$ complexes.

Interested in probing the L-type ligand effects further excess CO and $^t\text{BuNC}$ were added to $(^{\text{DIPP}}\text{CCC})\text{Fe(II)H(PMe}_3)(\text{N}_2)$ (Scheme 2.9). After monitoring by ^1H NMR spectroscopy for several hours the kinetic products $(^{\text{DIPP}}\text{CCC})\text{Fe(II)H(PMe}_3)(\text{CO})$ and $(^{\text{DIPP}}\text{CCC})\text{Fe(II)H(PMe}_3)(^t\text{BuNC})$ were identified. The dinitrogen stretch in $(^{\text{DIPP}}\text{CCC})\text{Fe(II)H(PMe}_3)(\text{N}_2)$ disappears and the C–O stretch at 1948 cm^{-1} (free 2143 cm^{-1}) can be observed for $(^{\text{DIPP}}\text{CCC})\text{Fe(II)H(PMe}_3)(\text{CO})$. The N–C stretch of $(^{\text{DIPP}}\text{CCC})\text{Fe(II)H(PMe}_3)(^t\text{BuNC})$ appears at 2016 cm^{-1} (free 2138 cm^{-1}) (Table 2.1). The ^1H NMR spectrum for both complexes feature a slightly upfield shifted hydride doublet resonance at -10.96 ppm ($J_{\text{P-H}} = 4.5\text{ Hz}$) for $(^{\text{DIPP}}\text{CCC})\text{Fe(II)H(PMe}_3)(\text{CO})$ and -10.45 ppm ($J_{\text{P-H}} = 5\text{ Hz}$) for $(^{\text{DIPP}}\text{CCC})\text{Fe(II)H(PMe}_3)(^t\text{BuNC})$. The minimal change in the P–H coupling constants indicate no change in the phosphine-hydride conformation and ^{31}P NMR spectroscopy also confirms retention of the PMe_3 ligand. Reliance on coupling constants alone, however, is inconclusive since no cis phosphine-hydride complex has been isolated with this system.

Monitoring the reactions by ^1H NMR spectroscopy over four days results in the collapse of the Fe–H resonance from a doublet to a singlet, indicating the reaction has proceeded to the thermodynamic products $(^{\text{DIPP}}\text{CCC})\text{Fe(II)H}(\text{CO})_2$ and $(^{\text{DIPP}}\text{CCC})\text{Fe(II)H}(^t\text{BuNC})_2$ and the new Fe–H resonances shift downfield to -8.41 ppm and -8.87 ppm , respectively (Scheme 2.9). Analysis

by IR spectroscopy shows two C–O stretches at 1983 and 1927 cm^{-1} for $(^{\text{DIPP}}\text{CCC})\text{Fe}(\text{II})\text{H}(\text{CO})_2$ and two C–N stretches for $(^{\text{DIPP}}\text{CCC})\text{Fe}(\text{II})\text{H}(\text{}^t\text{BuNC})_2$ at 2047 and 2002 cm^{-1} which is consistent with the C_s symmetric ^1H NMR spectra. These new stretches are distinct from the previously characterized mixed ligand species (Table 2.1).

Alternatively, complexes $(^{\text{DIPP}}\text{CCC})\text{Fe}(\text{II})\text{H}(\text{CO})_2$ and $(^{\text{DIPP}}\text{CCC})\text{Fe}(\text{II})\text{H}(\text{}^t\text{BuNC})_2$ can be synthesized by displacing the pyridine and N_2 ligands in $(^{\text{DIPP}}\text{CCC})\text{Fe}(\text{II})\text{H}(\text{py})(\text{N}_2)$ with excess CO or ${}^t\text{BuNC}$ in THF (Scheme 2.9). This results in an immediate color change from purple to pale yellow with no observation of mixed ligand species when monitored by ^1H NMR spectroscopy. Loss of pyridine can be tracked by ^1H NMR spectroscopy and generation of the desired complexes was accomplished in increased yields.

Comparing each of the Fe–H complexes synthesized gives us information about the electronics both of our complexes and ligand framework. The metal center is electron rich due to the strongly σ -donating ligand framework which causes it to transfer electron density onto the other ligands when possible. This is reflected in the Fe–H ^1H NMR resonance shift when switching

Complex	IR $\nu_{\text{L/L'}}$ (cm^{-1})	IR $\nu_{\text{Fe-H}}$ (cm^{-1})	^1H NMR (Fe-H, ppm)	^{31}P NMR (ppm)	$J_{\text{P-H}}$ (Hz)
$(^{\text{DIPP}}\text{CCC})\text{Fe}(\text{II})\text{H}(\text{PMe}_3)(\text{N}_2)$	2099 (N_2)	1722	-9.67 (d)	11	13
$(^{\text{DIPP}}\text{CCC})\text{Fe}(\text{II})\text{H}(\text{PPh}_3)(\text{N}_2)$	2099 (N_2)	1791	-11.11 (d)	50	22.5
$(^{\text{DIPP}}\text{CCC})\text{Fe}(\text{II})\text{H}(\text{py})(\text{N}_2)$	2081 (N_2)	1794	-18.70 (s)	-	-
$(^{\text{DIPP}}\text{CCC})\text{Fe}(\text{II})\text{H}(\text{PMe}_3)(\text{CO})$	1948	1723	-10.96 (d)	10.5	4.5
$(^{\text{DIPP}}\text{CCC})\text{Fe}(\text{II})\text{H}(\text{PMe}_3)(\text{}^t\text{BuNC})$	2016	1723	-10.45 (d)	14.9	5
$(^{\text{DIPP}}\text{CCC})\text{Fe}(\text{II})\text{H}(\text{CO})_2$	1983, 1927	1724	-8.41 (s)	-	-
$(^{\text{DIPP}}\text{CCC})\text{Fe}(\text{II})\text{H}(\text{}^t\text{BuNC})_2$	2047, 2002	1723	-8.87 (s)	-	-

Table 2.1. Characterization of $(^{\text{DIPP}}\text{CCC})\text{Fe}(\text{II})\text{H}(\text{L})(\text{L}')$ species.

to different L-type ligands. The overall trend observed is that the more π -accepting L-type ligands cause a downfield shift in the hydride resonance due to their ability to receive π -back-donation from the metal center (i.e. $\text{CO} > {}^t\text{BuNC} > \text{PR}_3 > \text{py}$).³⁵ $(^{\text{DIPP}}\text{CCC})\text{Fe}(\text{II})\text{H}(\text{py})(\text{N}_2)$ has the farthest upfield hydride resonance due to pyridine's lack of available p-orbital for π -back-donation (Figure 2.6, Table 2.1).

However, the kinetic products $(^{\text{DIPP}}\text{CCC})\text{Fe}(\text{II})\text{H}(\text{PMe}_3)(\text{CO})$ and $(^{\text{DIPP}}\text{CCC})\text{Fe}(\text{II})\text{H}(\text{PMe}_3)({}^t\text{BuNC})$ first experience an upfield shift of the Fe–H resonance from $(^{\text{DIPP}}\text{CCC})\text{Fe}(\text{II})\text{H}(\text{PMe}_3)(\text{N}_2)$ in their ${}^1\text{H}$ NMR spectra which is counterintuitive. Switching from a non- σ -donating L-type ligand (N_2) to one that is a stronger σ -donor (CO or ${}^t\text{BuNC}$), though still a good π -acceptor, results in this slightly upfield shift of the Fe–H resonance. Essentially, the σ -donation effect outweighs the ligand's π -accepting abilities. However, replacement of PMe_3 in $(^{\text{DIPP}}\text{CCC})\text{Fe}(\text{II})\text{H}(\text{PMe}_3)(\text{CO})$ and $(^{\text{DIPP}}\text{CCC})\text{Fe}(\text{II})\text{H}(\text{PMe}_3)({}^t\text{BuNC})$ with the second equivalent of CO or ${}^t\text{BuNC}$, respectively, places these ligands trans to the hydride resulting in a much larger effect on the hydridic ${}^1\text{H}$ NMR resonance. Both are stronger π -acceptors than PMe_3 so back-donation from the metal center to the ligand results in a downfield shift of the hydride resonance in the ${}^1\text{H}$ NMR spectrum (Figure 2.6).

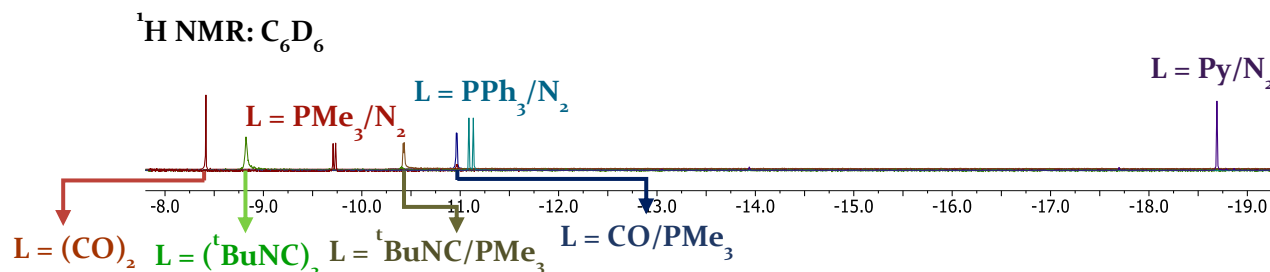


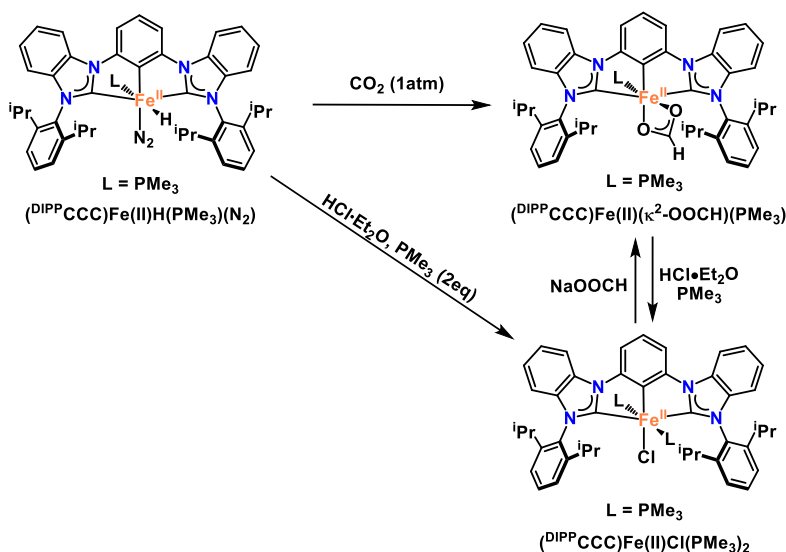
Figure 2.6. ${}^1\text{H}$ NMR spectra of $(^{\text{DIPP}}\text{CCC})\text{Fe}(\text{II})\text{H}(\text{L})(\text{L}')$.

Similarities can be drawn when comparing the hydride shifts and phosphorus coupling constants to the pincer system by Guan and co-workers, (POCOP)Fe(II)H(PMe₃)₂.²⁸ In Guan's system substitution of one PMe₃ ligand by CO first occurs trans to the hydride with a subsequent downfield shift of the hydride resonance from -14.87 ppm to -9.58 ppm in the ¹H NMR spectrum ($J_{P-H} = 52.0$ Hz). Heating (POCOP)Fe(II)H(PMe₃)(CO) to 80 °C for 12 h in toluene resulted in an upfield shift of the hydride resonance to -12.66 ppm ($J_{P-H} = 28.8$ Hz). The change in the coupling constant is consistent with ligand rearrangement where the hydride and PMe₃ are now trans to one another with the CO cis. This clearly shows that the placement of the CO ligand has a distinct effect upon the hydride-phosphorus coupling constant as well as the cis P–H coupling constant being larger than the trans. The movement of the hydride resonances in Guan's system is similar to what is observed for CO substitution in our system. However, unlike in Guan's system the possibility of ligand rearrangement in (DIPPCCC)Fe(II)H(PMe₃)(CO) and (DIPPCCC)Fe(II)H(PMe₃)(^tBuNC) was discounted due to several reasons; 1) the J_{P-H} coupling constants did not change significantly throughout the course of the reaction; 2) a significant downfield shift of the Fe-H resonance in the ¹H NMR spectrum was not observed due to the binding of the new strong π -acceptor ligand trans to the hydride; and 3) no other intermediates were observed by ¹H NMR during the conversion of the mixed ligand complexes to the final products. Finally, in both systems, additional CO generates the bis(carbonyl) iron hydride complex with a subsequent downfield shift of the hydride resonance.²⁸

Comparing the ¹³C NMR resonances of the *N*-heterocyclic carbene carbon, C_{NHC}, and aryl carbon, C_{Ar}, also shows the same electronic effects based on the L-type ligand with the latter exhibiting the most drastic change. The C_{NHC} resonances are 230.10 ppm (PPh₃), 229.28 ppm (py), 228.03 ppm (^tBuNC), and 220.05 ppm (CO). The lower solubility of (DIPPCCC)Fe(II)H(PMe₃)(N₂)

in benzene prohibited assignment of the C_{NHC} resonance. The C_{Ar} resonances follow the exact same trend as the Fe–H resonances in the ^1H NMR spectra; 191.93 ppm (py), 185.70 ppm (PMe_3), 183.01 ppm (PPh_3), 175.35 ppm ($^t\text{BuNC}$), and 174.75 ppm (CO). Here it can be seen that the addition of a second L-type ligand in the position trans to C_{Ar} results in a much more upfield shift for both $(^{\text{DIPP}}\text{CCC})\text{Fe}(\text{II})\text{H}(\text{CO})_2$ and $(^{\text{DIPP}}\text{CCC})\text{Fe}(\text{II})\text{H}(^t\text{BuNC})_2$. Both the latter complexes also exhibit two separate resonances in their ^{13}C NMR spectra for the carbon bound to the Fe center (CO and $^t\text{BuNC}$) which is consistent with complexes exhibiting C_s symmetry.

With these hydrides in hand their reactivity with CO_2 was investigated. The addition of 1 atm of $\text{CO}_2(\text{g})$ to $(^{\text{DIPP}}\text{CCC})\text{Fe}(\text{II})\text{H}(\text{PMe}_3)(\text{N}_2)$ led to insertion of the CO_2 into the Fe–H bond resulting in formation of a formate product, $(^{\text{DIPP}}\text{CCC})\text{Fe}(\text{II})(\kappa^2\text{-OOCH})(\text{PMe}_3)$, (Scheme 2.10). This was evident by the loss of the hydridic resonance in the ^1H NMR spectrum and the growth of a resonance at 6.02 ppm of the formate proton (Figure 2.7). Analysis by IR spectroscopy shows the loss of both the Fe–H and N_2 absorbances from $(^{\text{DIPP}}\text{CCC})\text{Fe}(\text{II})\text{H}(\text{PMe}_3)(\text{N}_2)$ and a new C–H stretch at 2815 cm^{-1} consistent with a bound formate fragment. Investigation of the ^{31}P NMR



Scheme 2.10. Reactivity of $(^{\text{DIPP}}\text{CCC})\text{Fe}(\text{II})\text{H}(\text{PMe}_3)(\text{N}_2)$.

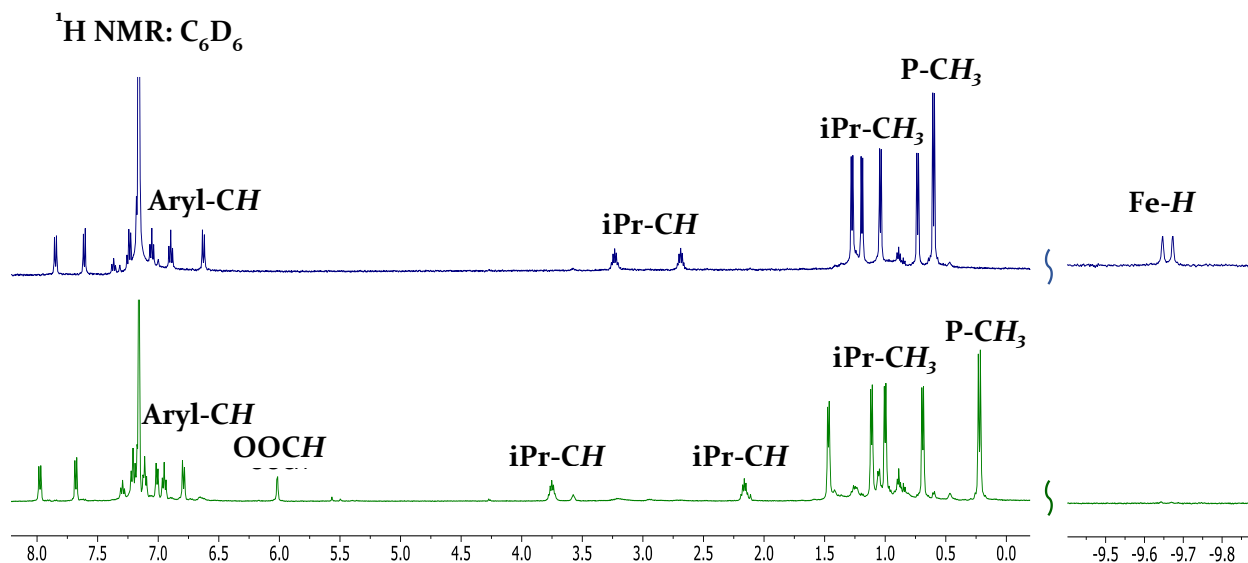


Figure 2.7. ^1H NMR spectrum of $(^{\text{DIPPCCC}}\text{Fe}(\text{II})\text{H}(\text{PMe}_3)(\text{N}_2))$ (top) and $(^{\text{DIPPCCC}}\text{Fe}(\text{II})(\kappa^2\text{-OOCH})(\text{PMe}_3))$ (bottom).

spectrum indicates retention of the PMe_3 ligand with a resonance at 42 ppm ($(^{\text{DIPPCCC}}\text{Fe}(\text{II})\text{H}(\text{PMe}_3)(\text{N}_2)) = 11$ ppm) and integration of the ^1H NMR indicates a single PMe_3 ligand and no additional solvent molecules bound to the Fe center. This indicates either a five-coordinate iron center or multi-atom bonded formate to obtain a diamagnetic ^1H NMR spectrum. The C–H IR absorbance falls within the region known for other $\text{M}-\kappa^2\text{-OOCH}$ complexes but $\text{M}-\kappa^1\text{-OOCH}$ complexes can also appear in this same region.^{36,37} Looking more closely at the fingerprint region, however, reveals a stretch at 1562 cm^{-1} . Comparing these stretches with other published Fe-formate complexes clearly indicates a $\kappa^2\text{-OOCH}$ binding mode. The clearest comparison by Jonas Peters shows $\text{Fe}(\text{II})(\kappa^1\text{-OOCH})$ ranges from $1644\text{-}1603\text{ cm}^{-1}$ while $\text{Fe}(\text{II})(\kappa^2\text{-OOCH})$ are slightly lower from $1585\text{-}1553\text{ cm}^{-1}$.³⁷ The most likely conformation of the product, therefore, is $(^{\text{DIPPCCC}}\text{Fe}(\text{II})(\kappa^2\text{-OOCH})(\text{PMe}_3))$. Efforts to crystallographically characterize this new formate species were unsuccessful and therefore independent synthesis was investigated.

The addition of $\text{HCl}\cdot\text{Et}_2\text{O}$ (1 equiv.) and PMe_3 (2 equiv.) to $(^{\text{DIPPCCC}}\text{Fe}(\text{II})\text{H}(\text{PMe}_3)(\text{N}_2))$ furnishes H_2 and $(^{\text{DIPPCCC}}\text{Fe}(\text{II})\text{Cl}(\text{PMe}_3)_2)$ in good yield (90%) (Scheme 2.10). Addition of

HCl•Et₂O without the extra L-type ligand led only to a mixture of unidentified products. The second equivalent of PMe₃ allows for the capture of any unreacted HCl•Et₂O which helps avoid complex decomposition. Single crystal X-ray diffraction of the complex, (DIPPCCC)Fe(II)Cl(PMe₃)₂, shows an octahedral geometry around the iron center with the chloride ligand bound trans to the C_{Ar} and two axial PMe₃ ligands (Figure 2.8). The ¹H NMR spectrum reveals a C_s symmetric complex and a single ³¹P NMR resonance at 22.90 ppm confirms this assignment. The ¹³C NMR C_{NHC} resonance appears at 225.91 ppm while the C_{Ar} resonance appears at 189.69 ppm. The use of non-coordinating acids to generate different Fe(II)–X complexes led to the generation of multiple inseparable products, possibly due to ligand rearrangements.

Treating (DIPPCCC)Fe(II)Cl(PMe₃)₂ with excess sodium formate led to the isolation of the same (DIPPCCC)Fe(II)(κ²-OOCH)(PMe₃) complex characterized above including loss of the second PMe₃ ligand as evident by integration of the ¹H NMR spectrum (Scheme 2.10). This loss of the second PMe₃ ligand supports the assignment of the formate being κ²-OOCH. It was previously shown that even using a strongly binding L-type ligand like CO took four days to replace PMe₃, therefore only a strong binding interaction, like κ²-OOCH, is likely to cause it to be displaced. Additionally, treating (DIPPCCC)Fe(II)(κ²-OOCH)(PMe₃) with one equivalent of HCl•Et₂O and PMe₃ led to re-isolation of (DIPPCCC)Fe(II)Cl(PMe₃)₂ (Scheme 2.10).

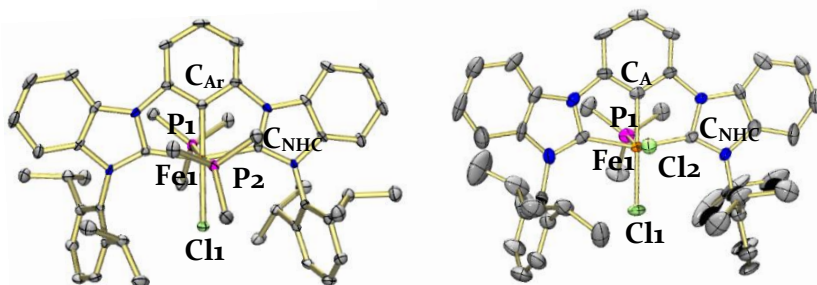
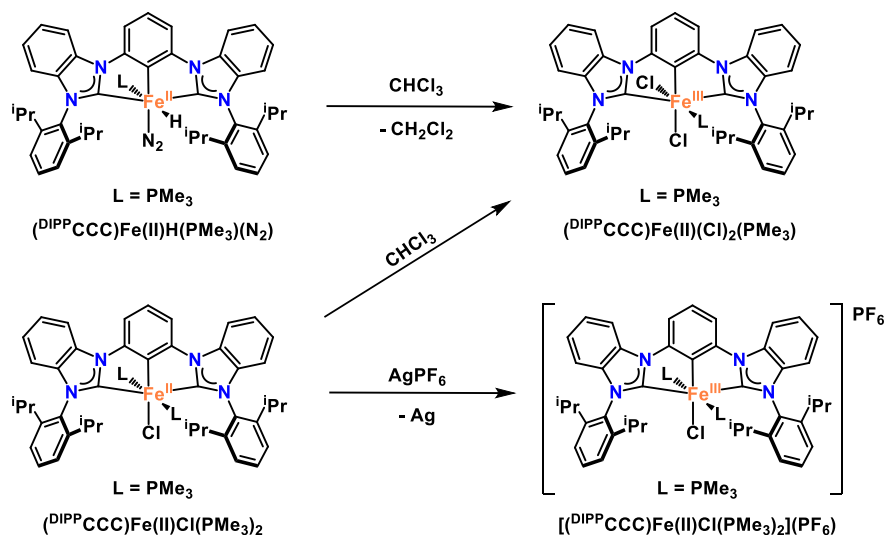


Figure 2.8. Molecular structures of (DIPPCCC)Fe(II)Cl(PMe₃)₂ (left) and (DIPPCCC)Fe(III)(Cl)₂(PMe₃) (right) shown with 50% and 30% probability ellipsoids, respectively. Solvent molecules and selected hydrogen atoms have been omitted for clarity.

The addition of CO₂ to (^{DIPP}CCC)Fe(II)H(py)(N₂) led to the isolation of a complex with a paramagnetic ¹H NMR spectrum instead of a diamagnetic species like (^{DIPP}CCC)Fe(II)(κ²-OOCH)(PMe₃). Both the Fe–H and N₂ stretches were lost as seen by IR spectroscopy. This complex could not be characterized crystallographically but the addition of PMe₃ gave the same (^{DIPP}CCC)Fe(II)(κ²-OOCH)(PMe₃) complex that was previously characterized. The addition of CO₂ to (^{DIPP}CCC)Fe(II)H(CO)₂ and (^{DIPP}CCC)Fe(II)H(^tBuNC)₂ showed no reaction, likely due to having two very strong binding L-type ligands giving more stable complexes. Unfortunately, (^{DIPP}CCC)Fe(II)(κ²-OOCH)(PMe₃) could not be further hydrogenated and was only released from the Fe center when a very strong acid, like HCl, was used. We hypothesize that the paramagnetic complex generated after adding CO₂ to (^{DIPP}CCC)Fe(II)H(py)(N₂) is still an Fe(II) species and the paramagnetic character is due to geometry rather than direct chemical oxidation to Fe(III). However, we were interested in determining whether other paramagnetic and/or higher oxidation states of iron could be supported by this ligand framework.

Treatment of either (^{DIPP}CCC)Fe(II)H(PMe₃)(N₂) or (^{DIPP}CCC)Fe(II)Cl(PMe₃)₂ with CHCl₃ yields (^{DIPP}CCC)Fe(III)Cl₂(PMe₃) (90%) with concomitant formation of CH₂Cl₂ as observed by ¹H NMR spectroscopy (Scheme 2.11). This compound exhibits a paramagnetic ¹H NMR spectrum with resonances ranging from 100 to -20 ppm. Analysis by X-ray crystallography depicts a slightly distorted octahedral Fe center with cis chloride ligands, 2.362(3) (axial) vs 2.264(3) Å (equatorial) (Figure 2.8). The use of the one-electron oxidant tritylchloride (ClCPh₃) led to partial conversion of (^{DIPP}CCC)Fe(II)Cl(PMe₃)₂ but was unable to generate the Fe(III) complex cleanly. The method of chloride abstraction from CHCl₃ is unknown. Alternatively, [(^{DIPP}CCC)Fe(III)Cl(PMe₃)₂](PF₆) could be generated upon the addition of AgPF₆ to (^{DIPP}CCC)Fe(II)Cl(PMe₃)₂ in DCM (Scheme 2.11). This complex also had a paramagnetic ¹H

NMR spectrum but was a much cleaner reaction and retained a single ^{31}P NMR signal at 26 ppm indicating retention of a C_s symmetric complex.



Scheme 2.11. Synthesis of $(^{\text{DIPP}}\text{CCC})\text{Fe}(\text{III})$ complexes.

Overall, we were able to isolate and characterize a variety of Fe(II) hydride complexes as well as investigate their reactivity using CO_2 . The independent synthesis of $(^{\text{DIPP}}\text{CCC})\text{Fe}(\text{II})(\kappa^2\text{-OOCH})(\text{PMe}_3)$ from $(^{\text{DIPP}}\text{CCC})\text{Fe}(\text{II})\text{Cl}(\text{PMe}_3)_2$ was accomplished and the catalytic hydrogenation of the formate fragment attempted. These complexes were not found to be a competent system for catalytic CO_2 hydrogenation. Further oxidation of the Fe center was carried out using chloroform and AgPF_6 to give two paramagnetic Fe(III) complexes.

2.4 Experimental Section

General Considerations. All air- and moisture-sensitive manipulations were performed using an MBraun inert atmosphere drybox with an atmosphere of nitrogen. The MBraun drybox was equipped with one -35°C freezer for cooling samples and crystallizations. Solvents for sensitive manipulations were dried and deoxygenated on a Glass Contour System (SG Water USA, Nashua, NH) and stored over 4 \AA molecular sieves purchased from Strem following literature procedure

prior to use.³⁸ Iron (II) chloride anhydrous (98%) was purchased from Strem and used as received. Trimethylphosphine (1.0 M in THF), tert-butylnocyanide (98%), hydrochloric acid (2.0 M in Et₂O), and pyridine (99.8%) were purchased from Sigma-Aldrich and used as received. Triphenylphosphine ($\geq 95\%$ (GC)) was purchased from Sigma-Aldrich and recrystallized using ethanol and dried before use. Lithium hexamethyldisilazide was purchased from Sigma-Aldrich and recrystallized under an inert atmosphere using toluene prior to use. Carbon monoxide (99.5%) and carbon dioxide (99.8%) was purchased from Specialty Gases of America and used as received. Iron (0) tetrakis(trimethylphosphine),²⁸ potassium graphite,³⁹ 1-(tert-butyl)-1H-benzo[d]imidazole,⁴⁰ and ^{DIPP}CCC (^{DIPP}CCC = bis(diisopropylphenyl-imidazol-2-ylidene)phenyl) ligand² were prepared according to literature procedures. Chloroform-*d*, and benzene-*d*₆ were purchased from Cambridge Isotope Labs and were degassed and stored over 4 Å molecular sieves prior to use. Celite® 545 (J. T. Baker) was dried in a Schlenk flask for 24 h under dynamic vacuum while heating to at least 150 °C prior to use in a glovebox.

¹H, ¹³C, and ³¹P NMR spectra were recorded on a Varian spectrometer operating at 500 MHz (¹H NMR), 126 MHz (¹³C NMR), and 202.4 MHz (³¹P NMR) at ambient temperature. All chemical shifts were reported relative to the peak of the residual solvent as a standard. Solid-state infrared spectra were recorded using a Perkin-Elmer Frontier FT-IR spectrophotometer equipped with a KRS5 Thallium Bromide/Iodide Universal Attenuated Total Reflectance accessory. Elemental analysis was performed by the University of Illinois at Urbana Champaign School of Chemical Sciences Microanalysis Laboratory in Urbana, IL.

Modified Preparation of 1,3-Bis(N-benzimidazolyl)benzene. Benzimidazole (7.0 g, 60 mmol), CuO (0.62 g, 8 mmol), and K₂CO₃ (8.2 g, 60 mmol) were combined in a 500 mL flask and dissolved in DMSO (30 mL). A reflux condenser was added to the flask and the entire system

flushed with N₂. 1,3-dibromobenzene (3.0 mL, 24 mmol) was syringed into the flask and the reaction heated to 150 °C for 48 hours. The reaction was then cooled to room temperature and diluted with DCM (300 mL). The reaction mixture was then filtered through basic alumina. Instead of concentrating the reaction mixture which requires pumping off DMSO, an aqueous/organic work-up was instead done with DCM and water. The DCM layers were then concentrated under reduced pressure to yield a pale yellow solid. This solid was washed with cold EtOAc to remove the yellow colored impurities yielding a pale-yellow solid in good yield (6.86 g, 92%). ¹H NMR (DMSO-d₆, 500 MHz): δ = 8.73 (s, 2H), 8.07 (s, 1H), 7.94 (m, 7H), 7.36 (p, J = 8.7 Hz, 4H). The ¹H NMR is in accordance with previously published literature values.³

Modified Preparation of 1,3-Bis(1'-methyl-3'-benzimidazolyl)benzene diiodide

[H₃(^{Me}CCC)]I₂. 1,3-bis(*N*-benzimidazolyl)benzene (0.7 g, 2.24 mmol) was dissolved in DMF (20 mL) and CH₃I (1.39 mL, 22.4 mmol) was added dropwise. The reaction was sealed and stirred at 40 °C for 24 hours. A white precipitate began forming within several hours. The precipitate was collected and rinsed with Et₂O and DCM. More precipitate was formed in the washes and recollected as well. The resulting white solid was dried yielding quantitative conversion to the desired benzimidazolium salt of the ligand. ¹H NMR (DMSO-d₆, 500 MHz): δ = 10.30 (s, 2H), 8.39 (s, 1H), 8.21 (d, J = 8.3 Hz, 2H), 8.21 (d, J = 8.3 Hz, 2H), 8.17 (b, 3H), 8.06 (d, J = 8.3 Hz, 2H), 7.80 (dt, J = 28.7 Hz, 8 Hz, 4H), 4.23, (s, 6H). The ¹H NMR is in accordance with previously published literature values.³

Preparation of 2-bromo-1,3-bis(bromomethyl)benzene. 2-bromo-1,3-dimethylbenzene (3.17 mL, 23.8 mmol), benzylperoxide (36.33 mg, 0.15 mmol), and NBS (8.85 g, 49.7 mmol) were added to a 250 mL round bottom flask and dissolved in CHCl₃ (150 mL). The reaction was refluxed for 12 hours and monitored by GC for completion. The reaction was then cooled to room

temperature and extra NBS precipitated and was filtered off. The reaction mixture was quenched with Na₂S₂O₃ (10% wt soln, 2x30 mL) going from a dark red color to yellow. The solvent was then removed under reduced pressure giving a yellow oil that solidified overnight. The product was recrystallized from hexanes to give a white solid as the product (yield). ¹H NMR (CDCl₃, 500 MHz): δ = 7.42 (d, J = 9.4 Hz, 2H), 7.29 (dt, J = 10 Hz, 8.9 Hz, 1H), 4.65 (s, 4H). The ¹H NMR is in accordance with previously published literature values.^{5,41}

Preparation of 1-benzyl-1H-benzo[d]imidazole. Benzimidazole (0.25 g, 2.1 mmol), benzyl bromide (0.25 mL, 2.1 mmol) and Na₂CO₃ (0.67 g, 6.3 mmol) were added to a bomb and dissolved in toluene (10 mL). The reaction was then sealed and heated at 135 °C for 12 hours. The resulting reaction mixture was filtered over celite to remove excess Na₂CO₃ and the filtrate concentrated under reduced pressure to give a yellow solid. The solid was recrystallized in DCM giving a slightly off-white solid as the product (0.36g, 82%). ¹H NMR (CDCl₃, 500 MHz): δ = 7.93 (s, 1H), 7.81 (d, J = 9 Hz, 1H), 7.27 (m, 6H), 7.16 (d, J = 8.5 Hz, 2H), 5.35 (s, 2H). The ¹H NMR is in accordance with previously published literature values.⁴²

Preparation of 1,1'-((2-bromo-1,3-phenylene)bis(methylene))bis(3-benzyl-1H-benzo[d]imidazole-3-ium) dibromide [H₂(^{Bz}CcC^{Br}cC)]Br₂. 1-benzyl-1H-benzo[d]imidazole (1.02 g, 4.9 mmol) and 2-bromo-1,3-bis(bromomethyl)benzene (0.84 g, 2.45 mmol) were added to a bomb, dissolved in toluene (20 mL), and heated to 135 °C for 12 hours. The solid that precipitated out of the solution was collected by filtration and washed with Et₂O and THF to remove any leftover starting materials. The resulting white solid was dried giving the product in excellent yield (1.6 g, 86%). ¹H NMR (CDCl₃, 500 MHz): δ = 11.29 (s, 2H), 8.09 (d, J = 10.4, 2H), 7.70 (d, J = 9.6, 2H), 7.62 (t, J = 9.5 Hz, 2H), 7.54 (m, 5H), 7.44 (m, 6H), 7.30 (m, 6H), 6.04 (s, 4H), 5.91 (s, 4H). The ¹H NMR matches the previously published ligand.^{4,5}

Preparation of 1,1'-((1,3-phenylene)bis(methylene))bis(3-benzyl-1H-benzo[d]imidazole-3-ium) dibromide [H₃^{(Bz)CcCcC}]Br₂. 1-benzyl-1H-benzo[d]imidazole (1.02 g, 4.9 mmol) and 1,3-bis(bromomethyl)benzene (0.64 g, 2.45 mmol) were added to a bomb, dissolved in toluene (20 mL), and heated to 135 °C for 12 hours. The solid that precipitated out of the solution was collected by filtration and washed with Et₂O and THF to remove any leftover starting materials. The resulting white solid was dried giving the product in excellent yield (1.5 g, 90%). ¹H NMR (CDCl₃, 500 MHz): δ = 11.84 (s, 2H), 8.22 (s, 1H), 7.67 (m, 2H), 7.47 (m, 9H), 7.32 (m, 6H), 7.22 (m, 6H), 5.79 (s, 4H), 5.24 (s, 4H). The ¹H NMR exhibits similar resonances to other alkyl substituted ligands of this type that have been previously published.^{4,5}

Preparation of 1-(tert-butyl)-1H-benzo[d]imidazole. The product was isolated as a yellow liquid according to literature procedures (1.93 g, 50%). ¹H NMR (CDCl₃, 500 MHz): δ = 8.02 (s, 1H), 7.81 (m, 1H), 7.64 (m, 1H), 7.26 (m, 2H), 1.76 (s, 9H).⁴⁰

Preparation of 1,1'-((2-bromo-1,3-phenylene)bis(methylene))bis(3-tert-butyl-1H-benzo[d]imidazole-3-ium) dibromide [H₂^{(tBu)CcC^{Br}cC}]Br₂. 1-(tert-butyl)-1H-benzo[d]imidazole (1.40 g, 8.0 mmol) and 2-bromo-1,3-bis(bromomethyl)benzene (1.37 g, 4.0 mmol) were added to a bomb and dissolved in toluene (40 mL). The bomb was sealed and heated to 135 °C for 48 hours. The product was collected as a white solid (2.62 g, 95%) that precipitated from the reaction mixture and was washed with Et₂O and THF. ¹H NMR (CDCl₃, 500 MHz): δ = 11.47 (s, 2H), 7.93 (m, 2H), 7.59 (m, 6H), 7.47 (d, J = 9.5, 2H), 7.31 (t, J = 8.1 Hz, 1H), 6.35 (s, 4H), 1.99 (s, 18H). The ¹H NMR matches the previously published ligand.⁶

Preparation of 1,1'-((1,3-phenylene)bis(methylene))bis(3-tert-butyl-1H-benzo[d]imidazole-3-ium) dibromide [H₃^{(tBu)CcCcC}]Br₂. 1-(tert-butyl)-1H-benzo[d]imidazole (0.11 g, 0.65 mmol) and 1,3-bis(bromomethyl)benzene (0.086 g, 0.33 mmol) were added to a bomb and dissolved in

toluene (20 mL). The bomb was sealed and heated to 135 °C for 48 hours. The product was collected as a white solid (0.20 g, 98%) that precipitated from the reaction mixture and was washed with Et₂O and THF. ¹H NMR (CDCl₃, 500 MHz): δ = 11.46 (s, 2H), 8.40 (b, 1H), 7.88 (m, 2H), 7.83 (m, 2H), 7.57 (m, 6H), 7.37 (t, J = 9.7 Hz, 1H), 6.04 (s, 4H), 2.00 (s, 18H). ¹³C NMR (CDCl₃, 126 MHz): δ = 141.61, 134.56, 132.57, 130.49, 130.25, 129.86, 129.56, 127.18, 126.68, 116.03, 114.47, 62.33, 50.49, 29.73. The ¹H NMR exhibits similar resonances to other alkyl substituted ligands of this type that have been previously published.⁶

General Preparation of Free Carbenes. A 20 mL scintillation vial was charged with [(^RCcC^RcC)]Br₂ and benzene:THF in a 3:1 mixture. Li(N(SiMe₃)₂) (2.1equiv) was dissolved in minimal THF and added dropwise to the ligand. The reaction was stirred at room temperature for 1hr during which a gradual color change took place to pale yellow. The reaction was filtered over celite and the volatiles removed under reduced pressure giving the free carbene as a pale-yellow precipitate in quantitative yield. The free carbenes were stable as solids stored at -35 °C for several days but lasted only a few hours in coordinating solvents.

Preparation of (^{Bz}CcC^{Br}cC). ¹H NMR (C₆D₆, 500 MHz): δ = 7.40 (d, J = 7.7 Hz, 2H), 7.36 (d, J = 7.6 Hz, 2H), 7.23 (d, J = 7.6 Hz, 4H), 7.12 (d, J = 7.6 Hz, 4H), 7.06 (t, J = 7.2 Hz, 4H), 7.65 (m, 5H), 6.29 (d, J = 7.6 Hz, 2H), 6.19 (m, 2H), 4.31 (d, J = 16.9 Hz, 1H), 3.96 (d, J = 15.9 Hz, 1H), 3.86 (m, 1H), 3.74 (d, J = 16 Hz, 1H).

Preparation of (^{tBu}CcC^{Br}cC). ¹H NMR (C₆D₆, 500 MHz): δ = 7.24 (d, J = 6.5 Hz, 2H), 7.06 (d, J = 7.3 Hz, 2H), 7.02 (d, J = 7.6 Hz, 2H), 6.89 (b, 5H), 5.92 (b, 4H), 1.72 (s, 18H).

Preparation of H^{(tBu)CcCcC}. ¹H NMR (C₆D₆, 500 MHz): δ = 8.75 (b, 1H), 7.21 (d, J = 7.9 Hz, 2H), 7.03 (d, J = 7.7 Hz, 2H), 7.00 (d, J = 7.5 Hz, 2H), 6.91 (m, 4H), 6.84 (t, J = 7.6 Hz, 1H), 5.74 (s, 4H) 1.70 (s, 18H).

Preparation of (BzCcCcC)Ni(II)Br. 1,1'-((2-bromo-1,3-phenylene)bis(methylene))bis(3-benzyl-1H-benzo[d]imidazole-3-ium) dibromide (50 mg, 0.066 mmol) and Li(N(SiMe₃)₂) (23.1 mg, 0.14 mmol) were dissolved in benzene (2 mL) and THF (2 mL) respectively and cooled to -35 °C. The base was then added to the frozen benzene solution and warmed to room temperature (~5 mins). Ni(COD)₂ (14.5 mg, 0.053 mmol) dissolved in THF was then added to the reaction dropwise. Ni was required to be the limiting reagent due to the difficulty of removing Ni(COD)₂ starting material from the resulting product. The reaction was then concentrated under reduced pressure and filtered over celite washing with hexanes and benzene. The benzene wash was concentrated to give a yellow solid as the product (20.9 mg, 0.032 mmol, 60% based on Ni). ¹H NMR (C₆D₆, 500 MHz): δ = 7.26 (d, J = 16.3 Hz, 4H), 7.14 (m, 2H), 6.89 (b, 4H), 6.85 (m, 6H), 6.76 (m, 6H), 6.67 (t, J = 7.3 Hz, 1H), 5.44 (d, J = 16.9 Hz, 2H), 5.30 (d, J = 13.2 Hz, 2H), 4.61 (d, J = 12.3 Hz, 2H).

Alternate Preparation of (BzCcCcC)Ni(II)Br. 1,1'-((2-bromo-1,3-phenylene)bis(methylene))bis(3-benzyl-1H-benzo[d]imidazole-3-ium) dibromide (50 mg, 0.066 mmol) and Li(N(SiMe₃)₂) (23.2 mg, 0.14 mmol) were dissolved cold THF (-35 °C) and stirred together at room temperature for one hour. NiCl₂py₄ (29.4 mg, 0.066 mmol) and KC₈ (31.2 mg, 0.23mmol) were dissolved separately in THF and then added to the free carbene generated *in situ* in that order. The reaction went from clear yellow to dark red. The reaction was stirred for four hours at room temperature and then concentrated under reduced pressure. The solid was washed with hexanes and then benzene and filtered over celite. The benzene was concentrated under reduced pressure giving (BzCcCcC)Ni(II)Br in good yield (34.6 mg, 80%).

Preparation of (^tBuCcCcC)Ni(II)Br. 1,1'-((2-bromo-1,3-phenylene)bis(methylene))bis(3-*t*-butyl-1H-benzo[d]imidazole-3-ium) dibromide (25 mg, 0.036 mmol) and Li(N(SiMe₃)₂) (12.8 mg, 0.076 mmol) were dissolved in benzene (2 mL) and THF (2 mL) respectively and cooled to -35 °C. The base was then added to the frozen benzene solution and warmed to room temperature (~5 mins). Ni(COD)₂ (8.0 mg, 0.029 mmol) dissolved in THF was then added to the reaction dropwise. Ni was required to be the limiting reagent due to the difficulty of removing Ni(COD)₂ starting material from the resulting product. The reaction was then concentrated under reduced pressure and filtered over celite washing with hexanes and benzene. The benzene wash was concentrated to give a yellow solid as the product (9.4 mg, 0.016 mmol, 55% based on Ni). ¹H NMR (C₆D₆, 500 MHz): δ = 7.17 (d, 2H), 6.98 (m, 4H), 6.89 (m, 2H), 6.78 (d, J = 7.3 Hz, 2H), 6.66 (t, J = 7.3 Hz, 1H), 5.90 (d, J = 13.6 Hz, 2H), 4.86 (d, J = 13.6 Hz, 2H), 2.05 (s, 18H).

Alternate Preparation of (^tBuCcCcC)Ni(II)Br. 1,1'-((2-bromo-1,3-phenylene)bis(methylene))bis(3-*t*-butyl-1H-benzo[d]imidazole-3-ium) dibromide (25 mg, 0.036 mmol) and Li(N(SiMe₃)₂) (12.8 mg, 0.076 mmol) were dissolved cold THF (-35 °C) and stirred together at room temperature for one hour. NiCl₂py₄ (16.2 mg, 0.036 mmol) and KC₈ (17.2 mg, 0.127 mmol) were dissolved separately in THF and then added to the free carbene generated *in situ* in that order. The reaction went from clear yellow to dark red with the addition of nickel. The reaction was stirred for four hours at room temperature and then concentrated under reduced pressure. The solid was washed with hexanes and then benzene and filtered over celite. The benzene was concentrated under reduced pressure giving product in good yield (19.2 mg, 90%).

Preparation of (^tBuCcCcC)Ni(II)H. A 20 mL scintillation vial was charged with (^tBuCcCcC)Ni(II)Br (0.025 g, 0.043 mmol) and approximately 2 mL of benzene and cooled to -35 °C. NaHBEt₃ (0.043 mL, 0.043 mmol) was added to the frozen reaction and thawed to room

temperature going from a yellow frozen solution to deep purple. The reaction was stirred at room temperature for 30 minutes, filtered through celite, and cooled to -35 °C. The frozen benzene was removed under reduced pressure yielding a dark purple solid in good yield (21 mg, 96%). ^1H NMR (C_6D_6 , 500 MHz): $\delta = 7.31$ (d, $J = 8.3$ Hz, 2H), 7.10 (d, $J = 7.5$ Hz, 4H), 7.02 (t, $J = 7.9$ Hz, 2H), 6.93 (m, 3H), 5.44 (d, $J = 13.5$ Hz, 2H), 5.10 (d, $J = 13.5$ Hz, 2H), 1.92 (s, 18H), -7.77 (s, 1H).

Preparation of $\text{H}_2(\text{DIPPCCC})\text{Fe}(\text{II})\text{Cl}_3$. A 20 mL scintillation vial was charged with $[\text{H}_3(\text{DIPPCCC})]\text{Cl}_2$ (0.071 g, 0.101 mmol) and approximately 2 mL of THF. In two separate vials, an equivalent of FeCl_2 (0.013 g, 0.101 mmol) and 1.1 equivalents of $\text{Li}(\text{N}(\text{SiMe}_3)_2)$ (0.019 g 0.111 mmol) were dissolved in approximately 2 mL of THF each. The FeCl_2 was added to the off-white solution of ligand and the $\text{Li}(\text{N}(\text{SiMe}_3)_2)$ was added drop-wise to the solution, resulting in an instantaneous color change to green-brown. After stirring for 3 hours, the color of the solution was orange with yellow precipitate. Solvents were removed under reduced pressure and the yellow residue was dissolved in DCM, filtered over celite, and the solvent again removed under reduced pressure. The product, $\text{H}_2(\text{DIPPCCC})\text{Fe}(\text{II})\text{Cl}_3$ was isolated as a yellow solid (1:1) (0.08 g, 0.101

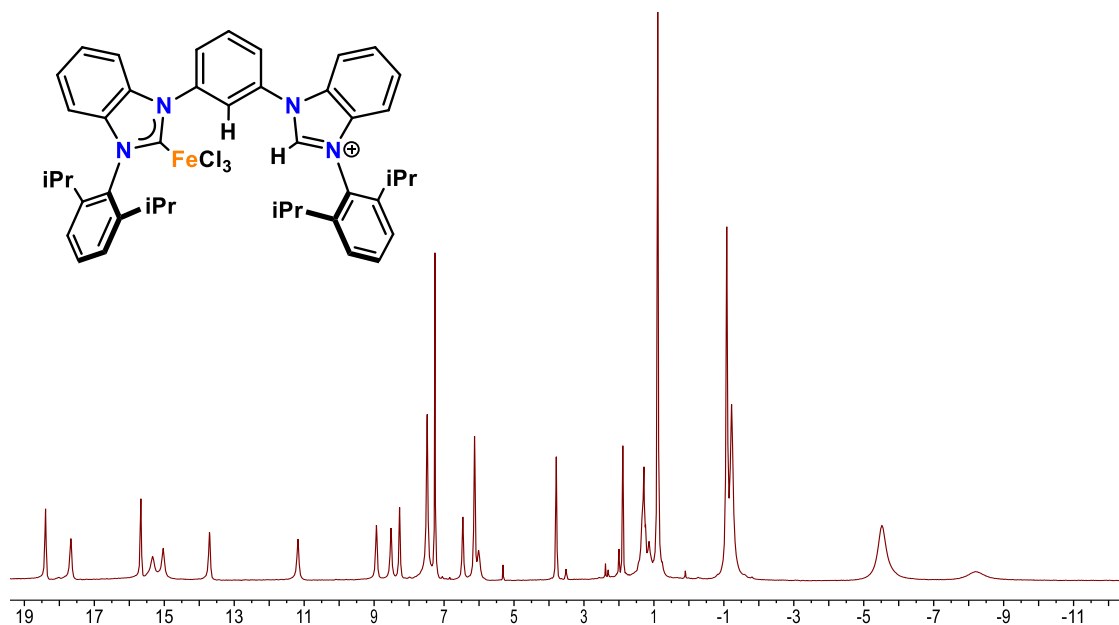


Figure 2.9. ^1H NMR spectrum of $\text{H}(\text{DIPPCCC})\text{Fe}(\text{II})\text{Cl}_3$ (CDCl_3).

mmol, 100 %). Crystals suitable for X-ray analysis were grown overnight from a concentrated solution of DCM and hexanes at -35 °C. Analysis for $C_{44}H_{49}N_4FeCl_3 \cdot CH_2Cl_2(0.1equiv)$: Calcd. C, 66.00; H, 5.93; N, 6.98. Found C, 65.84; H, 5.90; N, 7.10. 1H NMR ($CDCl_3$, 500 MHz): $\delta = 18.39, 17.67, 15.67, 15.53, 15.03, 13.71, 11.18, 8.93, 8.52, 8.27, 7.48, 6.46, 6.13, 1.28, 0.89, -1.08, -1.22, -5.52, -8.20$. $\mu_{eff} = 5.73(5) \mu_B$.

Initial Preparation of $(^{DIPP}CCC)Fe(II)H(PMe_3)(N_2)$. A 20 mL scintillation vial was charged with $[H_3(^{DIPP}CCC)]Cl_2$ (0.028 g, 0.040 mmol) and approximately 4 mL of toluene. With vigorous stirring, 2.1 equivalents of benzyl potassium (0.011 g, 0.084 mmol) was weighed by difference and added as an orange solid. After one hour of stirring at room temperature, the solution was filtered over Celite and the filtrate was cooled to -35 °C. In a separate vial, $Fe(PMe_3)_4$ (0.014 g, 0.039 mmol) was dissolved in approximately 3 mL of pentane. The yellow solution was cooled to -35 °C. The filtrate, containing the free carbene, $H^{DIPP}CCC$ generated *in situ*, was added dropwise to the iron(0) solution, resulting in a color change to brown. After three hours of stirring at room temperature, volatiles were removed under reduced pressure. The brown-yellow residue was triturated with pentane, affording the product as a yellow solid (9.5 mg, 0.012 mmol, 30%).

Preparation of $(^{DIPP}CCC)Fe(II)H(PMe_3)(N_2)$. A 20 mL scintillation vial was charged with $H_2(^{DIPP}CCC)Fe(II)Cl_3$ (0.030 g, 0.038 mmol) and approximately 2 mL of toluene. Two equivalents of PMe_3 (1.0 M THF, 0.08 mL, 0.076 mmol) was syringed into the vial. Three and a half equivalents of KC_8 (0.018 g, 0.133 mmol) was dissolved in 2 mL of THF and added dropwise to the solution. The reaction was stirred at room temperature overnight and the volatiles removed under reduced pressure. Pentane (2 mL) was added to the solid and filtered over celite, the filtrate was placed in the freezer at -35 °C to crystallize. Benzene was then added to the remaining solid and filtered over celite until no further color washed down. The volatiles were removed under

pressure from the filtrate and the product as a yellow-red solid was obtained in quantitative yield after collection of crystalline material from the pentane wash (0.030 mg, 0.038 mmol, 100%). Crystals suitable for X-ray analysis were grown overnight at room temperature from a concentrated solution of pentane and toluene (20:1). Analysis for $C_{47}H_{57}N_6FeP \cdot C_4H_8O$ (1equiv): Calcd. C, 70.9; H, 7.47; N, 9.73. Found C, 70.68; H, 6.93; N, 9.35. 1H NMR (C_6D_6 , 500 MHz): $\delta = -9.65$ (d, $J = 13$ Hz, 1H, Fe-H), 0.63 (d, $J = 7$ Hz, 9H, $P(CH_3)_3$), 0.76 (d, $J = 7$ Hz, 6H, iPr- CH_3), 1.04 (d, $J = 7$ Hz, 6H, iPr- CH_3), 1.20 (d, $J = 7$ Hz, 6H, iPr- CH_3), 1.34 (d, $J = 7$ Hz, 6H, iPr- CH_3), 2.68 (m, $J = 13$ Hz, 2H, iPr- CH), 3.23 (m, $J = 13$ Hz, 2H, iPr- CH), 6.30 (d, $J = 7$ Hz, 2H, Ar- CH), 6.89 (t, $J = 7$ Hz, 2H, Ar- CH), 7.05 (t, $J = 7$ Hz, 2H, Ar- CH), 7.18 (b, 4H, Ar- CH), 7.24 (d, $J = 7$ Hz, 2H, Ar- CH), 7.37 (t, $J = 7$ Hz, 1H, Ar- CH), 7.62 (d, $J = 7$ Hz, 2H, Ar- CH), 7.84 (d, $J = 7$ Hz, 2H, Ar- CH). ^{13}C NMR (C_6D_6 , 126 MHz): $\delta = 149.09, 146.99, 146.48, 140.90, 135.06, 132.20, 129.98, 128.59, 125.27, 123.62, 122.00, 121.13, 120.39, 110.51, 109.68, 105.94, 28.68, 28.46, 25.65, 25.06, 24.64, 23.77, 15.73, 15.57$. $^{31}P\{^1H\}$ NMR (C_6D_6 , 202.4MHz): $\delta = 11.02$ (1P, $P(CH_3)_3$). IR = 1723 cm^{-1} (Fe-H), 2099 cm^{-1} (N_2).

Preparation of $(DIPPCCC)Fe(II)H(PPh_3)(N_2)$. A 20 mL scintillation vial was charged with $H_2(DIPPCCC)Fe(II)Cl_3$ (0.030 g, 0.038 mmol) and approximately 2 mL of toluene. One equivalent of PPh_3 (0.01 g, 0.038 mmol) and 1.1 equivalents of $Li(N(SiMe_3)_2)$ (0.007 g, 0.042 mmol) were dissolved separately in 1 mL of toluene. Three and a half equivalents of potassium graphite (0.018 g, 0.133 mmol) was dissolved in 2 mL of THF. The $Li(N(SiMe_3)_2)$ was added to the vial of KC_8 and the PPh_3 to the $H_2(DIPPCCC)Fe(II)Cl_3$. The $Li(N(SiMe_3)_2)/KC_8$ mixture was slowly added dropwise to the solution. The reaction was stirred at room temperature overnight and the volatiles removed under reduced pressure. Pentane was added to the solid and filtered over celite until no further color was washed down. The volatiles were removed under pressure from the filtrate and

the product as an orange solid was obtained in quantitative yield (0.037 mg, 0.038 mmol, 100%). Analysis for $C_{62}H_{61}N_6FeP \cdot C_4H_8O(0.5equiv) \cdot CH_2Cl_2(0.5equiv)$: Calcd. C, 73.39; H, 6.30; N, 7.96. Found C, 73.41; H, 6.04; N, 7.55. 1H NMR (C_6D_6 , 500 MHz): $\delta = -11.15$ (d, $J = 22.5$ Hz, 1H, Fe-*H*), 0.70 (m, $J = 7.5$ Hz, 12H, iPr-*CH*₃), 0.90 (d, $J = 6.5$, 6H, iPr-*CH*₃), 1.10 (d, $J = 7$ Hz, 6H, iPr-*CH*₃), 2.53 (m, $J = 7$ Hz, 2H, iPr-*CH*), 2.89 (m, $J = 7$ Hz, 2H, iPr-*CH*), 6.57 (m, 6H, Ar-*CH*), 6.70 (t, $J = 7.5$ Hz, 2H, Ar-*CH*), 6.78 (t, $J = 8.5$ Hz, 4H, Ar-*CH*), 6.86 (t, $J = 7.5$ Hz, 2H, Ar-*CH*), 7.03 (m, 6H, Ar-*CH*), 7.27 (m, 6H, Ar-*CH*), 7.37 (d, $J = 7.5$ Hz, 2H, Ar-*CH*), 7.50 (t, $J = 7.5$ Hz, 2H, Ar-*CH*), 7.63 (d, $J = 8$ Hz, 2H, Ar-*CH*). ^{13}C NMR (C_6D_6 , 126 MHz): $\delta = 230.10, 183.01, 149.10, 147.74, 147.02, 141.43, 137.64, 135.80, 132.99, 132.91, 132.54, 129.90, 129.51, 127.07, 127.01, 125.27, 123.83, 121.80, 120.87, 120.78, 110.97, 109.84, 106.05, 29.38, 28.43, 25.50, 25.38, 24.26, 22.58$. $^{31}P\{^1H\}$ NMR (C_6D_6 , 202.4 MHz): $\delta = 50$ (1P, *PPh*₃). IR = 1791 cm^{-1} (Fe-H), 2099 cm^{-1} (N_2).

Preparation of $(DIPPCCC)Fe(II)H(py)(N_2)$. A 20 mL scintillation vial was charged with $H_2(DIPPCCC)Fe(II)Cl_3$ (0.030 g, 0.038 mmol) and approximately 2 mL of toluene. Excess pyridine (5 drops) was added to the vial and 1.1 equivalents of $Li(N(SiMe_3)_2)$ (0.007 g, 0.042 mmol) was dissolved in 2 mL of toluene. Three and a half equivalents of potassium graphite (0.018 g, 0.133 mmol) was dissolved in 2 mL of THF. The $Li(N(SiMe_3)_2)$ was added to the KC_8 and then slowly added dropwise to the reaction. The reaction was stirred at room temperature overnight and the volatiles removed under reduced pressure. Pentane was added to the solid and filtered over celite until no further color was washed down. The volatiles were removed under pressure from the filtrate and the product as a purple solid was obtained in quantitative yield (0.030 mg, 0.038 mmol, 100%). Analysis for $C_{49}H_{51}FeN_7 \cdot C_7H_8(1.5equiv) \cdot CH_2Cl_2(0.5equiv)$: Calcd. C, 74.73; H, 6.72; N, 9.61. Found C, 75.27; H, 6.64; N, 10.07. 1H NMR (C_6D_6 , 500 MHz): $\delta = -18.69$ (s, 1H, Fe-*H*),

0.78 (d, J = 6.5 Hz, 6H, iPr-CH₃), 0.79 (d, J = 6.5 Hz, 6H, iPr-CH₃), 0.85 (d, J = 6.5 Hz, 6H, iPr-CH₃), 1.24 (d, J = 6.5 Hz, iPr-CH₃), 2.64 (m, J = 7 Hz, 2H, iPr-CH), 2.84 (m, J = 7 Hz, 2H, iPr-CH), 6.01 (s, J = 6.5 Hz, 2H, Ar-CH), 6.40 (t, J = 7.5 Hz, 1H, Ar-CH), 6.63 (d, J = 7.5 Hz, 2H, Ar-CH), 6.88 (m, J = 7.5 Hz, 2H, Ar-CH), 7.04 (t, J = 7.5 Hz, 2H, Ar-CH), 7.20 (d, J = 8 Hz, 2H, Ar-CH), 7.25 (d, J = 7.5 Hz, 2H, Ar-CH), 7.33 (t, J = 7.5 Hz, 2H, Ar-CH), 7.48 (t, J = 7.5 Hz, 1H, Ar-CH), 7.74 (d, J = 8 Hz, 2H, Ar-CH), 7.87 (d, J = 8 Hz, 2H, Ar-CH), 8.12 (d, J = 5.5 Hz, 2H, Ar-CH). ¹³C NMR (C₆D₆, 126 MHz): δ = 229.28, 191.95, 154.47, 149.09, 148.69, 146.87, 140.49, 134.97, 132.70, 132.62, 130.06, 125.20, 123.80, 122.85, 122.00, 121.10, 120.96, 110.42, 109.78, 106.59, 28.64, 28.56, 26.14, 25.21, 24.29, 23.35. IR = 1794 cm⁻¹ (Fe-H), 2081 cm⁻¹ (N₂).

Preparation of (DIPPCCC)Fe(II)H(CO)₂. A 50 mL schlenk flask was charged with (DIPPCCC)Fe(II)H(PMe₃)(N₂) (0.020 g, 0.025 mmol) and approximately 5 mL of benzene. CO gas (4atm) was added to the flask after freeze pump thawing. The reaction was stirred at room temperature over four days, going slowly from red to pale yellow, and the volatiles were removed under reduced pressure. The product (DIPPCCC)Fe(II)H(CO)₂ was obtained as a pale yellow solid in high yield (0.015 mg, 0.02 mmol, 80%). Analysis for C₄₆H₄₆N₄O₂Fe·CH₂Cl₂(0.3equiv): Calcd. C, 72.39; H, 6.11; N, 7.29. Found C, 72.65; H, 5.96; N, 7.36. ¹H NMR (C₆D₆, 500 MHz): δ = 8.42 (s, 1H, Fe-H), 0.77 (d, J = 6.5 Hz, 6H, iPr-CH₃), 0.87 (d, J = 7 Hz, 6H, iPr-CH₃), 1.13 (d, J = 6.5 Hz, 6H, iPr-CH₃), 1.44 (d, J = 6.5 Hz, 6H, iPr-CH₃), 2.36 (m, J = 7 Hz, 2H, iPr-CH), 2.98 (m, J = 7 Hz, 2H, iPr-CH), 6.57 (d, J = 8 Hz, 2H, Ar-CH), 6.86 (t, J = 7.5 Hz, 2H, Ar-CH), 7.04 (t, J = 7.5 Hz, 2H, Ar-CH), 7.10 (d, J = 8 Hz, 2H, Ar-CH), 7.18 (m, 2H, Ar-CH) 7.23 (d, J = 8 Hz, 2H, Ar-CH), 7.43 (t, J = 8 Hz, 1H, Ar-CH), 7.61 (d, J = 8 Hz, 2H, Ar-CH), 7.72 (d, J = 8 Hz, 2H, Ar-CH). ¹³C NMR (C₆D₆, 126 MHz): δ = 220.05, 214.04, 209.82, 174.82, 147.81, 147.66, 146.91,

139.20, 133.57, 131.84, 130.63, 124.85, 124.49, 122.93, 122.88, 122.19, 111.07, 110.86, 108.16, 28.78, 28.60, 25.85, 24.84, 23.84, 23.54. IR = 1983, 1927 cm^{-1} (C-O).

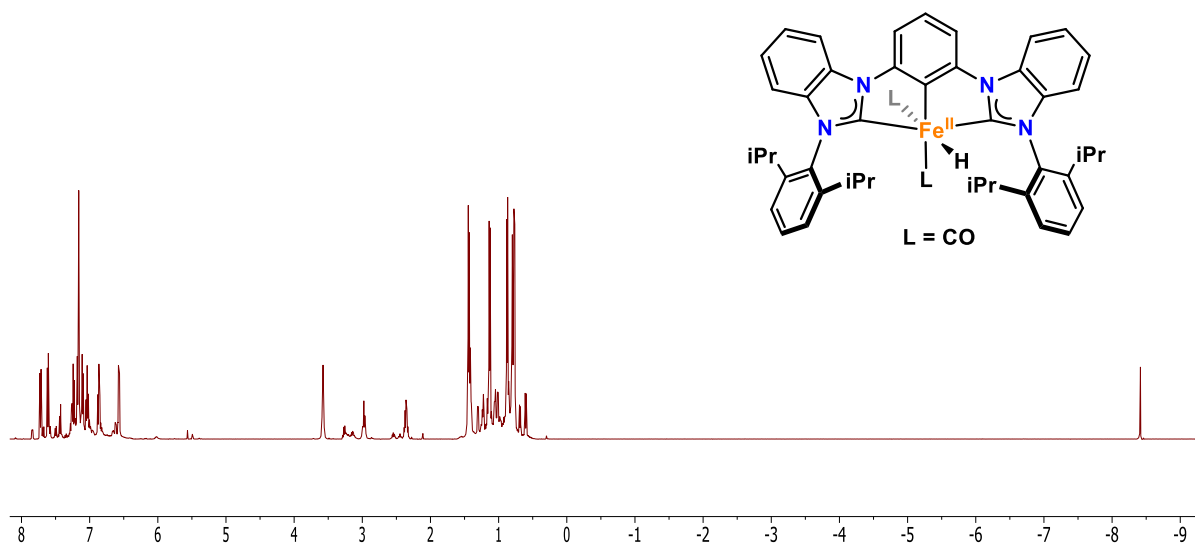


Figure 2.10. ^1H NMR spectrum of $(^{13}\text{C}_6\text{D}_6)\text{Fe}(\text{II})\text{H}(\text{CO})_2$ (C_6D_6).

Alternate Preparation of $(^{13}\text{C}_6\text{D}_6)\text{Fe}(\text{II})\text{H}(\text{CO})_2$. A 50 mL schlenk flask was charged with $(^{13}\text{C}_6\text{D}_6)\text{Fe}(\text{II})\text{H}(\text{py})(\text{N}_2)$ (0.020 g, 0.025 mmol) and approximately 5 mL of benzene. CO gas (4atm) was added to the flask after freeze pump thawing. The reaction immediately changed from purple to pale yellow. The volatiles were removed under reduced pressure and $(^{13}\text{C}_6\text{D}_6)\text{Fe}(\text{II})\text{H}(\text{CO})_2$ was obtained as a pale yellow solid in high yield (0.017 mg, 0.023 mmol, 90%).

Preparation of $(^{13}\text{C}_6\text{D}_6)\text{Fe}(\text{II})\text{H}(\text{tBuNC})_2$. A 20 mL scintillation vial was charged with $(^{13}\text{C}_6\text{D}_6)\text{Fe}(\text{II})\text{H}(\text{PMe}_3)(\text{N}_2)$ (0.020 g, 0.025 mmol) and approximately 5 mL of THF. Excess t-butylisocyanide (5eq, 0.014 mL, 0.125 mmol) was added to the vial. The reaction was stirred at room temperature for four days going slowly from orange to yellow/green. The volatiles were removed under reduced pressure and the product $(^{13}\text{C}_6\text{D}_6)\text{Fe}(\text{II})\text{H}(\text{tBuNC})_2$ was obtained as a

pale yellow solid in high yield (0.018 mg, 0.021 mmol, 85%). Analysis for $C_{54}H_{64}N_6Fe \cdot CH_2Cl_2(0.3\text{equiv})$: Calcd. C, 74.24; H, 7.41; N, 9.57. Found C, 74.36; H, 7.27; N, 9.21. 1H NMR (C_6D_6 , 500 MHz): $\delta = -8.82$ (s, 1H, Fe-*H*), 0.61 (s, 9H, $tBu-(CH_3)_3$), 0.62 (s, 9H, $tBu-(CH_3)_3$), 0.82 (d, $J = 6.5$ Hz, 6H, *iPr-CH*₃), 1.03 (d, $J = 7$ Hz, 6H, *iPr-CH*₃), 1.31 (d, $J = 6.5$ Hz, 6H, *iPr-CH*₃), 1.51 (d, $J = 7$ Hz, 6H, *iPr-CH*₃), 2.87 (septet, $J = 7$ Hz, 2H, *iPr-CH*), 3.34 (septet, $J = 7$ Hz, 2H, *iPr-CH*), 6.27 (d, $J = 8$ Hz, 2H, Ar-*CH*), 6.84 (t, $J = 7.5$ Hz, 2H, Ar-*CH*), 7.04 (t, $J = 7.5$ Hz, 2H, Ar-*CH*), 7.19 (d, $J = 8$ Hz, 2H, Ar-*CH*), 7.25 (d, $J = 7.5$ Hz, 2H, Ar-*CH*), 7.31 (t, $J = 7.5$ Hz, 2H, Ar-*CH*), 7.53 (t, $J = 8$ Hz, 1H, Ar-*CH*), 7.84 (d, $J = 7.5$ Hz, 2H, Ar-*CH*), 7.97 (d, $J = 8$ Hz, 2H, Ar-*CH*). ^{13}C NMR (C_6D_6 , 126 MHz): $\delta = 228.03, 187.33, 186.39, 175.31, 148.70, 147.96, 146.97, 140.85, 136.53, 132.06, 129.48, 125.14, 124.80, 122.10, 120.98, 120.02, 109.60, 109.49, 106.00, 55.39, 54.15, 31.27, 31.17, 28.69, 28.53, 25.14, 24.94, 24.59, 23.74$. IR = 2047, 2002 cm^{-1} (C-N).

Alternate Preparation of $(^{DIPP}CCC)Fe(II)H(tBuNC)_2$. A 20 mL scintillation vial was charged with $(^{DIPP}CCC)Fe(II)H(py)(N_2)$ (0.020 g, 0.025 mmol) and approximately 5 mL of THF. Excess *t*-

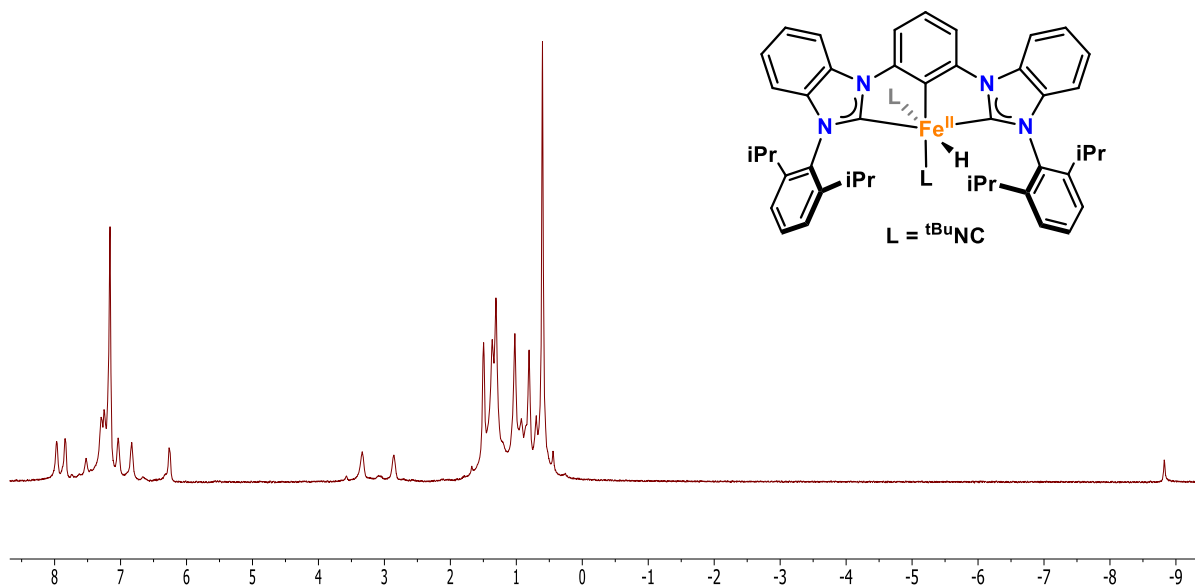


Figure 2.11. 1H NMR spectrum of $(^{DIPP}CCC)Fe(II)H(tBuNC)_2$ (C_6D_6).

butylisocyanide (3eq, 0.008 mL, 0.075 mmol) was added to the vial. The reaction immediately changed from purple to yellow/green. The volatiles were removed under reduced pressure and the product (^{DIPP}CCC)Fe(II)H(^tBuNC)₂ was obtained as a pale yellow solid in high yield (0.021 mg, 0.024 mmol, 95%).

Preparation of (^{DIPP}CCC)Fe(II)(κ²-OOCH)(PMe₃). A 50 mL schlenk flask was charged with (^{DIPP}CCC)Fe(II)H(PMe₃)(N₂) (0.020g, 0.025 mmol) and approximately 3 mL of benzene. The reaction was stirred at room temperature under an atmosphere of CO₂ for 36 hours. The volatiles were removed under reduced pressure and the product (^{DIPP}CCC)Fe(II)(κ²-OOCH)(PMe₃) was obtained as a red-purple solid. Pentane was added and the solution was filtered over celite and the filtrate was placed in the freezer at -35 °C to crystallize. Red-purple needle crystals were obtained in 60% yield (0.012g, 0.015 mmol). Concentrating the filtrate a second time yielded more red-purple crystals. ¹H NMR (C₆D₆, 21 °C): δ = 0.22 (d, J = 8.5 Hz, 9H, (P(CH₃)₃)₂), 0.69 (d, J = 6.5 Hz, 6H, iPr-CH₃), 1.00 (d, J = 7 Hz, 6H, iPr-CH₃), 1.11 (d, J = 6.5 Hz, 6H, iPr-CH₃), 1.47 (d, J = 7 Hz, 6H, iPr-CH₃), 2.16 (septet, J = 6.5 Hz, 2H, iPr-CH), 3.75 (septet, J = 7 Hz, 2H, iPr-CH), 6.02 (d, J = 4 Hz, 1H, OOCH), 6.79 (d, J = 8 Hz, 2H, Ar-CH), 6.95 (t, J = 7.5 Hz, 2H, Ar-CH), 7.01 (d, J = 7.5 Hz, 2H, Ar-CH), 7.11 (t, J = 8 Hz, 2H, Ar-CH), 7.18 (m, 2H, Ar-CH) 7.21 (t, J = 7.5 Hz, 2H, Ar-CH), 7.30 (t, J = 8 Hz, 1H, Ar-CH), 7.68 (d, J = 7.5 Hz, 2H, Ar-CH), 7.98 (d, J = 8 Hz, 2H, Ar-CH). IR = 2815 cm⁻¹ (OOCH), 1562 cm⁻¹ (OOCH), 1276 cm⁻¹ (OOCH).

Preparation of (^{DIPP}CCC)Fe(II)Cl(PMe₃)₂. A 20 mL scintillation vial was charged with (^{DIPP}CCC)Fe(II)H(PMe₃)(N₂) (0.020 g, 0.025 mmol) and approximately 3 mL of THF. With vigorous stirring, two equivalents of PMe₃ (1.0 M THF, 0.05 mL, 0.05 mmol) was syringed into the vial followed by 1.1 equivalents of HCl·Et₂O (2.0 M, 0.014 mL, 0.0275 mmol) resulting in a dark red solution. The solution was stirred overnight at room temperature and the volatiles were

removed under reduced pressure giving pure product (0.020 g, 0.023 mmol, 90%). Crystals suitable for X-ray analysis were grown from DCM. Analysis for $C_{50}H_{63}N_4FeClP_2 \cdot CH_2Cl_2(0.81equiv)$: Calcd. C, 64.78; H, 6.91; N, 5.95. Found C, 64.55; H, 6.69; N, 6.38. 1H NMR (C_6D_6 , 500 MHz): δ = 0.47 (s, 18H, $(P(CH_3)_3)_2$), 0.90 (d, J = 6.6 Hz, 12H, *iPr-CH₃*), 1.26 (d, J = 6.5 Hz, 12H, *iPr-CH₃*), 2.95 (m, J = 6.5 Hz, 4H, *iPr-CH*), 6.73 (d, J = 8 Hz, 2H, *Ar-CH*), 6.88 (t, J = 7.5 Hz, 2H, *Ar-CH*), 7.07 (t, J = 7.6 Hz, 2H, *Ar-CH*), 7.20 (d, J = 7.8 Hz, 4H, *Ar-CH*), 7.24, (t, J = 6.5 Hz, 2H, *Ar-CH*), 7.33 (t, J = 7 Hz, 1H, *Ar-CH*), 7.63 (d, J = 7.7 Hz, 2H, *Ar-CH*), 7.91 (d, J = 8 Hz, 2H, *Ar-CH*). ^{13}C NMR (C_6D_6 , 126 MHz): δ = 225.91, 189.69, 149.52, 147.67, 141.94, 135.62, 132.10, 129.79, 124.32, 122.23, 121.15, 118.6, 112.79, 109.29, 106.79, 29.21, 26.48, 23.69, 16.57. $^{31}P\{^1H\}$ NMR (C_6D_6 , 202.4MHz): δ = 22.90 (1P, $P(CH_3)_3$).

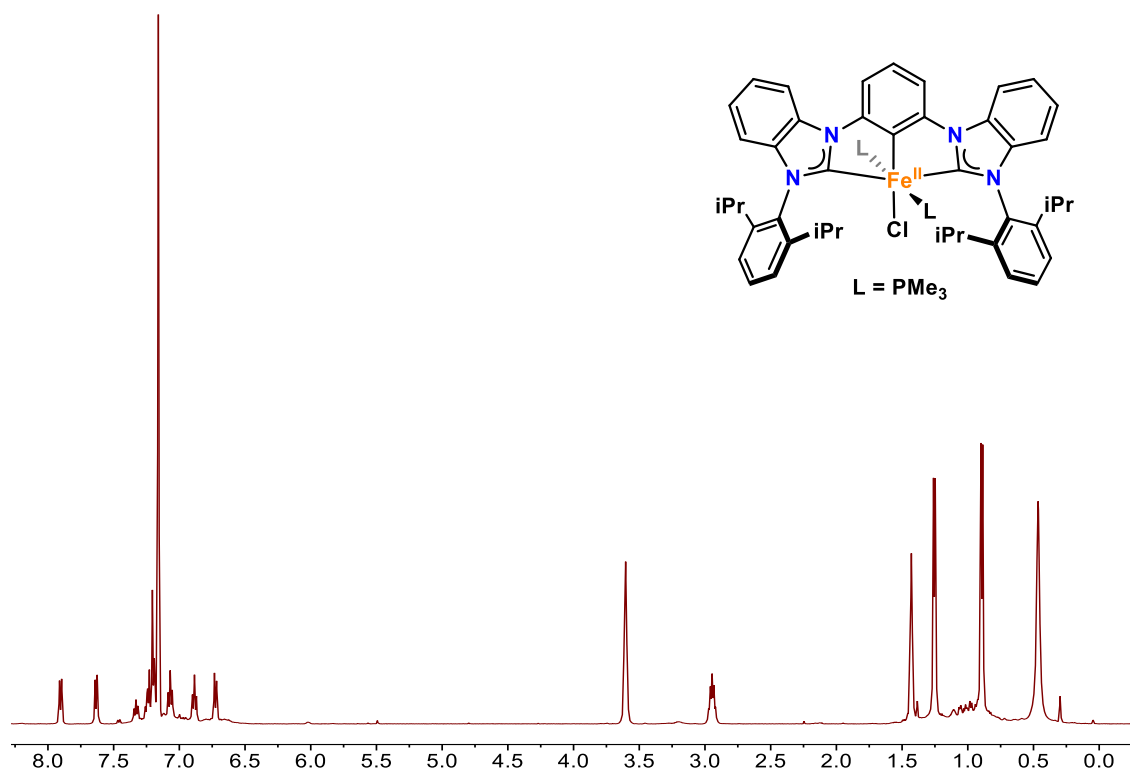


Figure 2.12. ^1H NMR spectrum of $(^{\text{DIPP}}\text{CCC})\text{Fe}(\text{II})\text{Cl}(\text{PMe}_3)_2$ (C_6D_6).

Preparation of $(^{\text{DIPP}}\text{CCC})\text{Fe}(\text{III})(\text{Cl})_2(\text{PMe}_3)$. A 20 mL scintillation vial was charged with $(^{\text{DIPP}}\text{CCC})\text{Fe}(\text{II})\text{Cl}(\text{PMe}_3)_2$ (0.020 g, 0.0229 mmol) and excess chloroform (CHCl_3) was added and stirred at room temperature for 20 minutes. The red solid changed to a dark green solution. The volatiles were then removed under reduced pressure to yield pure product (0.017 g, 0.021 mmol, 90%). Crystals suitable for X-ray analysis were grown from DCM and pentane. Analysis for $\text{C}_{47}\text{H}_{54}\text{N}_4\text{FeCl}_2\text{P}\cdot\text{CH}_2\text{Cl}_2$ (1.35equiv): Calcd. C, 61.3; H, 6.03; N, 5.91. Found C, 61.3; H, 5.68; N, 5.96. ^1H NMR (CDCl_3 , 500 MHz): $\delta = 100.51, 80.17, 20.49, 15.69, 11.21, 8.91, 8.56, 7.60, 7.40, 6.88, 6.44, 2.70, 2.37, 1.54, 1.41, 1.22, 1.09, 0.42, -1.19, -2.92, -19.35$. $\mu_{\text{eff}} = 2.81 \mu_{\text{B}}$.

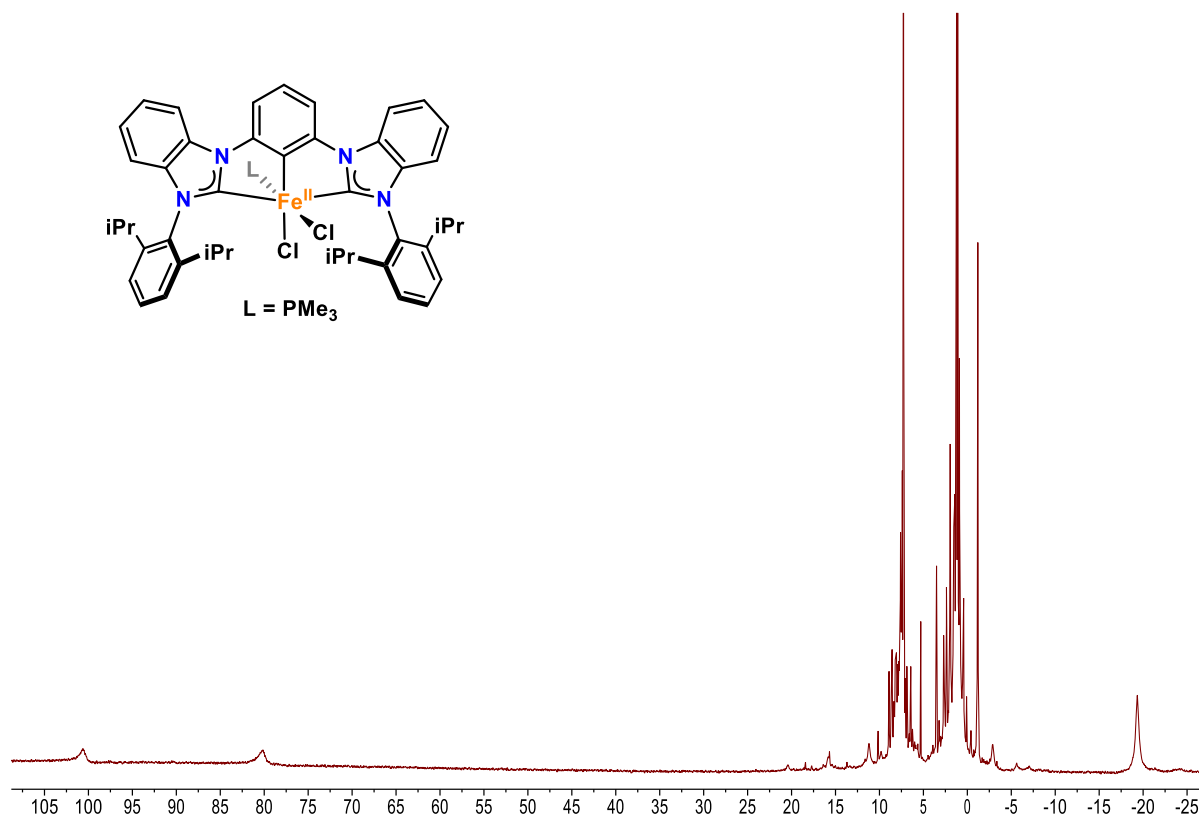


Figure 2.13. ^1H NMR spectrum of $(\text{DIPP})\text{Fe}(\text{III})\text{Cl}_2\text{PMe}_3$ (CDCl_3).

Preparation of [(^{DIPP}CCC)Fe(III)Cl(PMe₃)₂](PF₆). A 20 mL scintillation vial was charged with (^{DIPP}CCC)Fe(II)Cl(PMe₃)₂ (0.020 g, 0.0229 mmol) and approximately 3 mL of THF. Silver hexafluorophosphate (0.058 g, 0.0229 mmol) was dissolved in a separate vial in 2 mL of THF and added to the solution dropwise. The solution was stirred at room temperature overnight and the red solution changed to dark green with precipitate which was filtered off through celite. The volatiles were removed under reduced pressure yielding the product which was recrystallized by a slow diffusion of pentane into DCM (0.022 g, 0.023 mmol, 95%). Analysis for C₅₀H₆₃N₄FeCl₃PF₆·CH₂Cl₂(0.2equiv): Calcd. C, 58.24; H, 6.17; N, 5.41. Found C, 58.36; H, 6.36; N, 5.29. ¹H NMR (C₆D₆, 21 °C): δ = -19.52, -3.01, -1.24, 1.25, 1.88, 2.19, 4.50, 6.40, 7.53, 8.11, 3.49, 8.85, 10.91, 14.92, 19.52. ³¹P{¹H} NMR (C₆D₆, 21 °C): δ = 26.40 (1P, P(CH₃)₂), -143.50 (1P, PF₆). ¹⁹F{¹H} NMR (C₆D₆, 21 °C): δ = -72.05, -73.57.

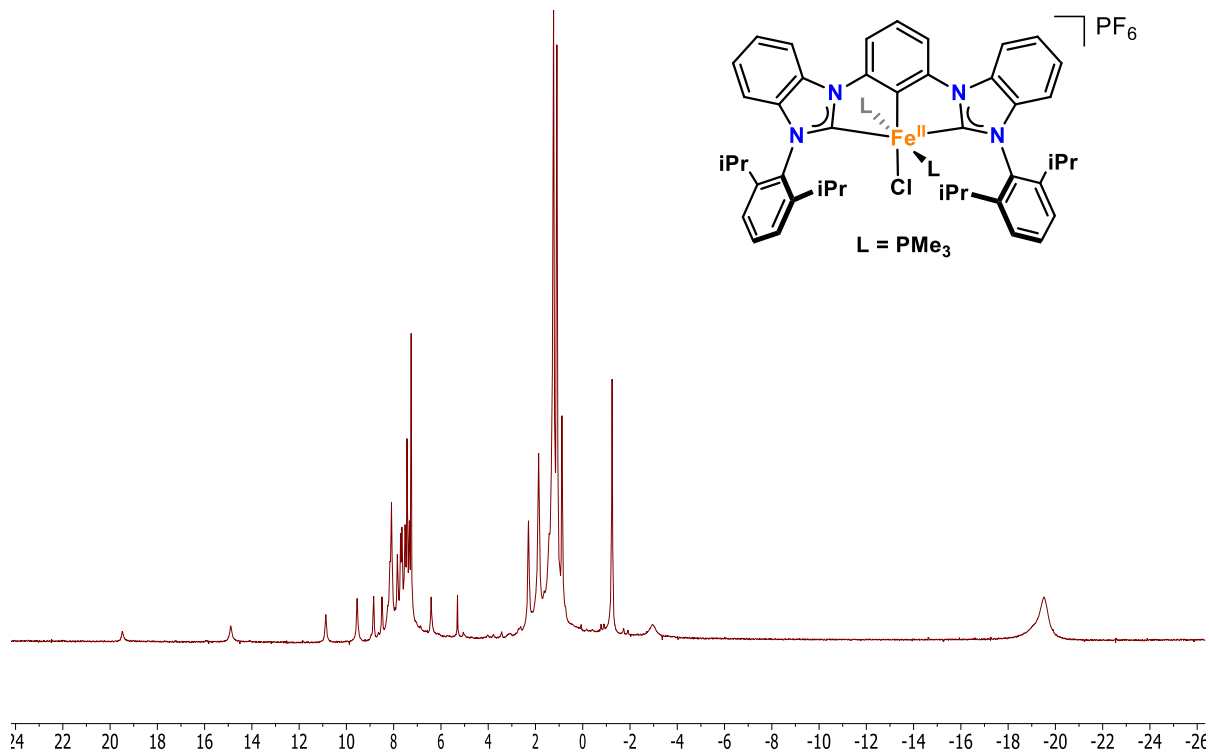


Figure 2.14. ¹H NMR spectrum of [(^{DIPP}CCC)Fe(III)Cl(PMe₃)₂](PF₆) (CDCl₃).

Compound	(^{Bz} CcCcC)Ni(II)Br	(^{tBu} CcCcC)Ni(II)Br
Empirical formula	C ₃₉ H ₃₂ N ₄ NiBr	C ₄₂ H ₄₅ N ₄ NiBr
Formula weight	695.31	744.44
Temperature/K	100.01	100.15
Crystal system	orthorhombic	triclinic
Space group	Pccn	P1
a/Å	18.8748(9)	9.2859(3)
b/Å	19.1500(8)	9.7065(4)
c/Å	17.1403(9)	19.8810(7)
α/°	90.00	98.1365(19)
β/°	90.00	90.0145(19)
γ/°	90.00	91.516(2)
Volume/Å ³	6195.4(5)	1773.27(11)
Z	8	1
Reflections collected	287307	29450
Independent reflections	9501 [R _{int} = 0.0503, R _{sigma} = 0.0149]	17519 [R _{int} = 0.0248, R _{sigma} = 0.0403]
Goodness-of-fit on F ²	1.069	1.064
Final R indexes [I ≥ 2σ(I)]	R ₁ = 0.0414, wR ₂ = 0.1046	R ₁ = 0.0275, wR ₂ = 0.0722
Final R indexes [all data]	R ₁ = 0.0504, wR ₂ = 0.1118	R ₁ = 0.0356, wR ₂ = 0.0849

Table 2.2. Crystallographic parameters for (^RCcCcC)Ni(II)Br (R = benzyl, t-butyl).

Compound	H ₂ (^{DIPP} CCC)Fe(II)Cl ₃	(^{DIPP} CCC)Fe(II)H(PMe ₃)(N ₂)
Empirical formula	C ₄₅ H ₅₁ N ₄ OCl ₅ Fe	C _{54.5} H ₇₃ N ₆ PFe
Formula weight	897.00	899.01
Temperature/K	100.0	100.0
Crystal system	monoclinic	triclinic
Space group	P2 ₁ /n	P-1
a/Å	16.2332(7)	12.0449(5)
b/Å	17.6703(7)	14.6183(6)
c/Å	16.3741(7)	15.7848(7)
α/°	90.00	107.2907(18)
β/°	98.5058(15)	108.0980(19)
γ/°	90.00	103.6701(19)
Volume/Å ³	4645.2(3)	2351.23(17)
Z	4	2
Reflections collected	42898	82887
Independent reflections	8519 [R _{int} = 0.0289, R _{sigma} = 0.0205]	17198 [R _{int} = 0.0426, R _{sigma} = 0.0367]
Goodness-of-fit on F ²	3.856	1.034
Final R indexes [I>=2σ (I)]	R ₁ = 0.2514, wR ₂ = 0.6416	R ₁ = 0.0427, wR ₂ = 0.1092
Final R indexes [all data]	R ₁ = 0.2691, wR ₂ = 0.6686	R ₁ = 0.0583, wR ₂ = 0.1191

Table 2.3. Crystallographic parameters for H₂(^{DIPP}CCC)Fe(II)Cl₃ and (^{DIPP}CCC)Fe(II)H(PMe₃)(N₂).

Compound	(^{DIPP} CCC)Fe(II)Cl(PMe ₃) ₂	(^{DIPP} CCC)Fe(III)(Cl) ₂ (PMe ₃)
Empirical formula	C ₅₀ H ₆₃ N ₄ P ₂ ClFe	C _{23.5} H ₂₇ ClFe _{0.5} N ₂ P _{0.5}
Formula weight	873.28	416.33
Temperature/K	100.04	112.56
Crystal system	monoclinic	triclinic
Space group	C2/c	P-1
a/Å	21.1714(11)	10.7730(17)
b/Å	11.0332(5)	14.849(2)
c/Å	18.8162(10)	16.687(2)
α/°	90	91.381(8)
β/°	90.101(2)	95.761(8)
γ/°	90	93.318(8)
Volume/Å ³	4395.2(4)	2650.2(7)
Z	4	4
Reflections collected	92760	18875
Independent reflections	4062 [R _{int} = 0.0472, R _{sigma} = 0.0135]	18875 [R _{int} = ?, R _{sigma} = 0.1107]
Goodness-of-fit on F ²	1.101	1.090
Final R indexes [I >= 2σ (I)]	R ₁ = 0.0479, wR ₂ = 0.1181	R ₁ = 0.0868, wR ₂ = 0.1972
Final R indexes [all data]	R ₁ = 0.0510, wR ₂ = 0.1201	R ₁ = 0.1375, wR ₂ = 0.2258

Table 2.4. Crystallographic parameters (^{DIPP}CCC)Fe(II)Cl(PMe₃)₂ and (^{DIPP}CCC)Fe(III)(Cl)₂(PMe₃).

2.5 References

1. Chianese, A. R.; Mo, A.; Lampland, N. L.; Swartz, R. L.; Bremer, P. T. Iridium Complexes of CCC-Pincer N-Heterocyclic Carbene Ligands: Synthesis and Catalytic C-H Functionalization. *Organometallics* **2010**, *29*, 3019-3026.
2. Ibrahim, A. D.; Tokmic, K.; Brennan, M. R.; Kim, D.; Matson, E. M.; Nilges, M. J.; Bertke, J. A.; Fout, A. R. Monoanionic bis(carbene) pincer complexes featuring cobalt(I-III) oxidation states. *Dalton Trans.* **2016**, *45*, 9805-9811.
3. Huckaba, A. J.; Hollis, T. K.; Howell, T. O.; Valle, H. U.; Wu, Y. Synthesis and Characterization of a 1,3-Phenylene-Bridged N-Alkyl Bis(benzimidazole) CCC-NHC Pincer Ligand Precursor: Homobimetallic Silver and Rhodium Complexes and the Catalytic Hydrosilylation of Phenylacetylene. *Organometallics* **2013**, *32*, 63-69.
4. Haque, R. A.; Iqbal, M. A.; Budagumpi, S.; Ahamed, M. B. K.; Majid, A. M. S. A.; Hasanudin, N. Binuclear *meta*-xylyl-linked Ag(I)-N-heterocyclic carbene complexes of N-alkyl/aryl-alkyl-substituted bis-benzimidazolium salts: synthesis, crystal structures and *in vitro* anticancer studies. *Appl. Organometal. Chem.* **2013**, *27*, 214-223.
5. Kose, O.; Saito, S. Cross-coupling reaction of alcohols for carbon-carbon bond formation using pincer-type NHC/palladium catalysts. *Org. Biomol. Chem.* **2010**, *8*, 896-900.
6. Ghavale, N.; Manjare, S. T.; Singh, H. B.; Butcher, R. J. Bis(chalcogenones) as pincer ligands: isolation and Heck activity of the selone-ligated unsymmetrical C,C,Se-Pd pincer complex. *Dalton Trans.* **2015**, *44*, 11893-11900.
7. Hahn, F. E.; Jahnke, M. C.; Pape, T. Synthesis of Pincer-Type Bis(benzimidazolin-2-ylidene) Palladium Complexes and Their Application in C-C Coupling Reactions. *Organometallics*, **2007**, *26*, 150-154.

8. Danopoulos, A. A.; Tulloch, A. A. D.; Winston, S.; Eastham, G.; Hursthouse, M. B. Chelating and 'pincer' dicarbene complexes of palladium; synthesis and structural studies. *Dalton Trans.* **2003**, 1009-1015.
9. Schultz, K. M.; Goldberg, K. I.; Gusev, D. G.; Heinekey, D. M. Synthesis, Structure, and Reactivity of Iridium NHC Pincer Complexes. *Organometallics* **2011**, *30*, 1429-1437.
10. Liu, X.; Pattacini, R.; Deglmann, P.; Braunstein, P. Do Short C-H-M (M = Cu(I), Ag(I)) Distances Represent Agostic Interactions in Pincer-Type Complexes? Unusual NHC Transmetalation from Cu(I) to Ag(I). *Organometallics* **2011**, *30*, 3302-3310.
11. Rubio, R. J.; Anadavan, G. T. S.; Bauer, E. B.; Hollis, T. K.; Cho, J.; Tham, F. S.; Donnadieu, B. Toward a general method for CCC N-heterocyclic carbene pincer synthesis: Metallation and transmetalation strategies for concurrent activation of three C-H bonds. *J. Organomet. Chem.* **2005**, *690*, 5353-5364.
12. Yan, X.; Xi, C. Advances in transmetalation reactions originated from organozirconium compounds. *Coord. Chem. Rev.* **2017**, *350*, 275-284.
13. Andavan, G. T. S.; Bauer, E. B.; Letko, C. S.; Hollis, T. K.; Tham, F. S. Synthesis and characterization of a free phenylene bis(N-heterocyclic carbene) and its di-Rh complex: Catalytic activity of the di-Rh and CCC-NHC Rh pincer complexes in intermolecular hydrosilylation of alkynes. *J. Organomet. Chem.* **2005**, *690*, 5938-5947.
14. Bauer, E. B.; Andavan, G. T. S.; Hollis, T. K.; Rubio, R. J.; Cho, J.; Kuchenbeiser, G. R.; Helgert, T. R.; Letko, C. S.; Tham, F. S. Air- and Water-Stable Catalysts for Hydroamination/Cyclization. Synthesis and Application of CCC-NHC Pincer Complexes of Rh and Ir. *Org. Lett.* **2008**, *10*, 1175-1178.

15. Zhang, X.; Wright, A. M.; DeYonker, N. J.; Hollis, T. K.; Hammer, N. I.; Webster, C. E.; Valente, E. J. Synthesis, Air Stability, Photobleaching, and DFT Modeling of Blue Light Emitting Platinum CCC-N-Heterocyclic Carbene Pincer Complexes. *Organometallics* **2012**, *31*, 1664-1672.
16. Hcukaba, A. J.; Cao, B.; Hollis, T. K.; Valle, H. U.; Kelly, J. T.; Hammer, N. I.; Oliver, A. G.; Webster, C. E. Platinum CCC-NHC benzimidazolyl pincer complexes: synthesis, characterization, photostability, and theoretical investigation of a blue-green emitter. *Dalton Trans.* **2013**, *42*, 8820-8826. – maybe don't need both Pt examples
17. Reilly, S. W.; Webster, C. E.; Hollis, T. K.; Valle, H. U. Transmetallation from CCC-NHC pincer Zr complexes in the synthesis of air-stable CCC-NHC pincer Co(III) complexes and initial hydroboration trials. *Dalton Trans.* **2016**, *45*, 2823-2828.
18. Alabau, R. G.; Eguillor, B.; Esler, J.; Esteruelas, M. A.; Oliván, M.; Oñate, E.; Tsai, J.; Xia, C. CCC-Pincer-NHC Osmium Complexes: New Types of Blue-Green Emissive Neutral Compounds for Organic Light-Emitting Devices (OLEDs). *Organometallics* **2014**, *33*, 5582-5596.
19. Lv, K.; Cui, D. Tridentate CCC-Pincer Bis(carbene)-Ligated Rare-Earth Metal Dibromides. Synthesis and Characterization. *Organometallics* **2008**, *27*, 5438-5440.
20. Matson, E. M.; Martinez, G. E.; Ibrahim, A. D.; Jackson, B. J.; Bertke, J. A.; Fout, A. R. Nickel(II) Pincer Carbene Complexes: Oxidative Addition of an Aryl C-H Bond to Form a Ni(II) Hydride. *Organometallics* **2014**, *34*, 399-407.
21. Ibrahim, A. D.; Entsminger, S. W.; Zhu, L.; Fout, A. R. A Highly Chemoselective Cobalt Catalyst for the Hydrosilylation of Alkenes using Tertiary Silanes and Hydrosiloxanes. *ACS Catal.* **2016**, *6*, 3589-3593.

22. Tokmic, K.; Markus, C. R.; Zhu, L.; Fout, A. R. Well-Defined Cobalt(I) Dihydrogen Catalyst: Experimental Evidence for a Co(I)/Co(III) Redox Process in Olefin Hydrogenation. *J. Am. Chem. Soc.* **2016**, *138*, 11907-11913.
23. Ibrahim, A.; Entsminger, S. W.; Fout, A. R. Insights into a Chemoselective Cobalt Catalyst for the Hydroboration of Alkenes and Nitriles. *ACS Catal.* **2017**, *7*, 3730-3734.
24. Tokmic, K.; Fout, A. R. Alkyne Semihydrogenation with a Well-Defined Nonclassical Co-H₂ Catalyst: A H₂ Spin on Isomerization and *E*-Selectivity. *J. Am. Chem. Soc.* **2016**, *138*, 13700-13705.
25. IUPAC. *Compendium of Chemical Terminology ("Gold Book)*. Compiled by A. D. McNaught and A. Wilkinson. Blackwell Scientific Publications: Oxford, 1997.
26. Evans, D. F. The Determination of the Paramagnetic Susceptibility of Substances in Solution by Nuclear Magnetic Resonance. *J. Chem. Soc.* **1959**, 2003–2005.
27. Figgis, B.N.; Lewis, J. *The Magnetochemistry of Complex Compounds*; In Lewis, J. and Wilkins, R.G. *Modern Coordination Chemistry*. New York: Wiley, 2015.
28. Bhattacharya, P.; Krause, J. A.; Guan, H. Iron hydride complexes bearing phosphinite-based pincer ligands: synthesis, reactivity, and catalytic application in hydrosilylation reactions. *Organometallics* **2011**, *30*, 4720-4729.
29. Otting, G.; Soler, L. P.; Messerle, B. A. Measurement of Magnitude and Sign of Heteronuclear Coupling Constants in Transition Metal Complexes. *J. Magn. Reson.* **1999**, *137*, 413-429.
30. Bampos, N.; Field, L. D.; Messerle, B. A. Measurement of heteronuclear coupling constants in organometallic complexes using high-resolution 2D NMR. *Organometallics* **1993**, *12*, 2529-2535.

31. Klawitter, I.; Meyer, S.; Demeshko, S.; Meyer, F. Nickel(II) and Iron(II) Complexes with Tetradentate NHC/Amide Hybrid Ligands. *Zeitschrift für Naturforsch. B* **2013**, *68b*, 458–466.
32. Huckaba, A. J.; Hollis, T. K.; Howell, T. O.; Valle, H. U.; Wu, Y. Synthesis and Characterization of a 1,3-Phenylene-Bridged N-Alkyl Bis(benzimidazole) CCC-NHC Pincer Ligand Precursor: Homobimetallic Silver and Rhodium Complexes and the Catalytic Hydrosilylation of Phenylacetylene. *Organometallics* **2013**, *32*, 63–69.
33. Raynal, M.; Cazin, C. S. J.; Vallée, C.; Olivier-Bourbigou, H.; Braunstein, P. A New Stable C(NHC)—CH—C(NHC)N-Heterocyclic Dicarbene Ligand: Its Mono- and Dinuclear Ir(I) and Ir(I)-Rh(I) Complexes. *Dalton Trans.* **2009**, *19*, 3824–3832.
34. Haav, K.; Saame, J.; Kütt, A.; Leito, I. Basicity of Phosphanes and Diphosphanes in Acetonitrile. *European J. Org. Chem.* **2012**, *11*, 2167–2172.
35. Coe, B. J.; Glenwright, S. J. Trans-effects in octahedral transition metal complexes. *Coord. Chem. Rev.* **2000**, *203*, 5-80.
36. Gibson, D. H. Carbon dioxide coordination chemistry: metal complexes and surface-bound species. What relationships? *Coord. Chem. Rev.* **1999**, *185-186*, 335-355.
37. Fong, H.; Peters, J. C. Hydricity of an Fe-H Species and Catalytic CO₂ Hydrogenation. *Inorg. Chem.* **2015**, *54*, 5124-5135 and references therein.
38. Pangborn, A. B.; Giardello, M. A.; Grubbs, R. H.; Rosen, R. K.; Timmers, F. J. Safe and Convenient Procedure for Solvent Purification. *Organometallics* **1996**, *15*, 1518–1520.
39. Wietz, I. S.; Rabinovitz, M. The Application of C₈K for Organic Synthesis: Reduction of Substituted Naphthalenes. *J. Chem. Soc. Perkin Trans.* **1993**, *1*, 117-120.

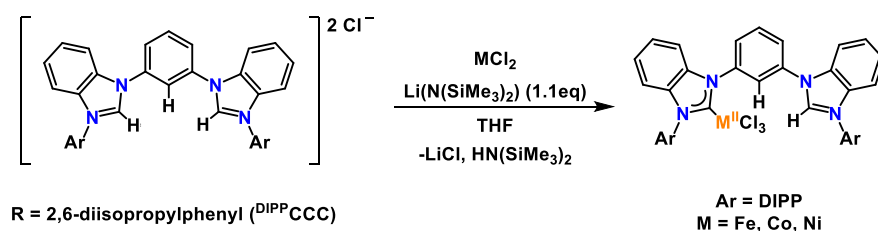
40. Li, Y.; Yang, L.; Chen, Q.; Cao, C.; Guan, P.; Pang, G.; Shi, Y. Synthesis, Structure, and Reactivity of Dicarbene Dipalladium Complexes. *Z. Anorg. Allg. Chem.*, **2013**, *639*, 575-581.
41. Dilworth, J. R.; Zheng, Y.; Griffiths, D. V. Binuclear complexes with ligands based on the 2,6-bis(diphenyl-phosphinomethyl)benzene framework. Syntheses and crystal structures of $[\text{Ir}_2\text{Cl}_2(\text{u-CO})\{2,6-(\text{Ph}_2\text{PCH}_2)_2\text{C}_6\text{H}_3\text{S}\}_2] \cdot 2\text{CH}_2\text{Cl}_2$, $[\text{Ni}_2\{2,6-(\text{Ph}_2\text{PCH}_2)_2\text{C}_6\text{H}_3\text{S}\}_2]9\text{PF}_6] \cdot \text{Et}_2\text{O} \cdot 0.5\text{CH}_2\text{Cl}_2$ and $[\text{Rh}_2\text{Cl}_2(\text{CO})_2\{1,3-\text{Ph}_2\text{PCH}_2)_2\text{C}_6\text{H}_4\}_2]$. *J. Chem. Soc., Dalton Trans.*, **1999**, *11*, 1877-1881.

Chapter 3

Extending the Metalation Methods

3.1 Zwitterionic Metalation Method

The new zwitterionic method of metalation with iron was successful in giving quantitative yield of the metalated complexes.¹ The extension of this method to other first-row transition metals would be beneficial since a major challenge facing the use of these ligands is their difficult and specific metalation. The method was first extended to nickel and cobalt since these metals have previously been shown to generate isolable pincer complexes with our ligand framework.²⁻⁴



Scheme 3.1. Synthesis of $\text{H}_2(\text{DIPPCCC})\text{M}(\text{II})\text{Cl}_3$ complexes.

The same procedure was used adding one equivalent of $\text{Li}(\text{N}(\text{SiMe}_3)_2)$ to $[\text{H}_3(\text{DIPPCCC})]\text{Cl}_2$ that was stirring in THF with the desired metal salt, $\text{M}(\text{II})\text{Cl}_2$ ($\text{M} = \text{Co}, \text{Ni}$) (Scheme 3.1). Both reactions changed color over several hours and the metal chloride salts, insoluble at first, went into solution as they reacted with the *in situ* generated carbene. The volatiles were removed under reduced pressure yielding a sticky residue that was dissolved using DCM or benzene, for cobalt and nickel respectively, and filtered over celite to remove the LiCl byproduct. The nickel zwitterionic complex, $\text{H}_2(\text{DIPPCCC})\text{Ni}(\text{II})\text{Cl}_3$, was much more soluble than its iron and cobalt analogues. The isolated complexes were a pale yellow for $\text{H}_2(\text{DIPPCCC})\text{Ni}(\text{II})\text{Cl}_3$ and a bright teal blue for $\text{H}_2(\text{DIPPCCC})\text{Co}(\text{II})\text{Cl}_3$. Investigating the latter by ^1H NMR spectroscopy revealed a broad, paramagnetic spectrum similar to the previously synthesized zwitterionic complex, $\text{H}_2(\text{DIPPCCC})\text{Fe}(\text{II})\text{Cl}_3$ (Figure 3.1). However, $\text{H}_2(\text{DIPPCCC})\text{Ni}(\text{II})\text{Cl}_3$, while still having somewhat

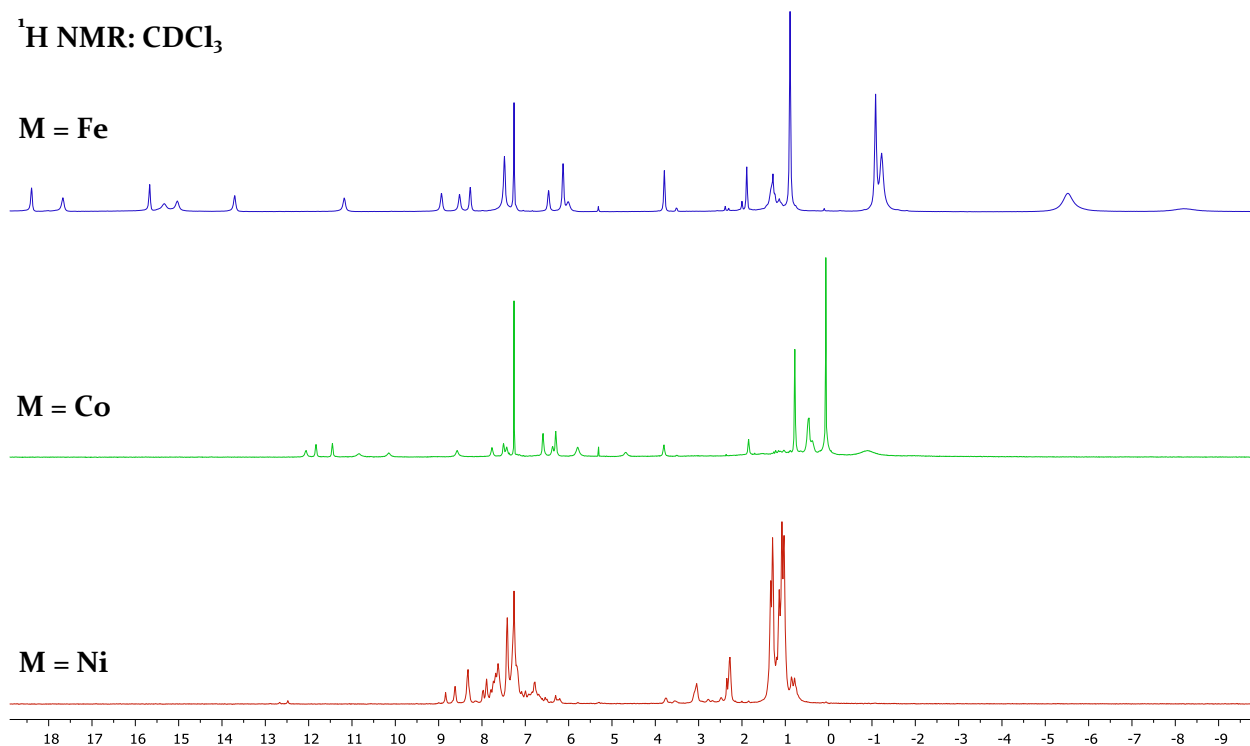
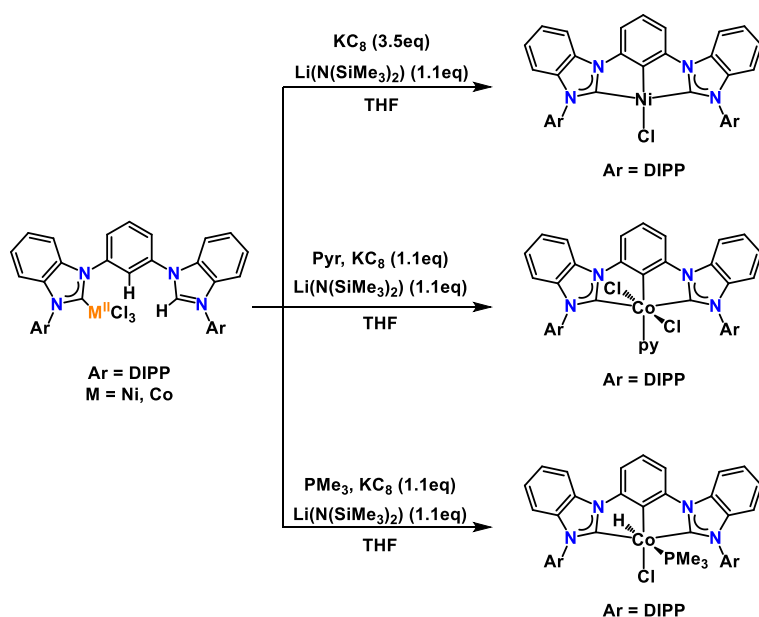


Figure 3.1. ¹H NMR spectra of H₂(^{DIPP}CCC)M(II)Cl₃ (M = Fe, Co, Ni).

broad resonances, is contained almost entirely within the diamagnetic window (Figure 3.1). This change in overall isotropic resonance shifts is likely due to the greater paramagnetic character of the Fe complex ($S = 2$) decreasing to Co ($S = 3/2$) and then Ni ($S = 1$) assuming a high-spin electronic configuration in a tetrahedral environment.⁵ While the complexes' increased solubility and change in color indicated a reaction occurred the salts, [H₃(^RCCC)]M(II)Cl₄, might have been synthesized instead. However, adding the metal salts, M(II)Cl₂ (M = Fe, Co, Ni), without base present did not lead to the same dramatic color changes nor the same ¹H NMR spectra.

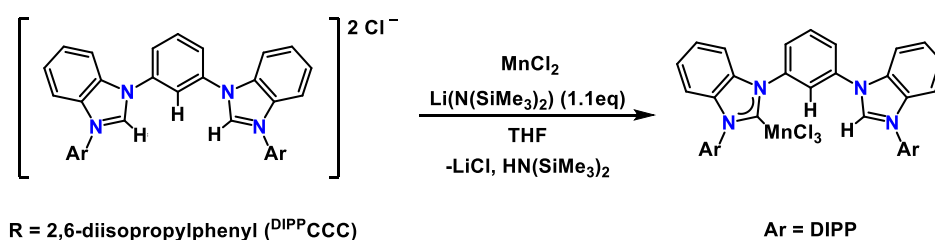
The zwitterionic complexes were then treated with a mixture of base (Li(N(SiMe₃)₂)) and reductant (KC₈). The nickel zwitterionic complex, H₂(^{DIPP}CCC)Ni(II)Cl₃, yielded (^{DIPP}CCC)Ni(II)Cl instead of the hydride likely due to the large amount of chloride present in solution as well as the hydride's inherent instability (Scheme 3.2). The ¹H NMR spectra matched the previously published complex.²



Scheme 3.2. Synthesis of $(^{\text{DIPP}}\text{CCC})\text{M}(\text{Cl}_x)(\text{L})$ complexes.

The reduction of $\text{H}_2(^{\text{DIPP}}\text{CCC})\text{Co}(\text{II})\text{Cl}_3$ required additional L-type ligands such as pyridine or PMe_3 . The addition of pyridine to the reaction yielded $(^{\text{DIPP}}\text{CCC})\text{Co}(\text{III})\text{Cl}_2\text{py}$. However, when PMe_3 was added the hydride complex, $(^{\text{DIPP}}\text{CCC})\text{Co}(\text{III})(\text{H})(\text{Cl})(\text{PMe}_3)$, was obtained instead (Scheme 3.2). The former complex had been previously independently synthesized and fully characterized but the latter species had only been synthesized using the $(^{\text{Mes}}\text{CCC})$ ligand. The ^1H NMR spectrum of $(^{\text{DIPP}}\text{CCC})\text{Co}(\text{III})\text{Cl}_2\text{py}$ matches the previously published complex.³ The ^1H NMR spectrum of $(^{\text{DIPP}}\text{CCC})\text{Co}(\text{III})(\text{H})(\text{Cl})(\text{PMe}_3)$ shows the hydridic resonance at -10.25 ppm ($J_{\text{P-H}} = 113$ Hz) as a doublet due to the phosphorus-hydride coupling compared to -10.0 ppm ($J_{\text{P-H}} = 109$ Hz) for $(^{\text{Mes}}\text{CCC})\text{Co}(\text{III})(\text{H})(\text{Cl})(\text{PMe}_3)$.⁴ The latter has been crystallographically characterized and shows the hydride and phosphorus in a trans configuration to each other. It can be assumed, therefore, that the diisopropylphenyl derivative has this same conformation due to the similar phosphorus-hydride coupling constants ($J_{\text{P-H}} = 113$ vs 109 Hz). All three complexes were obtained in quantitative yields through both reaction steps as was previously observed using iron.

After the successful synthesis of these complexes we turned our attention to the synthesis of the manganese complexes. The zwitterionic complex, $\text{H}_2(\text{DIPPCCC})\text{Mn}(\text{II})\text{Cl}_3$, was synthesized and characterized as a very faint yellow solid (Scheme 3.3). The zwitterionic complex is ^1H NMR silent but the color change and increased solubility indicates coordination of the metal to the carbene. Unfortunately, the *in situ* reduction of the manganese center using the previously described methodology did not appear to result in metalation of the ligand framework. The addition of various L-type ligands did not change this outcome as previously seen with cobalt. Other metalation methods were attempted but resulted in no discernible, isolable manganese complexes. Therefore, we decided to use transmetalation to attempt to coordinate manganese into these ligand frameworks.

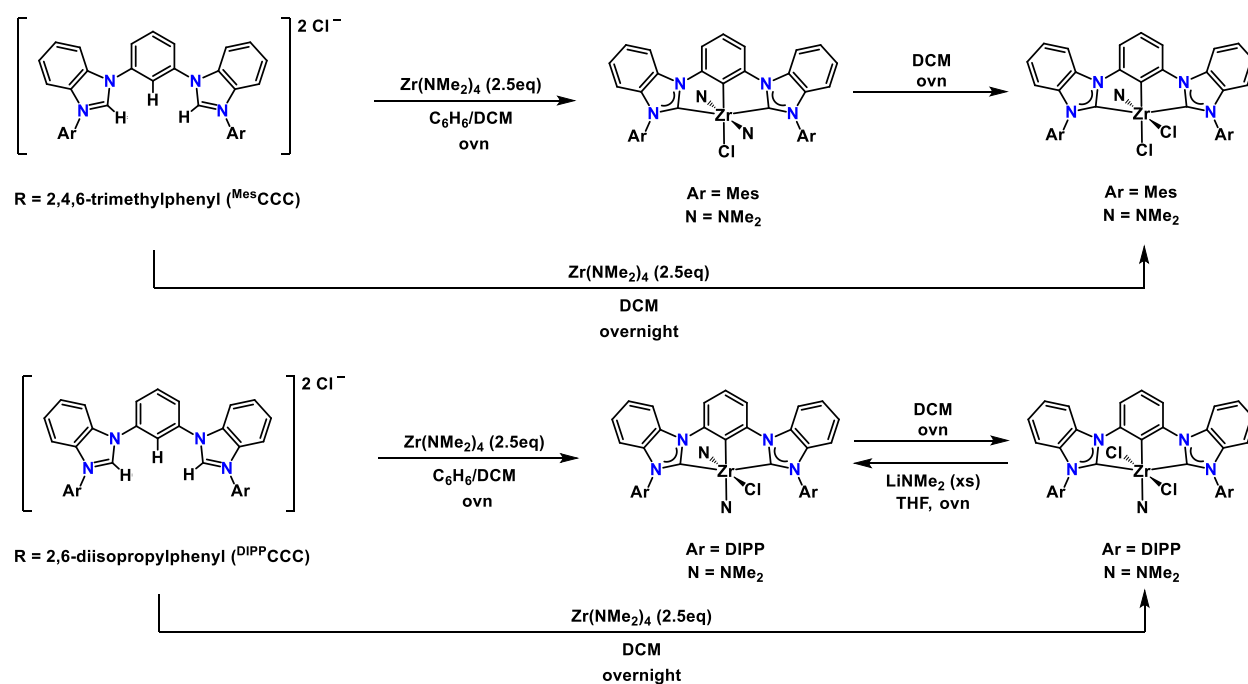


Scheme 3.3. Synthesis of $\text{H}_2(\text{DIPPCCC})\text{Mn}(\text{II})\text{Cl}_3$ complex.

3.2 Transmetalation Method using Zirconium

Transmetalation, the transfer of an organic group from one metal to another, is commonly invoked in many organic reactions including zirconium to other elements.⁶ However, zirconium pincer complexes have only been reported by Hollis and co-workers.⁶⁻¹⁰ This was accomplished by treating $[\text{H}_3(\text{}^n\text{BuCCC})]\text{I}_2$ ($\text{}^n\text{BuCCC}$ = 1,3-bis(1-butylimidazolium)benzene) with excess $\text{Zr}(\text{NMe}_2)_4$ to generate $(\text{}^n\text{BuCCC})\text{Zr}(\text{IV})\text{X}_3$ complexes. Hollis determined that the identity of the substituents on the zirconium complexes, halides or dimethylamides, was directly influenced by the metalation conditions. The group was also able to demonstrate transmetalation from these

zirconium complexes to cobalt, rhodium, palladium, and platinum.¹¹⁻¹⁷ Using similar reaction conditions $[\text{H}_3(\text{ArCCC})]\text{Cl}_2$ (Ar = DIPP or Mes) was treated with excess $\text{Zr}(\text{NMe}_2)_4$ in a benzene/DCM mixture. Zirconium complexes, $(\text{MesCCC})\text{Zr}(\text{IV})\text{Cl}(\text{NMe}_2)_2$ and $(\text{DIPPCCC})\text{Zr}(\text{IV})\text{Cl}(\text{NMe}_2)_2$, were obtained in quantitative yield (Scheme 3.4). Similar to Hollis' system a slight change in conditions led to the isolation of $(\text{MesCCC})\text{Zr}(\text{IV})\text{Cl}_2(\text{NMe}_2)$ and $(\text{DIPPCCC})\text{Zr}(\text{IV})\text{Cl}_2(\text{NMe}_2)$ instead (Scheme 3.4). Alternatively, stirring $(\text{ArCCC})\text{Zr}(\text{IV})\text{Cl}(\text{NMe}_2)_2$ (Ar = DIPP or Mes) with DCM overnight led to ligand exchange and the isolation of $(\text{ArCCC})\text{Zr}(\text{IV})\text{Cl}_2(\text{NMe}_2)$ (Ar = DIPP or Mes) (Scheme 3.4). Additionally, $(\text{DIPPCCC})\text{Zr}(\text{IV})\text{Cl}(\text{NMe}_2)_2$ could be regenerated from $(\text{DIPPCCC})\text{Zr}(\text{IV})\text{Cl}_2(\text{NMe}_2)$ with treating of excess LiNMe_2 in THF overnight (Scheme 3.4).



Scheme 3.4. Synthesis of $(\text{MesCCC})\text{Zr}(\text{IV})\text{X}_3$ (top) and $(\text{DIPPCCC})\text{Zr}(\text{IV})\text{X}_3$ (bottom).

Each of the zirconium complexes were characterized by ^1H NMR spectroscopy giving diamagnetic spectra (Figure 3.2). Integration of the spectra as well as the symmetry of the alkyl resonances helped to identify the geometry and identity of the products. The mesityl ligand variant,

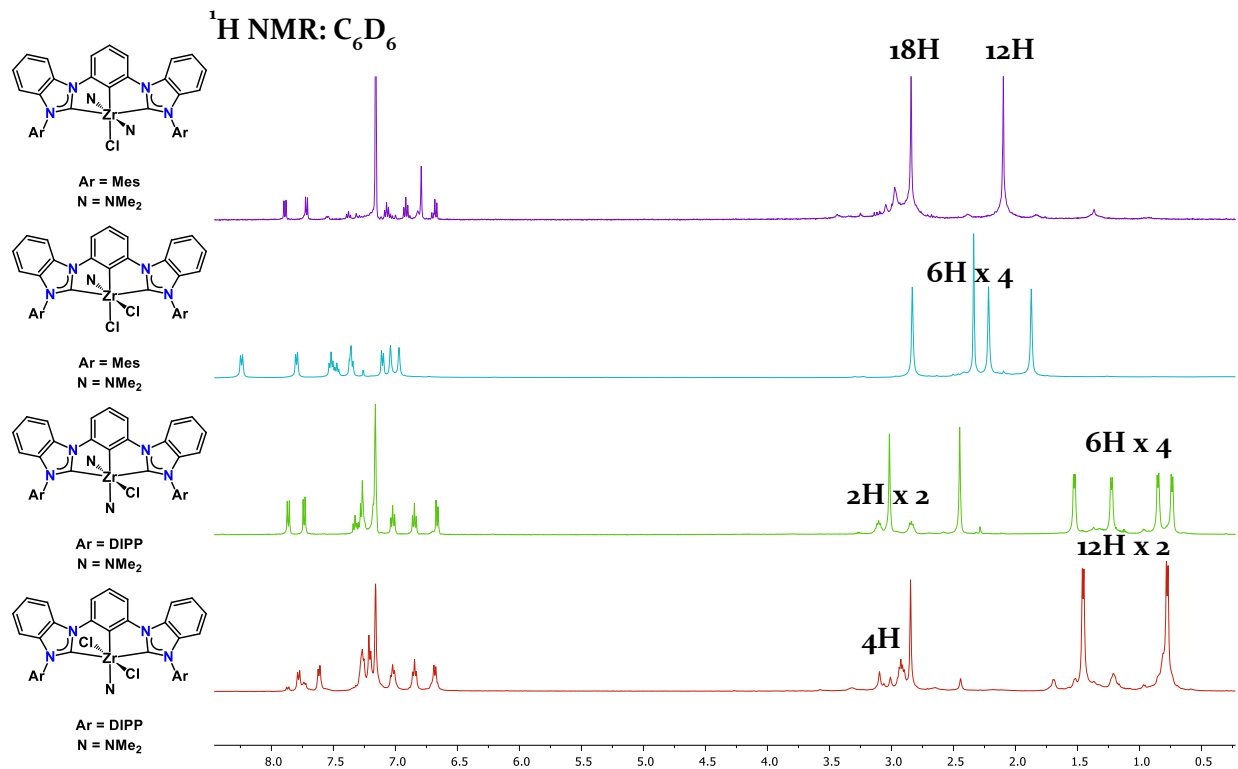


Figure 3.2. ^1H NMR spectra of $(^{\text{Mes}}\text{CCC})\text{Zr}(\text{IV})\text{Cl}(\text{NMe}_2)_2$ (top), $(^{\text{Mes}}\text{CCC})\text{Zr}(\text{IV})\text{Cl}_2(\text{NMe}_2)$ (second), $(^{\text{DIPP}}\text{CCC})\text{Zr}(\text{IV})\text{Cl}(\text{NMe}_2)_2$ (third), and $(^{\text{DIPP}}\text{CCC})\text{Zr}(\text{IV})\text{Cl}_2(\text{NMe}_2)$ (bottom).

$(^{\text{Mes}}\text{CCC})$, has three methyl groups that give either two (12H, 6H) or three resonances (6H x 3) based on whether the symmetry of the complex is C_2 or C_s , respectively. Similarly, the diisopropyl ligand variant, $(^{\text{DIPP}}\text{CCC})$, gives either a single septet (4H) and two doublet resonances (12H x 2) (C_2) or two septets (2H x 2) and four doublet resonances (6H x 4) (C_s). Any remaining alkyl resonances were attributed to either one or two dimethylamido groups. Interestingly, based on this information, the two ligands generate different isomers with the same formulas under identical reaction conditions. $(^{\text{Mes}}\text{CCC})\text{Zr}(\text{IV})\text{Cl}(\text{NMe}_2)_2$ gives a C_2 symmetric ^1H NMR spectra, based on the two methyl alkyl resonances, and a single overlapping peak integrates to two dimethylamido groups that must then be trans to one another (Figure 3.2, top). However, the $(^{\text{DIPP}}\text{CCC})\text{Zr}(\text{IV})\text{Cl}(\text{NMe}_2)_2$ complex, generated under the same reaction conditions, is C_s symmetric with two different resonances integrating to two dimethylamido groups indicating the

two must be in a cis configuration (Figure 3.2, third). This same trend is evident in $(^{\text{Mes}}\text{CCC})\text{Zr}(\text{IV})\text{Cl}_2(\text{NMe}_2)$ and $(^{\text{DIPP}}\text{CCC})\text{Zr}(\text{IV})\text{Cl}_2(\text{NMe}_2)$ where the former is C_s symmetric with the chlorides cis and the latter is C_2 symmetric with the chlorides trans to one another. Each ^1H NMR spectrum indicates a single dimethylamido group which in $(^{\text{Mes}}\text{CCC})\text{Zr}(\text{IV})\text{Cl}_2(\text{NMe}_2)$ must be trans to a chloride ligand and in $(^{\text{DIPP}}\text{CCC})\text{Zr}(\text{IV})\text{Cl}_2(\text{NMe}_2)$ must be trans to the aryl group of the ligand (Figure 3.2, second and bottom). This indicates that $(^{\text{Mes}}\text{CCC})$ prefers a configuration in which a chloride is trans to the phenyl backbone while $(^{\text{DIPP}}\text{CCC})$ prefers a dimethylamido ligand in that position. This could be attributed to either electronic or steric differences between the ligands or some combination of the two factors.

Characterization by X-ray crystallography was also carried out on $(^{\text{DIPP}}\text{CCC})\text{Zr}(\text{IV})\text{Cl}(\text{NMe}_2)_2$ to definitively determine the structure and, as identified by ^1H NMR spectroscopy, the chloride is axial to the plane of the ligand with the two dimethylamido groups cis to one another (Figure 3.3). Comparing

this structure to Hollis' complexes, $(^{\text{nBu}}\text{CCC})\text{Zr}(\text{IV})\text{X}_3$, show many similarities.⁷⁻¹⁰ The $\text{Zr}-\text{C}_{\text{NHC}}$ and $\text{Zr}-\text{C}_{\text{Ar}}$ bond lengths and bond angles are nearly identical among all the complexes but especially for its $(^{\text{nBu}}\text{CCC})\text{Zr}(\text{IV})\text{I}(\text{NMe}_2)_2$ congener with the same C_s symmetry as

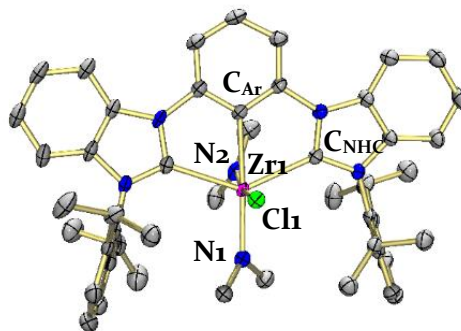
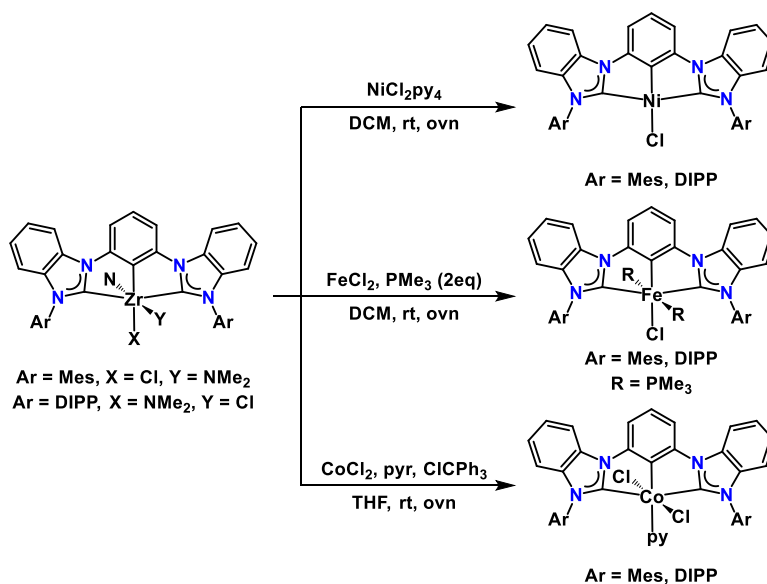


Figure 3.3. Molecular structure of $(^{\text{DIPP}}\text{CCC})\text{Zr}(\text{IV})\text{Cl}(\text{NMe}_2)_2$ shown with 50% probability ellipsoids. Solvent molecules and selected hydrogen atoms have been omitted for clarity.

$(^{\text{DIPP}}\text{CCC})\text{Zr}(\text{IV})\text{Cl}(\text{NMe}_2)_2$. The $\text{Zr}-\text{N}$ bond lengths are slightly longer in our complex which is likely due to the steric difference moving from n-butyl to diisopropylphenyl substituents.

Hollis reported the ability to generate his zirconium complexes *in situ* before undergoing transmetalation in one reaction vessel.¹¹⁻¹⁷ However, transmetalation to Fe, Co, or Ni did not occur upon the *in situ* generation of the zirconium complexes in our systems. Starting with the isolated zirconium complexes, on the other hand, led to easy transmetalation to Fe, Co, and Ni complexes using $(^{\text{Mes}}\text{CCC})\text{Zr}(\text{IV})\text{Cl}(\text{NMe}_2)_2$ and $(^{\text{DIPP}}\text{CCC})\text{Zr}(\text{IV})\text{Cl}(\text{NMe}_2)_2$ in quantitative yields (Scheme 3.5). Each of the product complexes were compared and matched by ^1H NMR spectroscopy to literature values except for $(^{\text{Mes}}\text{CCC})\text{Ni}(\text{II})\text{Cl}$ and $(^{\text{Mes}}\text{CCC})\text{Fe}(\text{II})\text{Cl}(\text{PMe}_3)_2$ which had not been previously reported. $(^{\text{Mes}}\text{CCC})\text{Ni}(\text{II})\text{Cl}$ was independently synthesized and the ^1H NMR spectrum of the transmetalated complex matched. $(^{\text{Mes}}\text{CCC})\text{Fe}(\text{II})\text{Cl}(\text{PMe}_3)_2$ has a single ^{31}P NMR resonance at 18.04 ppm indicating a C_2 symmetric complex which is corroborated by the ^1H NMR spectrum containing two alkyl mesityl resonances and a single broad PMe_3 resonance (See 3.3 Experimental). The zirconium bis(chloride) complexes, $(^{\text{Mes}}\text{CCC})\text{Zr}(\text{IV})\text{Cl}_2(\text{NMe}_2)$ and $(^{\text{DIPP}}\text{CCC})\text{Zr}(\text{IV})\text{Cl}_2(\text{NMe}_2)$, however, did not undergo transmetalation which could indicate increased insolubility or ligand substituents play an important role during transmetalation.



Scheme 3.5. Synthesis of $(^{\text{R}}\text{CCC})\text{M}(\text{II/III})(\text{Cl})_x(\text{L})_y$ complexes.

These transmetalation reactions offer an alternative metalation strategy compared to traditional methods for these CCC ligand frameworks. Our group has been able to develop other high yielding metalation methods, but they often require very specific conditions. The metalation methodology, even between the two similar ligand frameworks (^{Mes}CCC) and (^{DIPP}CCC), can require contrasting conditions and generate different final complexes. The zirconium transmetalation reactions were identical and essentially quantitative for each of the metals studied for either of the ligand frameworks. This method offers a very straightforward route to the metal complexes without extensive optimization of reaction parameters. It could likely be extended to other ligand derivatives as well, as changing the R-groups appended to the NHCs did not require a change in metalation conditions. Throughout the synthesis of these complexes it did not appear that any L₂M complexes were formed. This can likely be attributed to the more sterically hindered aryl groups off the NHCs which discourages the formation of these undesired products compared to Hollis' much smaller butyl groups where L₂M (M = Co) complexes could be isolated depending upon the transmetalation conditions.^{15,16}

Once the transmetalation methodology had been developed and verified on known complexes we attempted to metalate using manganese and copper. The zirconium complexes, (^{Ar}CCC)Zr(IV)Cl(NMe₂)₂ (Ar = Mes, DIPP), were treated with a variety of Mn and Cu metal sources along with various L-type ligands. No clearly identifiable complexes were able to be isolated and most often the zirconium starting complexes were re-isolated at the end indicating a complete lack of transmetalation occurring. Given the propensity of zirconium to transmetalate to copper in the literature it was somewhat surprising that we were not able to isolate the copper complexes.⁶ The relative electronegativity of Fe (1.83), Co (1.88), Ni (1.91), and Cu (1.90) varies only by 0.07 points which should indicate similar transmetalation reactivity.¹⁸ However, the use

of an electron rich, rigid pincer ligand could have contributed to the lack of transmetalation to copper. Again, examining the electronegativity differences, it is possible that Mn (1.55) is too similar to Zr (1.33) to undergo this transmetalation.¹⁸

The extension of the zwitterionic metalation methodology to cobalt and nickel has been accomplished in quantitative yields. The synthesis and characterization of four different zirconium complexes was undertaken and transmetalation to iron, cobalt, and nickel was observed for both the (^{Mes}CCC) and (^{DIPP}CCC) ligands. Unfortunately, these methods were not amenable to manganese and copper. However, this work represents the first time these zwitterionic complexes have been isolated, characterized, and subsequently reduced *in situ* to give the fully metalated complexes. It also represents the first report of transmetalation from zirconium to iron and one of the few nickel and cobalt examples.

3.3 Experimental Section

General Considerations. All air- and moisture-sensitive manipulations were performed using an MBraun inert atmosphere drybox with an atmosphere of nitrogen. The MBraun drybox was equipped with one -35 °C freezer for cooling samples and crystallizations. Solvents for sensitive manipulations were dried and deoxygenated on a Glass Contour System (SG Water USA, Nashua, NH) and stored over 4 Å molecular sieves purchased from Strem following literature procedure prior to use.¹⁹ Cobalt (II) chloride anhydrous (98%) and nickel (II) chloride anhydrous (98%) were purchased from Strem and used as received. Trimethylphosphine (1.0 M in THF) and pyridine (99.8%) were purchased from Sigma-Aldrich and used as received. Triphenylphosphine (≥ 95% (GC)) was purchased from Sigma-Aldrich and recrystallized using ethanol and dried before use. Lithium hexamethyldisilazide was purchased from Sigma-Aldrich and recrystallized under an inert atmosphere using toluene prior to use. Zirconium (IV) dimethylamide was purchased from

Oakwood and sublimed under a nitrogen atmosphere prior to use, clean Zr starting material was essential to generate the complexes cleanly. Potassium graphite,²⁰ and ^{DIPP}CCC (^{DIPP}CCC = bis(diisopropylphenyl-imidazol-2-ylidene)phenyl) ligand³ were prepared according to literature procedures. Chloroform-*d*, tetrahydrofuran-*d*₈, and benzene-*d*₆ were purchased from Cambridge Isotope Labs and were degassed and stored over 4 Å molecular sieves prior to use. Celite® 545 (J. T. Baker) was dried in a Schlenk flask for 24 h under dynamic vacuum while heating to at least 150 °C prior to use in a glovebox. ¹H, ¹³C, and ³¹P NMR spectra were recorded on a Varian spectrometer operating at 500 MHz (¹H NMR), 126 MHz (¹³C NMR), and 202.4 MHz (³¹P NMR) at ambient temperature. All chemical shifts were reported relative to the peak of the residual solvent as a standard.

Preparation of H₂(^{DIPP}CCC)Co(II)Cl₃. A 20 mL scintillation vial was charged with [H₃(^{DIPP}CCC)]Cl₂ (0.071 g, 0.101 mmol) and approximately 2 mL of THF. In two separate vials, an equivalent of CoCl₂ (0.013 g, 0.101 mmol) and 1.1 equivalents of Li(N(SiMe₃)₂) (0.019 g 0.111 mmol) were dissolved in approximately 2 mL of THF each. The CoCl₂ was added to the off-white solution of ligand and the Li(N(SiMe₃)₂) was added drop-wise to the solution, resulting in an instantaneous color change to light blue. After stirring for 3 hours, the color of the solution was bright teal. The solvent was removed under reduced pressure and the teal residue was dissolved in DCM, placed in the freezer at -35 °C for 5 minutes, filtered over celite, and the solvent again removed under reduced pressure. The product, H₂(^{DIPP}CCC)Co(II)Cl₃ was isolated as a bright teal blue powder (0.08 g, 0.101 mmol, >99 %). ¹H NMR (CDCl₃, 500 MHz): δ = 12.06, 11.83, 11.45, 10.83, 10.15, 8.57, 7.77, 7.50, 7.43, 6.59, 6.37, 6.30, 5.79, 4.67, 0.78, 0.47, 0.45, 0.06, -0.93. HRMS (ESI), calc. for C₄₄H₄₉Cl₂CoN₄O (M – Cl)⁺: 779.74; found 781.3.

Preparation of $\text{H}_2(\text{DIPPCCC})\text{Ni}(\text{II})\text{Cl}_3$. A 20 mL scintillation vial was charged with $[\text{H}_3(\text{DIPPCCC})]\text{Cl}_2$ (0.071 g, 0.101 mmol) and approximately 2 mL of THF. In two separate vials, an equivalent of NiCl_2 (0.013 g, 0.101 mmol) and 1.1 equivalents of $\text{Li}(\text{N}(\text{SiMe}_3)_2)$ (0.019 g 0.111 mmol) were dissolved in approximately 2 mL of THF each. The NiCl_2 was added to the off-white solution of ligand and the $\text{Li}(\text{N}(\text{SiMe}_3)_2)$ was added drop-wise to the solution, resulting in an instantaneous color change to yellow. After stirring for 3 hours the solvents were removed under reduced pressure and the yellow residue was dissolved in DCM, placed in the freezer at $-35\text{ }^\circ\text{C}$ for 5 minutes, filtered over celite, and the solvent again removed under reduced pressure. The product, $\text{H}_2(\text{DIPPCCC})\text{Ni}(\text{II})\text{Cl}_3$ was isolated as a pale yellow solid (0.077 g, 0.097 mmol, 96 %). ^1H NMR (CDCl_3 , 500 MHz): $\delta = 8.84, 8.63, 8.32, 7.97, 7.89, 7.74, 7.63, 7.42, 7.21, 6.78, 3.05, 2.28, 1.34, 1.29, 1.14, 1.07, 1.03, 0.85, 0.79$. HRMS (ESI), calc. for $\text{C}_{44}\text{H}_{47}\text{Cl}_3\text{N}_4\text{Ni}$ (M) $^+$: 796.93, found 796.40.

Preparation of $(\text{DIPPCCC})\text{Ni}(\text{II})\text{Cl}$. A 20 mL scintillation vial was charged with $\text{H}_2(\text{DIPPCCC})\text{NiCl}_3$ (0.030 g, 0.038 mmol) and approximately 2 mL of toluene. $\text{Li}(\text{N}(\text{SiMe}_3)_2)$ (0.007 g, 0.042 mmol, 1.1eq) was dissolved separately in 1 mL of toluene. Three and a half equivalents of potassium graphite (0.018 g, 0.133 mmol) was dissolved in 2 mL of THF. The $\text{Li}(\text{N}(\text{SiMe}_3)_2)$ was added to the vial of KC_8 and the mixture was slowly added dropwise to the complex. The reaction was stirred at room temperature overnight and the volatiles removed under reduced pressure. The precipitate was washed with pentane over celite and then dissolved in benzene. The volatiles were removed under pressure from the filtrate and the product as an orange-yellow solid was obtained in quantitative yield (0.031 g, 0.099 mmol, 98 %). ^1H NMR (C_6D_6 , 500 MHz): $\delta = 7.52$ (d, $J = 7.8$, 2H), 7.26-7.11 (m, 9H), 7.00 (t, $J = 7.9$, 2H), 6.82 (t, $J = 7.9$, 2H), 6.61

(d, $J = 8.8$ Hz, 2H), 2.64 (sept, $J = 6.6$ Hz, 4H), 1.47 (d, $J = 6.7$, 12H), 0.88 (d, $J = 6.6$, 12H). Matches literature compound.²

Preparation of $(\text{DIPPCCC})\text{Co}(\text{III})\text{Cl}_2(\text{Py})$. A 20 mL scintillation vial was charged with $\text{H}_2(\text{DIPPCCC})\text{Co}(\text{II})\text{Cl}_3$ (0.030 g, 0.038 mmol), pyridine (5 drops), and approximately 2 mL of toluene. $\text{Li}(\text{N}(\text{SiMe}_3)_2)$ (0.007 g, 0.042 mmol, 1.1eq) and potassium graphite (0.006 g, 0.042 mmol, 1.1eq) were dissolved separately in 2 mL of THF. The $\text{Li}(\text{N}(\text{SiMe}_3)_2)$ was added to the vial of KC_8 and the mixture was then slowly added dropwise to the complex. The reaction was stirred at room temperature overnight and the volatiles removed under reduced pressure. The solid was washed with hexanes and benzene to remove impurities and then dissolved in DCM and filtered over celite. The volatiles were removed under reduced pressure from the filtrate and the product as a green solid was obtained in quantitative yield (0.032 g, 0.038 mmol, >99 %). ^1H NMR (CDCl_3 , 500 MHz): $\delta = 8.82$ (d, $J = 4.8$ Hz, 2H), 8.27 (d, $J = 8.2$ Hz, 2H), 7.88 (d, $J = 7.8$ Hz, 2H), 7.55 (t, $J = 7.8$ Hz, 1H), 7.41 (t, $J = 7.6$ Hz, 2H), 7.21 (t, $J = 7.8$ Hz, 2H), 7.16 (t, $J = 7.7$ Hz, 4H), 6.96 (d, $J = 7.8$ Hz, 4H), 6.76 (d, $J = 8.1$ Hz, 2H), 6.41 (t, $J = 6.4$ Hz, 2H), 2.68 (septet, $J = 6.6$ Hz, 4H), 0.98 (d, $J = 6.5$ Hz, 12H), 0.68 (d, $J = 6.7$ Hz, 12H). Matches literature compound.³

Preparation of $(\text{DIPPCCC})\text{Co}(\text{III})\text{H}(\text{Cl})(\text{PMe}_3)$. A 20 mL scintillation vial was charged with $\text{H}_2(\text{DIPPCCC})\text{Co}(\text{II})\text{Cl}_3$ (0.030 g, 0.038 mmol), PMe_3 (0.038 mL, 0.038 mmol), and approximately 2 mL of toluene. $\text{Li}(\text{N}(\text{SiMe}_3)_2)$ 1.1 equivalents (0.007 g, 0.042 mmol) and 1.1 equivalents of potassium graphite (0.006 g, 0.042 mmol) were dissolved separately in 2 mL of THF. The $\text{Li}(\text{N}(\text{SiMe}_3)_2)$ was added to the vial of KC_8 and the mixture was then slowly added dropwise to the first solution. The reaction was stirred at room temperature overnight and the volatiles removed under reduced pressure. The solid was washed with hexanes to remove impurities and then dissolved in benzene and filtered over celite. The volatiles were removed under reduced pressure

from the filtrate and the product was obtained as a red solid (0.030 g, 0.037 mmol, 98 %). ^1H NMR (C_6D_6 , 500 MHz): $\delta = 7.72$ (d, $J = 6.8$ Hz, 2H), 7.63 (m, 1H), 7.42 (d, $J = 6.4$ Hz, 2H), 7.27 (m, 2H), 7.03 (d, $J = 8.9$ Hz, 4H), 6.86 (d, $J = 6.8$ Hz, 4H), 6.64 (d, $J = 7.5$ Hz, 2H), 3.12 (sept, $J = 6$ Hz, 2H), 2.63 (sept, $J = 6$ Hz, 2H), 1.36 (m, 12H), 1.00 (s, 9H), 0.70 (m, 12H), -10.25 (d, $J = 113$ Hz, 1H). ^{13}C NMR (C_6D_6 , 126 MHz): $\delta = 147.27, 146.21, 145.72, 140.94, 134.58, 131.19, 129.68, 128.59, 124.47, 123.26, 123.09, 122.39, 122.27, 112.26, 110.30, 107.28, 29.13, 28.73, 25.31, 24.39, 24.64, 24.05, 13.77, 13.61$. HRMS (ESI), calc. for $\text{C}_{47}\text{H}_{54}\text{ClCoN}_4\text{P}$ ($\text{M} - \text{H}$) $^+$: 799.31; found 799.31. Similar to $(^{\text{Mes}}\text{CCC})\text{Co}(\text{III})\text{H}(\text{Cl})(\text{PMe}_3)$ in the literature.⁴

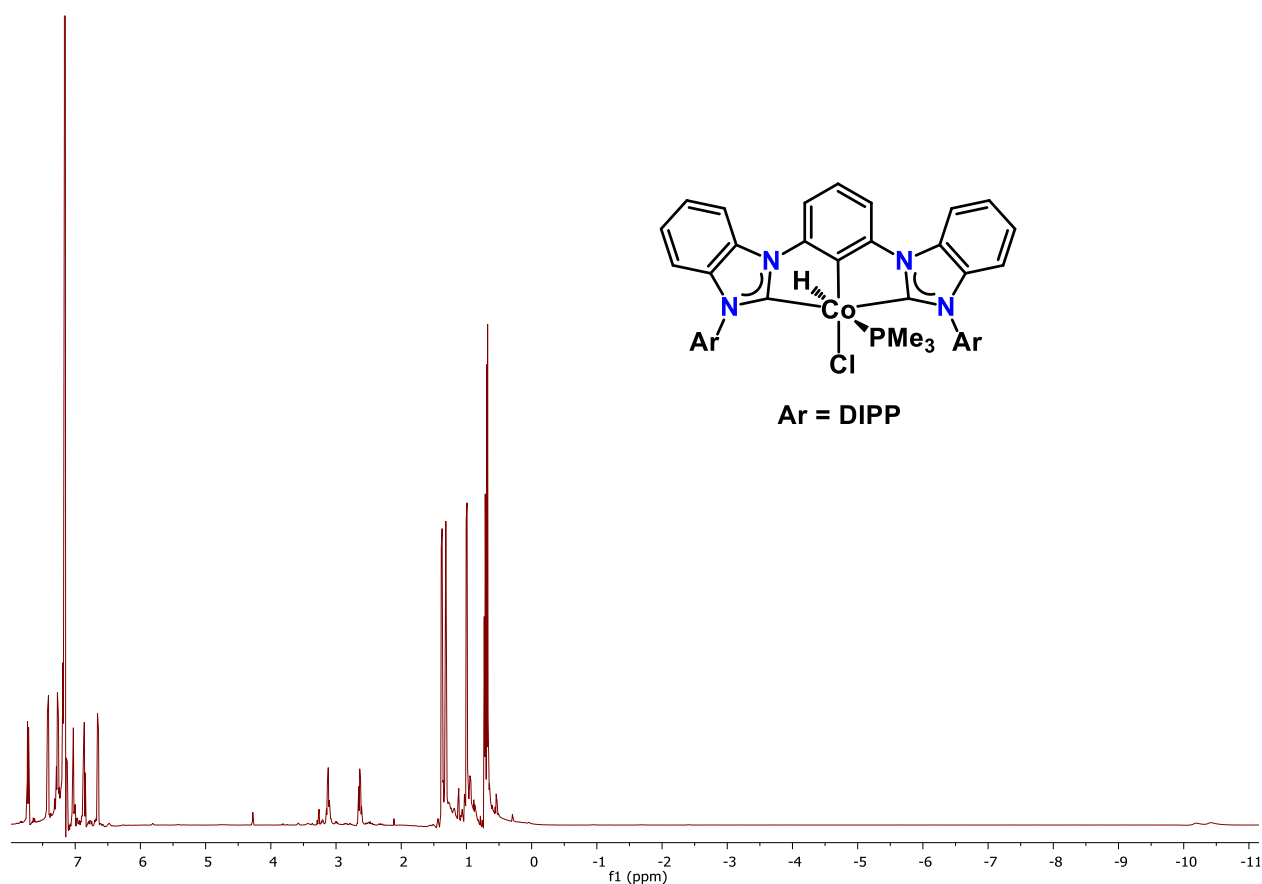


Figure 3.4. ^1H NMR spectrum of $(^{\text{DIPP}}\text{CCC})\text{Co}(\text{III})\text{H}(\text{Cl})(\text{PMe}_3)$ (C_6D_6).

Preparation of $(^{\text{Mes}}\text{CCC})\text{Zr}(\text{IV})\text{Cl}(\text{NMe}_2)_2$. A 20 mL scintillation vial was charged with $[\text{H}_3(^{\text{Mes}}\text{CCC})]\text{Cl}_2$ (0.030 g, 0.048 mmol) and 3 mL of benzene and placed in a -35 °C freezer until frozen. Two and a half equivalents of $\text{Zr}(\text{NMe}_2)_4$ (0.032 g, 0.121 mmol) was dissolved in a minimal

amount of DCM and placed in a -35 °C freezer for 5 minutes. The DCM solution was then added dropwise to the frozen benzene solution and warmed to room temperature. The reaction was stirred at room temperature overnight. The solvents were removed under reduced pressure and a hexanes/diethyl ether mixture (2 mL) was added to the yellow solid and stirred for 30 minutes. The reaction mixture was filtered over celite, discarding the wash, and the remaining yellow solid was dissolved in benzene. The volatiles were removed under reduced pressure yielding (^{Mes}CCC)Zr(IV)Cl(NMe₂)₂ as a pale yellow solid in excellent yield (0.035 g, 0.046 mmol, 96 %). ¹H NMR (C₆D₆, 500 MHz): δ = 7.92 (d, J = 8.4 Hz, 2H), 7.74 (d, J = 7.9 Hz, 2H), 7.43 (t, J = 7.8 Hz, 1H), 7.10 (t, J = 7.5 Hz, 2H), 6.93 (t, J = 7.9 Hz, 2H), 6.81 (s, 4H), 6.67 (d, J = 8.1 Hz, 2H), 2.80 (s, 12H), 2.11 (s, 6H), 2.05 (s, 12H). ¹³C NMR (CDCl₃, 126 MHz): δ = 204.46, 149.52, 139.28, 136.99, 136.00, 133.39, 131.98, 129.48, 128.59, 124.85, 124.76, 124.34, 124.05, 114.47, 113.03, 112.21, 111.84, 43.90, 21.04, 17.95. HRMS (ESI), calc. for C₃₈H₃₃ClN₄Zr (M – (NMe₂)₂)⁺: 670.14; found 670.36.

Preparation of (^{Mes}CCC)Zr(IV)Cl₂(NMe₂). A 20 mL scintillation vial was charged with [H₃(^{Mes}CCC)]Cl₂ (0.030 g, 0.048 mmol) and 3 mL of DCM and placed in a -35 °C freezer. Two and a half equivalents of Zr(NMe₂)₄ (0.032 g, 0.121 mmol) was dissolved in a minimal amount of DCM and placed in a -35 °C freezer for 5 minutes. The zirconium was then added dropwise to the ligand and warmed to room temperature. The reaction was stirred at room temperature overnight. The solvents were removed under reduced pressure and diethyl ether (2 mL) was added to the off-white solid and stirred for 30 minutes. The reaction mixture was filtered over celite, discarding the ether wash, and the remaining yellow solid was dissolved in DCM. The volatiles were removed under reduced pressure yielding (^{Mes}CCC)Zr(IV)Cl₂(NMe₂) as a yellow solid in excellent yield (0.036 g, 0.048 mmol, 100 %). Alternatively, if (^{Mes}CCC)Zr(IV)Cl(NMe₂)₂ is stirred with DCM

overnight almost complete conversion to (^{Mes}CCC)Zr(IV)Cl₂(NMe₂) can be seen. ¹H NMR (CDCl₃, 500 MHz): δ = 8.24 (d, J = 8.3 Hz, 2H), 7.80 (d, J = 7.8 Hz, 2H), 7.52 (t, J = 7.7 Hz, 2H), 7.47 (t, J = 8 Hz, 1H), 7.36 (t, J = 7.7 Hz, 2H), 7.10 (d, J = 8 Hz, 2H), 7.04 (s, 2H), 6.97 (s, 2H), 2.83 (s, 6H), 2.34 (s, 6H), 2.22 (s, 6H), 1.87 (s, 2H). ¹³C NMR (CDCl₃, 126 MHz): δ = 202.61, 167.68, 149.03, 139.94, 137.58, 135.83, 135.31, 131.91, 131.32, 130.24, 129.01, 128.75, 128.48, 125.15, 124.58, 113.90, 112.51, 112.41, 45.30, 21.43, 18.57, 17.17. HRMS (ESI), calc. for C₃₈H₃₃ClN₄Zr (M – (NMe₂)₂)⁺: 670.14; found 669.20.

Preparation of (^{DIPP}CCC)Zr(IV)Cl(NMe₂)₂. A 20 mL scintillation vial was charged with [H₃(^{DIPP}CCC)]Cl₂ (0.030 g, 0.043 mmol) and 3 mL of benzene and placed in a -35 °C freezer until frozen. Two and a half equivalents of Zr(NMe₂)₄ (0.029 g, 0.107 mmol) was dissolved in a minimal amount of DCM and placed in a -35 °C freezer for 5 minutes. The DCM solution was then added dropwise to the frozen benzene solution and warmed to room temperature. The reaction was stirred at room temperature overnight. The solvents were removed under reduced pressure and hexanes (2 mL) was added to the bright yellow solid and stirred for 30 minutes. The reaction mixture was filtered over celite, discarding the hexanes wash, and the remaining pale-yellow solid was dissolved in benzene. The volatiles were removed under reduced pressure yielding (^{DIPP}CCC)Zr(IV)Cl(NMe₂)₂ as a pale-yellow solid in excellent yield (0.034 g, 0.041 mmol, 95 %). ¹H NMR (C₆D₆, 500 MHz): δ = 7.88 (d, J = 8.2 Hz, 2H), 7.74 (d, J = 8.0 Hz, 2H), 7.32 (t, J = 7.9 Hz, 1H), 7.27 (m, 4H), 7.19 (m, 2H), 7.03 (t, J = 8.2 Hz, 2H), 6.85 (t, J = 8.0 Hz, 2H), 6.68 (d, J = 8.1 Hz, 2H), 3.11 (septet, J = 6.0 Hz, 2H), 3.02, (s, 6H), 2.84 (septet, J = 6.3 Hz, 2H), 2.44 (s, 6H), 1.52 (d, J = 5.9 Hz, 6H), 1.23 (d, J = 6.1 Hz, 6H), 0.85 (d, J = 6.1 Hz, 6H), 0.74 (d, J = 6.3 Hz, 6H). ¹³C NMR (C₆D₆, 126 MHz): δ = 205.80, 174.82, 149.22, 138.14, 133.65 131.78, 130.61,

128.59, 126.92, 125.50, 124.46, 124.01, 123.23 114.36, 113.62, 112.94, 46.89, 41.43, 28.76, 26.13, 25.72, 24.25, 23.76. HRMS (ESI), calc. for $C_{45}H_{48}N_4Zr$ (M)⁺: 719.24, found 719.48.

Preparation of $(^{DIPP}CCC)Zr(IV)Cl_2(NMe_2)$. A 20 mL scintillation vial was charged with $[H_3(^{DIPP}CCC)]Cl_2$ (0.030 g, 0.043 mmol) and 3 mL of DCM and placed in a -35 °C freezer. Two and a half equivalents of $Zr(NMe_2)_4$ (0.029 g, 0.107 mmol) was dissolved in a minimal amount of DCM and placed in a -35 °C freezer for 5 minutes. The zirconium was then added dropwise to the ligand and warmed to room temperature. The reaction was stirred at room temperature overnight. The solvents were removed under reduced pressure and diethyl ether (2 mL) was added to the off-white solid and stirred for 30 minutes. The reaction mixture was filtered over celite, discarding the ether wash, and the remaining yellow solid was dissolved in benzene. The volatiles were removed under reduced pressure yielding $(^{DIPP}CCC)Zr(IV)Cl_2(NMe_2)$ as a pale yellow solid in excellent yield (0.033 g, 0.040 mmol, 92 %). ¹H NMR (C_6D_6 , 500 MHz): δ = 7.78 (d, J = 8.4 Hz, 2H), 7.62 (d, J = 7.8 Hz, 2H), 7.27 (m, 5H), 7.21 (d, J = 7.5 Hz, 2H), 7.02 (t, J = 7.5 Hz, 2H), 6.85 (t, J = 7.3 Hz, 2H), 6.68 (d, J = 7.8 Hz, 2H), 2.92 (septet, J = 7 Hz, 4H), 2.85 (s, 6H), 1.45 (d, J = 6.3 Hz, 12H), 0.78 (d, J = 6.6 Hz, 12H). ¹³C NMR (C_6D_6 , 126 MHz): δ = 201.27, 170.77, 149.28, 147.94, 147.52, 137.25, 133.12, 131.43, 130.72, 128.59, 125.38, 124.96, 124.90, 124.65, 123.82, 114.62, 113.82, 113.19, 45.62, 28.85, 26.14, 23.75. HRMS (ESI), calc. for $C_{44}H_{45}Cl_2N_4Zr$ (M - (NMe₂))⁺: 792.00; found 793.23.

General Preparation of $(^RCCC)MCl_2L_y$ from $(^RCCC)Zr(IV)Cl(NMe_2)_2$. A 20 mL scintillation vial was charged with 25 mg of $(^RCCC)Zr(IV)Cl(NMe_2)_2$ and dissolved in 2 mL of DCM or THF. The desired L-type ligand (PMe₃ for Fe, pyridine for Co) was added to the dissolved zirconium complex. The M(II)Cl₂ (1 equiv.) was dissolved or suspended in DCM or THF and added dropwise to the solution. In the case for cobalt ClCPh₃ (1 equiv.) was dissolved in THF and added dropwise

after 5 minutes. The reaction was then stirred overnight at room temperature. The volatiles were removed under reduced pressure and the resulting precipitate was washed with hexanes and diethyl ether to remove any zirconium byproducts. The solid was then dissolved in benzene (DCM for cobalt) and filtered over celite. Removing the solvent resulted in the isolation of a colored solid in quantitative yield. The ^1H NMR spectra were compared and matched to published literature values or other independent synthesis, again except for $(^{\text{Mes}}\text{CCC})\text{Fe}(\text{II})\text{Cl}(\text{PMe}_3)_2$. The yields and ^1H NMR resonance values are given for each complex below.

Preparation of $(^{\text{DIPP}}\text{CCC})\text{Ni}(\text{II})\text{Cl}$. Yield (0.022 g, 0.030 mmol, >99 %). ^1H NMR (CDCl_3 , 500 MHz): $\delta = 7.51$ (d, $J = 8.2$ Hz, 2H), 7.22 (m, 3H), 7.16 (m, 2H), 7.13 (d, $J = 7.8$ Hz, 4H), 7.00 (t, $J = 8.3$ Hz, 2H), 6.82 (t, $J = 7.9$ Hz, 2H), 6.60 (d, $J = 8.1$ Hz, 2H), 2.64 (septet, $J = 6.9$ Hz, 4H), 1.47 (d, $J = 6.8$ Hz, 12H), 0.87 (d, $J = 6.9$ Hz, 12H). This complex was matched to literature values.²

Preparation of $(^{\text{Mes}}\text{CCC})\text{Ni}(\text{II})\text{Cl}$. Yield (0.021 g, 0.033 mmol, >99 %). This complex was later independently synthesized via regular metalation methods giving the same ^1H NMR spectrum. ^1H NMR (THF-d_8 , 500 MHz): $\delta = 8.25$ (d, $J = 8.2$ Hz, 2H), 7.63 (d, $J = 7.7$ Hz, 2H), 7.53 (t, $J = 7.6$ Hz, 2H), 7.45 (t, $J = 7.4$ Hz, 1H), 7.31 (t, $J = 7.4$ Hz, 2H), 6.80 (d, $J = 8.2$ Hz, 2H), 6.77 (s, 4H), 2.24 (s, 6H), 1.88 (s, 12H). ^{13}C NMR (THF-d_8 , 126 MHz): $\delta = 184.37, 148.73, 140.22, 136.45, 135.34, 130.57, 130.41, 128.82, 126.29, 125.20, 112.71, 112.21, 110.09, 21.04, 17.54$. HRMS (ESI), calc. for $\text{C}_{38}\text{H}_{33}\text{N}_4\text{Ni}$ ($\text{M} - \text{Cl}$)⁺: 603.20, found 603.21.

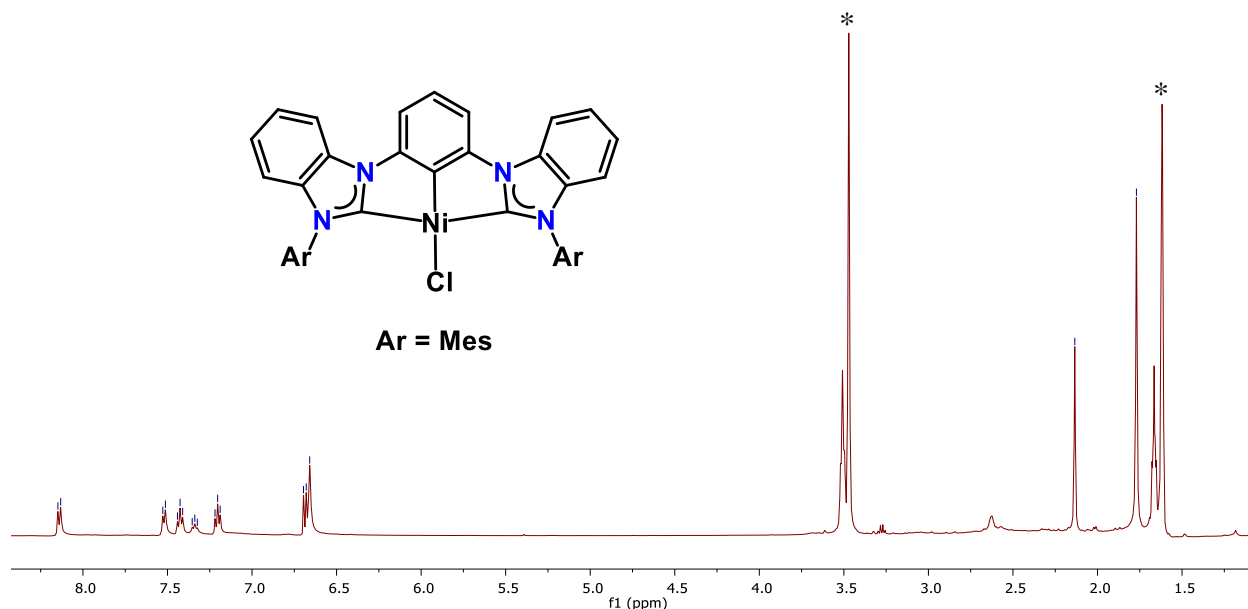


Figure 3.5. ^1H NMR spectrum of $(^{\text{Mes}}\text{CCC})\text{Ni}(\text{II})\text{Cl}$ (THF-d_8), *indicates solvent.

Preparation of $(^{\text{DIPP}}\text{CCC})\text{Fe}(\text{II})\text{Cl}(\text{PMe}_3)_2$. Yield (0.025 g, 0.029 mmol, 98 %). ^1H NMR (CDCl_3 , 500 MHz): $\delta = 7.90$ (d, $J = 7.9$ Hz, 2H), 7.63 (d, $J = 7.4$ Hz, 2H), 7.33 (t, $J = 7.9$ Hz, 1H), 7.24 (t, $J = 6.8$ Hz, 2H), 7.20 (d, $J = 7.8$ Hz, 4H), 7.07 (t, $J = 7.6$ Hz, 2H), 6.88 (t, $J = 7.4$ Hz, 2H), 6.72 (d, $J = 8$ Hz, 2H), 2.94 (septet, $J = 6.6$ Hz, 4H), 1.25 (d, $J = 6.3$ Hz, 12H), 0.89 (d, $J = 6.4$ Hz, 12H), 0.46 (s, 18H).

Preparation of $(^{\text{Mes}}\text{CCC})\text{Fe}(\text{II})\text{Cl}(\text{PMe}_3)_2$. Gives a red solid, $(^{\text{Mes}}\text{CCC})\text{Fe}(\text{II})\text{Cl}(\text{PMe}_3)_2$, in excellent yield (0.023 g, 0.029 mmol, 89 %). ^1H NMR (THF-d_8 , 500 MHz): $\delta = 8.36$ (d, $J = 6.8$ Hz, 2H), 7.98 (d, $J = 6.2$ Hz, 2H), 7.64 (t, $J = 6.2$ Hz, 1H), 7.53 (t, $J = 6.4$ Hz, 2H), 7.38 (t, $J = 6.8$ Hz, 2H), 7.16 (s, 4H), 6.97 (d, $J = 7.8$ Hz, 2H), 2.38 (s, 6H), 2.09 (s, 12H), 0.57 (s, 18H). ^{13}C NMR (THF-d_8 , 126 MHz): $\delta = 219.86, 148.23, 140.86, 138.87, 138.42, 137.22, 136.73, 133.42, 132.33, 131.64, 129.84, 127.14, 125.52, 125.02, 113.98, 111.63, 111.48, 22.31, 21.39, 21.26$. $^{31}\text{P}\{^1\text{H}\}$ NMR (THF-d_8 , 202.4 MHz): $\delta = 18.04$. HRMS (ESI), calc. for $\text{C}_{44}\text{H}_{51}\text{N}_4\text{P}_2\text{Fe} (\text{M} - \text{Cl})^+$: 753.29, found 752.29.

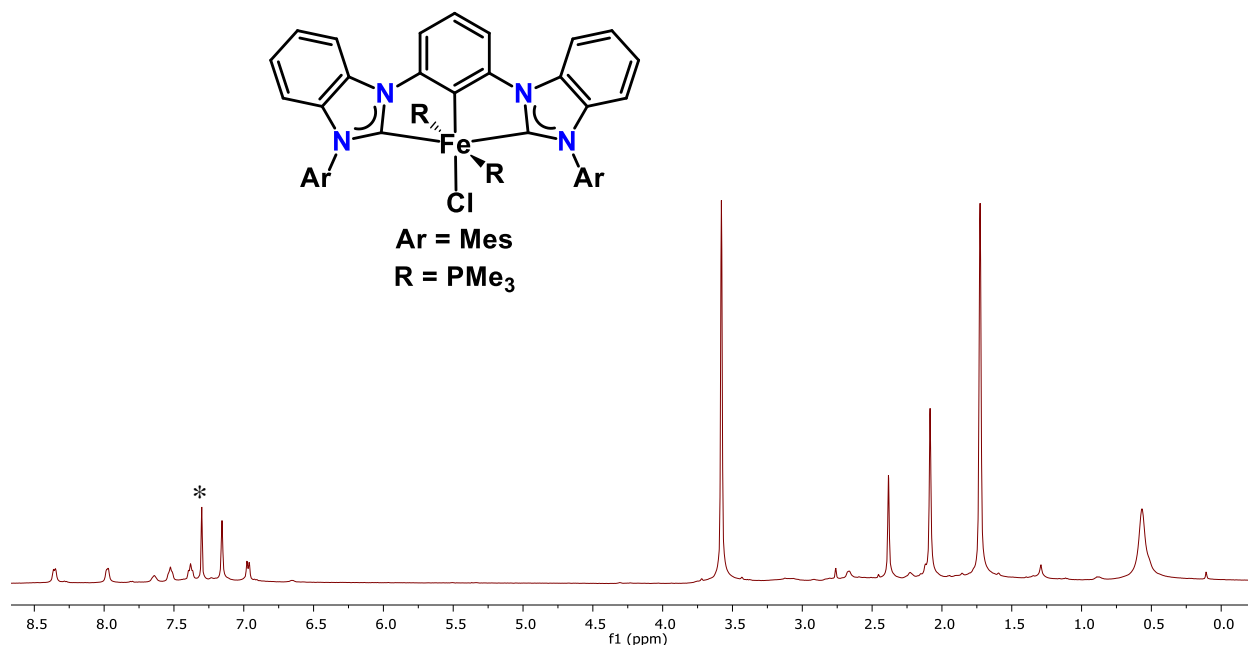


Figure 3.6. ^1H NMR spectrum of $(^{\text{Mes}}\text{CCC})\text{Fe}(\text{II})\text{Cl}(\text{PMe}_3)_2$ (THF-d_8), *indicates solvent.

Preparation of $(^{\text{DIPP}}\text{CCC})\text{Co}(\text{III})\text{Cl}_2(\text{N}_2)$. Yield (0.025 g, 0.030 mmol, >99 %). ^1H NMR (CDCl_3 , 500 MHz): $\delta = 8.82$ (d, $J = 4.8$ Hz, 2H), 8.27 (d, $J = 8.2$ Hz, 2H), 7.88 (d, $J = 7.8$ Hz, 2H), 7.55 (t, $J = 7.8$ Hz, 1H), 7.41 (t, $J = 7.6$ Hz, 2H), 7.21 (t, $J = 7.8$ Hz, 2H), 7.16 (t, $J = 7.7$ Hz, 2H), 6.96 (d, $J = 7.8$ Hz, 4H), 6.76 (d, $J = 8.1$ Hz, 2H), 6.41 (t, $J = 6.4$ Hz, 2H), 2.68 (septet, $J = 6.6$ Hz, 4H), 0.98 (d, $J = 6.5$ Hz, 12H), 0.68 (d, $J = 6.7$ Hz, 12H). This complex was matched to literature values.³

Preparation of $(^{\text{Mes}}\text{CCC})\text{Co}(\text{III})\text{Cl}_2\text{py}$. Yield (0.023 g, 0.031 mmol, 94 %). ^1H NMR (CDCl_3 , 500 MHz): $\delta = 8.78$ (d, $J = 4.9$ Hz, 2H), 8.25 (d, $J = 8.1$ Hz, 2H), 7.83 (d, $J = 7.8$ Hz, 2H), 7.55 (t, $J = 7.9$ Hz, 1H), 7.43 (t, $J = 7.7$ Hz, 2H), 7.31 (m, 1H), 7.20 (t, $J = 7.6$ Hz, 2H), 6.78 (d, $J = 8$ Hz, 2H), 6.52 (m, 6H), 2.19 (s, 6H), 1.83 (s, 12H). This complex was matched to literature values.³

3.4 References

1. IUPAC. *Compendium of Chemical Terminology* ("Gold Book). Compiled by A. D. McNaught and A. Wilkinson. Blackwell Scientific Publications: Oxford, 1997.
2. Matson, E. M.; Martinez, G. E.; Ibrahim, A. D.; Jackson, B. J.; Bertke, J. A.; Fout, A. R. Nickel(II) Pincer Carbene Complexes: Oxidative Addition of an Aryl C-H Bond to Form a Ni(II) Hydride. *Organometallics* **2014**, *34*, 399-407.
3. Ibrahim, A. D.; Tokmic, K.; Brennan, M. R.; Kim, D.; Matson, E. M.; Nilges, M. J.; Bertke, J. A.; Fout, A. R. Monoanionic bis(carbene) pincer complexes featuring cobalt(I-III) oxidation states. *Dalton Trans.* **2016**, *45*, 9805-9811.
4. Tokmic, K.; Markus, C. R.; Zhu, L.; Fout, A. R. Well-Defined Cobalt(I) Dihydrogen Catalyst: Experimental Evidence for a Co(I)/Co(III) Redox Process in Olefin Hydrogenation. *J. Am. Chem. Soc.* **2016**, *138*, 11907-11913.
5. Satterlee, J. D. Fundamental Concepts of NMR in Paramagnetic Systems Part I: The Isotropic Shift. *Concepts Magn. Reson.* **1990**, *2*, 69-70.
6. Yan, X.; Xi, C. Advances in transmetalation reactions originated from organozirconium compounds. *Coord. Chem. Rev.* **2017**, *350*, 275-284.
7. Rubio, R. J.; Anadavan, G. T. S.; Bauer, E. B.; Hollis, T. K.; Cho, J.; Tham, F. S.; Donnadieu, B. Toward a general method for CCC *N*-heterocyclic carbene pincer synthesis: Metallation and transmetallation strategies for concurrent activation of three C-H bonds. *J. Organomet. Chem.* **2005**, *690*, 5353-5364.
8. Cho, J.; Hollis, T. K.; Valente, E.; Trate, J. M.; CCC-N-heterocyclic carbene pincer complexes: Synthesis, characterization and hydroamination activity of a hafnium complex. *J. Organomet. Chem.* **2011**, *696*, 373-377.

9. Valle, H. U.; Akurathi, G.; Cho, J.; Clark, W. D.; Chakraborty, A.; Hollis, T. K. CCC-NHC Pincer Zr Diamido Complexes: Synthesis, Characterisation, and Catalytic Activity in Hydroamination/Cyclisation of Unactivated Amino-Alkenes, -Alkynes, and Allenes. *Aust. J. Chem.* **2016**, *69*, 565-572.
10. Clark, W. D.; Leigh, K. N.; Webster, C. E.; Hollis, T. K. Experimental and Computational Studies of the Mechanisms of Hydroamination/Cyclisation of Unactivated α,ω -Amino-alkenes with CCC-NHC Pincer Zr Complexes. *Aust. J. Chem.* **2016**, *69*, 573-582.
11. Andavan, G. T. S.; Bauer, E. B.; Letko, C. S.; Hollis, T. K.; Tham, F. S. Synthesis and characterization of a free phenylene bis(N-heterocycliccarbene) and its di-Rh complex: Catalytic activity of the di-Rh and CCC-NHC Rh pincer complexes in intermolecular hydrosilylation of alkynes. *J. Organomet. Chem.* **2005**, *690*, 5938-5947.
12. Bauer, E. B.; Andavan, G. T. S.; Hollis, T. K.; Rubio, R. J.; Cho, J.; Kuchenbeiser, G. R.; Helgert, T. R.; Letko, C. S.; Tham, F. S. Air- and Water-Stable Catalysts for Hydroamination/Cyclization. Synthesis and Application of CCC-NHC Pincer Complexes of Rh and Ir. *Org. Lett.* **2008**, *10*, 1175-1178.
13. Zhang, X.; Wright, A. M.; DeYonker, N. J.; Hollis, T. K.; Hammer, N. I.; Webster, C. E.; Valente, E. J. Synthesis, Air Stability, Photobleaching, and DFT Modeling of Blue Light Emitting Platinum CCC-N-Heterocyclic Carbene Pincer Complexes. *Organometallics* **2012**, *31*, 1664-1672.
14. Hcukaba, A. J.; Cao, B.; Hollis, T. K.; Valle, H. U.; Kelly, J. T.; Hammer, N. I.; Oliver, A. G.; Webster, C. E. Platinum CCC-NHC benzimidazolyl pincer complexes: synthesis, characterization, photostability, and theoretical investigation of a blue-green emitter. *Dalton Trans.* **2013**, *42*, 8820-8826.

15. Reilly, S. W.; Webster, C. E.; Hollis, T. K.; Valle, H. U. Transmetallation from CCC-NHC pincer Zr complexes in the synthesis of air-stable CCC-NHC pincer Co(III) complexes and initial hydroboration trials. *Dalton Trans.* **2016**, *45*, 2823-2828.
16. Denny, J. A.; Lamb, R. W.; Reilly, S. W.; Donnadieu, B.; Webster, C. E.; Hollis, T. K. Investigation of metalation/transmetallation reactions to synthesize a series of CCC-NHC Co pincer complexes and their X-ray structures. *Polyhedron* **2018**, *151*, 568-574.
17. Cope, J. D.; Liyanage, N. P.; Kelley, P. J.; Denny, J. A.; Valente, E. J.; Webster, C. E.; Delcamp, J. H.; Hollis, T. K. Electrocatalytic reduction of CO₂ with CCC-NHC pincer nickel complexes. *Chem. Commun.* **2017**, *53*, 9442-9445.
18. Brown, Geoffrey (2012). *The Inaccessible Earth: An integrated view to its structure and composition.* Springer: Netherlands, 1993.
19. Pangborn, A. B.; Giardello, M. A.; Grubbs, R. H.; Rosen, R. K.; Timmers, F. J. Safe and Convenient Procedure for Solvent Purification. *Organometallics* **1996**, *15*, 1518–1520.
20. Wietz, I. S.; Rabinovitz, M. The Application of C₈K for Organic Synthesis: Reduction of Substituted Naphthalenes. *J. Chem. Soc. Perkin Trans.* **1993**, *1*, 117-120.

Chapter 4

Cobalt Catalyzed Nitrile Hydrogenation to Primary Amines

4.1 Introduction¹

The development of systems for the selective formation of primary amines, particularly from nitriles being the most atom-economical route, is of interest due to their wide uses in the bulk and fine chemical industries.^{1,2} The hydrogenation of nitriles to primary amines takes place in two separate steps first going through the primary imine intermediate (Figure 4.1). The difficulty of product selectivity arises from the ability of the generated primary amine to intercept this intermediate and, upon the loss of ammonia, generate the secondary aldimine side product. This product can also undergo further hydrogenation to the secondary amine or subsequent condensation to the tertiary amine.¹

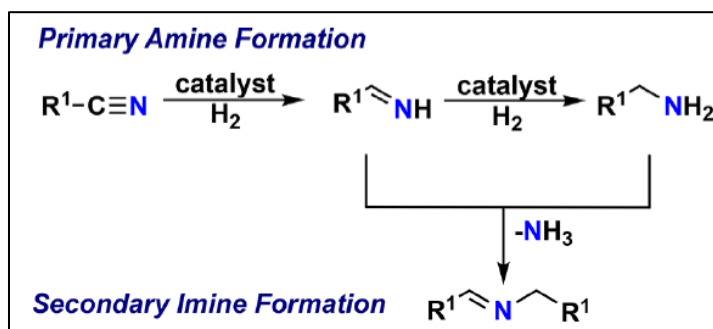


Figure 4.1. Hydrogenation of nitriles.

Heterogeneous nitrile hydrogenation processes often suffer from low functional group tolerance and reduced selectivity for the primary amine due to these side reactions, including secondary and tertiary amine formation.¹⁻⁵ Homogeneous nitrile hydrogenation catalysts are typically more selective with milder reaction conditions, but are less active than their heterogeneous counterparts and tend to require more expensive second- and third-row transition

¹ Portions of this chapter are reproduced from the following publication with permission from the authors: Tokmic, K.;* Jackson, B. J.;* Salazar, A.; Woods, T. J.; Fout, A. R. Cobalt-Catalyzed and Lewis Acid-Assisted Nitrile Hydrogenation to Primary Amines: A Combined Effort. *J. Am. Chem. Soc.* **2017**, *139*, 13554-13561.

metal catalysts.⁶⁻¹⁷ Replacing these expensive catalysts with late first-row transition metals offers a cheaper and much more environmentally benign alternative.^{18,19}

Homogeneous nitrile hydrogenation using late first-row transition metals has been undertaken by Beller and Milstein for manganese,²⁰ iron,²¹⁻²³ and cobalt^{24,25} with systems that are very selective for primary amines, though they still require high hydrogen pressure and extended reaction times (Table 4.1). Often the reactivity is attributed to ligand-assisted hydrogenation and not a completely metal-centered process, where the mechanism has been elucidated. Therefore, we were interested in determining whether our system was competent for this transformation under milder conditions as well as its operative mechanism.

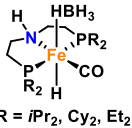
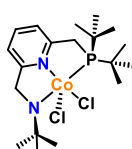
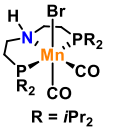
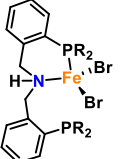
Catalyst	Loading	Pressure	Temperature	Time	Catalyst	Loading	Pressure	Temperature	Time
	1 mol%	30 bar	70, 100, 130°C	3 hrs		3 mol%	30 bar	135°C	36-60 hrs
	3 mol%	50 bar	120°C	24-60 hrs	$\text{Co}(\text{acac})_3$				
	3 mol%	60 bar	140°C	16-60 hrs	$\text{Cy}_2\text{P}-\text{CH}_2-\text{CH}_2-\text{P}(\text{Cy}_2)_2$	4 mol%	30 bar	80, 100, 120°C	18 hrs

Table 4.1. Literature examples to other first-row nitrile hydrogenation catalysts.²⁰⁻²⁵

Our group has reported that the hydrogenation of alkenes and *E*-selective semi-hydrogenation of alkynes can be carried out by $(^{\text{Mes}}\text{CCC})\text{Co}(\text{I})(\text{H}_2)\text{PPh}_3$ using very mild conditions.^{26,27} Mechanistic insights, including para-hydrogen induced polarization (PHIP) transfer NMR spectroscopy, indicated a metal-centered Co(I/III) process for these transformations. However, this complex is both air and moisture sensitive which limits its ease of use so a change to using the air-stable $(^{\text{Mes}}\text{CCC})\text{Co}(\text{III})\text{Cl}_2\text{py}$ with an *in situ* activator was targeted. The use of

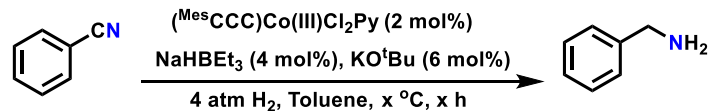
Grignard, metal hydride, or metal alkoxides as *in situ* activators has been investigated by a number of groups.²⁸⁻³³ Encouraged by our previous studies using Co(I) hydrogenation catalysts³⁴ we sought to use NaHBET₃ as the *in situ* activator for our catalysis. Herein the selective hydrogenation of nitriles to primary amines using a bench-stable catalyst precursor, (^{Mes}CCC)Co(III)Cl₂py (py = pyridine), *in situ* activator, NaHBET₃, and low H₂ pressure (4 atm) is described.

4.2 Optimization of Reaction Parameters and Substrate Scope

The initial reaction parameters were modeled after previously published cobalt nitrile hydrogenation systems using benzonitrile as the model substrate.^{23,24} The use of (^{Mes}CCC)Co(III)Cl₂py (2 mol%), NaHBET₃ (4 mol%), and 4 atm of H₂ in toluene at 115 °C for 8 h resulted in the complete conversion of benzonitrile, but with selectivity to the secondary aldimine as seen by GC-MS (Table 4.2, Entry 2). Adding KO^tBu (6 mol%) resulted in complete conversion and selectivity for the primary amine with a yield of 97% (Table 4.2, Entry 1). The addition of the base helps to prevent the formation of the secondary aldimine as has been previously reported in other systems.^{1,2} A variety of other bases including K(N(SiMe₃)₂), NaOEt, NaO^tBu, and NaOPent were also tested ranging from 76-95% yield, but KO^tBu proved to give the best yield of the amine (Table S4.5). The amount of base caused only a small variance in selectivity but 6 mol% was found to give the best yield of primary amine (Table S4.5). Various controls excluding the catalyst, *in situ* activator (NaHBET₃), or hydrogen showed no conversion of the starting material (Table S4.5).

Using 1 atm of H₂ led to the same conversion as 4 atm (>99%) but much lower selectivity for the primary amine (50%) (Table 4.2, Entry 3). Lowering the temperature to 100 °C or 80 °C still resulted in complete conversion of the starting material but less selectivity for the primary amine (Table 4.2, Entry 5 & 6). Carrying out the catalysis just above room temperature at 30 °C

gave 0% conversion of the starting material (Table 4.2, Entry 4). Monitoring the reaction at shorter reaction times (2, 4, and 6 hrs) showed similar conversions and less selectivity for the primary amine likely due to decomposition of the primary imine on the instrument itself (Table 4.2, Entry 7-9). It is also possible that the equilibrium between the secondary imine and primary imine is reversed with longer reaction times but later studies monitoring by ^1H NMR spectroscopy proved this false. While primary imines are known to be unstable and typically transient this was our first indication that monitoring by GC-MS wasn't the best method for full quantification of these reaction mixtures.



Entry	Temperature	Time	Conversion	Yield ^a
1	115 °C	8 hrs	>99	97%
2 ^b	115 °C	8 hrs	>99	- ^b
3 ^c	115 °C	8 hrs	>99	50%
4	30 °C	8 hrs	0	-
5	80 °C	8 hrs	>99	60%
6	100 °C	8 hrs	>99	87%
7	115 °C	2 hrs	95	51%
8	115 °C	4 hrs	97	86%
9	115 °C	6 hrs	>99	92%

^aPrimary amine, via GC-MS, remaining balance secondary aldimine.

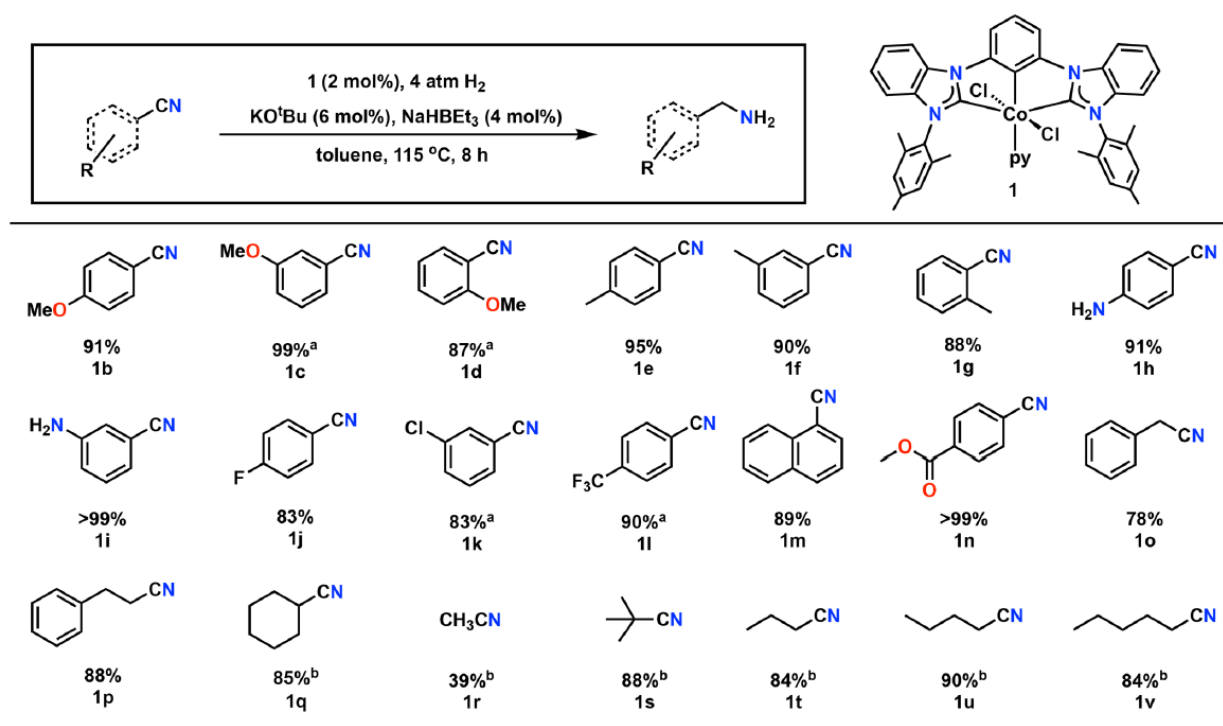
^bNo base, secondary aldimine only. ^c1 atm H₂.

Table 4.2. Optimization of reaction conditions.

We were also interested in whether other cobalt sources could undergo this transformation under these or similar conditions. $(\text{PPh}_3)_2\text{Co}(\text{I})(\text{N}(\text{SiMe}_3)_2)$, $(\text{PPh}_3)_3\text{Co}(\text{I})\text{Cl}$, and $\text{Co}(\text{III})(\text{acac})_3$ were subjected to these same reaction conditions, with NaHBEt_3 as the reductant where relevant, but no conversion of the starting material was observed under any conditions (Table S4.5).^{35,36}

The optimized reaction conditions (toluene, 115 °C, 8 h, 4 atm H₂, KO^tBu 6 mol%) were determined and the scope of this reaction was investigated. Conversion was determined by GC-MS where applicable (>99%) and the isolated yields are of the hydrochloride salts. A variety of

aromatic and aliphatic nitriles were found to be hydrogenated efficiently and selectively to their primary amines (Table 4.3). Electron-donating aromatic substrates including methoxy, methyl, and naphthyl were hydrogenated with high yields including those with more sterically hindered ortho-substitution (**1b-1g, 1m**). The ortho- and meta-substituted methoxy substrates required slightly higher catalyst loadings likely due to steric interactions. Electron-withdrawing aromatic substrates like fluoro, chloro, and trifluoromethyl proceeded with good but slight lower yields (**1j-1l**). Anilines (**1h, 1i**) were tolerated under these reaction conditions but not in the ortho position which could be due to a bidentate interaction with the metal center. Phenols in any position were not tolerated and appeared to result in decomposition of the catalyst as seen by distinct color changes even before the addition of H₂. Para-methylester benzonitrile (**1n**) was hydrogenated in very high yield with the ester fragment intact but ketone or aldehyde functionalities in the same position



[‡]Conversion (>99%) determined by GC-MS. Yields were of the isolated hydrochloride salts. ^aCatalyst (4 mol %), NaHBET₃ (8 mol %), KO^tBu (12 mol %). ^bGC-MS conversion was not determined; yields were of the isolated hydrochloride salts.

Table 4.3. Nitrile hydrogenation substrate scope.

resulted in zero conversion of the starting material. Aromatic nitro functional groups also shut down the catalysis and gave no conversion of the starting nitrile.

Aliphatic substrates were hydrogenated in very good yields including phenylacetonitrile (**1o**) and phenylpropionitrile (**1p**). The cyclic non-aromatic cyclohexylnitrile (**1q**) gave complete conversion and an isolated yield of 85%. All the alkyl substrates that were too light to be analyzed by the GC-MS method are given as only isolated yields instead. Three, four, and five carbon alkyl nitriles were isolated in very good yields (**1t-1v**). Additionally, two substrates not seen before for first-row homogeneous nitrile hydrogenation are acetonitrile (**1r**) and *t*-butylnitrile (**1s**). Ethyl amine is a widely used chemical in industry and hydrogenation of acetonitrile presents an atom-economical route to this product.³⁷ The sterically hindered *t*-butylnitrile (**1s**) was also isolated in excellent yield (88%).

This transformation demonstrates the utility of this system in hydrogenating nitriles with excellent reactivity and selectivity to their primary amines. Additionally, the reaction can be scaled up while still retaining the same yield of the product (*p*-MePhCN, 200 mg, 97% yield). The optimized conditions use a very low pressure of hydrogen and short reaction times compared to other first-row transition metal systems (Table 4.1). Beller's PNP Fe pincer complex operates on some of the mildest conditions that have been published but, again, still requires 30 bar of hydrogen pressure.^{21,22} All the first-row catalyst systems for nitrile hydrogenation in the literature use 30-60 bar of pressure compared to our system at 4 bar H₂ (Table 4.1).²⁰⁻²⁵ The lower hydrogen pressure also allowed the use of standard Schlenk lines and tubes instead of requiring high pressure reaction apparatuses. After establishing the catalytic competence of our system, we next examined the mechanism of this transformation in greater detail with particular emphasis on identifying any two-electron processes as observed in our previous studies.^{26,27,38,39}

4.3 Mechanistic Studies

Para-hydrogen induced polarization (PHIP) is an extremely powerful tool to study the placement of a molecule of H₂ onto a substrate by NMR spectroscopy.⁴⁰⁻⁵⁴ Our lab has previously reported PHIP transfer NMR studies of Co(η^2 -H₂) bis(carbene) pincer complexes for the hydrogenation of carbon-carbon bonds.^{26,27} We were interested to see if we could extend this technique to the hydrogenation of nitriles.

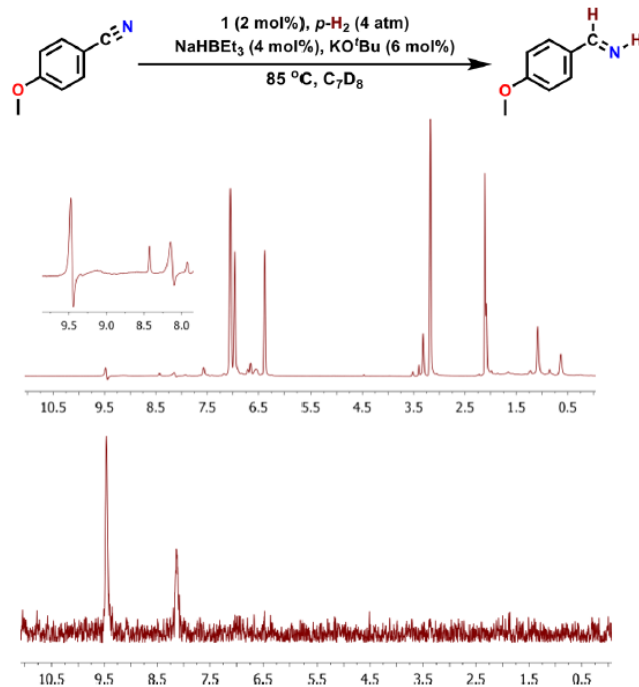


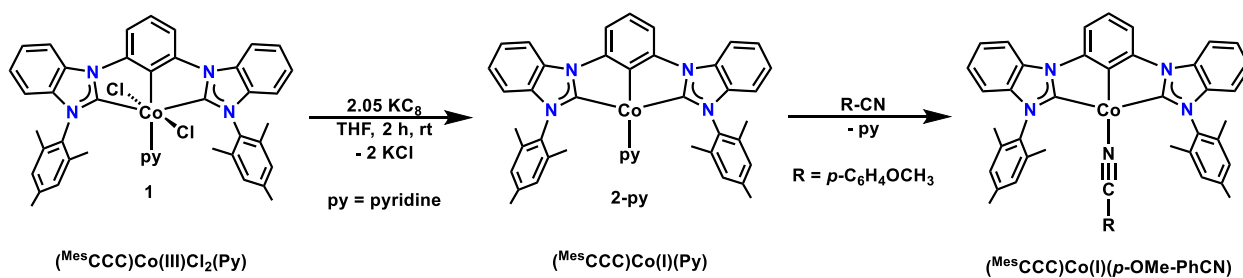
Figure 4.2 PHIP data 45° pulse (top) and ¹H NMR OPSY (bottom).

PHIP transfer NMR spectroscopy results from the hyperpolarization of H₂ to *p*-H₂ and signals can be seen in the ¹H NMR spectrum for each of these hydrogen atoms as long as they are added pairwise to magnetically distinct positions of the substrate. In the studies undertaken with the hydrogenation of nitriles a 45° pulse and a double quantum OPSY (only *para*-hydrogen spectroscopy) filter in the ¹H NMR experiment was used.⁵² We chose para-methoxybenzotrile as the model substrate since the methoxy group provides a clearly discernible handle in the ¹H NMR spectrum for each of the possible hydrogenation products. The addition of *p*-H₂ to a toluene-*d*₈ solution consisting of para-methoxybenzotrile, (^{Mes}CCC)Co(III)Cl₂py (2 mol%), NaHBEt₃ (4 mol%), and KO^tBu (6 mol%) resulted in the observation of hyperpolarized resonances only when heated above 85 °C (Figure 4.2). The primary imine resonances were clearly seen by this method, but though primary amine resonances appeared they were not polarized by *p*-H₂. This indicates that *p*-H₂ was added pairwise to the nitrile moiety to generate the primary imine but that the process

of hydrogenation from the imine to the amine could be going through a different mechanism.⁵⁵⁻⁵⁸ These results indicate that a Co(I/III) mechanism is most likely operative as observed in our previous hydrogenation studies. This is the first time the hyperpolarization of resonances using *p*-H₂ have been observed using polar functionalities through a hydrogenative process.⁵⁸⁻⁶⁵

Interested in identifying our active catalytic species we set out to isolate the Co(I) complex generated upon the addition of two equivalents of NaHBET₃ to (^{Mes}CCC)Co(III)Cl₂py. Initial reactions indicated the reduction of the Co(III) center to a diamagnetic, C₂ symmetric Co(I) complex that displayed broadened features by ¹H NMR spectroscopy. Solution IR spectroscopy of the brown complex revealed an intense absorption at 2081 cm⁻¹ tentatively assigned as (^{Mes}CCC)Co(I)(N₂) (vide infra). An alternate reduction using potassium graphite (KC₈, 2equiv) yielded (^{Mes}CCC)Co(I)(py) in 80% yield (Scheme 4.1). Crystals suitable for X-ray diffraction show a square planar geometry around cobalt (Figure S4.1). Analysis by ¹H NMR spectroscopy indicates a diamagnetic C₂ symmetric complex and IR spectroscopy shows no N₂ stretching frequency as previously observed when reducing using NaHBET₃. This is likely due to the Lewis acid coordinating to pyridine allowing N₂ to bind to the metal. This was confirmed by adding BEt₃ to (^{Mes}CCC)Co(I)(py) and identifying the BEt₃-pyr adduct by ¹H and ¹¹B NMR spectroscopy.

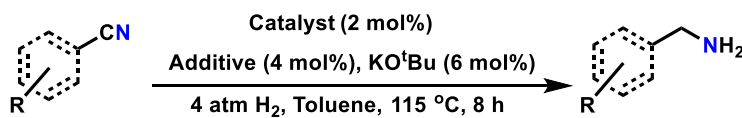
Interested in understanding the metal-substrate interactions during catalysis we then treated (^{Mes}CCC)Co(I)(py) with *para*-OMe-PhCN which yielded (^{Mes}CCC)Co(I)(*p*-OMe-PhCN) where the



Scheme 4.1. Synthesis of (^{Mes}CCC)Co(I)(py) and (^{Mes}CCC)Co(I)(*p*-OMe-PhCN).

pyridine ligand has been replaced by the nitrile (Scheme 4.1). Characterization by ^1H NMR spectroscopy showed a very similar spectrum to $(^{\text{Mes}}\text{CCC})\text{Co}(\text{I})(\text{py})$ and integrations consistent with one nitrile per cobalt center. Examining this species by IR spectroscopy shows an absorbance at 2084 cm^{-1} which is red shifted by 32 cm^{-1} from the free nitrile (2216 cm^{-1}) indicative of an end-on binding mode.⁶⁶

Having established that the nitrile coordinates to the reduced cobalt species in an end-on fashion, we next explored the competency of both Co(I) catalysts for nitrile hydrogenation. Using $(^{\text{Mes}}\text{CCC})\text{Co}(\text{I})(\text{py})$ (2 mol%), KO^tBu (6 mol%), and 4 atm of H_2 the hydrogenation of *p*-methylbenzonitrile did not proceed, and only starting material was recovered (Table 4.4, Entry 1). Under optimized catalytic conditions, two equivalents of NaHBET_3 activates the pre-catalyst, with subsequent formation of BET_3 . To our surprise, the addition of two equivalents of BET_3 (4 mol%) to the $(^{\text{Mes}}\text{CCC})\text{Co}(\text{I})(\text{py})$ catalyzed reaction enabled the hydrogenation to proceed with a similarly high yield to the original reaction (Table 4.4, Entry 2 & 3). This result suggests the borane, acting as a Lewis acid, is intimately involved in the catalysis. To further evaluate the necessity of Lewis acids in the catalysis, BPh_3 , LiOTf , and $\text{Ca}(\text{OTf})_2$ were targeted. The addition of each Lewis acid



Entry	Catalyst	Additive	Substrate	Yield ^a
1	$\text{Co}(\text{I})(\text{Py})$	-	$\text{R} = p\text{-Me}$	0% ^b
2	$\text{Co}(\text{III})\text{Cl}_2(\text{Py})$	NaHBET_3	$\text{R} = p\text{-Me}$	95%
3	$\text{Co}(\text{I})(\text{Py})$	BET_3	$\text{R} = p\text{-Me}$	91%
4	$\text{Co}(\text{I})(\text{Py})$	LiOTf	$\text{R} = p\text{-Me}$	82%
5	$\text{Co}(\text{I})(\text{Py})$	$\text{Ca}(\text{OTf})_2$	$\text{R} = p\text{-Me}$	70%
6	$\text{Co}(\text{I})(\text{Py})$	BPh_3	$\text{R} = p\text{-Me}$	98%
7	$\text{Co}(\text{III})\text{Cl}_2(\text{Py})$	NaHBET_3	$\text{R} = p\text{-OMe}$	91%
8	$\text{Co}(\text{I})(p\text{-OMe-PhCN})$	BET_3	$\text{R} = p\text{-OMe}$	92%

^aIsolated yield of the hydrochloride salt. ^bStarting material only.

Table 4.4. Lewis acid screen for catalysis.

to the catalytic reaction resulted in the hydrogenation of para-methylbenzotrile to the primary amine in good yields (Table 4.4, Entry 4-6). This indicates that the reaction requires a Lewis Acid to proceed. The triflate Lewis acids had a slightly lower yield likely due to their lower solubility in toluene. Using instead (^{Mes}CCC)Co(I)(*p*-OMe-PhCN) as the catalyst (2 mol%), two equivalents of BEt₃ (4 mol%), and KO^tBu (6 mol%) resulted in the hydrogenation of para-methoxybenzotrile, again with a similar yield to the original reaction, indicating that pyridine or pyridine-borane adducts are not necessary for the catalysis to proceed (Table 4.4, Entry 7 & 8).

We next wanted to confirm that a Co(I/III) reaction mechanism was still operative starting with our Co(I) catalysts instead of the Co(III) with *in situ* activation. Upon the addition of p-H₂ to a toluene-d₈ solution containing para-methoxybenzotrile, (^{Mes}CCC)Co(I)(py) (2 mol%), NaO^tBu (6 mol%), and BEt₃ (4 mol%) heated to 75 °C the same PASADENA effects were observed as starting with the Co(III) catalyst. On the basis of the PHIP transfer ¹H NMR data, the first step in the hydrogenation of nitriles conforms with the concerted nature of H₂ addition, which is consistent with our previous studies of the cobalt-catalyzed hydrogenation of carbon-carbon multiple bonds using (^{Mes}CCC)Co(I)H(PPh₃).^{26,27} Interested in the reaction profile we next monitored the reaction by ¹H NMR spectroscopy.

Monitoring the hydrogenation of para-methoxybenzotrile by ¹H NMR spectroscopy reveals an immediate decline in the nitrile starting material going to the primary imine initially (Figure 4.3). This is then consumed and followed by a steady increase in the primary amine throughout the reaction. The formation of the secondary aldimine is essentially zero during the entire reaction. This indicates that the temperature and added base are in fact preventing the equilibrium from taking place between the primary imine/amine and the secondary aldimine.

Adding one equivalent of amine to the reaction mixture did not change the reaction time indicating the increased amine concentration did not inhibit catalytic turnover.

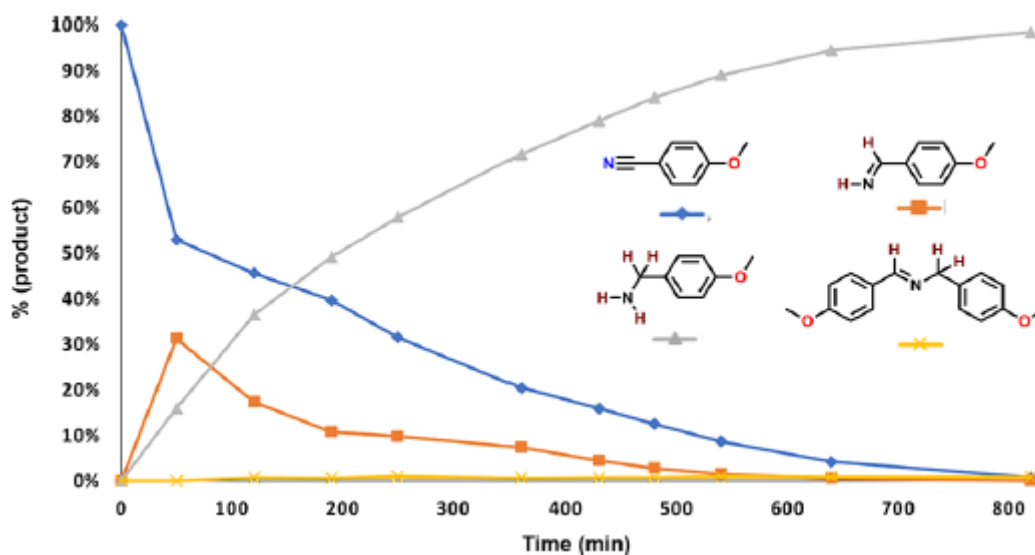
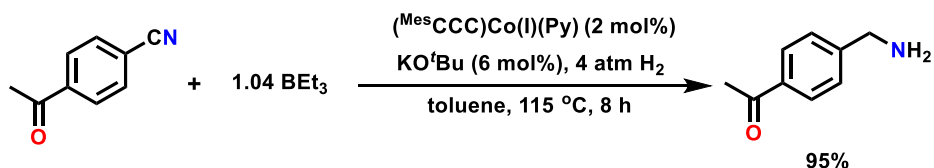


Figure 4.3. Reaction profile of the hydrogenation of *p*-methoxybenzonitrile with $(^{\text{Mes}}\text{CCC})\text{Co}(\text{I})(\text{py})$ (2 mol%), BEt_3 (4 mol%), and NaO^tBu (6 mol%) in toluene-d_8 under 4 atm of H_2 at 115 °C.

Knowing the Lewis acid is essential for the hydrogenation of the nitrile to the primary imine we next questioned if the presence of a Lewis acid was necessary for the hydrogenation of the primary imine to the primary amine to proceed. Use of a primary imine surrogate, *N*-benzylideneamine, under regular catalytic conditions in the absence of Lewis acid gave 10% conversion to the secondary amine as observed by GC-MS. In contrast, the addition of BEt_3 (4 mol%) resulted in 90% conversion to the primary amine. Therefore, the Lewis acid can also facilitate the second hydrogenation step, but it is not necessary for the reaction to occur.

In view of these findings on the importance of the Lewis acid we next re-examined the hydrogenation of *para*-acetylbenzonitrile, a substrate that proved unamenable towards hydrogenation under the previous reaction conditions (*vide supra*). We recognized that the Lewis acid is necessary for catalysis, so it was postulated that an interaction of the Lewis acid with the ketone functionality could inhibit catalytic turnover. Accordingly, the addition of 1.04 equivalents

of BEt_3 with respect to the substrate, to account for coordination to the ketone and the amount needed to hydrogenate the nitrile, furnished the primary amine in 95% yield (Scheme 4.2). Notably, the ketone functionality was not reduced under these conditions, which is a distinct difference from the iron,²² ruthenium,^{67,68} and palladium⁶⁹ systems. The increase in Lewis acid equivalents was applied to formyl and thiophene functionalities but did not improve catalysis.



Scheme 4.2. Hydrogenation of 4-acetylbenzotrile with stoichiometric Lewis acid.

Computational modeling and experimental data have shown that reactivity of the Lewis acidic boranes (BF_3 and $\text{B}(\text{C}_6\text{F}_5)_3$) with nitriles results in an electrostatic interaction in the subsequent adduct formation.^{70,71} Interested in understanding if a nitrile-borane interaction was present we treated a solution of $(^{\text{Mes}}\text{CCC})\text{Co}(\text{I})(p\text{-OMe-PhCN})$ with BEt_3 , and the mixture was monitored by ^1H NMR spectroscopy. Unfortunately, there was no change in the ^1H NMR spectrum at room temperature nor when heating to 100 °C. Likewise, examining the reaction by IR spectroscopy revealed no change in the $\text{C}\equiv\text{N}$ stretch, and coordination of N_2 was not observed. We next wanted to make the pre-formed nitrile-borane adduct which was accomplished by treating para-methoxybenzotrile with BPh_3 in hexanes.⁷² The isolated adduct was characterized, added to $(^{\text{Mes}}\text{CCC})\text{Co}(\text{I})(\text{py})$, and monitored by ^1H NMR spectroscopy where the formation of $(^{\text{Mes}}\text{CCC})\text{Co}(\text{I})(p\text{-OMe-PhCN})$ was observed. No nitrile-borane interaction was observed by either ^{11}B NMR or IR spectroscopy.

Nonetheless, while the nitrile was found to coordinate to the cobalt center only end-on at ambient temperatures, we propose that under catalytic conditions the coordination mode changes to accommodate the pairwise addition of H_2 onto the metal center as indicated by the PHIP NMR

data. One possibility involves a side-on coordination mode of the nitrile through the $C\equiv N$ π -orbital proceeding through a three-center bonding geometry. In the side-on coordination mode the $C\equiv N$ bond would be more amenable toward functionalization, and the nitrogen lone pair would be available to interact with a Lewis acid in a similar fashion as observed in bisphosphine nickel(0) complexes.⁷³⁻⁷⁵ A computational study by Jiao and co-workers reported that the energy difference decreases between end-on and side-on coordination modes of acetonitrile in cobalt complexes with increasing electron-donating ability of the ligands and, therefore, the nitrile group becomes more negatively charged.⁷⁶ On the basis of these studies and those presented herein, the most viable role of the Lewis acid in the observed catalysis is depicted (Figure 4.4).

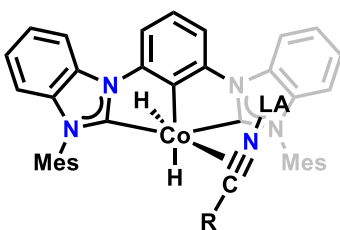


Figure 4.4. Proposed coordination of Lewis acid to the cobalt-bound nitrile.

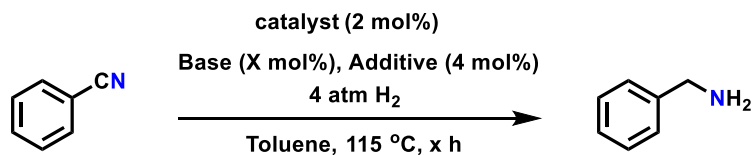
In conclusion, the catalytic activity of a cobalt bis(carbene) pincer system was extended toward the hydrogenation of a broad scope of nitriles with excellent selectivity toward the primary amines. Through the course of our studies, it was determined that the hydrogenation does not proceed without the addition of catalytic amounts of a Lewis acid. On the basis of the mechanistic studies herein and corroborating literature precedents, the nature of the Lewis acid is proposed to facilitate a side-on coordination of the nitrile to the cobalt center, permitting a pairwise transfer of H_2 through a $Co(I/III)$ redox process. Furthermore, supplemented by insights gleaned from the mechanistic studies, a nitrile featuring a ketone functionality was amenable toward the selective hydrogenation of only the nitrile, with the addition of super-stoichiometric amounts of Lewis acid. Finally, in our approach investigating a bench stable hydrogenation pre-catalyst accompanied by

in situ activation by NaHBET_3 , the presumed innocence of the Lewis acid byproduct was contested, and it proved to hold a substantial role in the observed catalysis.

4.4 Experimental Section

General Considerations. All manipulations of air- and moisture-sensitive compounds were carried out in the absence of water and dioxygen in an MBraun inert atmosphere drybox under a dinitrogen atmosphere except where specified otherwise. All glassware was oven dried for a minimum of 8 h and cooled in an evacuated antechamber prior to use in the drybox. Solvents for sensitive manipulations were dried and deoxygenated on a Glass Contour System (SG Water USA, Nashua, NH) and stored over 4 Å molecular sieves purchased from Strem following a literature procedure prior to use.⁷⁷ Toluene- d_8 and benzene- d_6 were purchased from Cambridge Isotope Labs and were degassed and stored over 4 Å molecular sieves prior to use. Dimethyl sulfoxide- d_6 was purchased from Cambridge Isotope Labs and stored over 4 Å molecular sieves prior to use. Deuterium oxide was purchased from Sigma-Aldrich and used as received. Sodium triethylborohydride solution (1.0 M in toluene) and triethylborane solution (1.0 M in hexanes) were purchased from Sigma-Aldrich. Celite® 545 (J. T. Baker) was dried in a Schlenk flask for 24 h under dynamic vacuum while heating to at least 150°C prior to use in a glovebox. All nitrile substrates were purchased from Sigma-Aldrich or Alfa Aesar and the solids were re-crystallized and dried prior to use. NMR Spectra were recorded at room temperature on a Varian spectrometer operating at 500 or 600 MHz (^1H NMR) and 126 MHz (^{13}C NMR) (U500, VXR500, UI500NB, UI600) and referenced to the residual HDO , $\text{C}_2\text{D}_5\text{HSO}$, HC_7D_7 , and $\text{C}_6\text{D}_5\text{H}$ resonance (δ in parts per million, and J in Hz) unless otherwise noted. Potassium graphite (KC_8)⁷⁸ was prepared

according to literature procedures. (^{Mes}CCC)CoCl₂py (**1**)³⁴ was prepared according to literature procedures.



Entry	Catalyst	Additive	Base	Time	Yield ^a
1	^{Mes} Co(III)Cl ₂ Pyr	none	KO ^t Bu (6 mol%)	8 hrs	- ^c
2 ^b	^{Mes} Co(III)Cl ₂ Pyr	NaHBET ₃	KO ^t Bu (6 mol%)	8 hrs	- ^c
3	none	NaHBET ₃	KO ^t Bu (6 mol%)	8 hrs	- ^c
4	Co(III)(acac) ₃	NaHBET ₃	KO ^t Bu (6 mol%)	8 hrs	- ^c
5	Co(III)(acac) ₃	NaHBET ₃	none	8 hrs	- ^c
6	Co(I)(NTMS ₂)(PPh ₃) ₂	none	KO ^t Bu (6 mol%)	8 hrs	- ^c
7	Co(I)(NTMS ₂)(PPh ₃) ₂	BEt ₃	KO ^t Bu (6 mol%)	8 hrs	- ^c
8	Co(I)Cl(PPh ₃) ₃	none	KO ^t Bu (6 mol%)	8 hrs	- ^c
9	^{Mes} Co(III)Cl ₂ Pyr	NaHBET ₃	KO ^t Bu (2 mol%)	8 hrs	83%
10	^{Mes} Co(III)Cl ₂ Pyr	NaHBET ₃	KO ^t Bu (8 mol%)	8 hrs	96%
11	^{Mes} Co(III)Cl ₂ Pyr	NaHBET ₃	K(N(SiMe ₃) ₂) (6 mol%)	8 hrs	95%
12	^{Mes} Co(III)Cl ₂ Pyr	NaHBET ₃	NaOEt (6 mol%)	8 hrs	93%
13	^{Mes} Co(III)Cl ₂ Pyr	NaHBET ₃	NaO ^t Bu (6 mol%)	8 hrs	93%
14	^{Mes} Co(III)Cl ₂ Pyr	NaHBET ₃	NaOPent (6 mol%)	8 hrs	92%
15	^{Mes} Co(III)Cl ₂ Pyr	NaHBET ₃	KO ^t Bu (6 mol%)	18 hrs	79%
16	^{Mes} Co(III)Cl ₂ Pyr	NaHBET ₃	KO ^t Bu (6 mol%)	20 hrs	76%

^aPrimary amine via GC-MS, remaining balance secondary aldimine. ^bNo H₂. ^cStarting material only.

Table 4.5. Controls and optimization of benzonitrile hydrogenation.

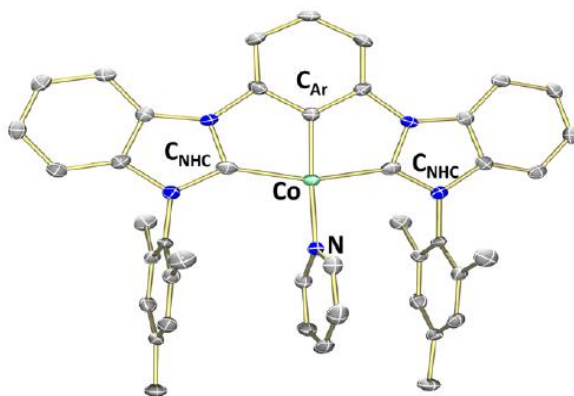


Figure 4.5. Molecular structure of (^{Mes}CCC)Co(I)(py) shown with 50% probability ellipsoids. Solvent molecules and H atoms have been omitted for clarity.*

*See paper for crystallographic parameters.

Synthesis of Cobalt(I) Complexes

Preparation of $(^{\text{Mes}}\text{CCC})\text{Co-py}$ (2-py**):** A 20 mL scintillation vial was charged with $(^{\text{Mes}}\text{CCC})\text{CoCl}_2\text{py}$ (0.100 g, 0.133 mmol) and THF (10 mL). A suspension of KC_8 (0.038 g, 0.281 mmol) in THF (5 mL) was added to the mixture. After stirring for 2 hours, the dark brown suspension was filtered over Celite and concentrated to a dark solid under reduced pressure. The product was then extracted into benzene (3 x 5 mL), filtered over Celite, and lyophilized under reduced pressure to a dark brown solid (0.072 g, 0.105 mmol, 80%). NMR data (in benzene- d_6 , 25 °C): ^1H δ = 8.03 (d, J = 5.4, 2H), 7.79 (t, J = 7.4, 1H), 7.65 (d, J = 7.6, 2H), 7.23 (t, J = 7.8, 3H), 7.00 (t, J = 7.5, 3H), 6.66 (d, J = 7.8, 4H), 6.31 (s, 5H), 1.96 (s, 6H), 1.83 (s, 12H). ^{13}C δ = 147.4, 139.7, 137.1, 136.1, 135.1, 133.1, 129.1, 128.6, 127.5, 122.3, 122.2, 110.0, 108.5, 105.9, 20.9, 17.8. HRMS (ESI), calc. for $\text{C}_{43}\text{H}_{39}\text{CoN}_5$ ($\text{M} + \text{H}$) $^+$: calculated 684.2537; found 684.2543.

Preparation of $(^{\text{Mes}}\text{CCC})\text{Co}(p\text{-NCC}_6\text{H}_4\text{OCH}_3)$ (2-NCArOCH₃**):** A 20 mL scintillation vial was charged with $(^{\text{Mes}}\text{CCC})\text{CoCl}_2\text{py}$ (0.072 g, 0.095 mmol) and THF (10 mL). A suspension of KC_8 (0.026 g, 0.194 mmol) in THF (5 mL) was added to the mixture. After stirring for 2 hours, the dark brown suspension, **2-py**, was filtered over Celite and a solution of 4-methoxybenzotrile (0.013 g, 0.095 mmol) was added. After stirring the mixture for 1 h, the solution was concentrated to a solid under reduced pressure. The product was then extracted into benzene (3 x 5 mL), filtered over Celite, and lyophilized under reduced pressure to a brown solid (0.055g, 0.074 mmol, 79%). Alternatively, **2-NCArOCH₃** can also be prepared by the addition of 1 equiv of 4-methoxybenzotrile to **2-py** following the same work up procedure. NMR data (in benzene- d_6 , 25 °C): ^1H δ = 7.92 (d, J = 8.0, 2H), 7.65-7.57 (m, 3H), 7.32 (s, 1H), 7.00 (s, 1H), 6.95 (t, J = 7.6, 2H), 6.64 (t, J = 8.1, 4H), 6.47 (s, 4H), 6.43 (d, J = 8.5, 2H), 3.20 (s, 3H), 2.03 (s, 12H), 1.74 (s, 6H). The low solubility of **2-NCArOCH₃** in benzene precluded the collection of ^{13}C NMR data.

HRMS (ESI), calc. for $C_{46}H_{40}CoN_5O$ (M)⁺: calculated 737.2565; found 737.2583. ATR-IR: 2184 cm^{-1} (Co-N \equiv CR).

***In situ* Stoichiometric Reactivity Studies**

Treatment of (^{Mes}CCC)CoCl₂py with 2 equivalence of NaHBEt₃

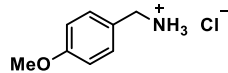
A 4 mL scintillation vial was charged with **1** (0.004 g, 0.006 mmol), NaHBEt₃ (1.0 M in toluene, 12 μ L, 0.011 mmol) and toluene (2 mL). Solution IR (C_7H_8): 2082 cm^{-1} (Co-N₂). (See Figure S9)

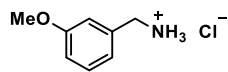
General Procedure: Nitrile Hydrogenation

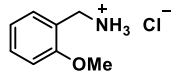
A 50 mL schlenk tube was charged with **1** (2 mg, 0.0027 mmol) and KO^tBu (0.9 mg, 0.008 mmol) in toluene (2 mL) and two equivalents of NaHBEt₃ (5.4 μ L, 0.0054 mmol) were added. The nitrile was added last and the total volume raised to 4 mL of toluene. It was then subjected to two freeze pump thaw cycles and placed under 1 atm of H₂ gas at 77K. The mixture was allowed to warm to room temperature, resulting in 4 atm of H₂ gas. The flask was placed in a 115 °C oil bath for 8hrs. The reaction was then removed from the oil bath and cooled to room temperature, the H₂ gas vented, and the reaction analyzed by GC-MS to determine conversion. In all cases the nitrile starting material was not detected by GC-MS after the completion of the reaction. The resulting reaction mixture was diluted with 15 mL of diethyl ether before HCl (0.1 mL, 0.1M, MeOH) was added and stirred at room temperature overnight. A fine green and white precipitate was obtained after removing the solvent under reduced pressure. The solid was then washed with either 5 mL diethyl ether or dichloromethane depending on the solubility and filtered through a Celite plug.

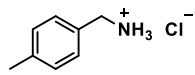
The product was then washed down in methanol and the solvents removed under reduced pressure yielding a fine white powder which was characterized by ^1H , ^{13}C , and ^{19}F NMR spectroscopy where appropriate. All catalytic yields are the average of duplicate or triplicate runs. The spectra were compared to published literature examples of these species that already contain HR-MS data. Substrate i was not found in the literature and so was further characterized by HR-MS.

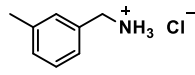
NMR Data for Isolated HCl Salts of Primary Amines:*

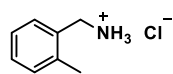
 **(4-methoxyphenyl)methanamine hydrochloride: (1b)^a** ^1H NMR (DMSO, 500 MHz): δ = 7.38 (d, J = 10.5, 2H), 7.02 (d, J = 10.5, 2H), 4.09 (s, 2H), 3.82 (s, 3H). ^{13}C NMR (DMSO, 126 MHz): 159.44, 130.66, 125.23, 114.61, 55.40, 42.67.

 **(3-methoxyphenyl)methanamine hydrochloride: (1c)^b** ^1H NMR (DMSO, 500 MHz): δ = 8.46 (s, 3H), 7.31 (t, J = 8, 1H), 7.15 (s, 1H), 7.04 (d, J = 7, 1H), 6.93 (d, J = 8, 1H), 3.97 (s, 2H), 3.76 (s, 3H). ^{13}C NMR (DMSO, 126 MHz): 159.26, 135.69, 129.58, 120.95, 114.48, 113.89, 55.20, 42.04.

 **(2-methoxyphenyl)methanamine hydrochloride: (1d)^b** ^1H NMR (DMSO, 500 MHz): δ = 8.38 (s, 3H), 7.39 (m, 2H), 7.06 (d, J = 10, 1H), 6.97 (t, J = 9.5, 1H), 3.94 (s, 2H), 3.83 (s, 3H). ^{13}C NMR (DMSO, 126 MHz): 157.13, 130.24, 121.73, 120.23, 110.87, 55.52, 37.42.

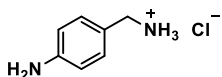
 **p-tolylmethanamine hydrochloride: (1e)^b** ^1H NMR (DMSO, 500 MHz): δ = 8.57 (s, 3H), 7.56 (d, J = 7.5, 2H), 7.41 (d, J = 8, 2H), 4.14 (s, 2H), 2.70 (s, 3H). ^{13}C NMR (DMSO, 126 MHz): 137.70, 131.20, 129.07, 129.01, 41.89, 20.82.

 **m-tolylmethanamine hydrochloride: (1f)^a** ^1H NMR (DMSO, 500 MHz): δ = 8.61 (s, 3H), 7.29 (m, 3H), 7.17 (d, J = 7.5, 1H), 3.94 (s, 2H), 2.30 (s, 3H). ^{13}C NMR (DMSO, 126 MHz): 137.42, 133.87, 129.28, 128.65, 128.18, 125.74, 41.96, 20.71.



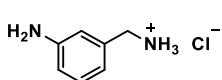
o-tolylmethanamine hydrochloride: (1g)^c ¹H NMR (DMSO, 500 MHz): δ = 8.46 (s, 3H), 7.42 (d, J = 7, 1H), 7.25 (m, 3H), 3.99 (s, 2H), 2.35 (s, 3H). ¹³C NMR

(DMSO, 126 MHz): 136.39, 132.16, 130.03, 129.02, 128.16, 125.75, 39.32, 18.57.



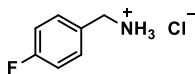
4-(aminomethyl)aniline dihydrochloride: (1h)^b ¹H NMR (D₂O, 500 MHz): δ = 7.20 (d, J = 7, 2H), 6.80 (d, J = 10, 2H), 3.99 (s, 2H). ¹³C NMR (D₂O, 126

MHz): 147.16, 130.36, 130.32, 123.26, 116.59, 42.89.



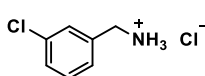
3-(aminomethyl)aniline dihydrochloride: (1i) ¹H NMR (D₂O, 500 MHz): δ = 7.25 (t, J = 9.5, 1H), 6.84 (m, 3H), 4.04 (s, 2H). ¹³C NMR (D₂O, 126 MHz):

147.04, 134.09, 130.34, 119.53, 116.99, 116.36, 43.23. HRMS (ESI), calc. for C₇H₁₁N₂Cl⁺: calculated 123.0917; found 123.0922.



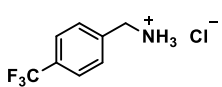
(4-fluorophenyl)methanamine hydrochloride: (1j)^b ¹H NMR (DMSO, 500 MHz): δ = 8.42 (s, 3H), 7.55 (m, 2H), 7.26 (m, 2H), 4.00 (s, 2H). ¹³C NMR

(DMSO, 126 MHz): 162.07 (d, J = 306.3), 131.43 (t, J = 8.7), 130.51 (d, J = 2.8), 115.35 (dd, J = 26.9, 6.1), 41.36 (t, J = 7.1). ¹⁹F NMR (DMSO, 470 MHz): δ = -114.47.



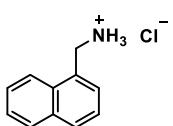
(3-chlorophenyl)methanamine hydrochloride: (1k)^c ¹H NMR (DMSO, 500 MHz): δ = 8.55 (s, 3H), 7.64 (s, 1H), 7.46 (m, 3H), 4.02 (s, 2H). ¹³C NMR

(DMSO, 126 MHz): 136.64, 132.99, 130.35, 128.91, 128.22, 127.76, 41.42.



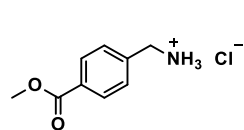
(4-(trifluoromethyl)phenyl)methanamine hydrochloride: (1l)^b ¹H NMR (DMSO, 500 MHz): δ = 8.54 (s, 3H), 7.79 (d, J = 7.5, 2H), 7.73 (d, J = 7, 2H),

4.12 (s, 2H). ¹³C NMR (DMSO, 126 MHz): 139.09, 129.80, 128.77 (q, J = 31.5), 125.28 (q, J = 3.8), 124.11 (q, J = 272), 41.51. ¹⁹F NMR (DMSO, 470 MHz): δ = 61.50.



naphthalen-1-ylmethanamine hydrochloride: (1m)^b ¹H NMR (DMSO, 500 MHz): δ = 8.58 (s, 3H), 8.15 (d, J = 8, 1H), 7.99 (m, 2H), 7.61 (m, 4H), 4.51 (s,

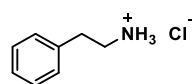
2H). ^{13}C NMR (DMSO, 126 MHz): 133.19, 130.66, 130.14, 128.95, 128.62, 127.24, 126.72, 126.19, 125.35, 123.48, 39.15.



(4-(methoxycarbonyl)phenyl)methanaminium chloride: (1n)^b ^1H NMR

(DMSO, 500 MHz): δ = 8.75 (s, 3H), 7.96 (d, J = 8.5, 2H), 7.67 (d, J = 8, 2H),

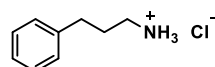
4.09 (s, 2H), 3.85 (s, 3H). ^{13}C NMR (DMSO, 126 MHz): 165.89, 129.37, 129.21, 129.18, 52.24, 41.68.



2-phenylethan-1-amine hydrochloride: (1o)^b ^1H NMR (DMSO, 500 MHz): δ

= 8.28 (s, 3H), 7.32 (m, 2H), 7.24 (m, 3H), 2.96 (m, 4H). ^{13}C NMR (DMSO, 126

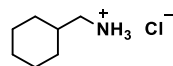
MHz): 137.52, 128.63, 128.61, 126.68, 39.93, 32.93.



3-phenylpropan-1-amine hydrochloride: (1p)^b ^1H NMR (DMSO, 500 MHz):

δ = 8.19 (s, 3H), 7.29 (m, 2H), 7.19 (m, 3H), 2.74 (m, 2H), 2.64 (m, 2H), 1.87

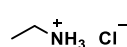
(m, 2H). ^{13}C NMR (DMSO, 126 MHz): 140.94, 128.39, 128.28, 125.99, 38.27, 31.92, 28.80.



cyclohexylmethanamine hydrochloride: (1q)^b ^1H NMR (DMSO, 500 MHz): δ =

8.05 (s, 3H), 2.60 (d, J = 6.4, 2H), 1.70 (m, 4H), 1.58 (m, 2H), 1.15 (m, 3H), 0.90

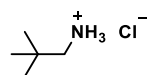
(m, 2H). ^{13}C NMR (DMSO, 126 MHz): 44.35, 35.37, 29.83, 25.67, 25.07.



ethanamine hydrochloride: (1r)^d ^1H NMR (DMSO, 500 MHz): δ = 8.02 (s, 3H),

2.79 (q, J = 7.5, 2H), 1.15 (t, J = 7.3, 3H). ^1H NMR (D₂O, 500MHz): δ = 3.03 (qd, J = 7.5, 2H),

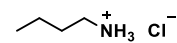
1.26 (t, J = 7, 3H). ^{13}C NMR (DMSO, 126 MHz): 34.02, 12.51.

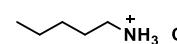


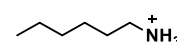
2,2-dimethylpropan-1-amine hydrochloride: (1s)^c ^1H NMR (DMSO, 500 MHz): δ

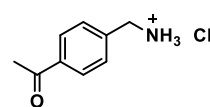
= 8.11 (s, 3H), 2.58 (s, 2H), 0.94 (s, 9H). ^{13}C NMR (DMSO, 126 MHz): 49.68, 30.13,

26.91.

 **butan-1-amine hydrochloride: (1t)^e** ¹H NMR (DMSO, 500 MHz): δ = 8.13 (s, 3H), 2.72 (t, J = 8.6, 2H), 1.53 (m, 2H), 1.31 (m, 2H), 0.87 (t, J = 8.8, 3H). ¹³C NMR (DMSO, 126 MHz): 38.38, 28.98, 19.18, 13.51.

 **pentan-1-amine hydrochloride: (1u)^f** ¹H NMR (DMSO, 500 MHz): δ = 8.12 (s, 3H), 2.71 (t, J = 7.5, 2H), 1.55 (m, 2H), 1.27 (m, 4H), 0.86 (t, J = 6.8, 3H). ¹³C NMR (DMSO, 126 MHz): 38.62, 28.01, 26.57, 21.66, 13.76.

 **hexan-1-amine hydrochloride: (1v)^f** ¹H NMR (DMSO, 500 MHz): δ = 8.13 (s, 3H), 2.71 (t, J = 7.3, 2H), 1.55 (m, 2H), 1.25 (m, 8H), 0.85 (t, J = 6.8, 3H). ¹³C NMR (DMSO, 126 MHz): 38.67, 31.07, 28.23, 26.92, 25.86, 22.00, 13.94.

 **1-[4-(aminomethyl)phenyl]ethan-1-one hydrochloride: (1w)^g** ¹H NMR (DMSO, 500 MHz): δ = 8.51 (s, 3H), 7.97 (d, J = 8.5, 2H), 7.66 (d, J = 8, 2H), 4.09 (s, 2H), 2.58 (s, 3H). ¹³C NMR (DMSO, 126 MHz): 197.63, 139.23, 136.55, 129.08, 128.28, 41.68, 26.83. ATR-IR (ATR): 1696.80 cm⁻¹ (C=O).

HR-MS data

^aBornschein, C.; Werkmeister, S.; Junge, K.; Beller, M. TBAF-catalyzed hydrosilylation for the reduction of aromatic nitriles. *New J. Chem.* **2013**, *37*, 2061-2065.

^bBornschein, C.; Werkmeister, S.; Wendt, B.; Jiao, H.; Alberico, E.; Baumann, W.; Junge, H.; Junge, K.; Beller, M. Mild and selective hydrogenation of aromatic and aliphatic (di)nitriles with a well-defined iron pincer complex. *Nat. Comm.* **2014**, *5*, 1-11.

^cGandhamsetty, N.; Jeong, J.; Park, J.; Park, S.; Chang, S. Boron-catalyzed silylative reduction of nitriles in accessing primary amines and imines. *J. Org. Chem.* **2015**, *80*, 7281-7287.

^dJackson, D. M.; Ashley, R. L.; Brownfield, C. B.; Morrison, D. R.; Morrison, R. W. Rapid conventional and microwave-assisted decarboxylation of l-histidine and other amino acids via organocatalysis with r-carvone under superheated conditions. *Synthetic Communications* **2015**, *45*, 2691-2700.

^eChen, X.; Zhou, S.; Qian, C. Hydrogen transfer reduction of nitriles in DBU based ionic liquids. *Arkivoc*, **2012**, *8*, 128-136.

^fWerkmeister, S.; Junge, K.; Wendt, B.; Spannenberg, A.; Jiao, H.; Bornschein, C.; Beller, M. *Chem. Eur. J.* **2014**, *20*, 4227-4231.

^gMurai, N.; Miyano, M.; Yonaga, M.; Tanaka, K. One-Pot primary aminomethylation of aryl and heteroaryl halides with sodium phthalimidomethyltrifluoroborate. *Org. Lett.* **2012**, *14* (11), 2818-2821.

*See paper for actual substrate ¹H NMR spectra

^1H NMR Spectrum, 500 MHz, C_6D_6 (2-py)

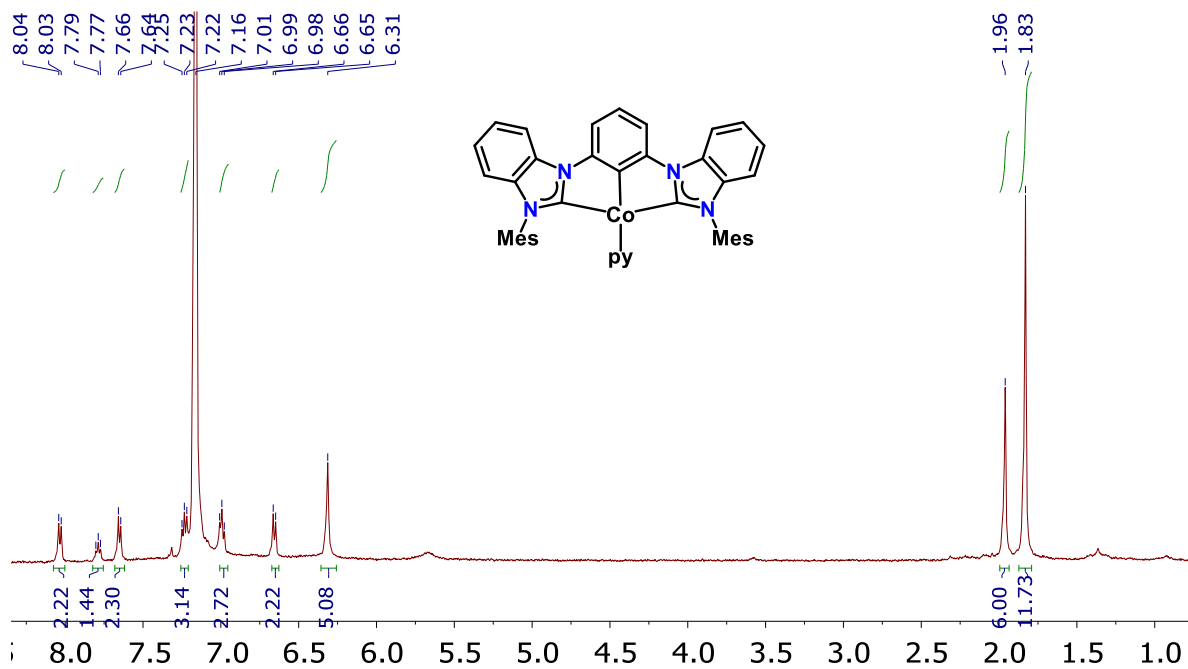


Figure 4.6. ^1H NMR (C_6D_6 , 500 MHz) spectrum of $(^{\text{Mes}}\text{CCC})\text{Co-py}$ (2-py).

^{13}C NMR Spectrum, 126 MHz, C_6D_6 (2-py)

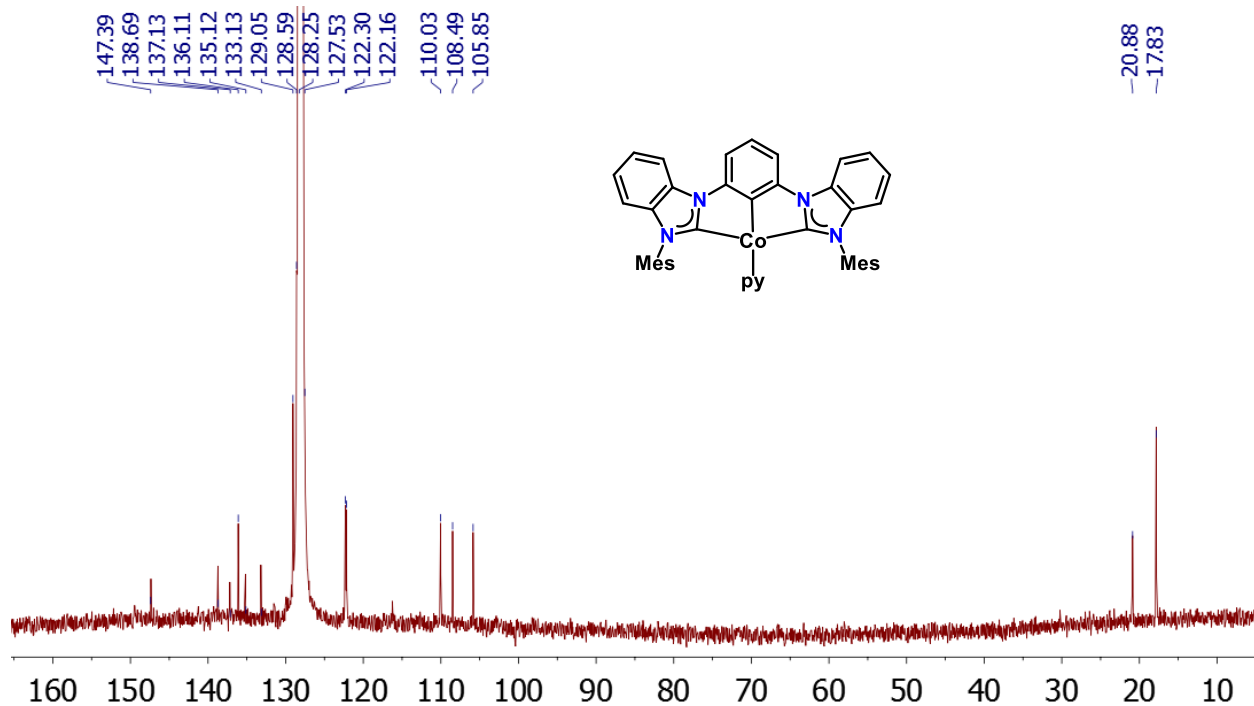


Figure 4.7. ^{13}C NMR (C_6D_6 , 126 MHz) spectrum of $(^{\text{Mes}}\text{CCC})\text{Co-py}$ (2-py).

¹H NMR Spectrum, 500 MHz, C₆D₆ (2-NCArOCH₃)

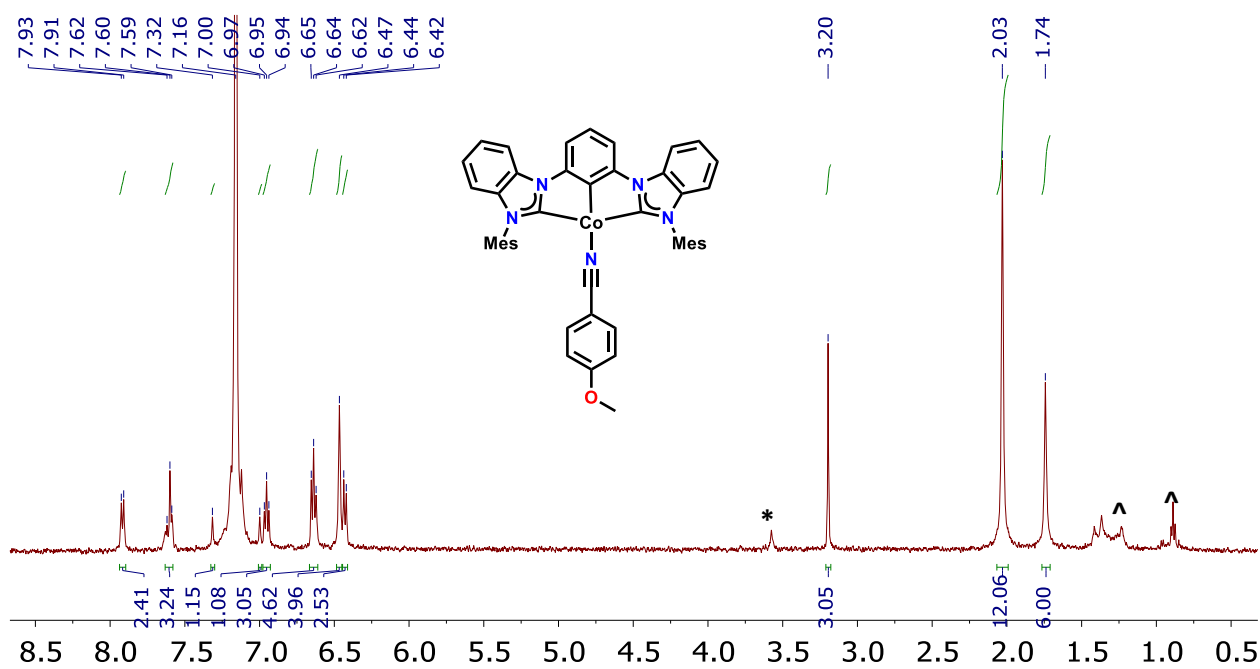
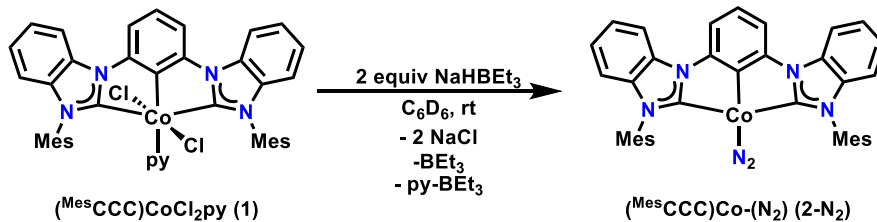
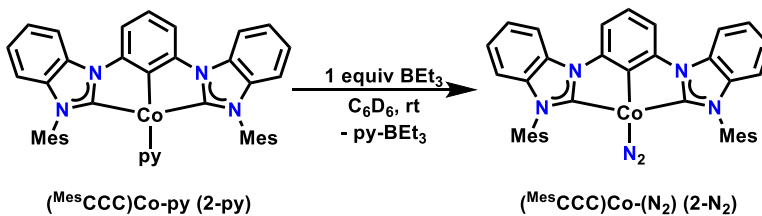
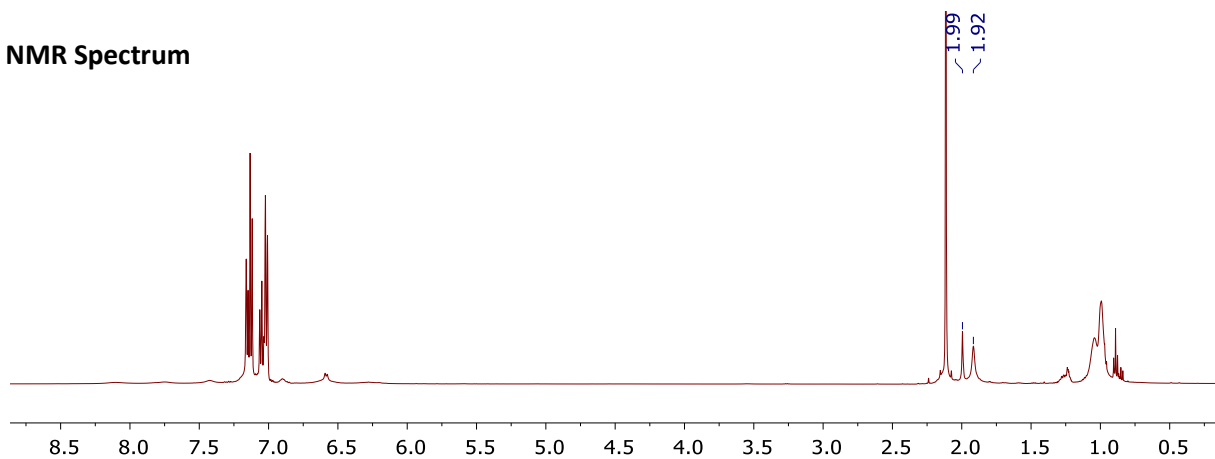


Figure 4.8. ¹H NMR (C₆D₆, 500 MHz) spectrum of (^{Mes}CCC)Co(*p*-NCC₆H₄OCH₃) (2-NCArOCH₃). (*denotes THF, ^denotes H grease).

¹H NMR Spectra, 500 MHz, C₆D₆. **1** reaction with 2 equiv. NaHBET₃ and 2-py reaction with BEt₃.



¹H NMR Spectrum



¹H NMR Spectrum

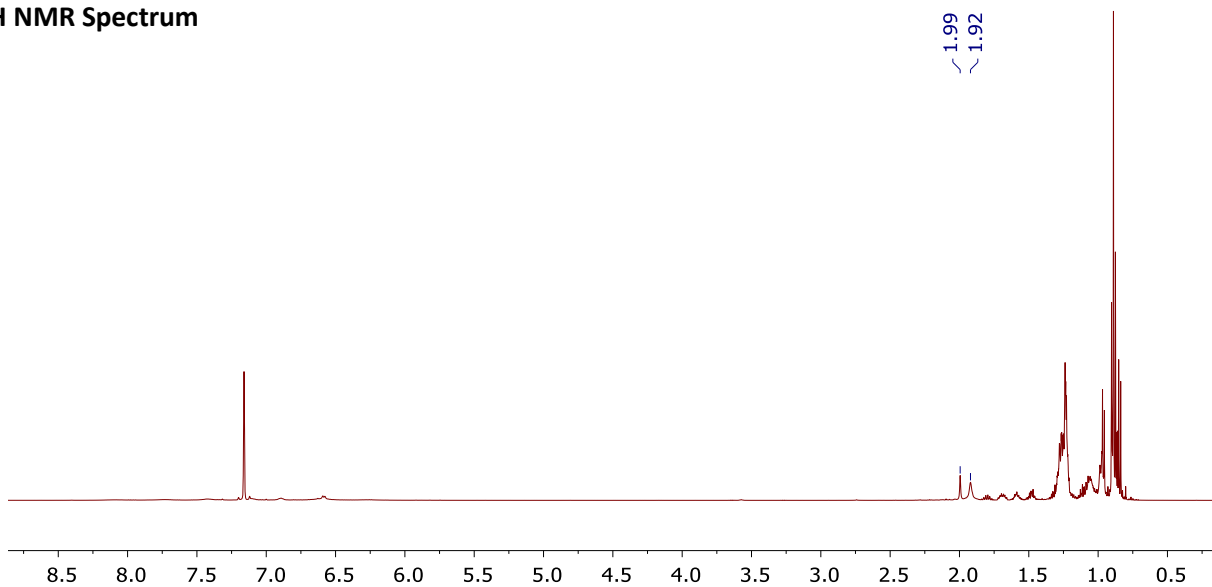


Figure 4.9. ¹H NMR (C₆D₆, 500 MHz) spectrum of **1** reaction with 2 equiv of NaHBET₃ (1.0 M toluene) (top) and **2-py** reaction with BEt₃ (1.0 M hexanes) (bottom).

***Para*-hydrogen (*p*-H₂) Induced Polarization (PHIP) NMR Studies**

Sample preparation using 1. A standard J. Young NMR tube was charged with 4-methoxybenzotrile (17.6 mg, 0.133 mmol), KO^tBu (1.0 mg, 0.0089 mmol) and **1** (2.0 mg, 0.0027 mmol) in *ca.* ½ ml of toluene-*d*₈. A solution of NaHBET₃ (1.0 M in toluene, 5.3 µL, 0.0053 mmol) was added and the color the solution turned brown. The sample was subjected to two freeze-pump-thaw cycles and *p*-H₂ gas (1 atm) was added at 77K on a high-vacuum line. The sample was kept frozen in liquid nitrogen and warmed to ambient temperature and shaken immediately prior to inserting into the NMR spectrometer (Following ALTADENA conditions). No polarization was observed at 30 °C and 60 °C. Upon warming the probe temperature to 85 °C, polarization of the imine functionality was observed (see Figure S11). In the case of 4-(trifluoromethyl)benzotrile, polarization of the imine functionality was observed upon warming the probe temperature to 80 °C (see Figure S12).

Sample preparation using 2-py. A standard J. Young NMR tube was charged with 4-methoxybenzotrile (9.7 mg, 0.0731 mmol), NaO^tBu (0.4 mg, 0.0416 mmol), **2-py** (1.0 mg, 0.00146 mmol) and BEt₃ (1.0 M in hexane, 3.0 µL, 0.003 mmol) in *ca.* 1 ml of toluene-*d*₈. The sample was subjected to two freeze-pump-thaw cycles and *p*-H₂ gas (1 atm) was added at 77K on a high-vacuum line. The sample was kept frozen in liquid nitrogen and warmed to ambient temperature and shaken immediately prior to inserting into the NMR spectrometer. No polarization was observed at 25 °C. Upon warming the probe temperature to 65 °C, 70 °C and 75 °C, polarization of the H atoms of the imine functionality were observed (at 75 °C, the signals were more pronounced and are depicted in Figure S13). In the case of 4-(trifluoromethyl)benzotrile, polarization of the imine functionality was observed upon warming the probe temperature to 55 °C and 65 °C. At 65 °C the imine signals were more pronounced and are depicted in Figure S14.

NMR Spectrometer. All PHIP NMR data presented herein were collected on a Varian UNITY Inova 600 NB High-Resolution NMR Console with a 5mm Varian AutoTuneX $^1\text{H}/\text{X}$ PFG Z probe, $\text{X} = ^{31}\text{P}-^{15}\text{N}$. All spectra were collected in toluene- d_8 and the residual solvent resonance ($\text{C}_6\text{D}_5\text{CD}_3$) was referenced to 2.08 ppm. ^1H NMR spectra were recorded using 45° pulse angle. The spectral window of 30ppm was used in both proton and ^1H -OPSY experiments. ^1H -OPSY NMR data was collected via a double quantum coherence pathway using the pulse sequence below (**Figure S10**). The ^1H -OPSY spectra are anti-phase peaks, and they are displayed with absolute mode (phase correction) in the following spectra.^{79,80}

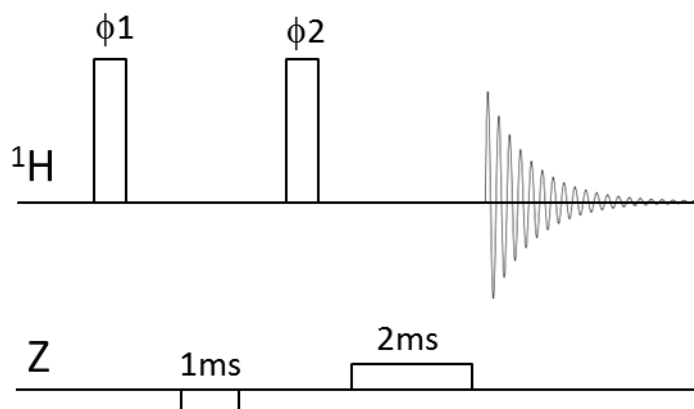


Figure 4.10. Double quantum OPSY pulse sequence (OPSY-d): the vertical bar at ^1H channel represents $\pi/2$ pulse. Phase cycle: $\phi 1$: $(y)_4(x)_4$, $\phi 2$: $(x)_4(y)_4$, rec: $(x)_4(y)_4$. Z Gradient: 50 G/cm rectangular gradient was used. First gradient was applied for 1ms in the opposite direction of the second gradient which was applied for 2ms. 0.5ms gradient recovery delays were used after each gradient. The acquisition time was 4 seconds and no delay between scans was used.

Generation of *para*-hydrogen. A parahydrogen converter was used to generate the *para*- H_2 enriched hydrogen gas. This consisted of copper tubing filled with a hydrous ferric oxide catalyst that was cooled to 14 K using a closed-cycle helium cryostat. A detailed description of the converter can be found in Tom *et al.*, which was able to consistently convert naturally occurring

hydrogen gas (3:1 *ortho:para*) to 99.99% *para*-H₂.⁸¹ For practical and convenience purposes, a lecture bottle was filled with *p*-H₂ to 50 psi.

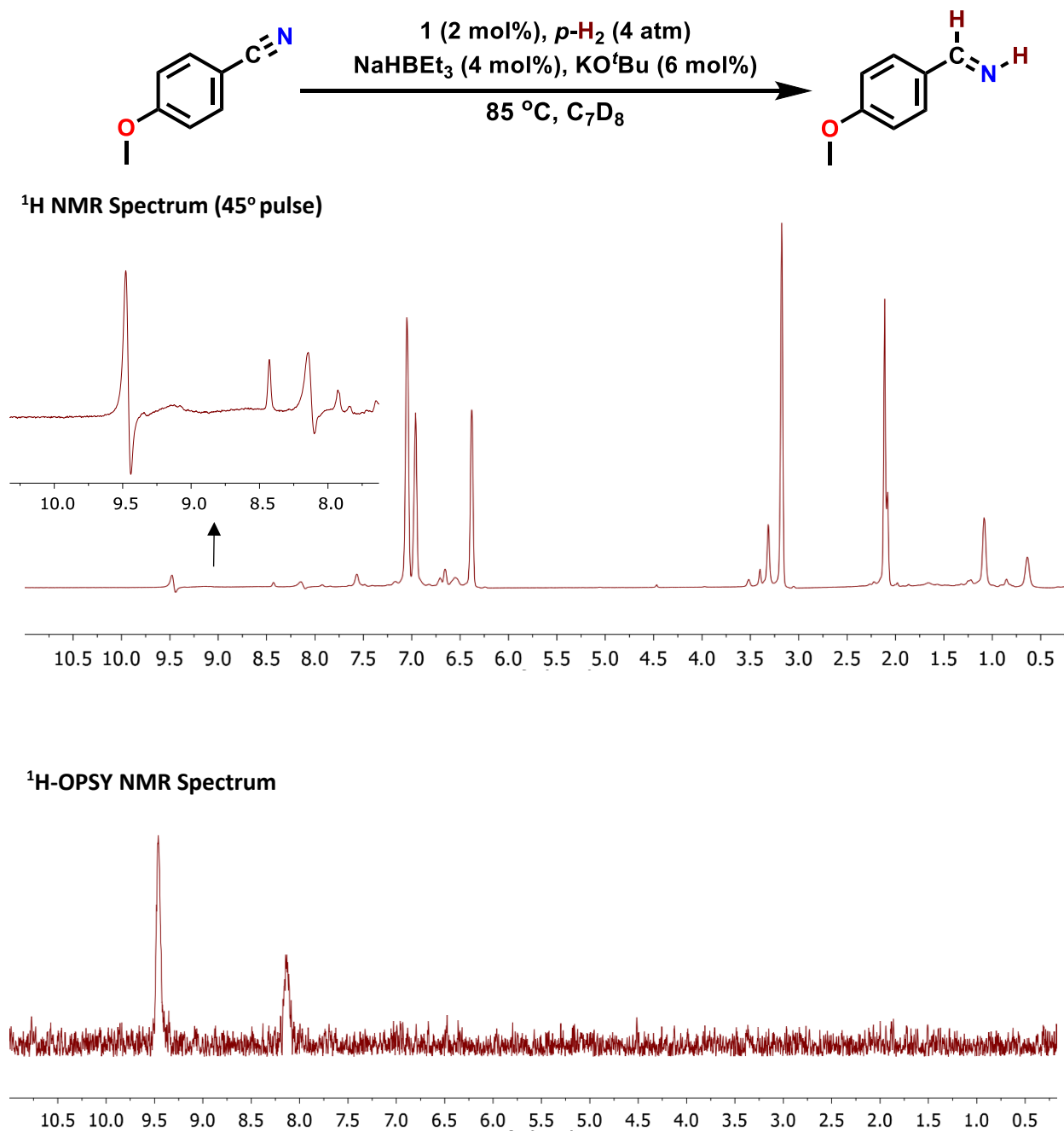
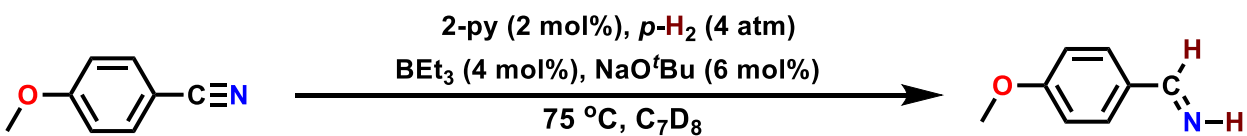


Figure 4.11. ¹H NMR (C₇D₈, 600 MHz, 45° pulse) spectrum of **1** (2 mol%), NaHBET₃ (4 mol%), KO^tBu (6 mol%) and 4-methoxybenzointrile under 4 atm of *p*-H₂ at 85 °C (top). ¹H-OPSY NMR (C₇D₈, 600 MHz) spectrum of **1** (2 mol%), NaHBET₃ (4 mol%), KO^tBu (6 mol%) and 4-methoxybenzointrile under 4 atm of *p*-H₂ at 85 °C (bottom).



¹H NMR Spectrum (45° pulse)

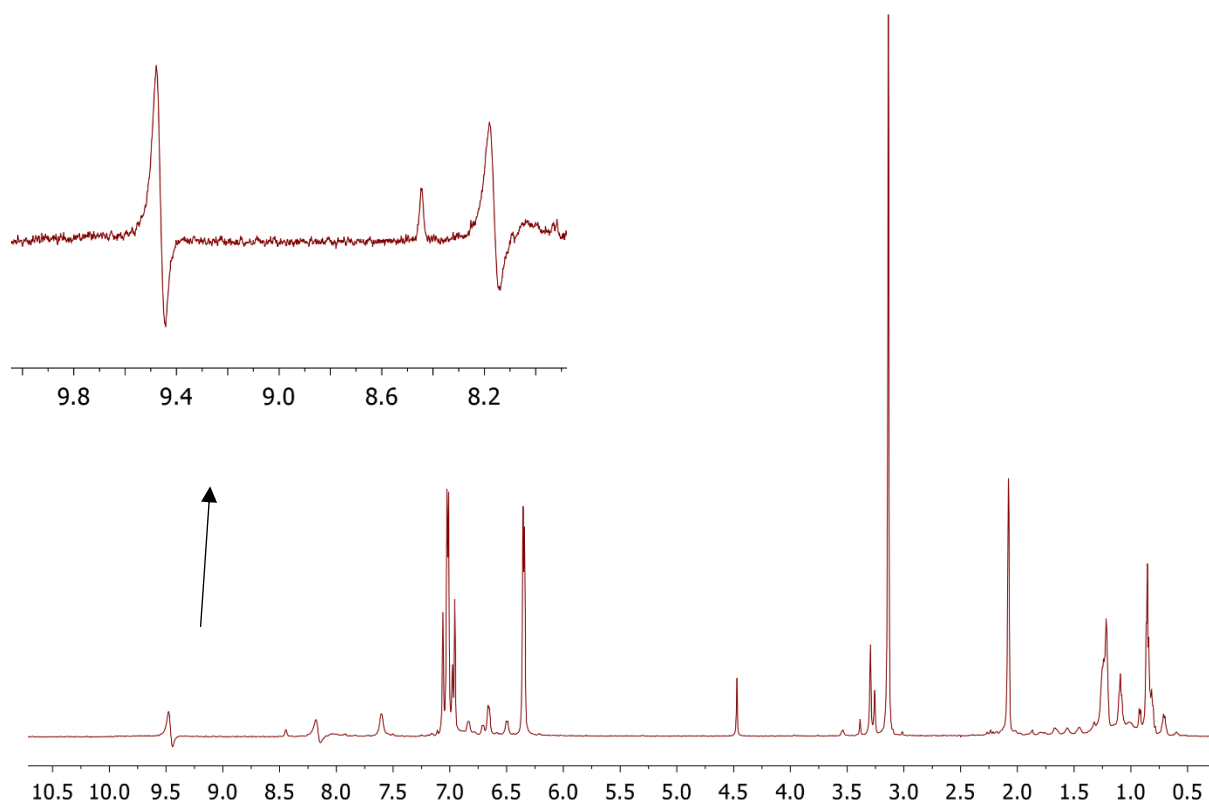


Figure 4.12. ¹H NMR (C₇D₈, 600 MHz, 45° pulse) spectrum of **2-py** (2 mol%), BEt₃ (4 mol%), NaO^tBu (6 mol%) and 4-methoxybenzotrile under 4 atm of *p*-H₂ at 75 °C.

Amine concentration experiment with 4-methoxybenzylamine and 4-tolunitrile or 4-methoxybenzotrile

A standard J. Young NMR tube was charged with 4-tolunitrile (4.3 mg, 0.0367 mmol) or 4-methoxybenzotrile (4.9 mg, 0.0367 mmol), 4-methoxybenzylamine (5 μ L, 0.367 mmol), NaO^tBu (0.2 mg, 0.002 mmol), **2-py** (0.5 mg, 0.0007 mmol) and BEt₃ (1.0 M in hexane, 1.5 μ L, 0.0015 mmol) in *ca.* ½ mL of toluene-*d*₈. The sample was subjected to two freeze-pump-thaw cycles and H₂ gas (1 atm) was added at 77K on a high-vacuum line. After heating the reaction for 9 h in at 115 °C, the H₂ was vented and complete conversion to the primary amine product was observed for 4-tolunitrile by GC-MS analysis. When 4-methoxybenzotrile was used, only the amine product was observed by GC-MS.

***In situ* NMR monitoring of a catalytic run**

A standard J. Young NMR tube was charged with 4-methoxybenzotrile (4.9 mg, 0.0365 mmol), NaO^tBu (0.2 mg, 0.002 mmol), **2-py** (0.5 mg, 0.0007 mmol), BEt₃ (1.0 M in hexane, 1.5 μ L, 0.0015 mmol) and triphenyl methane (4.46 mg, 0.0182 mmol, internal standard) in *ca.* ½ mL of toluene-*d*₈. The sample was subjected to two freeze-pump-thaw cycles and H₂ gas (1 atm) was added at 77K on a high-vacuum line. After warming the NMR tube to ambient temperature, the reaction was heated in a 115 °C oil bath. For each time point, the reaction was removed from the oil bath, allowed to cool to ambient temperature, washed with hexanes to remove the excess oil and an ¹H NMR spectrum was recorded (**Figure S15**).

In situ NMR monitoring of a catalytic run

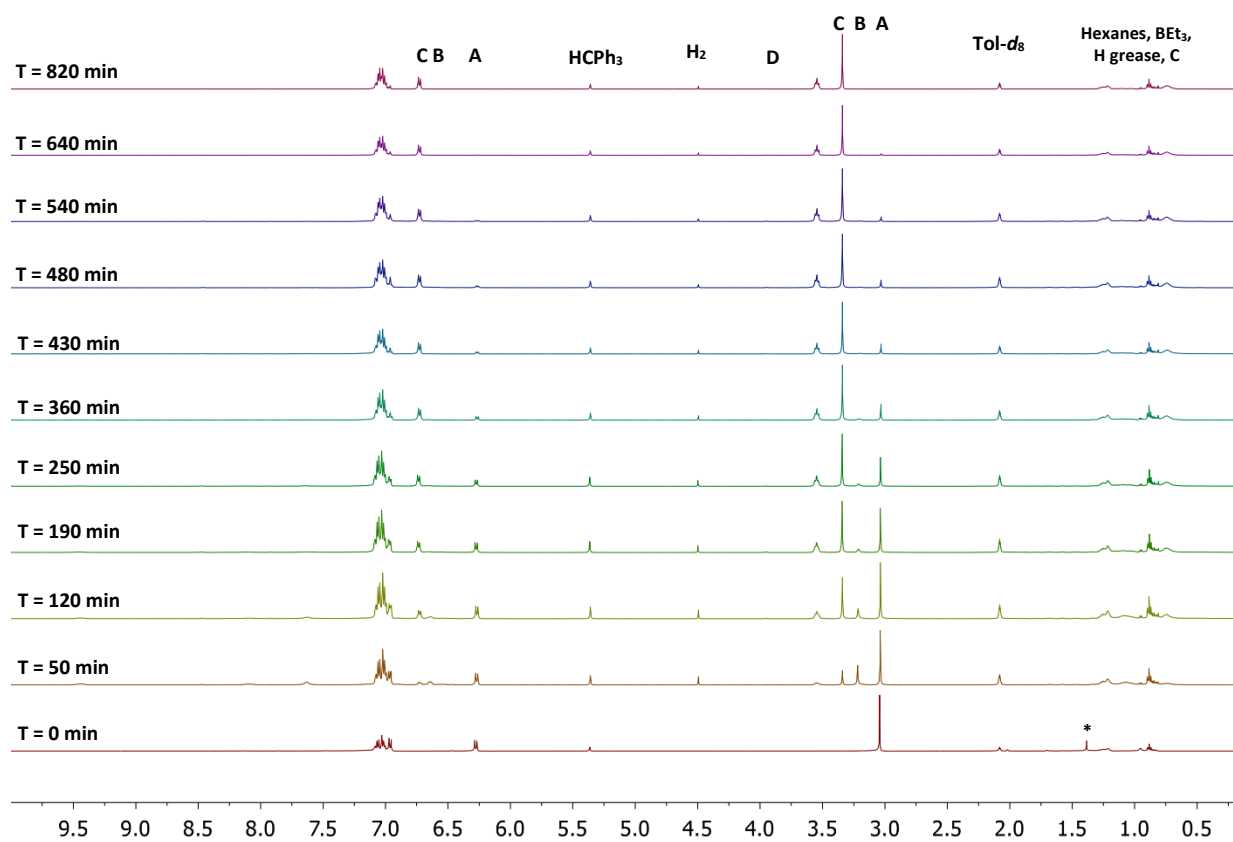
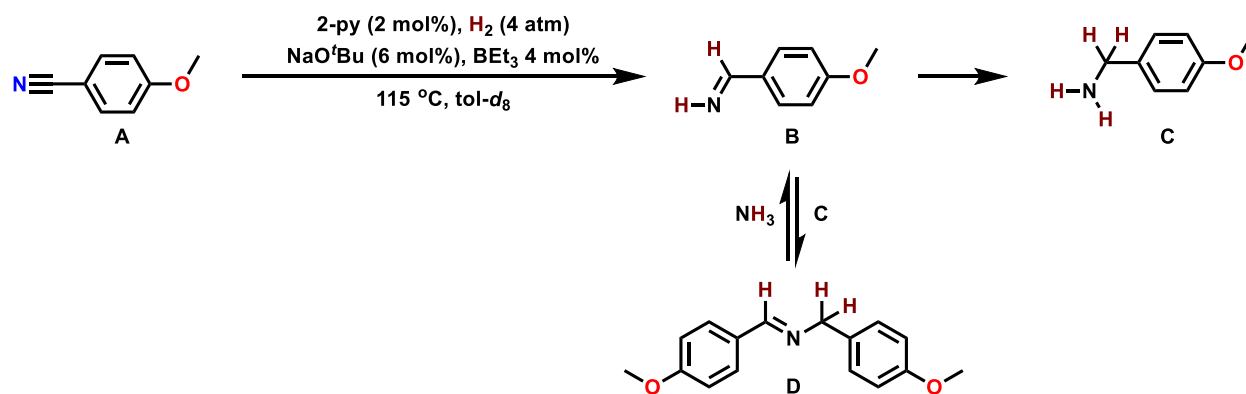


Figure 4.13. ¹H NMR (C₇D₈, 500 MHz) spectra of **2-py** (2 mol%), BEt₃ (4 mol%), NaO^tBu (6 mol%) and 4-methoxybenzonitrile under 4 atm of H₂ taken at different timepoints during the hydrogenation reaction.

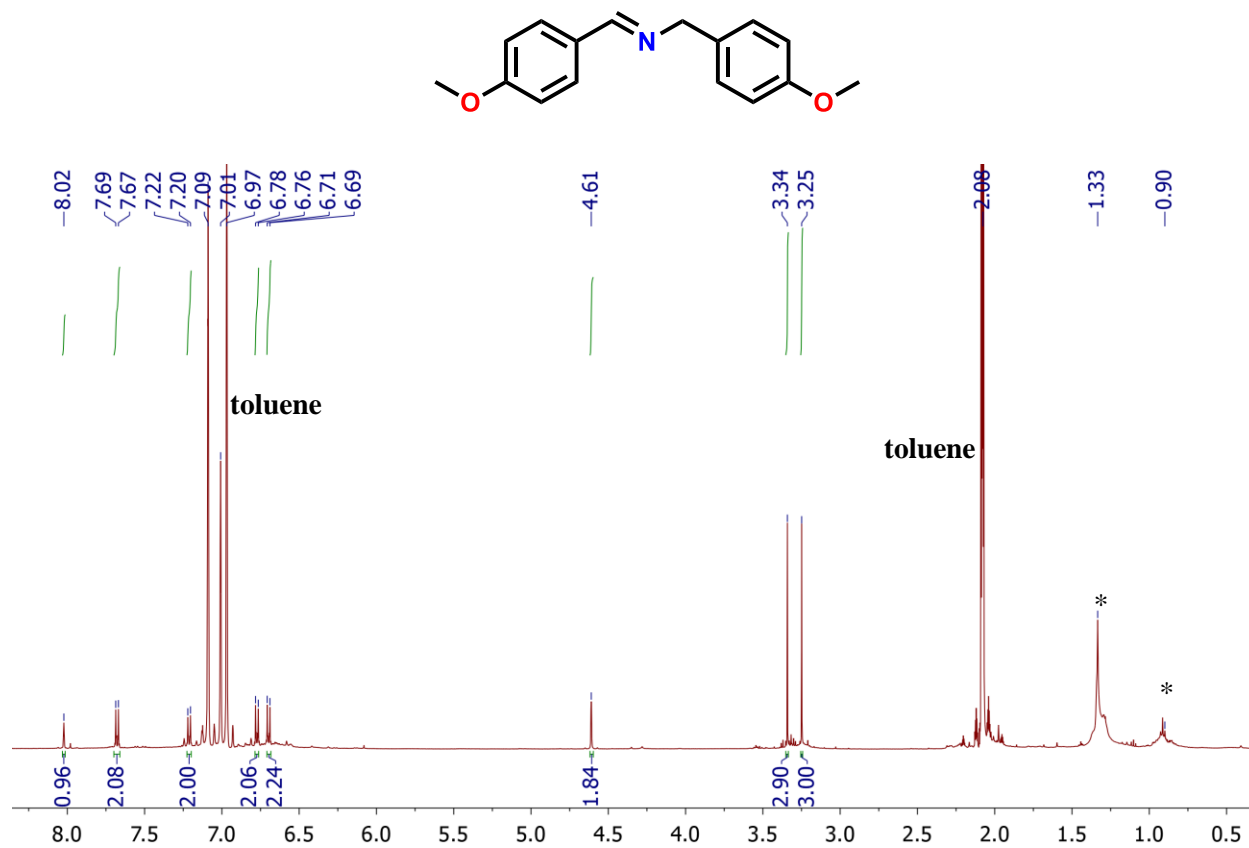


Figure 4.14. ^1H NMR (C_7D_8 , 500 MHz) spectra N-(4-methoxybenzyl)-1-(4-methoxyphenyl)methanimine. (*denotes H grease)

^1H NMR data (in toluene- d_8 , 25 °C, 500 MHz): ^1H δ = 8.02 (s, 1H), 7.68 (d, J = 8.8, 2H), 7.21 (d, J = 8.8, 2H), 6.77 (d, J = 8.6, 2H), 6.70 (d, J = 8.7, 2H), 4.61 (s, 2H), 3.34 (s, 3H), 3.25 (s, 3H).

4.5 References

1. Bagal, D. B.; Bhanage, B. Recent Advances in Transition Metal-Catalyzed Hydrogenation of Nitriles. *Adv. Synth. Catal.* **2015**, *357*, 883–900 and references therein.
2. Blaser, H.; Malan, C.; Pugin, B.; Spindler, F.; Steiner, H.; Studer, M. Selective Hydrogenation for Fine Chemicals: Recent Trends and New Developments. *Adv. Synth. Catal.* **2003**, *345*, 103–151.
3. Banwell, M. G.; Jones, M. T.; Reekie, T. A.; Schwartz, B. D.; Tan, S. H.; White, L. V. Raney® cobalt – an underutilized reagent for the selective cleavage of C-X and N-O bonds. *Org. Biomol. Chem.* **2014**, *12*, 7433–7444.
4. Amundsen, L. H.; Nelson, L. S. Reduction of Nitriles to Primary Amines with Lithium Aluminum Hydride. *J. Am. Chem. Soc.* **1951**, *73*, 242–244.
5. Hudlicky, M. *Reductions in Organic Chemistry*, John Wiley & Sons: New York, 1984.
6. Rajesh, K.; Dudle, B.; Blacque, Ol.; Berke, H. Homogeneous Hydrogenations of Nitriles Catalyzed by Rhenium Complexes. *Adv. Synth. Catal.* **2011**, *353*, 1479–1484.
7. Li, T.; Bergner, I.; Haque, F. N.; Zimmer-De Iuliis, M.; Song, D.; Morris, R. H. Hydrogenation of Benzonitrile to Benzylamine Catalyzed by Ruthenium Hydride Complexes with P-NH-NH-P Tetradentate Ligands: Evidence for a Hydridic-Protonic Outer Sphere Mechanism. *Organometallics* **2007**, *26*, 5940–5949.
8. Enthaler, S.; Junge, K.; Addis, D.; Erre, G.; Beller, M. A Practical and Benign Synthesis of Primary Amines through Ruthenium-Catalyzed Reduction of Nitriles. *ChemSusChem* **2008**, *1*, 1006–1010.

9. Addis, D.; Enthaler, S.; Junge, K.; Wendt, B.; Beller, M. Ruthenium N-heterocyclic carbene catalysts for selective reduction of nitriles to primary amines. *Tetrahedron Lett.* **2009**, *50*, 3654–3656.
10. Gunanathan, C.; Holscher, M.; Leitner, W. Reduction of Nitriles to Amines with H₂ Catalyzed by Nonclassical Ruthenium Hydrides – Water-Promoted Selectivity for Primary Amines and Mechanistic Investigations. *Eur. J. Inorg. Chem.* **2011**, 3381–3386.
11. Miao, X.; Bidange, J.; Dixneuf, P. H.; Fischmeister, C.; Bruneau, C.; Dubois, J.; Couturier, J. Ruthenium-Benzylidenes and Ruthenium-Indenylidenes as Efficient Catalysts for the Hydrogenation of Aliphatic Nitriles into Primary Amines. *ChemCatChem* **2012**, *4*, 1911–1916.
12. Werkmeister, S.; Junge, K.; Wendt, B.; Spannenberg, A.; Jiao, H.; Bornschein, C.; Beller, M. Ruthenium/Imidazolylphosphine Catalysis: Hydrogenation of Aliphatic and Aromatic Nitriles to Form Amines. *Chem. Eur. J.* **2014**, *20*, 4227–4231.
13. Adam, R.; Bheeter, C. B.; Jackstell, R.; Beller, M. A Mild and Base-Free Protocol for the Ruthenium-Catalyzed Hydrogenation of Aliphatic and Aromatic Nitriles with Tridentate Phosphine Ligands. *ChemCatChem* **2016**, *8*, 1329–1334.
14. Adam, R.; Alberico, E.; Baumann, W.; Drexler, H.; Jackstell, R.; Junge, H.; Beller, M. NNP-Type Pincer IMidazolylphosphine Ruthenium Complexes: Efficient Base-Free Hydrogenation of Aromatic and Aliphatic Nitriles under Mild Conditions. *Chem. - Eur. J.* **2016**, *22*, 4991–5002.
15. Reguillo, R.; Grellier, M.; Vautravers, N.; Vendier, L.; Sabo-Etienne, S. Ruthenium-Catalyzed Hydrogenation of Nitriles: Insights into the Mechanism. *J. Am. Chem. Soc.* **2010**, *132*, 7854–7855.

16. Yoshida, T.; Okano, T.; Otsuka, S. Catalytic Hydrogenation of Nitriles and Dehydrogenation of Amines with Rhodium(I) Hydrido Compounds $[\text{RhH}(\text{PPr}^i_3)_3]$ and $[\text{Rh}_2\text{H}_2(\mu\text{-N}_2)\{\text{P}(\text{cyclohexyl})_3\}_4]$. *J. Chem. Soc., Chem. Commun.* **1979**, 870–871.
17. Xie, X.; Liotta, C. L.; Eckert, C. CO_2 -Protected Amine Formation from Nitrile and Imine Hydrogenation in Gas-Expanded Liquids. *Ind. Eng. Chem. Res.* **2004**, *43*, 7907–7911.
18. Anastas, P. T.; Kirchhoff, M. M. Origins, Current Status, and Future Challenges of Green Chemistry. *Acc. Chem. Res.* **2002**, *35*, 686–694.
19. Bullock, R. M. Abundant Metals Give Precious Hydrogenation Performance. *Science* **2013**, *342*, 1054–1055.
20. Elangovan, S.; Topf, C.; Fischer, S.; Jiao, H.; Spannenberg, A.; Baumann, W.; Ludwig, R.; Junge, K.; Beller, M. Selective Catalytic Hydrogenations of Nitriles, Ketones, and Aldehydes by Well-Defined Manganese Pincer Complexes. *J. Am. Chem. Soc.* **2016**, *138*, 8809–8814.
21. Bornschein, C.; Werkmeister, S.; Wendt, B.; Jiao, H.; Alberico, E.; Baumann, W.; Junge, H.; Junge, K.; Beller, M. Mild and selective hydrogenation of aromatic and aliphatic (di)nitriles with a well-defined iron pincer complex. *Nat. Commun.* **2014**, *5*, 4111.
22. Lange, S.; Elangovan, S.; Cordes, C.; Spannenberg, A.; Jiao, H.; Junge, H.; Bachmann, S.; Scalone, M.; Topf, C.; Junge, K.; Beller, M. Selective catalytic hydrogenation of nitriles to primary amines using iron pincer complexes. *Catal. Sci. Technol.* **2016**, *6*, 4768–4772.
23. Chakraborty, S.; Leitus, G.; Milstein, D. Selective hydrogenation of nitriles to primary amines catalyzed by a novel iron complex. *Chem. Commun.* **2016**, *52*, 1812–1815.

24. Adam, R.; Bheeter, C. B.; Cabrero-Antonino, J. R.; Junge, K.; Jackstell, R.; Beller, M. Selective Hydrogenation of Nitriles to Primary Amines by using a Cobalt Phosphine Catalyst. *ChemSusChem* **2017**, *10*, 842–846.
25. Mukherjee, A.; Srimani, D.; Chakraborty, S.; Ben-David, Y.; Milstein, D. Selective Hydrogenation of Nitriles to Primary Amines Catalyzed by a Cobalt Pincer Complex. *J. Am. Chem. Soc.* **2015**, *137*, 8888–8891.
26. Tokmic, K.; Markus, C. R.; Zhu, L.; Fout, A. R. Well-Defined Cobalt(I) Dihydrogen Catalyst: Experimental Evidence for a Co(I)/Co(III) Redox Process in Olefin Hydrogenation. *J. Am. Chem. Soc.* **2016**, *138*, 11907–11913.
27. Tokmic, K.; Fout, A. R. Alkyne Semihydrogenation with a Well-Defined Nonclassical Co-H₂ Catalyst: A H₂ Spin on Isomerization and *E*-Selectivity. *J. Am. Chem. Soc.* **2016**, *138*, 13700–13705.
28. Friedfeld, M. R.; Shevlin, M.; Hoyt, J. M.; Krska, S. W.; Tudge, M. T.; Chirik, P. J. Cobalt Precursors for High-Throughput Discovery of Base Metal Asymmetric Alkene Hydrogenation Catalysts. *Science* **2013**, *342*, 1076–1080.
29. Greenhalgh, M. D.; Thomas, S. P. Chemo-, regio-, and stereoselective iron-catalysed hydroboration of alkenes and alkynes. *Chem. Commun.* **2013**, *49*, 11230–11232.
30. Chen, C.; Hecht, M. B.; Kavara, A.; Brennessel, W. W.; Mercado, B. Q.; Weix, D. J.; Holland, P. L. Rapid, Reioconvergent, Solvent-Free Alkene Hydrosilylation with a Cobalt Catalyst. *J. Am. Chem. Soc.* **2015**, *137*, 13244–13247.
31. Léonard, N. G.; Bezdek, M. J.; Chirik, P. J. Cobalt-Catalyzed C(sp²)-H Borylation with an Air-Stable, Readily Prepared Terpyridine Cobalt(II) Bis(acetate) Precatalyst. *Organometallics* **2017**, *36*, 142–150.

32. Obligacion, J. V.; Bezdek, M. J.; Chirik, P. J. C(sp²)-H Borylation of Fluorinated Arenes Using an Air-Stable Cobalt Precatalyst: Electronically Enhanced Site Selectivity Enables Synthetic Opportunities. *J. Am. Chem. Soc.* **2017**, *139*, 2825–2832.
33. Docherty, J. H.; Peng, J.; Dominey, A. P.; Thomas, S. P. Activation and discovery of earth-abundant metal catalysts using sodium *tert*-butoxide. *Nat. Chem.* **2017**, *9*, 595–600.
34. Ibrahim, D. A.; Tokmic, K.; Brennan, M. R.; Kim, D.; Matson, E. M.; Nilges, M. J.; Bertke, J. A.; Fout, A. R. Monoanionic bis(carbene) pincer complexes featuring cobalt(I-III) oxidation states. *Dalton Trans.* **2016**, *45*, 9805–9811.
35. Brennan, M. R.; Kim, D. K.; Fout, A. R. A synthetic and mechanistic investigation into the cobalt(I) catalyzed amination of aryl halides. *Chem. Sci.* **2014**, *5*, 4831–4839.
36. Scheuermann, M. L.; Johnson, E. J.; Chirik, P. Alkene Isomerization-Hydroboration Promoted by Phosphine-Ligated Cobalt Catalysts. *J. Org. Lett.* **2015**, *17*, 2716–2719.
37. Eller, K., Henkes, E., Rossbacher, R.; Höke, H. *Amines, Aliphatic. Ullmann's Encyclopedia of Industrial Chemistry*; Wiley-VCH: Weinheim, Germany, 2002; pp 647–692.
38. Ibrahim, A. D.; Entsminger, S. W.; Zhu, L.; Fout, A. R. A Highly Chemoselective Cobalt Catalyst for the Hydrosilylation of Alkenes using Tertiary Silanes and Hydrosiloxanes. *ACS Catal.* **2016**, *6*, 3589–3593.
39. Ibrahim, A. D.; Entsminger, S. W.; Fout, A. R. Insights into a Chemoselective Cobalt Catalyst for the Hydroboration of Alkenes and Nitriles. *ACS Catal.* **2017**, *7*, 3730–3734.
40. Kovtunov, K. V.; Beck, I. E.; Bukhtiyarov, V. I.; Koptug, I. V. Observation of Parahydrogen-Induced Polarization in Heterogeneous Hydrogenation on Supported Metal Catalysts. *Angew. Chem., Int. Ed.* **2008**, *47*, 1492–1495.

41. Balu, A. M.; Duckett, S. B.; Luque, R. *Para*-hydrogen induced polarisation effects in liquid phase hydrogenations catalysed by supported metal nanoparticles. *Dalton Trans.* **2009**, 5074–5076.
42. Irfan, M.; Eshuis, N.; Spannring, P.; Tessari, M.; Feiters, M. C.; Rutjes, F. P. J. T. Liquid-Phase Parahydrogen-Induced Polarization (PHIP) with Ligand-Capped Platinum Nanoparticles. *J. Phys. Chem. C* **2014**, *118*, 13313–13319.
43. Burueva, D. B.; Salnikov, O. G.; Kovtunov, K. V.; Romanov, A. S.; Kovtunova, L. M.; Khudorozhkov, A. K.; Bukhtiyarov, A. V.; Prosvirin, I. P.; Bukhtiyarov, V. I.; Koptug, I. V. Hydrogenation of Unsaturated Six-Membered Cyclic Hydrocarbons Studied by the Parahydrogen-Induced Polarization Technique. *J. Phys. Chem. C* **2016**, *120*, 13541–13548.
44. Salnikov, O. G.; Liu, H.; Fedorov, A.; Burueva, D. B.; Kovtunov, K. V.; Copéret, C.; Koptug, I. V. Pairwise hydrogen addition in the selective semihydrogenation of alkynes on silica-supported Cu catalysts. *Chem. Sci.* **2017**, *8*, 2426–2430.
45. Eisenberg, R. Parahydrogen-induced polarization: a new spin on reactions with molecular hydrogen. *Acc. Chem. Res.* **1991**, *24*, 110–116.
46. Duckett, S. B.; Wood, N. J. Parahydrogen-based NMR methods as a mechanistic probe in inorganic chemistry. *Coord. Chem. Rev.* **2008**, *252*, 2278–2291.
47. Duckett, S. B.; Mewis, R. E. Application of *Parahydrogen* Induced Polarization Techniques in NMR Spectroscopy and Imaging. *Acc. Chem. Res.* **2012**, *45*, 1247–1257 and references therein.
48. Leutzsch, M.; Wolf, M. L.; Gupta, P.; Fuchs, M.; Thiel, W.; Farès, C.; Fürstner, A. Formation of Ruthenium Carbenes by *gem*-Hydrogen Transfer to Internal Alkynes:

- Implications for Alkyne *trans*-Hydrogenation. *Angew. Chem., Int. Ed.* **2015**, *54*, 12431–12436.
49. Guan, D.; Holmes, A. J.; Lopez-Serrano, J.; Duckett, S. B. Following palladium catalyzed methoxycarbonylation by hyperpolarized NMR spectroscopy: a *parahydrogen* based investigation. *Catal. Sci. Technol.* **2017**, *7*, 2101–2109.
50. Zhivonitko, V. V.; Telkki, V. V.; Chernichenko, K.; Repo, T.; Leskela, M.; Sumerin, V.; Koptuyg, I. V. Tweezers for *parahydrogen*: A Metal-Free Probe of Nonequilibrium Nuclear Spin States of H₂ Molecules. *J. Am. Chem. Soc.* **2014**, *136*, 598–601.
51. Longobardi, L. E.; Russell, C. A.; Green, M.; Townsend, N. S.; Wang, K.; Holmes, A. J.; Duckett, S. B.; McGrady, J. E.; Stephan, D. W. Hydrogen Activation by an Aromatic Triphosphenzene. *J. Am. Chem. Soc.* **2014**, *136*, 13453–13457.
52. Aguilar, J. A.; Elliott, P. I. P.; Lopez-Serrano, J.; Adams, R. W.; Duckett, S. B. Only *parahydrogen* spectroscopy (OPSY), a technique for the selective observation of *parahydrogen* enhanced NMR signals. *Chem. Commun.* **2007**, *11*, 1183–1185.
53. Bowers, C. R.; Weitekamp, D. P. Transformation of Symmetrization Order to Nuclear-Spin Magnetization by Chemical Reaction and Nuclear Magnetic Resonance. *Phys. Rev. Lett.* **1986**, *57*, 2645–2648.
54. Bowers, C. R.; Weitekamp, D. P. *Parahydrogen* and synthesis allow dramatically enhanced nuclear alignment. *J. Am. Chem. Soc.* **1987**, *109*, 5541–5542.
55. Clapham, S. E.; Hadzovic, A.; Morris, R. H. Mechanisms of the H₂-hydrogenation and transfer hydrogenation of polar bonds catalyzed by ruthenium hydride complexes. *Coord. Chem. Rev.* **2004**, *248*, 2201–2237.

56. Takemoto, S.; Kawamura, H.; Yamada, Y.; Okada, T.; Ono, A.; Yoshikawa, E.; Mizobe, Y.; Hidai, M. Ruthenium Complexes Containing Bis(diarylamido)/Thioether Ligands: Synthesis and Their Catalysis for the Hydrogenation of Benzonitrile. *Organometallics* **2002**, *21*, 3897–3904.
57. Eisenberg, R.; Eisenschmid, T. C.; Chinn, M. S.; Kirss, R. U. Parahydrogen-Induced Polarization and Polarization Transfer in Hydrogenation and Oxidative Addition Reactions. *Adv. Chem. Ser.* **1992**, *230*, 47–74.
58. Eisenberg, R. Parahydrogen Induced Polarization: A New Magnifying Glass for Examining Reactions with Hydrogen. *J. Chin. Chem. Soc.* **1995**, *42*, 471–481.
59. Theis, T.; Truong, M. L.; Coffey, A. M.; Shchepin, R. V.; Waddell, K. W.; Shi, F.; Goodson, B. M.; Warren, W. S.; Chekmenev, E. Y. Microtesla SABRE Enables 10% Nitrogen-15 Nuclear Spin Polarization. *J. Am. Chem. Soc.* **2015**, *137*, 1404–1407.
60. Truong, M. L.; Theis, T.; Coffey, A. M.; Shchepin, R. V.; Waddell, K. W.; Shi, F.; Goodson, B. M.; Warren, W. S.; Chekmenev, E. Y. ¹⁵N Hyperpolarization by Reversible Exchange Using SABRE-SHEATH. *J. Phys. Chem. C* **2015**, *119*, 8786–8797.
61. Zhivonitko, V. V.; Skovpin, I. V.; Koptyug, I. V. Strong ³¹P nuclear spin hyperpolarization produced *via* reversible chemical interaction with parahydrogen. *Chem. Commun.* **2015**, *51*, 2506–2509.
62. Pravdivtsev, A. N.; Yurkovskaya, A. V.; Zimmermann, H.; Vieth, H.; Ivanov, K. L. Transfer of SABRE-derived hyperpolarization to spin-1/2 heteronuclei. *RSC Adv.* **2015**, *5*, 63615–63623.

63. Mewis, R. E.; Green, R. A.; Cockett, M. C. R.; Cowley, M. J.; Duckett, S. B.; Green, G. G. R.; John, R. O.; Rayner, P. J.; Williamson, D. C. Strategies for the Hyperpolarization of Acetonitrile and Related Ligands by SABRE. *J. Phys. Chem. B* **2015**, *119*, 1416–1425.
64. Logan, A. W. J.; Theis, T.; Colell, J. F. P.; Warren, W. S.; Malcolmson, S. J. Hyperpolarization of Nitrogen-15 Schiff Bases by Reversible Exchange Catalysis with *para*-Hydrogen. *Chem. Eur. J.* **2016**, *22*, 10777–10782.
65. Colell, J. F. P.; Emondts, M.; Logan, A. W. J.; Shen, K.; Bae, J.; Shchepin, R. V.; Ortiz, G. X.; Spannring, P.; Wang, Q.; Malcolmson, S. J.; Chekmenev, E. Y.; Feiters, M. C.; Rutjes, F. P. J. T.; Blümich, B.; Theis, T.; Warren, S. W. Direct Hyperpolarization of Nitrogen-15 in Aqueous Media with Parahydrogen in Reversible Exchange. *J. Am. Chem. Soc.* **2017**, *139*, 7761–7767.
66. Michelin, R. A.; Mozzon, M.; Bertani, R. Reactions of transition metal-coordinated nitriles. *Coord. Chem. Rev.* **1996**, *147*, 299–338.
67. Lu, Z.; Williams, T. J. A dual site catalyst for mild, selective nitrile reduction. *Chem. Commun.* **2014**, *50*, 5391–5393.
68. Paul, B.; Chakrabarti, K.; Kundu, S. Optimum bifunctionality in a 2-(2-pyridyl-2-ol)-1,10-phenanthroline based ruthenium complex for transfer hydrogenation of ketones and nitriles: impact of the number of 2-hydroxypyridine fragments. *Dalton Trans.* **2016**, *45*, 11162–11171.
69. Guyon, C.; Baron, M.; Lemaire, M.; Popowycz, F.; Métay, E. Commutative reduction of aromatic ketones to arylmethylenes/alcohols by hypophosphites catalyzed by Pd/C under biphasic conditions. *Tetrahedron* **2014**, *70*, 2088–2095.

70. Jacobsen, H.; Berke, H.; Döring, S.; Kehr, G.; Erker, G.; Fröhlich, R.; Meyer, O. Lewis Acid Properties of Tris(pentafluorophenyl)borane. Structure and Bonding in L-B(C₆F₅)₃ Complexes. *Organometallics* **1999**, *18*, 1724–1735.
71. Smith, E. L.; Sadowsky, D.; Cramer, C. J.; Phillips, J. A. Structure, Bonding, and Energetic Properties of Nitrile-Borane Complexes: RCN-BH₃. *J. Phys. Chem. A* **2011**, *115*, 1955–1964.
72. Prepared following procedure within Jacobsen, H.; Berke, H.; Döring, S.; Kehr, G.; Erker, G.; Fröhlich, R.; Meyer, O. Lewis Acid Properties of Tris(pentafluorophenyl)borane. Structure and Bonding in L-B(C₆F₅)₃ Complexes. *Organometallics* **1999**, *18*, 1724–1735.
73. García, J. J.; Jones, W. D. Reversible Cleavage of Carbon-Carbon Bonds in Benzonitrile Using Nickel(0). *Organometallics* **2000**, *19*, 5544–5545.
74. García, J. J.; Brunkan, N. M.; Jones, W. D. Cleavage of Carbon-Carbon Bonds in Aromatic Nitriles Using Nickel(0). *J. Am. Chem. Soc.* **2002**, *124*, 9547–9555.
75. Ateşin, T. A.; Li, T.; Lachaize, S.; Brennessel, W. W.; García, J. J.; Jones, W. D. Experimental and Theoretical Examination of C-CN and C-H Bond Activations of Acetonitrile Using Zerovalent Nickel. *J. Am. Chem. Soc.* **2007**, *129*, 7562–7569.
76. Huo, C.; Zeng, T.; Li, Y.; Beller, M.; Jiao, H. Switching *End-on* into *Side-on* C:N Coordination: A Computational Approach. *Organometallics* **2005**, *24*, 6037–6042.
77. Pangborn, A. B.; Giardello, M. A.; Grubbs, R. H.; Rosen, R. K.; Timmers, F. J. Safe and Convenient Procedure for Solvent Purification. *Organometallics* **1996**, *15*, 1518–1520.
78. Wietz, I. S.; Rabinovitz, M. The application of C₈K for organic synthesis: reduction of substituted naphthalenes. *J. Chem. Soc. Perkin Trans.* **1993**, *1*, 117–120.

79. Aguilar, J. A.; Adam, R. W.; Duckett, S. B.; Green, G. G. R.; Kandiah, R. Selective detection of hyperpolarized NMR signals derived from *para*-hydrogen using the Only *Para*-hydrogen Spectroscopy (OPSY) approach. *J. Magn. Reson.* **2011**, *208*, 49-57.
80. Duckett, S. B.; Green, G. G. R.; Cowley, M. J. Pulse sequencing with hyperpolarisable nuclei. US Patent 20,110,274,626, November 10, 2011.
81. Tom, B. A.; Bhasker, S.; Miyamoto, Y.; Momose, T.; McCall, B. J. Producing and quantifying enriched *para*-H₂. *Rev. Sci. Instrum.* **2009**, *80*, 016108 (1-3).

Chapter 5

Cobalt Catalyzed Semi-Hydrogenation of Nitriles and Lewis Acid Controlled Condensation to Secondary Aldimines

5.1 Introduction

Nitrile hydrogenation presents a particular challenge to chemists due to the complex mixture of products that can be formed. Due to the two-step nature of the hydrogenation the primary imine intermediate is susceptible not only to degradation but also nucleophilic attack by the primary amine. The secondary aldimine produced from this condensation reaction can also be further hydrogenated or functionalized to give the secondary amines and tertiary amines, respectively. Several methods, including the addition of base and increasing temperature and hydrogen pressure, can be used to control selectivity for the primary amines but the secondary aldimines also represent interesting synthetic products.¹⁻²

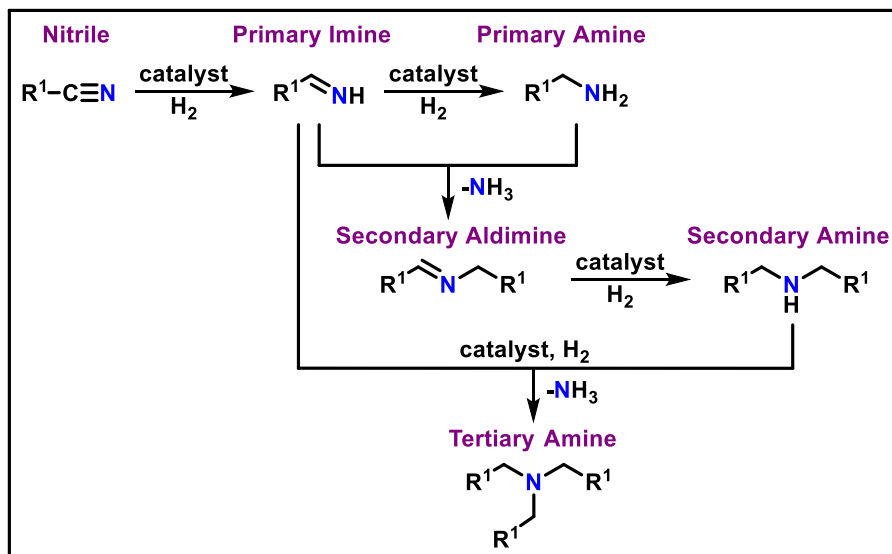


Figure 5.1. Hydrogenation of nitriles.

Imines are reactive intermediates which can easily undergo further functionalization including condensations, cyclizations, C–H additions, [3+2] cycloadditions, reductive and A^3 coupling, and enantioselective reduction and C–C bond formation to name only a few.¹⁻¹¹ However, this propensity to undergo further reactivity can also inhibit the synthesis and isolation

of these products. Secondary aldimines, specifically, are often synthesized through the condensation of aldehydes with primary amines but can also be obtained from the aerobic oxidation of secondary amines, primary amines, or alcohols, the dehydrogenation of secondary amines, and a dehydrogenative synthesis from alcohols and primary amines has also recently been reported.¹²⁻²⁰ Often these synthetic methods require multiple coupling partners and suffer from reduced functional group tolerance. The synthesis of secondary aldimines using nitriles, therefore, represents the most atom economical route to these products.¹

Homogenous catalysts capable of hydrogenating nitriles to primary amines are somewhat limited²¹⁻³³ though it has lately been extended²¹⁻³³ to also include first-row transition metal catalysts.³⁴⁻⁴⁰ Beller, Milstein, and most recently our group have reported systems capable of hydrogenating nitriles selectively to primary amines using Fe,³⁴⁻³⁶ Mn,³⁷ and Co.³⁸⁻⁴⁰ However, changing the selectivity to generate the secondary aldimines exclusively is not as straightforward as it might seem since over-hydrogenation to the secondary amines and tertiary amines is common for many catalysts.¹ The synthesis of secondary aldimines from nitriles has been reported for Ru, Mo, Fe, and Ni catalysts.⁴¹⁻⁴⁶ Cobalt catalysts capable of nitrile hydrogenation to primary amines have been reported³⁸⁻⁴⁰ but only one example selective for the secondary aldimines has been published.⁴⁷

We recently reported the selective hydrogenation of nitriles to primary amines using a Co(III) catalyst with *in situ* activator.⁴⁰ The use of higher temperature and a base were found to be necessary to avoid secondary aldimine formation during the catalysis. Therefore, we were subsequently interested in determining if modification of the reaction parameters could generate the secondary aldimine product selectively. Herein, the hydrogenation of nitriles to primary imines and amines is followed by condensation to selectively form the secondary aldimine products. A distinct dependence on temperature and the identity and amount of Lewis acid was also discovered.

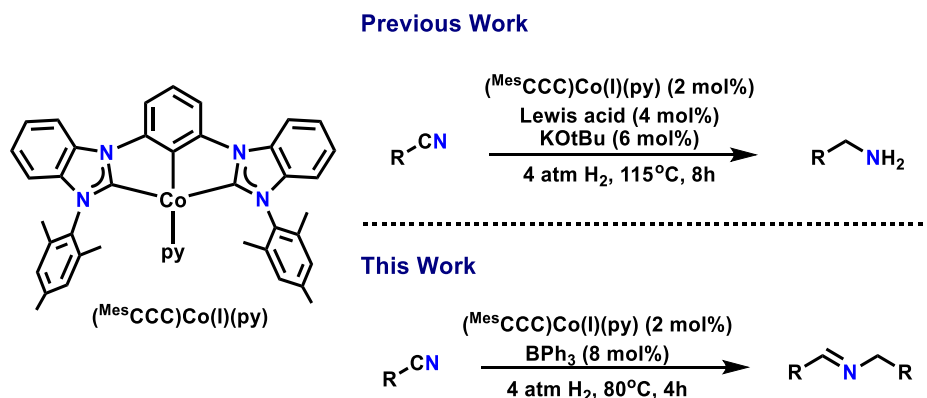
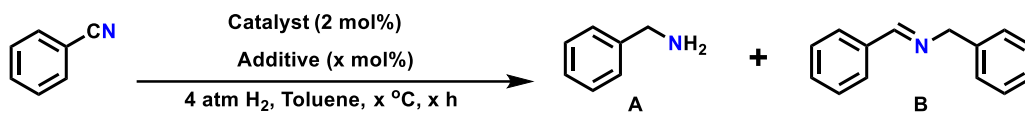


Figure 5.2. Hydrogenation of nitriles with $(^{\text{Mes}}\text{CCC})\text{Co}(\text{I})(\text{py})$.

5.2 Optimization of Reaction Parameters and Substrate Scope

Our initial investigations into this transformation began with the optimized reaction parameters for primary amine selectivity previously reported, toluene at 115 °C, 8 h, 4 atm H₂, $(^{\text{Mes}}\text{CCC})\text{Co}(\text{III})\text{Cl}_2\text{py}$ (2 mol%), NaHBET₃ (4 mol%), and KO^tBu (6 mol%) (Table 1.1, Entry 1).⁴⁰ Benzonitrile was initially used as the model substrate for this reaction. Our previous studies identified that the secondary aldimine was obtained in the absence of base (Table 1.1, Entry 2). However, when extending these same reaction conditions to other substrates we discovered this was not always the case as a mixture of products was obtained (Table 1.1, Entry 3).

Previous studies indicated a lower temperature generated more of the secondary aldimine product even in the presence of base.⁴⁰ This phenomenon has also been observed and studied closely in the literature specifically with a ruthenium system.⁴⁴ Lowering the reaction temperature to 80 °C still generated a substantial amount of primary amine but the amount of secondary aldimine produced did increase (Table 1.1, Entry 4). The reaction time was reduced to four hours since conversion was determined to be complete within that period (See 5.4 Experimental). Using the $(^{\text{Mes}}\text{CCC})\text{Co}(\text{I})(\text{py})$ catalyst previously reported with the addition of BPh₃ in increased amounts (8 mol%) gave a similar result to starting from the Co(III) catalyst (Table 1.1, Entry 5).



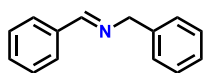
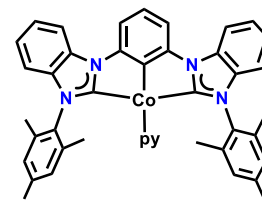
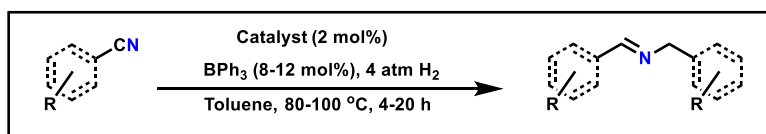
Entry	Catalyst	Substrate	Temperature	Time	Additive	Amount	Base ^c	Yield A ^a	Yield B ^a
1 ^b	Co(III)Cl ₂ py	PhCN	115 °C	8 hrs	NaHBEt ₃	4 mol%	KO ^t Bu	97%	3%
2 ^b	Co(III)Cl ₂ py	PhCN	115 °C	8 hrs	NaHBEt ₃	4 mol%	-	0%	>99%
3	Co(III)Cl ₂ py	4-MePhCN	115 °C	4 hrs	NaHBEt ₃	4 mol%	-	67%	33%
4	Co(III)Cl ₂ py	4-MePhCN	80 °C	4 hrs	NaHBEt ₃	4 mol%	-	59%	41%
5	Co(I)(py)	4-MePhCN	80 °C	4 hrs	BEt ₃	8 mol%	-	55%	45%
6	Co(III)Cl ₂ py	4-MePhCN	80 °C	4 hrs	NaHBEt ₃ + BPh ₃	8 mol%	-	2%	98%
7	Co(I)(py)	4-MePhCN	80 °C	4 hrs	BPh ₃	8 mol%	-	0%	>99%

^aConversion >99% for all reactions, weighted yield via GC-MS. ^bPrevious studies. ^cBase (6 mol%)

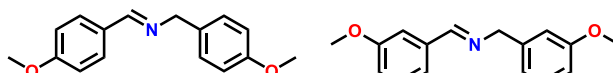
Table 5.1. Optimization of reaction parameters.

Taking inspiration from our previous work, where different Lewis acids effected yield of the product, we hypothesized that the identity of the Lewis acid might have some effect. Adding BPh₃ (4 mol%, 1:1 BEt₃) to the Co(III) catalyzed reaction resulted in the selective formation of the secondary aldimine (Table 1.1, Entry 6). This indicates a distinct shift in the selectivity based on the identity of the Lewis acid. Due to the already complex reaction mixture a pre-formed Co(I) catalyst and BPh₃ were used giving the same selective formation of the secondary aldimine (Table 1.1, Entry 7). The optimal amount of BPh₃ was found to be four equivalents (8 mol%) relative to catalyst as determined using multiple substrates. Limiting the reaction to one Lewis acid simplifies the possible interactions even though it prohibits starting with a bench stable pre-catalyst. Henceforth, we set out to determine the substrate scope of this reaction using (^{Mes}CCC)Co(I)(py) and BPh₃.

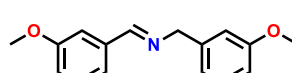
The optimized reaction conditions using (^{Mes}CCC)Co(I)(py) (2 mol%) (toluene, 80 °C, 4 hrs, 4 atm H₂, BPh₃ (8 mol%)) were applied to a variety of substrates, both aromatic and aliphatic. Substitution in the ortho-, meta-, and para-positions was tolerated using methyl or methoxy groups with excellent yields (Table 5.2) The methoxy substituted aryl substrates required slightly longer reaction times to go to completion and the meta-substituted required a higher catalyst loading (4



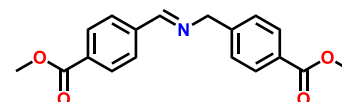
GCMS >99%
Isolated >99%
4 h



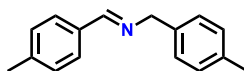
GCMS >99%
Isolated 94%
6 h



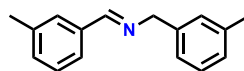
GCMS >99%
Isolated 99%
6 h, 4 mol% cat



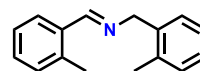
GCMS >99%
Isolated >99%
6 h, 12 mol% LA



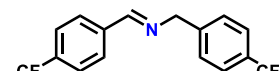
GCMS >99%
Isolated >99%
4 h



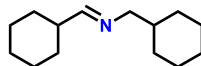
GCMS >99%
Isolated 95%
4 h



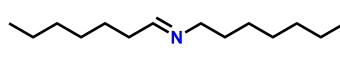
GCMS >99%
Isolated 79%
6 h, 12 mol% LA



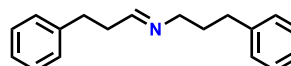
GCMS >99%
Isolated 80%
4 h



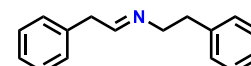
GCMS >99%
Isolated 63%^b
100°C, 16 h



GCMS 59%
Isolated 45%^b
100°C, 20 h, 4 mol% cat.



GCMS 63%
Isolated 40%^b
100°C, 20 h, 4 mol% cat.



GCMS 86%
Isolated 52%^b
100°C, 18 h

^aConversion determined by GC-MS, yields are isolated. ^bIsolated yield of secondary amine HCl salt.

Table 5.2. Nitrile hydrogenation substrate scope.

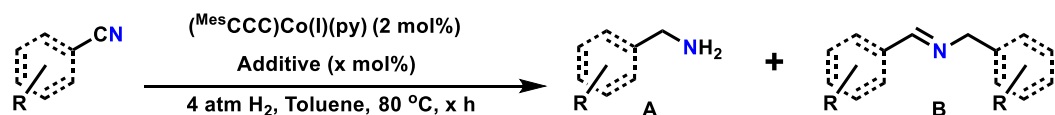
mol%) which was also observed in our previous nitrile hydrogenation studies.⁴⁰ The sterically hindered ortho-substituted tolunitrile (Table 5.2) also required a slightly longer reaction time (6 hrs) and a larger amount of Lewis acid (12 mol%, 6 equiv. to catalyst). The isolated yield (79%) was slightly lower for this particular substrate as well, though GC-MS conversion shows only the secondary aldimine product. Electron-withdrawing groups in the form of para-methylester and para-trifluoromethyl groups were also tolerated (Table 5.2). The latter with the optimized conditions and the former with a higher loading of Lewis acid and longer reaction time (12 mol%, 6 hrs).

Applying nitrile hydrogenation systems to alkyl substrates presents a significant challenge. Many literature studies struggle to achieve high yields or even effective hydrogenation using these substrates. We found that much longer reaction times (16-20 hrs) were required to achieve adequate conversion along with slightly higher catalyst loadings (4 mol%) and elevated temperatures (100 °C). Cyclohexyl nitrile was completely converted to its secondary aldimine based on GC-MS yields but the difficulty of isolating the reactive product gave a much lower yield (30%). The alkyl secondary aldimines decomposed quickly, even under an inert atmosphere, so an alternate method of purification was undertaken. The hydrochloride salts of the secondary amines were instead isolated and the yield of the reaction determined, similar to the method previously utilized for the isolation of the primary amines.⁴⁰ This method was used for the four non-aryl substrates (Table 5.2). Few of the alkyl substrates went to complete conversion, even with increased catalyst loading, but no primary amines were detected by GC or GC-MS. This allowed for the isolation of the secondary amine hydrochloride salts with no primary amine salts present. The alkyl and aliphatic substrates were isolated in good yields (Table 5.2).

Surprisingly, a number of substrates that were competent in our previous nitrile hydrogenation studies either did not yield the secondary aldimine or did not hydrogenate under the modified reaction conditions. For example, the aniline substrates were not hydrogenated at 80 °C. Increasing the temperature to 100 °C allowed for the hydrogenation to proceed for the meta substituted substrate, but only the primary amine was generated. Meta-chlorobenzonitrile gave similar results to the meta-aniline substrate. Naphthylcyanide was hydrogenated at either temperature but only with selectivity for the primary amine.⁴⁰ Interested in examining this transformation further mechanistic studies were carried out.

5.3 Mechanistic Insights

The specificity of this reaction for a single Lewis acid, BPh₃, is distinctly different from our original studies. Optimization of the reaction conditions for nitrile hydrogenation to the primary amines revealed no dependence on the amount of Lewis acid and only a small amount of variability ($\pm 20\%$) in yield based on the identity of Lewis acid. However, in the case of our secondary aldimine studies a direct selectivity dependence on both the amount and type of Lewis acid was observed. The optimized catalytic conditions using BEt₃ generated only 45% yield of the secondary aldimine (Table 5.3, Entry 1). Using those same conditions but substituting BPh₃ gave quantitative yield of the secondary aldimine (Table 5.3, Entry 2). LiOTf, previously competent for nitrile hydrogenation to the primary amines, gave a very low yield of the secondary aldimine under these conditions (Table 5.3, Entry 3). Another Lewis acid that was previously competent for our Lewis acid-assisted nitrile hydrogenation, Ca(OTf)₂, was unable to assist under these conditions and no conversion was observed (Table 5.3, Entry 4).⁴⁰ However, the lower solubility of these triflates at 80 °C versus 115 °C could also be contributing to the lack of reactivity.



Entry	Substrate	Time	Additive	Amount	Conversion	Yield A ^a	Yield B ^a
1	4-MePhCN	4 hrs	BEt ₃	8 mol%	>99%	55%	45%
2	4-MePhCN	4 hrs	BPh ₃	8 mol%	>99%	0%	>99%
3	4-MePhCN	4 hrs	LiOTf	8 mol%	64%	23%	42%
4	4-MePhCN	4 hrs	Ca(OTf) ₂	8 mol%	0%	-	-
5	4-MeEsterPhCN	6 hrs	BPh ₃	8 mol%	>99%	70%	30%
6	4-MeEsterPhCN	6 hrs	BPh ₃	12 mol%	>99%	0%	>99%
7	2-MePhCN	6 hrs	BPh ₃	8 mol%	>99%	28%	72%
8	2-MePhCN	6 hrs	BPh ₃	12 mol%	>99%	0%	>99%

^aYields and conversion determined by weighted yield via GC-MS.

Table 5.3. Lewis acid dependence in catalysis.

Additionally, when more difficult substrates were addressed in this catalysis, a dependence on the amount of Lewis acid for selectivity was identified. Hydrogenating 4-MeEsterPhCN under regular catalytic conditions, with a slightly longer reaction time (6 h), generated only a small amount of the desired secondary aldimine product (30%) (Table 5.3, Entry 5). However, increasing the loading of BPh₃ to 12 mol% instead gave the secondary aldimine exclusively (>99%) (Table 5.3, Entry 6). Similarly, 2-MePhCN also required increased loading of the Lewis acid to achieve quantitative conversion to the secondary aldimine selectively (Table 5.3, Entry 7-8).

These results suggest that both the identity and amount of Lewis acid plays an ^{intimate} role in the selectivity during catalysis. Since no previous Lewis acid dependence was determined when hydrogenating the nitriles to primary amines selectively we propose that BPh₃ is helping to increase the rate of the condensation reaction. Examples of this reactivity in the literature require much longer reaction times than we observed which also helps to indicate the Lewis acid's role in both the condensation reaction and nitrile hydrogenation. The reaction, as previously established, is in fact a Lewis-acid assisted process since hydrogenation does not occur in the absence of a Lewis acid.

We initially proposed that the interaction of the Lewis acid helps promote the side-on coordination of the nitrile to the metal center and activate it to undergo subsequent hydrogenation to the primary imine (Figure 5.3). Based on this work and the Lewis acid dependence discovered we also propose that BPh₃ places an essential role in the condensation reaction between the primary imine and primary amine. Unfortunately, we were unable to determine its exact role but hypothesize that it could act either through sequestration of the generated NH₃ or stabilization of reactive intermediates.

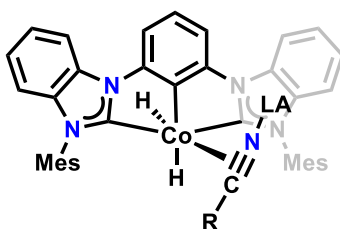


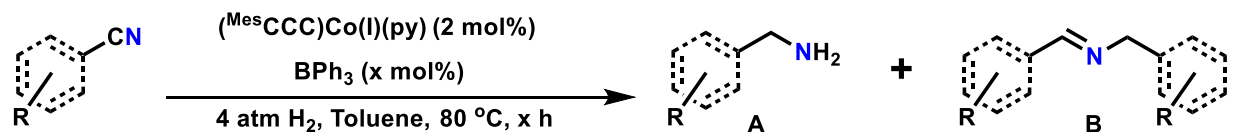
Figure 5.3. Proposed coordination of Lewis acid to the cobalt-bound nitrile.

Overall a very efficient nitrile hydrogenation reaction with mild conditions was carried out using $(^{\text{Mes}}\text{CCC})\text{Co}(\text{I})(\text{py})$ as the catalyst with BPh_3 playing an active role during the transformation. The reaction times were significantly shorter than other previously published nitrile hydrogenation catalysts and is similar to the two ruthenium literature examples in terms of hydrogen pressure.⁴¹⁻⁴⁶ This study also represents, to our knowledge, only the second example of a cobalt catalyst performing the hydrogenation of nitriles with selectivity to the secondary aldimines. Investigations into the mechanism and cross-coupled or cross-condensation of nitriles with other amines to create asymmetric secondary aldimines is currently on-going.

5.4 Experimental Section

General Considerations. All manipulations of air- and moisture-sensitive compounds were carried out in the absence of water and dioxygen in an MBraun inert atmosphere drybox under a dinitrogen atmosphere except where specified otherwise. All glassware was oven dried for a minimum of 8 h and cooled in an evacuated antechamber prior to use in the drybox. Solvents for sensitive manipulations were dried and deoxygenated on a Glass Contour System (SG Water USA, Nashua, NH) and stored over 4 Å molecular sieves purchased from Strem following a literature procedure prior to use.⁴⁸ Toluene- d_8 , benzene- d_6 , and chloroform- d were purchased from Cambridge Isotope Labs and were degassed and stored over 4 Å molecular sieves prior to use. Triethylborane solution (1.0 M in hexanes) was purchased from Sigma-Aldrich. Triphenylborane

was purchased from Oakwood Chemical and re-crystallized from diethyl ether prior to use. Lithium triflate (anhydrous) and calcium triflate (anhydrous) were purchased from Sigma-Aldrich and used as received. Celite® 545 (J. T. Baker) was dried in a Schlenk flask for 24 h under dynamic vacuum while heating to at least 150 °C prior to use in a glovebox. All nitrile substrates were purchased from Sigma-Aldrich or Alfa Aesar and the solids were re-crystallized and dried prior to use. NMR Spectra were recorded at room temperature on a Varian spectrometer operating at 500 or 600 MHz (¹H NMR) and 126 MHz (¹³C NMR) (U500, VXR500, UI500NB, UI600) and referenced to the residual solvent. Potassium graphite (KC₈)⁴⁹ was prepared according to literature procedures. (^{Mes}CCC)CoCl₂py (**1**)⁵⁰ and (^{Mes}CCC)Co(I)(Py)⁴⁰ were prepared according to literature procedures.



Entry	Substrate	Time	BPh ₃ (x mol%)	Yield A ^a	Yield B ^a
1	4-MePhCN	4 hrs	4 mol%	0%	>99%
2	4-MePhCN	4 hrs	8 mol%	0%	>99%
3	3-MePhCN	4 hrs	4 mol%	38%	62%
4	3-MePhCN	4 hrs	8 mol%	0%	>99%
5	4-OMePhCN	6 hrs	4 mol%	6%	94%
6	4-OMePhCN	6 hrs	8 mol%	0%	>99%
7	4-CF ₃ PhCN	4 hrs	4 mol%	54%	46%
8	4-CF ₃ PhCN	4 hrs	8 mol%	0%	>99%

^aYields and conversion (>99%) determined by weighted yield via GC-MS.

Table 5.4. Optimization of BPh₃ amount.

Entry	Substrate	Temperature	Conversion	Yield A ^a	Yield B ^a
1		80 °C	0%	0%	0%
		100 °C	0%	0%	0%
2		80 °C	0%	0%	0%
		100 °C	>99%	>99%	0%
3 ^b		80 °C	0%	0%	0%
		100 °C	0%	0%	0%
4		80 °C	>99%	>99%	0%
		100 °C	>99%	>99%	0%

^aYields and conversion determined by weighted yield via GC-MS.

Table 5.5. Substrates not selective for the secondary aldimine.

Literature Procedure - Synthesis of Cobalt(I) Complexes⁴⁰

Preparation of (^{Mes}CCC)Co-py: A 20 mL scintillation vial was charged with (^{Mes}CCC)CoCl₂py⁵⁰ (0.100 g, 0.133 mmol) and THF (10 mL). A suspension of KC₈ (0.038 g, 0.281 mmol) in THF (5 mL) was added to the mixture. After stirring for 2 hours, the dark brown suspension was filtered over Celite and concentrated to a dark solid under reduced pressure. The product was then extracted into benzene (3 x 5 mL), filtered over Celite, and lyophilized under reduced pressure to a dark brown solid (0.072 g, 0.105 mmol, 80%). NMR data (in benzene-*d*₆, 25 °C): ¹H δ = 8.03 (d, J = 5.4, 2H), 7.79 (t, J = 7.4, 1H), 7.65 (d, J = 7.6, 2H), 7.23 (t, J = 7.8, 3H), 7.00 (t, J = 7.5, 3H), 6.66 (d, J = 7.8, 4H), 6.31 (s, 5H), 1.96 (s, 6H), 1.83 (s, 12H). ¹³C δ = 147.4, 139.7, 137.1, 136.1, 135.1, 133.1, 129.1, 128.6, 127.5, 122.3, 122.2, 110.0, 108.5, 105.9, 20.9, 17.8. HRMS (ESI), calc. for C₄₃H₃₉CoN₅ (M + H)⁺: calculated 684.2537; found 684.2543.

General Procedure: Nitrile Hydrogenation and Condensation

A 50 mL schlenk tube was charged with (^{Mes}CCC)Co(I)(py) (2 mg, 0.0027 mmol) in toluene (2 mL). BPh₃ (8-12 mol%) was dissolved in toluene (1 mL) and added to the flask. The nitrile was added and the total volume raised to 4 mL of toluene. It was then subjected to two freeze pump thaw cycles and placed under 1 atm of H₂ gas at 77K. The mixture was allowed to warm to room temperature, resulting in 4 atm of H₂ gas. The flask was heated in an oil bath (80 – 100 °C, 4 – 20hrs). The reaction was then removed from the oil bath, cooled to room temperature, brought into the glovebox, the H₂ gas vented, and the reaction analyzed by GC-MS to determine conversion. The volatiles were removed under reduced pressure and hexanes or diethyl ether added to the remaining oil before filtering through celite. After the volatiles were removed a very pale yellow solid or liquid was analyzed by ¹H, ¹³C, and ¹⁹F NMR spectroscopy where appropriate. All catalytic yields are the average of duplicate or triplicate isolated runs. The spectra were compared to published literature examples of these species that already contain HR-MS data.^{a-c} Substrates Bis(cyclohexylmethyl)amine hydrochloride, diheptylamine hydrochloride, bis(3-phenylpropyl)amine hydrochloride, and diphenethylamine hydrochloride were not found in the literature and so was further characterized by HR-MS.

Experimental for Secondary Imine (Substrates)

^aN-benzylidenebenzylamine: ¹H NMR (CDCl₃, 500 MHz): δ = 8.32 (s, 1H), 7.74 (m, 2H), 7.34 (dd, J = 5.1, 1.9 Hz, 4H), 7.27 (m, 2H), 7.19 (m, 2H), 4.75 (s, 2H). ¹³C NMR (CDCl₃, 126 MHz): 162.13, 139.38, 136.23, 130.90, 128.3, 128.62, 128.39, 128.09, 127.11, 65.20.

^aN-(4-methoxybenzylidene)-1-(4-methoxyphenyl)methylamine: ¹H NMR (CDCl₃, 500 MHz): δ = 8.29 (s, 1H), 7.71 (d, J = 8.7 Hz, 2H), 7.24 (d, J = 8.3 Hz, 2H), 6.91 (d, J = 8.7 Hz, 2H), 6.87

(d, J = 8.5 Hz, 2H), 4.72 (s, 2H), 3.83 (s, 3H), 3.79 (s, 3H). ^{13}C NMR (CDCl_3 , 126 MHz): 161.72, 161.05, 158.70, 131.73, 129.91, 129.27, 129.24, 113.96, 64.54, 55.47, 55.40.

^aN -(3-methoxybenzylidene)-1-(3-methoxyphenyl)methylamine: ^1H NMR (CDCl_3 , 500 MHz): δ = 8.36 (s, 1H), 7.4 (q, J = 1.2 Hz, 1H), 7.3 (m, 3H), 6.99 (dq, J = 7.6, 1.4 Hz, 2H), 6.92 (m, 2H), 6.82 (dd, J = 8.2, 2.1 Hz, 1H), 4.81 (s, 2H), 3.85 (s, 3H), 3.81 (s, 3H). ^{13}C NMR (CDCl_3 , 126 MHz): 126.18, 159.98, 159.86, 140.92, 137.66, 134.36, 129.69, 129.62, 127.49, 121.81, 120.44, 117.74, 113.72, 112.55, 111.65, 65.04, 55.52, 55.35.

^bN -(4-methylesterbenzylidene)-1-(4-methylesterphenyl)methylamine: ^1H NMR (CDCl_3 , 500 MHz): δ = 8.46 (s, 1H), 8.10 (d, J = 8 Hz, 2H), 8.03 (d, J = 8 Hz, 2H), 7.86 (d, J = 8 Hz, 2H), 7.43 (d, J = 8 Hz, 2H), 7.34 (d, J = 6.8 Hz, 2H), 4.90 (s, 2H), 3.94 (s, 3H), 3.91 (s, 3H). ^{13}C NMR (CDCl_3 , 126 MHz): 167.09, 144.47, 140.01, 133.95, 132.33, 130.13, 128.42, 128.04, 127.74, 127.38, 127.08, 125.97, 52.54, 52.34.

^aN -(4-methylbenzylidene)-1-(4-methylphenyl)methylamine: ^1H NMR (CDCl_3 , 500 MHz): δ = 8.35 (s, 1H), 7.68 (d, J = 8.1 Hz, 2H), 7.23 (m, 4H), 7.16 (d, J = 7.8 Hz, 2H), 4.78 (s, 2H), 2.39 (s, 3H), 2.35 (s, 3H). ^{13}C NMR (CDCl_3 , 126 MHz): 161.82, 141.10, 136.64, 136.44, 133.70, 129.42, 129.27, 128.35, 128.07, 64.95, 21.66, 21.26.

^aN -(3-methylbenzylidene)-1-(3-methylphenyl)methylamine: ^1H NMR (CDCl_3 , 500 MHz): δ = 8.38 (s, 1H), 7.67 (m, 1H), 7.56 (d, J = 7.6 Hz, 2H), 7.35 (t, J = 7.7 Hz, 1H), 7.31 (m, 1H), 7.25 (m, 1H), 7.16 (m, 2H), 7.10 (d, J = 7.4 Hz, 1H), 4.80 (s, 2H), 2.40 (s, 3H), 2.37 (s, 3H). ^{13}C NMR (CDCl_3 , 126 MHz): 162.22, 139.29, 138.45, 138.22, 136.26, 131.67, 128.88, 128.58, 128.51, 127.84, 127.58, 125.98, 125.19, 65.27, 21.55, 21.38.

^aN -(2-methylbenzylidene)-1-(2-methylphenyl)methylamine: ^1H NMR (CDCl_3 , 500 MHz): Small amount of BPh_3 present. δ = 8.69 (s, 1H), 7.95 (dd, J = 7.8, 0.8 Hz, 1H), 7.38 (dd, J = 7.9,

1.4 Hz, 1H), 7.28 (m, 3H), 7.17 (m, 2H), 7.16 (m, 1H), 4.82 (s, 2H), 2.50 (s, 3H), 2.38 (s, 3H). ¹³C NMR (CDCl₃, 126 MHz): 160.66, 137.84, 137.74, 136.22, 133.70, 130.93, 130.39, 130.22, 128.35, 127.74, 127.15, 126.31, 126.19, 63.44, 19.54, 19.45.

^cN-(4-trifluoromethylbenzylidene)-1-(4-trifluoromethylphenyl)methylamine: ¹H NMR (CDCl₃, 500 MHz): δ = 8.47 (s, 1H), 7.91 (d, J = 8 Hz, 2H), 7.69 (d, J = 8.1 Hz, 2H), 7.62 (d, J = 8.1 Hz, 2H), 7.48 (d, J = 8 Hz, 2H), 4.90 (s, 2H). ¹⁹F NMR (CDCl₃, 470 MHz): -62.48, -62.86. ¹³C NMR (CDCl₃, 126 MHz): 161.23, 143.14, 139.15, 128.67, 128.27, 125.82, 125.63, 64.57.

Aliphatic and alkyl substrates were isolated as the hydrochloride salts of the secondary amines.

Bis(cyclohexylmethyl)amine hydrochloride: ¹H NMR (DMSO, 500 MHz): δ = 2.65 (m, 2H), 2.42 (m, 2H), 1.73 (m, 12H), 1.26 (m, 8H), 0.80 (m, 3H). HRMS (ESI), calc. for C₁₄H₂₇N (M - HCl)⁺: 209.21, found 209.38.

Diheptylamine hydrochloride: ¹H NMR (DMSO, 500 MHz): δ = 2.80 (s, 4H), 1.55 (s, 4H), 1.27 (b, 12H), 0.88 (s, 6H).

Bis(3-phenylpropyl)amine hydrochloride: ¹H NMR (DMSO, 500 MHz): δ = 8.32 (b, 2H), 7.29 (m, 4H), 7.21 (m, 6H), 2.83 (t, J = 7.2 Hz, 2H), 2.75 (t, J = 7 Hz, 2H), 2.64 (t, J = 7.5 Hz, 4H), 1.93 (m, 2H), 1.86 (m, 2H). ¹³C NMR (DMSO, 126 MHz): 140.89, 128.40, 128.26, 126.01, 46.31, 38.27, 32.04, 31.88, 28.74, 27.24. HRMS (ESI), calc. for C₁₈H₂₄N (M - Cl)⁺: 254.19, found 255.82.

Diphenethylamine hydrochloride: ¹H NMR (DMSO, 500 MHz): δ = 8.54 (b, 2H), 7.33 (m, 4H), 7.25 (m, 6H), 3.12 (b, 2H), 3.00 (t, J = 6.8 Hz, 4H), 2.91 (m, 2H). ¹³C NMR (DMSO, 126 MHz): 137.52, 128.60, 126.66, 47.83, 32.93, 31.70. HRMS (ESI), calc. for C₁₆H₂₀N (M - Cl)⁺: 226.16, found 226.82.

HR-MS Data

^aHuang, B.; Tian, H.; Lin, S.; Xie, M.; Yu, X.; Xu, Q. Cu(I)/TEMPO-catalyzed aerobic oxidative synthesis of imines directly from primary and secondary amines under ambient and neat conditions. *Tetrahedron Lett.* **2013**, *54*, 2861-2864.

^bBosanac, T.; Wilcox, C. S. Precipiton Reagents: Precipiton Phosphines ofr Solution-Phase Reductions. *Org. Lett.* **2004**, *6*, 2321-2324. (But it cites this one: Ashton, P. R.; Glink, P. T.; Stoddart, J. F.; Tasker, P. A.; White, A. J. P.; Williams, D. J. Self-Assembling [2]- and [3]Rotzoxanes from Secondary Dialkylammonium Salts and Crown Ethers**. *Chem. Eur. J.* **1996**, *2*, 729-736.

^cMarui, K.; Nomoto, A.; Akashi, H.; Ogawa, A. Green Oxidation of Amines to Imines Based on the Development of Novel Catalytic Systems Using Molecular Oxygen or Hydrogen Peroxide. *Synthesis*, **2016**, *48*, 31-42.

5.5 References

1. Bagal, D. B.; Bhanage, B. Recent Advances in Transition Metal-Catalyzed Hydrogenation of Nitriles. *Adv. Synth. Catal.* **2015**, *357*, 883–900 and references therein.
2. Werkmeister, S.; Junge, K.; Beller, M. Catalytic Hydrogenation of Carboxylic Acid Esters, Amides, and Nitriles with Homogeneous Catalysts. *Org. Process. Res. Dev.* **2014**, *18*, 289-302 and references therein.
3. Saha, D.; Bagchi, S.; Sharma, A. Metal-catalyzed synthesis of cyclic imines: a versatile scaffold in organic synthesis. *Chem. Heterocycl. Compd.* **2018**, *54*, 302-313.
4. Hummel, J. R.; Boerth, J. A.; Ellman, J. A. Transition-Metal_Catalyzed C-H Bond Addition to Carbonyls, Imines, and Related Polarized π Bonds. *Chem. Rev.* **2017**, *117*, 963-9227.
5. John-Campbell, S.; Bull, J. A. Transient imines as ‘next generation’ directing groups for the catalytic functionalisation of C-H bonds in a single operation. *Org. Biomol. Chem.* **2018**, *16*, 4582-4595.
6. Grošelj, U.; Svete, J.; Al Mamari, H. H.; Požgan, F.; Štefane, B. Metal-catalyzed [3+2] cycloadditions of azomethine imines. *Chem. Heterocycl. Compd.* **2018**, *54*, 214-240.
7. Holmes, M.; Schwartz, L. A.; Krische, M. J. Intermolecular Metal-Catalyzed Reductive Coupling of Dienes, Allenes, and Enynes with Carbonyl Compounds and Imines. *Chem. Rev.* **2018**, *118*, 6026-6052.
8. Uhlig, N.; Yoo, W.; Li, C. Catalytic Nucleophilic Addition of Alkynes to Imines: The A³ (Aldehyde-Alkyne-Amine) Coupling. In *Modern Alkyne Chemistry: Catalytic and Atom-Economic Transformations*; Trost, B. M.; Li, C., Ed.; Wiley-VCH: Weinheim, Germany, 2015; Vol. 9; p 239-267.

9. Kobayashi, S.; Ishitani, H. Catalytic Enantioselective Addition to Imines. *Chem. Rev.* **1999**, *99*, 1069-1094.
10. Gröger, H. Catalytic Enantioselective Strecker Reactions and Analogous Syntheses. *Chem. Rev.* **2003**, *103*, 2795-2827.
11. Kobayashi, S.; Mori, Y.; Fossey, J. S.; Salter, M. M. Catalytic Enantioselective Formation of C-C Bonds by Addition to Imines and Hydrazones: A Ten-Year Update. *Chem. Rev.* **2011**, *111*, 2626-2704.
12. Paquin, L.; Hamelin, J.; Texier-Boullet, F. Efficient Microwave-Assisted Solvent-Free Synthesis of N-Substituted Aldimines. *Synthesis* **2006**, *10*, 1652-1656.
13. Moarles, S.; Guijarro, F. G.; Ruano, J. L. G.; Cid, M. B. A General Aminocatalytic Method for the Synthesis of Aldimines. *J. Am. Chem. Soc.* **2014**, *136*, 1082-1089.
14. Reeves, J. T.; Visco, M. D.; Marsini, M. A.; Grinberg, N.; Busacca, C. A.; Mattson, A. E.; Senanayake, C. H. A General Method for Imine Formation Using B(OCH₂CF₃)₃. *Org. Lett.* **2015**, *17*, 2442-2445.
15. Wendlandt, A. E.; Stahl, S. S. Chemoselective Organocatalytic Aerobic Oxidation of Primary Amines to Secondary Imines. *Org. Lett.* **2012**, *14*, 2850-2853.
16. Han, L.; Xing, P.; Jiang, B. Selective Aerobic Oxidation of Alcohols to Aldehydes, Carboxylic Acids, and Imines Catalyzed by a Ag-NHC Complex. *Org. Lett.* **2014**, *16*, 3428-3431.
17. Chen, B.; Wang, L.; Gao, S. Recent Advances in Aerobic Oxidation of Alcohols and Amines to Imines. *ACS Catal.* **2015**, *5*, 5851-5876.

18. Gu, X.; Chen, W.; Morales-Morales, D.; Jensen, C. M. Dehydrogenation of secondary amines to imines catalyzed by an iridium PCP pincer complex: initial aliphatic or direct amino dehydrogenation? *J. Mol. Catal. A.* **2002**, *189*, 119-124.
19. Kamiguchi, S.; Ikeda, N.; Nagashima, S.; Kurokawa, H.; Miura, H.; Chihara, T. Catalytic Condensation of Primary Amines, Dehydrogenation of Secondary Amines, and Dealkylation of Tertiary Amiens over Solid-State Rhenium Sulfide Clusters with an Octahedral Metal Framework. *J. Clust. Sci.* **2009**, *20*, 683-693.
20. Maggi, A.; Madsen, R. Dehydrogenative Synthesis of Imines from Alcohols and Amines Catalyzed by a Ruthenium N-Heterocyclic Carbene Complex. *Organometallics* **2012**, *31*, 451-455.
21. Yoshida, T.; Okano, T.; Otsuka, S. Catalytic Hydrogenation of Nitriles and Dehydrogenation of Amines with Rhodium(I) Hydrido Compounds $[\text{RhH}(\text{PPr}^i_3)_3]$ and $[\text{Rh}_2\text{H}_2(\mu\text{-N}_2)\{\text{P}(\text{cyclohexyl})_3\}_4]$. *J.C.S. Chem. Commun.* **1979**, 870–871.
22. Xie, X.; Liotta, C. L.; Eckert, C. CO₂-Protected Amine Formation from Nitrile and Imine Hydrogenation in Gas-Expanded Liquids. *Ind. Eng. Chem. Res.* **2004**, *43*, 7907–7911.
23. Li, T.; Bergner, I.; Haque, F. N.; Zimmer-De Iuliis, M.; Song, D.; Morris, R. H. Hydrogenation of Benzonitrile to Benzylamien Catalyzed by Ruthenium Hydride Complexes with P-NH-NH-P Tetradentate Ligands: Evidence for a Hydridic-Protonic Outer Sphere Mechanism. *Organometallics* **2007**, *26*, 5940–5949.
24. Enthaler, S.; Junge, K.; Addis, D.; Erre, G.; Beller, M. A Practical and Benign Synthesis of Primary Amines through Ruthenium-Catalyzed Reduction of Nitriles. *ChemSusChem* **2008**, *1*, 1006–1010.

25. Enthaler, S.; Addis, D.; Junge, K.; Erre, G.; Beller, M. A General and Environmentally Benign Catalytic Reduction of Nitriles to Primary Amines. *Chem. Eur. J.* **2008**, *14*, 9491-9494.
26. Addis, D.; Enthaler, S.; Junge, K.; Wendt, B.; Beller, M. Ruthenium N-heterocyclic carbene catalysts for selective reduction of nitriles to primary amines. *Tetrahedron Lett.* **2009**, *50*, 3654–3656.
27. Reguillo, R.; Grellier, M.; Vautravers, N.; Vendier, L.; Sabo-Etienne, S. Ruthenium-Catalyzed Hydrogenation of Nitriles: Insights into the Mechanism. *J. Am. Chem. Soc.* **2010**, *132*, 7854–7855.
28. Gunanathan, C.; Holscher, M.; Leitner, W. Reduction of Nitriles to Amines with H₂ Catalyzed by Nonclassical Ruthenium Hydrides – Water-Promoted Selectivity for Primary Amines and Mechanistic Investigations. *Eur. J. Inorg. Chem.* **2011**, *2011*, 3381–3386.
29. Rajesh, K.; Dudle, B.; Blacque, O.; Berke, H. Homogeneous Hydrogenations of Nitriles Catalyzed by Rhenium Complexes. *Adv. Synth. Catal.* **2011**, *353*, 1479–1484.
30. Miao, X.; Bidange, J.; Dixneuf, P. H.; Fischmeister, C.; Bruneau, C.; Dubois, J.; Couturier, J. Ruthenium-Benzylidenes and Ruthenium-Indenylidenes as Efficient Catalysts for the Hydrogenation of Aliphatic Nitriles into Primary Amines. *ChemCatChem* **2012**, *4*, 1911–1916.
31. Werkmeister, S.; Junge, K.; Wendt, B.; Spannenberg, A.; Jiao, H.; Bornschein, C.; Beller, M. Ruthenium/Imidazolylphosphine Catalysis: Hydrogenation of Aliphatic and Aromatic Nitriles to Form Amines. *Chem. Eur. J.* **2014**, *20*, 4227–4231.

32. Adam, R.; Bheeter, C. B.; Jackstell, R.; Beller, M. A Mild and Base-Free Protocol for the Ruthenium-Catalyzed Hydrogenation of Aliphatic and Aromatic Nitriles with Tridentate Phosphine Ligands. *ChemCatChem* **2016**, *8*, 1329–1334.
33. Adam, R.; Alberico, E.; Baumann, W.; Drexler, H.; Jackstell, R.; Junge, H.; Beller, M. NNP-Type Pincer Imidazolylphosphine Ruthenium Complexes: Efficient Base-Free Hydrogenation of Aromatic and Aliphatic Nitriles under Mild Conditions. *Chem. Eur. J.* **2016**, *22*, 4991–5002.
34. Bornschein, C.; Werkmeister, S.; Wendt, B.; Jiao, H.; Alberico, E.; Baumann, W.; Junge, H.; Junge, K.; Beller, M. Mild and selective hydrogenation of aromatic and aliphatic (di)nitriles with a well-defined iron pincer complex. *Nat. Commun.* **2014**, *5*, 4111.
35. Lange, S.; Elangovan, S.; Cordes, C.; Spannenberg, A.; Jiao, H.; Junge, H.; Bachmann, S.; Scalone, M.; Topf, C.; Junge, K.; Beller, M. Selective catalytic hydrogenation of nitriles to primary amines using iron pincer complexes. *Catal. Sci. Technol.* **2016**, *6*, 4768–4772.
36. Chakraborty, S.; Leitus, G.; Milstein, D. Selective hydrogenation of nitriles to primary amines catalyzed by a novel iron complex. *Chem. Commun.* **2016**, *52*, 1812–1815.
37. Elangovan, S.; Topf, C.; Fischer, S.; Jiao, H.; Spannenberg, A.; Baumann, W.; Ludwig, R.; Junge, K.; Beller, M. Selective Catalytic Hydrogenations of Nitriles, Ketones, and Aldehydes by Well-Defined Manganese Pincer Complexes. *J. Am. Chem. Soc.* **2016**, *138*, 8809–8814.
38. Mukherjee, A.; Srimani, D.; Chakraborty, S.; Ben-David, Y.; Milstein, D. Selective Hydrogenation of Nitriles to Primary Amines Catalyzed by a Cobalt Pincer Complex. *J. Am. Chem. Soc.* **2015**, *137*, 8888–8891.

39. Adam, R.; Bheeter, C. B.; Cabrero-Antonino, J. R.; Junge, K.; Jackstell, R.; Beller, M. Selective Hydrogenation of Nitriles to Primary Amines by using a Cobalt Phosphine Catalyst. *ChemSusChem* **2017**, *10*, 842–846.
40. Tokmic, K.;* Jackson, B. J.;* Salazar, A.; Woods, T. J.; Fout, A. R. Cobalt-Catalyzed and Lewis Acid-Assisted Nitrile Hydrogenation to Primary Amines: A Combined Effort. *J. Am. Chem. Soc.* **2017**, *139*, 13554-13561.
41. Zerecero-Silva, P.; Jimenez-Solar, I.; Crestani, M. G.; Arévalo, A.; Barrios-Francisco, R.; García, J. J. Catalytic hydrogenation of aromatic nitriles and dinitriles with nickel compounds. *Appl. Catal., A* **2009**, *363*, 230-234.
42. Srimani, D.; Feller, M.; Ben-David, Y.; Milstein, D. Catalytic coupling of nitriles with amines to selectively form imines under mild hydrogen pressure. *Chem. Commun.* **2012**, *48*, 11853-11855.
43. Chakraborty, S.; Berke, H. Homogeneous Hydrogenation of Nitriles Catalyzed by Molybdenum and Tungsten Amides. *ACS Catal.* **2014**, *4*, 2191-2194.
44. Choi, J.; Precht, M. H. G. Tuneable Hydrogenation of Nitriles into Imines or Amines with a Ruthenium Pincer Complex under Mild Conditions. *ChemCatChem* **2015**, *7*, 1023-1028.
45. Chakraborty, S.; Milstein, D. Selective Hydrogenation of Nitriles to Secondary Imines Catalyzed by an Iron Pincer Complex. *ACS Catal.* **2017**, *7*, 3968-3972.
46. Chakraborty, S.; Leitius, G.; Milstein D. Iron-Catalyzed Mild and Selective Hydrogenative Cross-Coupling of Nitriles and Amines To Form Secondary Aldimines. *Angew. Chem. Int. Ed.* **2017**, *56*, 2074-2078.

47. Li, H.; Al-Dakhil, A.; Lupp, D.; Gholap, S. S.; Lai, Z.; Liang, L.; Huang, K. Cobalt-Catalyzed Selective Hydrogenation of Nitriles to Secondary Imines. *Org. Lett.* **2018**, *20*, 6430-6435.
48. Pangborn, A. B.; Giardello, M. A.; Grubbs, R. H.; Rosen, R. K.; Timmers, F. J. Safe and Convenient Procedure for Solvent Purification. *Organometallics* **1996**, *15*, 1518–1520.
49. Wietz, I. S.; Rabinovitz, M. The Application of C₈K for Organic Synthesis: Reduction of Substituted Naphthalenes. *J. Chem. Soc. Perkin Trans.* **1993**, *1*, 117-120.
50. Ibrahim, D. A.; Tokmic, K.; Brennan, M. R.; Kim, D.; Matson, E. M.; Nilges, M. J.; Bertke, J. A.; Fout, A. R. Monoanionic bis(carbene) pincer complexes featuring cobalt(I-III) oxidation states. *Dalton Trans.* **2016**, *45*, 9805–9811.